



Analysis and modelling of N₂O emissions in partial nitrification and anammox process

Longqi Lang

► To cite this version:

Longqi Lang. Analysis and modelling of N₂O emissions in partial nitrification and anammox process. Biochemistry [q-bio.BM]. INSA de Toulouse, 2019. English. NNT : 2019ISAT0042 . tel-03523675

HAL Id: tel-03523675

<https://theses.hal.science/tel-03523675>

Submitted on 12 Jan 2022

HAL is a multi-disciplinary open access archive for the deposit and dissemination of scientific research documents, whether they are published or not. The documents may come from teaching and research institutions in France or abroad, or from public or private research centers.

L'archive ouverte pluridisciplinaire **HAL**, est destinée au dépôt et à la diffusion de documents scientifiques de niveau recherche, publiés ou non, émanant des établissements d'enseignement et de recherche français ou étrangers, des laboratoires publics ou privés.



THÈSE

En vue de l'obtention du DOCTORAT DE L'UNIVERSITÉ DE TOULOUSE

Délivré par l'Institut National des Sciences Appliquées de
Toulouse

Présentée et soutenue par
Longqi LANG

Le 25 avril 2019

**Analyse et modélisation des émissions de N₂O dans un procédé
de nitrification partielle et anammox**

Ecole doctorale : **MEGEP - Mécanique, Energétique, Génie civil, Procédés**

Spécialité : **Génie des Procédés et de l'Environnement**

Unité de recherche :

LISBP - Laboratoire d'Ingénierie des Systèmes Biologiques et des Procédés

Thèse dirigée par
Mathieu SPERANDIO

Jury

M. Fabrice BÉLINE, Rapporteur
M. Nicolas BERNET, Rapporteur
Mme Eveline VOLCKE, Examinatrice
Mme Ahlem FILALI, Examinatrice
M. Mathieu SEBILO, Examineur
M. Mathieu SPERANDIO, Directeur de thèse

Acronym	Description
AerAOB	A erobic a mmonium o xidizing b acteria
AMO	A mmonia m onooxygenase
Anammox	A naerobic a mmonia o xidation
AnAOB	A naerobic a mmonium o xidizing b acteria
AOOs	A mmonium o xidizing o rganisms: including AerAOB and AnAOB (possibly AOA)
AOA	A mmonium o xidizing a rchaea
ASMN	A ctivated s ludge m odel for n itrogen
ASM-ICE	A ctivated s ludge m odel with i ndirect c oupling of e lectrons
CANON	C ompletely a utotrophic n itrogen r emoval o ver n itrite
CAS	C onventional a ctivate s ludge
Comammox	C omplete a mmonia o xidation
Cyt P460	C ytrochrome P460
Fe(II)	F errous iron
FISH	F luorescence i n s itu h ybridization
FNA	F ree n itrous a cid
HAO	H ydroxylamine o xidoreductase
HET	H eterotrophic d enitrifiers
HRT	H ydraulic r etention t ime
Hzs	h ydrazine s ynthase
NAR	M embrane-bound n itrate r eductase
ND	A utotrophic d enitrification of nitrite
NDHA	NN , ND , h eterotrophic d enitrification and a biotic pathways
NeNirK	N.europaea n itrite r eductase
NirK	Copper n itrite r eductase
NirS	cytochrome cd1-type n itrite r eductase
NN	i ncomplete NH ₂ OH oxidation
NoR	N itric o xide r eductase
NorB	M embrane-bound n itric o xide r eductase
NOB	N itrite oxidizing bacteria
Nos	N itrous oxide r eductase
OHO	O rganic h eterotroph o rganism
OLAND	O xygen limited a utotrophic n itrification/ d enitrification
OUT	O perational t axonomic u nit
PN	P artial n itrification
PNA	P artial n itritation and a nammox
PSD	P article s ize d istribution
QCLAS	Q uantum c ascade l aser a bsorption s pectroscopy
RBC	R otating b iological c ontactor
SBR	S equencing b atch r eactor
SP	S ite P reference: difference of ¹⁵ N abundance in central (α) and outer (β) position
WWTP	W astewater t reatment p lant
WWTS	W astewater t reatment s ystem
3-D	T hree- d imensional

Symbol	Characterization	Unit
AUR	Ammonium Uptake Rate	mg N L ⁻¹ h ⁻¹
DO	Dissolved Oxygen	mg O ₂ L ⁻¹
K _{La}	Transfer coefficient for oxygen	h ⁻¹
NAPR	Nitrate Production Rate	mg N L ⁻¹ h ⁻¹
NAUR	Nitrate Uptake Rate	mg N L ⁻¹ h ⁻¹
N ₂	Dinitrogen gas	
NH ₃	Ammonia	
NH ₄ ⁺	Ammonium	
NO ₂ ⁻	Nitrite	mg N L ⁻¹
NO ₃ ⁻	Nitrate	mg N L ⁻¹
NIUR	Nitrite Uptake Rate	mg N L ⁻¹ h ⁻¹
NO	Nitric oxide	
NO-EC	NO Emission Concentration	ppm
N ₂ O-EC	N ₂ O Emission Concentration	ppm
NO-EF	NO Emission Factor	%
N ₂ O-EF	N ₂ O Emission Factor	%
NO-ER	NO Emission Rate	mg N L ⁻¹ d ⁻¹
N ₂ O-ER	N ₂ O Emission Rate	mg N L ⁻¹ d ⁻¹
NLR	Nitrogen Loading Rate	kg NH ₄ ⁺ m ³ d ⁻¹
NRR	Nitrogen Removal Rate	kg NH ₄ ⁺ m ³ d ⁻¹
R	Isotope ratio for nitrogen (¹⁵ N/ ¹⁴ N) or oxygen (¹⁸ O/ ¹⁶ O)	1
SAUR	Specific Ammonium Uptake Rate	mg N g VSS ⁻¹ h ⁻¹
TSS	Total Suspended Solid	g L ⁻¹
VSS	Volatile Suspended Solid	g L ⁻¹
Q _{air}	Air flow rate	L h ⁻¹
δ ¹⁵ N-NH ₄ ⁺	Net isotope effect with NH ₄ ⁺ as substrate	‰
δ ¹⁵ N-NO ₂ ⁻	Net isotope effect with NO ₂ ⁻ as substrate	‰
δ ¹⁵ N-NO ₃ ⁻	Net isotope effect with NO ₃ ⁻ as substrate	‰
δ ¹⁵ N-N ₂ O	Net isotope effect with N ₂ O as substrate	‰

Résumé

Au cours des dernières décennies, le procédé couplant nitrification partielle et le procédé anammox (PNA) ont suscité beaucoup d'intérêt en raison d'un faible besoin énergétique et de l'évitement de la source de carbone organique externe par rapport aux systèmes biologiques classiques d'élimination de l'azote. Cependant, des émissions importantes de N_2O ont été signalées comme un inconvénient majeur de ce procédé. Le gaz N_2O est non seulement un gaz à effet de serre puissant, mais également une substance qui appauvrit la couche d'ozone dans la troposphère. Ce travail vise en premier lieu à une meilleure calibration des modèles de production de N_2O associés aux organismes oxydants de l'ammonium (AOO) pour la prévision des émissions des systèmes PNA. Deuxièmement, l'objectif était de mieux comprendre le mécanisme de production de N_2O dans le système PNA, la dynamique de ces émissions et l'influence du débit d'air.

Au début, deux modèles étaient disponibles pour modéliser les émissions de N_2O par les AOO. Par conséquent, leur capacité prédictive et leur calibration ont été évaluées sur la base de trois études de cas. Après la calibration simultanée avec les taux AOR et N_2O -R, les deux modèles étaient finalement capable de décrire les flux de N_2O expérimentaux et l'effet respectif du nitrite et de l'oxygène. En effet, ces deux paramètres sont cruciaux dans les systèmes PNA. Un modèle complet a ensuite été développé pour les systèmes PNA comprenant différentes voies biologiques de N_2O .

Les performances d'un procédé PN/A pour les boues granulaires combinant un faible débit d'air et un contrôle du point de consigne de l'OD terminal ont été étudiées. Le procédé a fonctionné avec succès pendant plus de 300 jours, contrôlé par le taux de transfert d'oxygène. Une diminution à long terme de la demande en oxygène jusqu'à $1,62 \pm 0,15$ a été observée en compagnie de l'augmentation de l'AUR. Les raisons de cette faible demande en oxygène ont été discutées, notamment un court-circuit possible par le NO. Une ségrégation des communautés microbiennes a été observée suivant les différentes tailles des agrégats. Les résultats du séquençage ont indiqué que *Nitrosomonas* était le principal AOO présent principalement dans les plus petits granules, alors que le genre Anammox était le *Ca. Kuenenia* et était le gène le plus abondant dans les plus gros granules. NOB a également coexisté dans le système avec le gène *nitrospira*.

Le facteur d'émission de N_2O a augmenté très progressivement lors du démarrage du procédé PNA (5 mois) de $0,4 \pm 0,1\%$ à $5,8 \pm 0,3\%$. Les différences dans la réponse à court et à long terme des émissions de N_2O suite à une variation du débit d'air ont été démontrées, révélant la complexité de la dynamique d'émission du N_2O . La raison de ces observations est discutée en relation avec l'identification de la voie en utilisant la signature isotopique du N_2O . L'étude confirme l'importance de la réduction des nitrites dans les filières de production et suggère également la contribution de la biomasse hétérotrophe alors qu'elle n'a pas été complètement démontrée. Le taux d'émission de N_2O a progressivement diminué jusqu'à 2,3% à la fin de l'étude.

Mots clés: Nitrification partielle et anammox (PNA); Organismes oxydants de l'ammonium (AOO); Facteur d'émission d'oxyde nitreux (N_2O_{EF}); DO limitation; Préférence de site (SP); Modélisation de l'oxyde nitreux; Ségrégation microbienne; Réduction des nitrites

Abstract

In recent decades, the process combining partial nitritation and the anammox (PNA) has aroused a lot of interest due to a low energy requirement and the avoidance of external organic carbon resource compared to conventional biological systems for nitrogen removal. However, significant N₂O emissions have been reported as a major drawback of this process. N₂O gas is not only a powerful greenhouse gas, but also a substance that can deplete the ozone layer in the troposphere. This work aims firstly at a better calibration of the N₂O production models associated with ammonium oxidizing organisms (AOOs) for predicting the emissions from PNA systems. Second, the objective was to better understand the N₂O production mechanism in the PNA system, the dynamics of these emissions and the influence of the air flow rate.

In the beginning, two models were available to model N₂O emissions by AOOs. Consequently, their predictive capacity and their calibration were evaluated on the basis of three case studies. After the simultaneous calibration with the ammonium oxidation rate (AOR) and N₂O emission rate (N₂O-R), the two models were finally able to describe the experimental N₂O fluxes and the respective effect of nitrite and oxygen. Indeed, these two parameters are crucial in PNA systems. A complete model was then developed for PNA systems comprising different biological N₂O pathways.

The performance of a PNA process for granular sludge combining a low air flow and a setpoint control of the terminal DO have been studied. The process had been working successfully for over 300 days, controlled by the oxygen transfer rate. A long-term decrease in oxygen demand to 1.62 ± 0.15 has been observed along with the increase in AOR. The reasons for this low oxygen demand have been discussed, in particular a possible short circuit by NO. Segregation of microbial communities was observed according to the different sizes of the aggregates. The sequencing results indicated that *Nitrosomonas* was the main AOO and present mainly in the smallest granules, while the genus Anammox was *Ca. Kuenenia* and was the most abundant gene in the largest granules. NOB also coexisted in the system with the *nitrospira* gene.

The N₂O emission factor gradually increased during the start-up of the PNA process (5 months) from $0.4 \pm 0.1\%$ to $5.8 \pm 0.3\%$. Different responses of N₂O emissions between the short-term and long-term following a change in air flow have been demonstrated, revealing the complexity of the N₂O emission dynamics. The reason for these observations is discussed in relation to the pathway identification using the isotopic signature of N₂O. The study confirms the importance of reducing nitrites in production chains and also suggests the contribution of heterotrophic biomass but it has not been fully demonstrated. The N₂O emission rate gradually decreased to 2.3% at the end of this study.

Key words: Partial nitritation and anammox (PNA); Ammonium oxidizing organisms (AOOs); Nitrous oxide emission factor (N₂O_{EF}); DO limitation; Site preference (SP); Nitrous oxide modelling; Microbial segregation; Nitrite reduction

Summary

<i>General introduction</i>	3
<i>Chapter 1: Literature overview</i>	9
1. MICROBIAL PROCESSES INVOLVED IN THE NITROGEN CONVERSION AND N ₂ O EMISSIONS.....	10
1.1 Nitrification pathways	10
1.2 Denitrification pathways	17
1.3 Anammox pathways	19
1.4 Contribution of abiotic N ₂ O pathways	22
1.5 Isotopic fractionation technique for tracking N ₂ O pathways	24
2. PNA CONTROL AND OPERATION	30
2.1 Global stoichiometry.....	30
2.2 Current operational and control strategies for PNA	30
2.3 Considering N ₂ O emission in the PNA process control?	33
3. THESIS OBJECTIVES AND CHAPTER OVERVIEW	39
 <i>Chapter 2: Comparison of different two-pathway models for describing the combined effect of DO and nitrite on the nitrous oxide production by ammonia-oxidizing bacteria</i>	53
1. INTRODUCTION	54
2. MATERIALS AND METHODS	56
2.1 Experimental Data	56
2.2 Mathematical Models.....	57
2.3 Model Calibration	58
3. RESULTS.....	59
Case 1: Combined DO and NO ₂ ⁻ effect on culture 1	59
Case 2: DO effect at low NO ₂ ⁻ level with culture 2	61
Case 3: Nitrite effect in culture 3	63
4. DISCUSSION.....	64
5. CONCLUSION	66
6. ACKNOWLEDGE	66
 <i>Chapter 3: One-stage partial nitrification anammox under oxygen limitation: performance, stoichiometry, N₂O emission and microbial segregation</i>	77
1. INTRODUCTION	78
2. MATERIALS AND METHODS	80
2.1 SBR operational mode	80
2.2 Aeration control and oxygen transfer rate	81
2.3 Chemical analysis.....	82
2.4 Particle size distribution (PSD), sieving and microbial analysis.....	83
2.5 Calculation and stoichiometry analysis	85
3. RESULTS.....	86
3.1 Process performances.....	86
3.2 Activity and biomass growth	87
3.3 Typical batch cycles.....	89
3.4 Granular sludge size distribution	91
3.5 Microbial community identification: 16 sRNA and FISH	93
4. DISCUSSION.....	97
4.1 PNA performances and stoichiometry under oxygen limitation	97
4.2 Biomass segregation: consequence on N ₂ O emissions?	98
5. CONCLUSIONS.....	99
6. APPENDIX	100
6.1 Recovery period	100
6.2 Transfer coefficient measurements.....	101
 <i>Chapter 4: Long-term and short-term dynamics of N₂O emission in PNA process under oxygen</i>	

<i>limitation</i>	107
1. INTRODUCTION	108
2. MATERIALS AND METHODS	110
2.1 Reactor operation	110
2.2 Aeration control and oxygen transfer rate	111
2.3 Chemicals analysis and specific batch tests	112
2.4 Isotopes analysis	112
2.5 Calculations	113
3. RESULTS	114
3.1 Typical N ₂ O patterns during batch cycles	114
3.2 Long term evolution of N ₂ O emission during intensification period	115
3.3 Operational parameters influencing initial N ₂ O peak: DO setpoint, aeration during feeding	118
3.4 Influence of air flow rate on N ₂ O emission (short and long term)	121
3.5 Isotopes analysis	123
3.6 N ₂ O emission rate during specific batch tests	124
4. DISCUSSION	125
4.1 Dynamic and range of N ₂ O emission under O ₂ limitation	125
4.2 Dominance of ND pathway and nitrite stimulating effect	126
4.3 Long term vs short term effects of aeration	127
5. CONCLUSIONS	128
6. APPENDIX	129
 <i>Chapter 5: Modelling N₂O emission from PNA process under oxygen limitation: Preliminary results and prospects</i>	135
1. INTRODUCTION	136
2. MODEL DESCRIPTION	136
3. RESULTS AND DISCUSSION	137
3.1. Model calibration for PNA at extremely low DO	137
3.2 Effect of NOB repression on the N ₂ O emission	138
3.3 Effect of air flow rate (K _{La} variation)	139
3.4. Pathways analysis	141
4. CONCLUSION	142
5. APPENDIX	144
5.1. Parameter, matrix and process description in the biofilm model	144
5.2 Effect of Temperature and pH dependency	151
5.3 The effect of DO on the ND pathway	152
5.3 Gas transfer calculations	152
 <i>Chapter 6: Conclusions and perspectives</i>	155
1. CONCLUSIONS	156
1.1 Properties of the one stage PNA process under OTR-controlled condition	156
1.2 Deeper insights into the N ₂ O emission dynamics	157
1.3 Deeper insights into the N ₂ O emission pathways	157
1.4 Combined effect of DO and nitrite on N ₂ O emission: modelling progress	158
2. FUTURE PERSPECTIVES	159
2.1 N ₂ O mitigation measures	159
2.2 Modelling aspects	159

General introduction

Nitrogen is the essential chemical element for the survival of all living creature and the fourth most abundant element in the cellular biomass (Stein and Klotz, 2016). However, excessive release of inorganic-N can lead to serious environmental problems such as the acidification of the freshwater system, eutrophication of aquatic ecosystems and also impair the ability of aquatic animals to survive, grow and reproduce (Camargo and Alonso, 2006). Ammonium (NH_4^+), nitrite (NO_2^-) and nitrate (NO_3^-) constitute the most common nitrogenous inorganic compounds found in aquatic ecosystems (Cervantes, 2009). Naturally these compounds can present as a result of atmospheric deposition, surface and groundwater runoff, dissolution of nitrogen-rich geological deposits, N_2 fixation by certain prokaryotes and biological degradation of organic matter (Camargo and Alonso, 2006). However, during the recent decades, human activities including the point and non-point sources have substantially increased the availability of inorganic nitrogen over large regions of Earth (Camargo and Alonso, 2006). Additionally, organic nitrogen can also indirectly cause the pollution by converting to the inorganic nitrogen (Smil, 2001). Both chemical and microbial methods have been developed to solve this problem. Compared with the chemical method, microbial technologies have the benefits of low environmental pollution and low costs, therefore technologies based on the microorganisms capable of converting nitrogen with high pollution potential into the nitrogen forms with low potential, are successively developed to treat the inorganic nitrogen pollution from the wastewater treatment systems. The basic idea of the most commonly used microbial nitrogen removal is to convert the inorganic-N pollutants from the wastewater into the harmless dinitrogen gas as the final product (Figures 1.1 and 6.1).

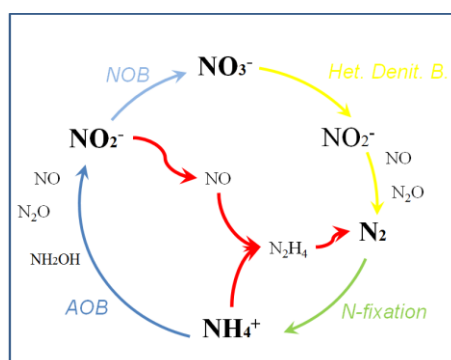


Figure 1.1: Major inorganic-N transformation pathways in wastewater systems

New alternatives have been established regarding the autotrophic system. Partial nitrification coupled to anaerobic ammonium oxidation, PNA for short, is a representative autotrophic nitrogen removal process which have received growing interests over the last decades (Jetten et al., 1997; Wett, 2007; Clippeleir et al., 2013). The concept of PNA process centered on the short-cut ammonium removal from an intermediate, nitrite, which is first produced by ammonium oxidizing organisms (AOOs) and then directly utilized to oxidize the ammonium into the harmless dinitrogen by the anaerobic ammonium oxidizing organisms (Anammox) (Connan et al., 2018). Compared with the conventional nitrification and denitrification, PNA route allows to save 65% of oxygen (less aeration) and 100% of organic matter requirement. Within the last decades, economic potential spurred the growing attention and brought fruitful advances on the single-stage PNA process (Cao et al., 2017; Agrawal et al., 2018; Baeten et al., 2019).

Until 2014, over 100 full-scale installations have been implemented worldwide and over 1000 publications concentrated on this topic (Lackner et al., 2014). Significant efforts have been successfully made from the lab-scale to pilot-scale then to full-scale applications (Sliekers et

al., 2002; Joss et al., 2009; Agrawal et al., 2018). The process can be used to treat the anaerobic digesters in the sidestream wastewater treatment with higher N load (De Clippeleir et al., 2009; Vázquez-Padín et al., 2009), also the mainstream line of the WWTP with lower N-load and higher seasonal variation of the temperature (Lotti et al., 2015).

The autotrophic PNA process can be realized either in one (combined PNA) or two reactors (Cao et al., 2017). For the two-stage system, reactors can be optimized separately and therefore the nitrite competition with NOB for the anammox can be avoided under anoxic condition (Pérez et al., 2014). However, considering the lower investment (infrastructures and operation) of the combined PNA process over the two-reactor system, one stage PNA gained more attention regarding to the nitrogen removal from the NH_4^+ -rich wastewater.

However, an important issue attracted the researchers regarding the PNA process: higher N_2O emission related to short-cut pathways compared to conventional nitrogen removal route. N_2O gas is not only a potential greenhouse gas with 300 times higher radiative forcing than carbon dioxide (IPCC, 2014), but also predicted to be the dominant tropospheric ozone depleting substance emitted in the 21st century (Ravishankara et al., 2009). Additionally, N_2O can easily react with multiple chemical N-forms in the lifecycle threatening the human health, and therefore unwanted even at trace levels (Kanter et al., 2017).

Besson et al. (2017) recently demonstrated that an excess of 1% of the N_2O emission factor from PNA process compared to conventional NDN can totally compensated the other benefits of such process in term of global warming potential. A potent advantage for the one stage PNA process is the lower nitrous oxide (N_2O) emissions over the two-reactor process (Okabe et al., 2011; Ali et al., 2016). However the range of N_2O emission reported in literature is highly variable (0.1 to more than 12%) and likely to be significantly higher than traditional N/DN in activated sludge for instance.

The current understanding does not enable us to establish a sustainable PNA process that performs maximum nitrogen removal and guarantying minimum N_2O emission. Most of the literature to date on the combined PNA process focused on the operation and control strategies which repress the NOB activity and avoid the oxygen inhibition on anammox. More insights into the biomass adaptation to the limiting-oxygen limitation are needed for investigating N_2O mitigation strategies.

Therefore this thesis aimed to acquire more comprehensive insights into the one stage PNA process, by establishing a long-term study on SBR process with low air flux and terminal DO set point control. The idea is to explore the performance and stoichiometry under extremely low DO, linking the N_2O emissions to operating conditions, with microbial community change, while mathematical models were finally used to explain the experimental observations. The **first** chapter is the literature study; the **second** chapter focus on the two-pathway models of ammonium oxidizing bacteria which explain the combined effect of DO and nitrite on N_2O production from a PN process; the **third** chapter summarizes the operational results of the PNA process, as well as the stoichiometry and microbial analysis; in chapter **four** the extensive N_2O monitoring from the PNA process will be analyzed and the pathways were explored using isotopic signature; finally in the **last** chapter a preliminary work on integrated 1-D model for PNA granular sludge with N_2O emission is presented.

References

- Agrawal, S., Seuntjens, D., Cocker, P.D., Lackner, S., Vlaeminck, S.E., 2018. Success of mainstream partial nitritation/anammox demands integration of engineering, microbiome and modeling insights. *Curr. Opin. Biotechnol., Energy biotechnology • Environmental biotechnology* 50, 214–221. <https://doi.org/10.1016/j.copbio.2018.01.013>
- Ali, M., Rathnayake, R.M.L.D., Zhang, L., Ishii, S., Kindaichi, T., Satoh, H., Toyoda, S., Yoshida, N., Okabe, S., 2016. Source identification of nitrous oxide emission pathways from a single-stage nitritation-anammox granular reactor. *Water Res.* 102, 147–157. <https://doi.org/10.1016/j.watres.2016.06.034>
- Baeten, J.E., Batstone, D.J., Schraa, O.J., van Loosdrecht, M.C.M., Volcke, E.I.P., 2019. Modelling anaerobic, aerobic and partial nitritation-anammox granular sludge reactors - A review. *Water Res.* 149, 322–341. <https://doi.org/10.1016/j.watres.2018.11.026>
- Besson, M., Tiruta-Barna, L., Spérandio, M., 2017. Environmental Assessment of Anammox Process in Mainstream with WWTP Modeling Coupled to Life Cycle Assessment, in: *Lecture Notes in Civil Engineering. Presented at the Frontiers International Conference on Wastewater Treatment and Modelling*, Springer, Cham, pp. 392–397. https://doi.org/10.1007/978-3-319-58421-8_62
- Camargo, J.A., Alonso, Á., 2006. Ecological and toxicological effects of inorganic nitrogen pollution in aquatic ecosystems: A global assessment. *Environ. Int.* 32, 831–849. <https://doi.org/10.1016/j.envint.2006.05.002>
- Cao, Y., Loosdrecht, M.C.M. van, Daigger, G.T., 2017. Mainstream partial nitritation–anammox in municipal wastewater treatment: status, bottlenecks, and further studies. *Appl. Microbiol. Biotechnol.* 101, 1365–1383. <https://doi.org/10.1007/s00253-016-8058-7>
- Cervantes, F.J. (Ed.), 2009. *Environmental Technologies to Treat Nitrogen Pollution: Principles and Engineering*. IWA Publishing, London.
- Clippeleir, H.D., Vlaeminck, S.E., Wilde, F.D., Daeninck, K., Mosquera, M., Boeckx, P., Verstraete, W., Boon, N., 2013. One-stage partial nitritation/anammox at 15 °C on pretreated sewage: feasibility demonstration at lab-scale. *Appl. Microbiol. Biotechnol.* 97, 10199–10210. <https://doi.org/10.1007/s00253-013-4744-x>
- Connan, R., Dabert, P., Moya-Espinosa, M., Bridoux, G., Béline, F., Magrí, A., 2018. Coupling of partial nitritation and anammox in two- and one-stage systems: Process operation, N₂O emission and microbial community. *J. Clean. Prod.* 203, 559–573. <https://doi.org/10.1016/j.jclepro.2018.08.258>
- De Clippeleir, H., Vlaeminck, S.E., Carballa, M., Verstraete, W., 2009. A low volumetric exchange ratio allows high autotrophic nitrogen removal in a sequencing batch reactor. *Bioresour. Technol.* 100, 5010–5015. <https://doi.org/10.1016/j.biortech.2009.05.031>
- IPCC, 2014. *Climate Change 2014: Synthesis Report. Contribution of Working Groups I, II and III to the Fifth Assessment Report of the Intergovernmental Panel on Climate Change [Core Writing Team, R.K. Pachauri and L.A. Meyer (eds.)]*. Geneva, Switzerland, p. 151.
- Jetten, M.S.M., Horn, S.J., van Loosdrecht, M.C.M., 1997. Towards a more sustainable municipal wastewater treatment system. *Water Sci. Technol., Sustainable Sanitation* 35, 171–180. [https://doi.org/10.1016/S0273-1223\(97\)00195-9](https://doi.org/10.1016/S0273-1223(97)00195-9)
- Joss, A., Salzgeber, D., Eugster, J., König, R., Rottermann, K., Burger, S., Fabijan, P., Leumann, S., Mohn, J., Siegrist, H., 2009. Full-Scale Nitrogen Removal from Digester Liquid with Partial Nitritation and Anammox in One SBR. *Environ. Sci. Technol.* 43, 5301–5306. <https://doi.org/10.1021/es900107w>
- Kanter, D.R., Wentz, J.A., Galloway, J.N., Moomaw, W.R., Winiwarter, W., 2017. Managing a forgotten greenhouse gas under existing U.S. law: An interdisciplinary analysis. *Environ. Sci. Policy* 67, 44–51. <https://doi.org/10.1016/j.envsci.2016.11.003>

- Lackner, S., Gilbert, E.M., Vlaeminck, S.E., Joss, A., Horn, H., van Loosdrecht, M.C.M., 2014. Full-scale partial nitritation/anammox experiences – An application survey. *Water Res.* 55, 292–303. <https://doi.org/10.1016/j.watres.2014.02.032>
- Lotti, T., Kleerebezem, R., Hu, Z., Kartal, B., de Kreuk, M.K., van Erp Taalman Kip, C., Kruit, J., Hendrickx, T.L.G., van Loosdrecht, M.C.M., 2015. Pilot-scale evaluation of anammox-based mainstream nitrogen removal from municipal wastewater. *Environ. Technol.* 36, 1167–1177. <https://doi.org/10.1080/09593330.2014.982722>
- Okabe, S., Oshiki, M., Takahashi, Y., Satoh, H., 2011. N₂O emission from a partial nitrification–anammox process and identification of a key biological process of N₂O emission from anammox granules. *Water Res.* 45, 6461–6470. <https://doi.org/10.1016/j.watres.2011.09.040>
- Pérez, J., Lotti, T., Kleerebezem, R., Picioreanu, C., van Loosdrecht, M.C.M., 2014. Outcompeting nitrite-oxidizing bacteria in single-stage nitrogen removal in sewage treatment plants: A model-based study. *Water Res.* 66, 208–218. <https://doi.org/10.1016/j.watres.2014.08.028>
- Ravishankara, A.R., Daniel, J.S., Portmann, R.W., 2009. Nitrous Oxide (N₂O): The Dominant Ozone-Depleting Substance Emitted in the 21st Century. *Science* 326, 123–125. <https://doi.org/10.1126/science.1176985>
- Sliekers, A.O., Derwort, N., Gomez, J.L.C., Strous, M., Kuenen, J.G., Jetten, M.S.M., 2002. Completely autotrophic nitrogen removal over nitrite in one single reactor. *Water Res.* 36, 2475–2482. [https://doi.org/10.1016/S0043-1354\(01\)00476-6](https://doi.org/10.1016/S0043-1354(01)00476-6)
- Smil, V., 2001. *Enriching the Earth: Fritz Haber, Carl Bosch, and the Transformation of World Food Production*. MIT Press.
- Stein, L.Y., Klotz, M.G., 2016. The nitrogen cycle. *Curr. Biol.* 26, R94–R98. <https://doi.org/10.1016/j.cub.2015.12.021>
- Vázquez-Padín, J.R., Pozo, M.J., Jarpa, M., Figueroa, M., Franco, A., Mosquera-Corral, A., Campos, J.L., Méndez, R., 2009. Treatment of anaerobic sludge digester effluents by the CANON process in an air pulsing SBR. *J. Hazard. Mater.* 166, 336–341. <https://doi.org/10.1016/j.jhazmat.2008.11.055>
- Wett, B., 2007. Development and implementation of a robust deammonification process. *Water Sci. Technol.* 56, 81–88. <https://doi.org/10.2166/wst.2007.611>

Chapter 1: Literature overview

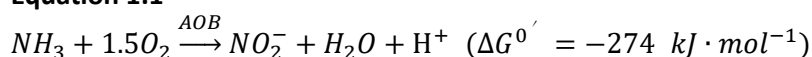
1. Microbial processes involved in the nitrogen conversion and N₂O emissions

1.1 Nitrification pathways

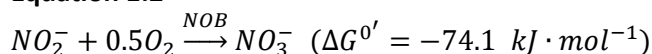
Nitrification is the biological process by which ammonia is oxidized to nitrite (Equation 1.1: nitritation) and then to nitrate (Equation 1.2: nitratation). This process was discovered at the end of the nineteenth century and found a division of labour between two different groups of bacteria, both of which have been isolated (Brock, 1999). Traditionally, ammonia oxidation is mainly catalyzed by autotrophic ammonia-oxidizing bacteria (AOB) whereas nitrite oxidation is catalyzed by nitrite oxidizing bacteria (NOB). Compared with heterotrophic organisms, growth of the nitrifiers is slow even in optimal conditions.

Nitratation, a more rapid process over nitritation under ambient temperature and conventional conditions, is the oxidation of nitrite (NO₂⁻) to nitrate (NO₃⁻) with no detectable intermediate. This reaction is carried out by an enzyme nitrite oxidoreductase (NOR) from the nitrite-oxidizing bacteria (NOB) (Equation 1.2). The extra oxygen atom in nitrate is derived from water (Poughon et al., 2001).

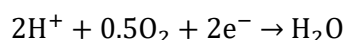
Equation 1.1



Equation 1.2



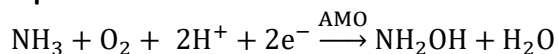
Equation 1.3



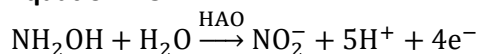
Sub-step pathways of ammonium oxidation

During nitritation, ammonia (NH₃), the actual substrate instead of ammonium (NH₄⁺) (Suzuki et al., 1974), is oxidized to nitrite (NO₂⁻) via a two sub-steps oxidation (Equations 1.4 and 1.5). First ammonia is converted to hydroxylamine (NH₂OH) via a membrane-bound enzyme ammonium monooxygenase (AMO) and next oxidized to nitrite by a hydroxylamine reductase (HAO) (Kowalchuk and Stephen, 2001). Four electrons are released from the oxidation of NH₂OH, two of which are used for the ammonia oxidation and another two are used for energy production and reduction of water (Equation 1.3).

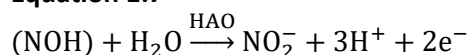
Equation 1.4



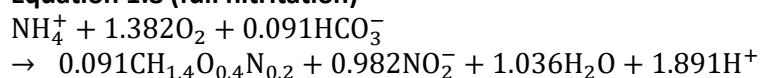
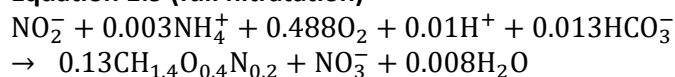
Equation 1.5



The oxidation from NH₂OH to nitrite is further split into two separate reactions as proposed in an energy model (Poughon et al., 2001). With the aid of metabolic flux analysis, Poughon et al. (2001) validated a complete energy model to describe the distribution of electrons coming from NH₃ and NO₂⁻ oxidation through the transport chain in the case of Nitrosomonas species. It was suggested that the tyrosine residues attached to the haem P460 and arrangement of haem cluster allow HAO transiently to accept two electrons at the same time, which splits the second step of nitritation (Equation 1.5) into two separate reactions (Equations 1.6 and 1.7).

Equation 1.6**Equation 1.7****Stoichiometry considering the anabolism**

It should be noted that during the autotroph growth, not all ammonium inside the bacterial cells is nitrified; part of ammonium is used for cell growth as nitrogen source where carbon dioxide serves as carbon source. Therefore by considering the growth yield and oxygen consumption for AOB and NOB organisms, the biochemistry of two reactions could be accurately described in full stoichiometries for nitritation (Equation 1.8) and nitrataion (Equation 1.9).

Equation 1.8 (full nitritation)**Equation 1.9 (full nitrataion)**

Therefore, the biomass growth yields for AOB and NOB are here assumed to be 0.1470 mg cells mg $\text{NH}_4\text{-N}^{-1}$ oxidized and 0.0202 mg cells mg $\text{NO}_2\text{-N}^{-1}$ oxidized, respectively. Oxygen consumption ratios in the equations are 3.16 mg O_2 mg $\text{NH}_4\text{-N}^{-1}$ oxidized and 1.11 mg O_2 mg $\text{NO}_2\text{-N}^{-1}$ oxidized, respectively (Cervantes, 2009).

Microbiology

Nitrification, is mainly performed by autotrophic AOB (Soliman and Eldyasti, 2018). Although studies showed that AOA was also able to carry out this reaction (Zhang et al., 2011), the enrichment and cultivation of AOA is linked to strict operating condition, such as high temperature (Torre et al., 2008; Courtens et al., 2016), and addition of antibiotics (Chen et al., 2017).

Since the first AOB isolation in the 1890s, five AOB genera have been recognized and confined to the Proteobacteria class (Soliman and Eldyasti, 2018), four of which were grouped in the β -subclass: *Nitrosomonas*, *Nitrospira*, *Nitrosovibrio* and *Nitrosolobus* (Woese et al., 1984), while *Nitrosococcus* belonged within the γ -subclass (Junier et al., 2010). Thereinto, *Nitrosomonas* and *Nitrospira* are two most important genera of AOB in activated sludge (Purkhold et al., 2000; Park and Noguera, 2004; Terada et al., 2013). DO concentrations can influence AOB species dominance. Low DO is reported to favor the proliferation of members of *N. europaea* lineage in full-scale and lab-scale reactors (Park and Noguera, 2004). Process configuration (SBR or CSTR) can also lead to the shift of the main AOB community (Terada et al., 2013). Terada et al. (2013) showed the abundance of *Nitrosomonas* lineage in SBR (76%) was twice as much as that in the CSTR (38%). In contrast, *Nitrospira* spp. grew well (42%) in the CSTR while seldom observed (less than 2%) in the SBR (and can thus be interpreted as K-strategist).

Since the first isolated NOB genus *Nitrobacter* in 1892, another four genera have been found as, *Nitrococcus*, *Nitrospira*, *Nitrolancetus hollandicus*, as well as *Nitrospina* (only in marine

environments). In wastewater treatment systems, *Nitrospira* spp. and *Nitrobacter* spp. represent the most dominant NOB. Sorokin et al. (2012) successfully isolated *Nitrolanceetus hollandicus* from a nitrifying reactor, which belonged to the widespread phylum *Chloroflexi* and had a low affinity for nitrite ($K_s=1\text{mM}$).

A great diversity of members of the genus *Nitrospira* have been found in wastewater treatment plants, while most strains of *Nitrospira* remain uncultured, and the few isolates grow slowly and are difficult to maintain in the laboratory (Daims and Wagner, 2018). The only previously known thermotolerant NOB belongs to the genus *Nitrospira* (Lebedeva et al., 2011). These organisms are inactive below 37°C and inhibited already by nitrite concentrations of 6mM , and do not utilize formate or other organic compounds.

Recent studies showed that the complete nitrification from ammonia to nitrate can be shortened from the two-step into one-step, called 'Comammox' (completely ammonium oxidation). After its theoretical prediction by Costa et al. (2006), Kessel et al. (2015) firstly discovered the enriched comammox species (*Nitrospira*) containing a novel amoA sequence group. Since then, *Nitrospira* have been successively identified in a wide range of engineered systems (Lawson and Lucker, 2018). One distinct characteristic of *Nitrospira* is that the AMO encoded by Comammox is phylogenetically distinct from the AMO forms of canonical AOB and AOA (Daims et al., 2015; Kessel et al., 2015).

Apparent oxygen affinity constants for AOB and NOB

Nitrification is very sensitive to low DO concentrations. Although nitrifying bacteria have very high affinities for oxygen (i.e. low K_{O_2} value), the local DO inside the aggregates or biofilm in wastewater treatment processes can be much lower than the bulk DO concentration (Cervantes, 2009).

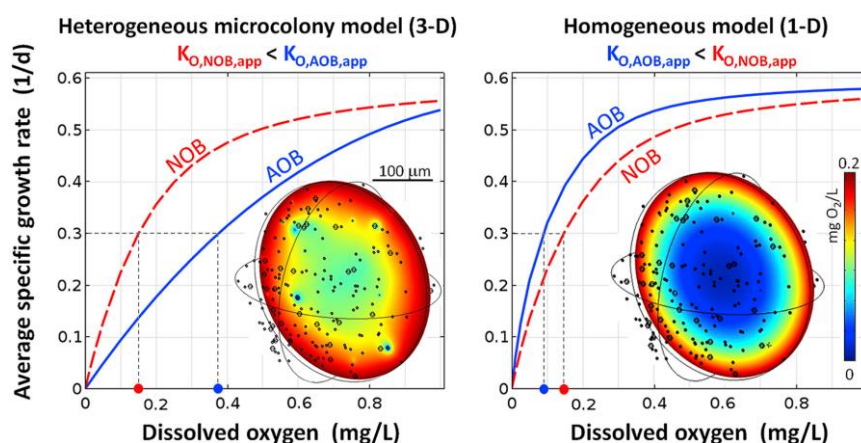


Figure 1.2: Comparison between the 3-D model and usual 1-D homogeneous model in predicting the apparent oxygen affinity constants for AOB and NOB (Picioreanu et al., 2016)

Regarding to the oxygen affinity for AOB and NOB, the comparison between the two parameters is not consistent among different studies (Sliekers et al., 2005; Regmi et al., 2014). This variation can be due to the provided oxygen amount referred with the nitrogen load. In a CANON reactor, AOB had a K_{O_2} of 0.074 and $0.20 \text{ mg O}_2 \text{ L}^{-1}$ under oxygen-limiting and oxygen-just-sufficient conditions, while for NOB was $0.042 \text{ mg O}_2 \text{ L}^{-1}$ when oxygen was sufficient while cannot be determined under the oxygen-limiting conditions. The value of oxygen affinity constant can also be due to the process configuration. In a pilot-scale CSTR, Regmi et al. (2014) determined the half saturation coefficient of 1.2 and $0.2 \text{ mg O}_2 \text{ L}^{-1}$ for AOB and NOB

respectively. However, Manser *et al.* (2005) evaluated the impact of membrane separation and mass transfer effects on the kinetics of nitrifiers by establishing two parallel reactors, a MBR and a CAS with the same settling. Saturation coefficient values obtained in this study was much lower for AOB but much higher for NOB. For AOB, K_{O_2} value increased from 0.18 to 0.79 mg O_2 L⁻¹ from the MBR to CAS, while for NOB, the increased from 0.13 to 0.47 mg O_2 L⁻¹.

A systematic statistical analysis of K_{O_2} conducted by Vannecke and Volcke (2015) by reviewing over 25 publications for AOB and NOB respectively showed that AOB tend to have a higher oxygen affinity than NOB (AOB: 0.40 mg O_2 L⁻¹; NOB: 0.97 mg O_2 L⁻¹ at 30 °C) considering the average value.

Actually, the intrinsic half-saturation coefficients (i.e., not affected by diffusion) show a better (low K_s value) affinity for oxygen for AOB than for NOB measurements in flocs (Blackburne *et al.*, 2008), but measurements in flocs often produced reversed apparent values. Picioreanu *et al.* (2016) applied a 3-D diffusion-reaction model to assess the impact of cell cluster size on apparent K_{O_2} in nitrifying sludge and biofilms. The modelling results demonstrated that although the intrinsic affinity (K_{O_2}) value (0.03 mg O_2 L⁻¹) is lower for AOB than for NOB (0.06 mg O_2 L⁻¹), the apparent coefficient value is just the inverse: stronger mass transfer limitations in the bigger AOB microcolonies than smaller NOB microcolonies, resulted in the drastic declined apparent oxygen affinity for AOB than for NOB: 0.19 and 0.37 mg O_2 L⁻¹ for AOB inside small floc (80µm) and large flocs (400µm), while 0.09 and 0.15 mg O_2 L⁻¹ for NOB species. This reversion of the half-saturation coefficient for AOB and NOB could be explained by the two important considerations in the 3-D model incorporating both lower oxygen yield and smaller colony size for NOB than that for AOB.

Two major N₂O pathways by AOB

Currently many studies were focused on the N₂O production by AOB who is well known as the main and decisive bacteria in the most nitrifying systems (Colliver and Stephenson, 2000; Spérandio *et al.*, 2016). Therefore, revolving around the AOB, there are two proposed mechanisms of N₂O production (Chandran *et al.*, 2011; Wunderlin *et al.*, 2012): The first N₂O production pathway involved the incomplete oxidation of NH₂OH to NO by HAO enzyme and subsequent reduction to N₂O catalyzed by the NOR enzyme (noted “**NN**”) (Ni *et al.*, 2013b; Pocquet *et al.*, 2016). While the second N₂O pathway through the autotrophic denitrification of nitrite (noted “**ND**”) i.e. the reduction of nitrite to NO by the NirK enzyme, followed by the reduction of NO to N₂O by the Nor enzyme (Ni *et al.*, 2014; Peng *et al.*, 2015; Pocquet *et al.*, 2016).

Strictly speaking, ND pathway is a denitrification process because both processes are reduction processes. Existence of NirK and Nor with the absence of Nos was later described as the fundamental reason for N₂O accumulation in autotrophic denitrification by AOB. ND is active during aerobic conditions and especially promoted during O₂-limiting conditions and high NO₂⁻ conditions. Chandran *et al.* (2011) summarized that presence of non-limiting substrate concentration and the switch between anoxic and oxic conditions can both lead to the N₂O production, the latter of which is much more common in the engineered nitrogen-removal systems. The reconstruction of metabolic N₂O pathways in that review provided the opportunity to achieving the simultaneous minimization of aqueous and gaseous nitrogen pollutions via what can be termed environmentally sustainable engineering design of sewage-treatment processes.

Initially, ND pathway by *N.europaea* received more attentions (Wrage *et al.*, 2001; Beaumont

et al., 2004). The finding of Lawton *et al.* (2013) provided the molecular insights into the extracted enzyme NeNirK from *N.europaea*. The crystal structure of this enzyme revealed a constrained substrate channel due to the presence of Met-128 and a second water channel that might function as an egress for displaced water molecules, enabling it to function in an aerobic environment. Later, it was confirmed that this ability is not only for this specific species but widespread, probably as a general trait in the β -proteobacterial AOB. Shaw *et al.* (2006) detected the ND activity in six *nitrosospiras* which are representatives of three major phylogenetic clusters in the cultured *Nitrosospira* lineage, in addition to the previously known activity of *nitrosomonas*. The characterization of the N_2O production and ND in seven strains of AOB representative of clusters 0, 2 and 3 in the cultured *Nitrosospira* lineage showing that up to 13.5% of produced N_2O was derived from the exogenously applied $^{15}N-NO_2^-$ for all AOB species under aerobic conditions.

Despite the major AOB species are considered to produce most of the N_2O , recent microbial advances of the nitrification also indicated that the minority of microflora can proliferate during certain environmental systems (Annavaiah et al., 2018). In addition, the NOB, AOA, and comammox microorganisms might also play an indirect role in N_2O formation by affecting the availability of NH_3 and NO_2^- (Sabba et al., 2018). These complex phenomenon still lack of sufficient in depth studies.

N_2O production models by AOB: from single-pathway to two-pathway

As the N_2O production mechanism by AOB are becoming clearer, several mechanistic models have been proposed based on single-pathway or two-pathways by AOB (Ni and Yuan, 2015). Single-pathway model considered either ND or NN pathway, while two-pathway models considered both mechanisms. Considering only ND pathway, two primary models proposed by Ni et al. (2011) and Mampaey et al. (2013) shared the similarity of two-step NO_2^- reduction to N_2O while differed mainly the step number of NH_3 oxidation to NO_2^- and the way of DO inhibition. Compared with the original model respectively, the modification of the former model by Pocquet et al. (2013) neglected the DO limitation on the ND pathway but considered the pH influence, while the latter model was modified by Guo and Vanrolleghem (2014) through switching the Monod inhibition to Haldane function in order to describe the multi-aspect influence of DO, and adding one reduction factor on NO reduction to N_2O . Single-pathway models considering only NN pathway were reported respectively by Law et al. (2012) and Ni et al. (2013a). Different intermediates were used in the model, NOH for the former and NO for the latter. Additionally, DO has no inhibitory effect on NO reduction for the latter. All those single-pathway models considered the cell growth, but the original (Mampaey et al., 2013) and modified ND pathway model (Guo and Vanrolleghem, 2014) assumed the energy resource from all step processes, which is different from others with NH_2OH oxidation as the main resource.

Single-pathway model had simple model structure but could be used only under specific conditions (Ni et al., 2013b; Spérandio et al., 2016). Overcoming the limitation of single-pathway N_2O models, the first 2-pathway model was proposed by Ni et al. (2014) linking all biochemical redox processes through a pool of electron carriers as new model components. The extended version of this model is based on decoupling approach with both electron and energy (ATP) balance, enabling to describe the dependency of N_2O production by AOB on IC concentration (Peng et al., 2016). The second 2-pathway model developed by Pocquet et al. (2016) considered five pure enzymatic reactions. It was calibrated to describe not only the data from batch experiments with various accumulated levels of nitrite, especially the trends

observed for the NO/N₂O ratio as well as N₂O-EF, but also the long term N₂O emission data from a SBR process with variations of nitrite, pH and DO. Until now, most of the applications of the 2-pathway models in predicting the N₂O emission from the nitrification-related systems were in the suspended systems (Ni et al., 2015; Pocquet et al., 2016), calibration experiences to more complex system such as the biofilm system are still lacking.

Potential N₂O pathways

Unlike the well-accepted ND and NN pathways by AOB with the characteristic of the successive enzymatic reactions, N₂O could be potentially assessed through kinetics with the catalyst of extracted cytochromes.

Upadhyay et al. (2006) reported that ferrous cytochrome C554 (cyt C554) has significant NO reductase activity. The tetraheme cyt C554 from *Nitrosomonas europaea* is considered to function as an electron-transfer protein from hydroxylamine oxidoreductase (HAO), which may be important during ammonium oxidation at low DO concentration to detoxify NO. However, no direct N₂O measurements were demonstrated to confirm the existence of this pathway.

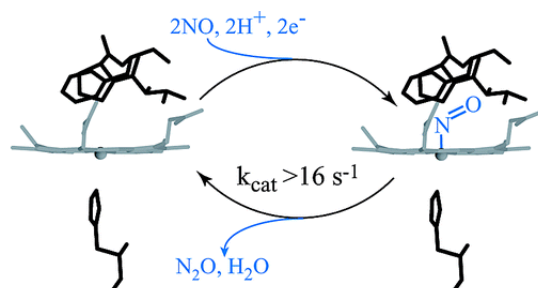
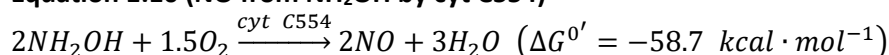


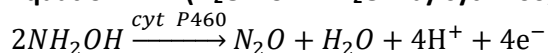
Figure 1.3: Potential N₂O production pathway through cyt C554 from *N. europaea*.(Upadhyay et al., 2006)

Equation 1.10 (NO from NH₂OH by cyt C554)



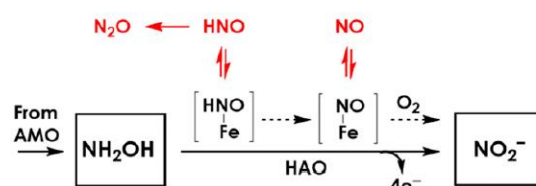
Caranto *et al.* (2016) found that N₂O is the enzymatic product of anaerobic NH₂OH oxidation mediated by *N. europaea* cyt P460. This pathway proceeds through an NH₂OH-bound form that is oxidized by three electrons to {Fe-NO} that then reacts with NH₂OH to form N₂O in the rate limiting step, which is different from the NN and ND pathway, establishing an alternative oxidative pathway to produce N₂O under limiting-oxygen condition.

Equation 1.11 (N₂O from NH₂OH by cyt P460)



The work conducted by Caranto and Lancaster. (2017) revealed that NO is an additional obligate intermediate and three electrons were released during the oxidation of NH₂OH to NO under both aerobic and anaerobic conditions (Figure 1.4). The termination of NO allows for additional free energy to be withdraw via subsequent oxidation to NO₂⁻ by an as-yet-unidentified enzyme. A decrease in the rate of NO oxidation to NO₂⁻ might be expected at low DO concentrations, and this may help explain the observed increase in N₂O emissions at low DO or during transitions from oxic to anoxic. The presently afforded revision of HAO's activity should facilitate understanding of the sources and rates of NO and N₂O emissions from AOB.

NH₂OH obligate intermediate model



NH₂OH/NO obligate intermediate model

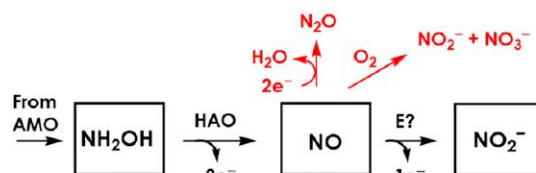


Figure 1.4: Two models for obligate intermediates of NH₃ oxidation to NO₂⁻ production by AOB (Caranto and Lancaster, 2017)

It is not demonstrated that all of the observed AOB communities can share the same N₂O production routes. Moreover the recent new findings definitely suggested that the N₂O formation during the nitrification process is not only a simple consecutive enzymatic reaction, but also one type of diverse/alternative adaptation for the biomass performing the nitrification when meeting with the different environmental condition, no matter it is stimulating or inhibiting. Notably, the chemical reactions might also happen during the nitrification, which is detailed in part 1.4 of this chapter.

1.2 Denitrification pathways

Denitrification is initially nominated to describe one phenomenon (e.g. nitrogen loss in N cycle) and was recognized by Kluver as an anaerobic respiration process. Denitrifying bacteria in the water systems involve numerous physiological and morphological characteristics, most of the denitrifying bacteria being facultative. However, the capacity to denitrify has been also found in some Archaea and Fungi (Thorndycroft et al., 2007).

Denitrification by heterotrophic bacteria

The complete heterotrophic denitrification consists of sequential reductive reactions from NO_3^- to NO_2^- , NO, N_2O and finally to N_2 , carried out by heterotrophs (Conthe et al., 2019). At the same time, four different enzymes are involved in those processes: NAR, NiR, NoR and NoS. Each enzyme uses a redox active metal cofactor, such as molybdenum for NO_3^- reduction, iron or copper for nitrite reduction, iron for NO reduction and copper of N_2O reduction (Richardson et al., 2009). Therefore, heterotrophic denitrifiers have two abilities: producing and consuming N_2O . Depending on the environmental conditions regulating enzymatic rates (NOR and NOS) heterotrophic processes are either a possible source (NOR rate > NOS rate), or in contrast can play as a sink of N_2O (NOS rate > NOR rate) (Figure 1.5).

Denitrification as an N_2O sink in the denitrification process

During the heterotrophic denitrification, N_2O gas can be both produced and consumed by the denitrifying organisms unlike the AOB are invariably net sources of N_2O (Figure 1.5). The ability to emit N_2O will be strongly dependent on the intrinsic capacity of its heterotrophic denitrifying community to reduce N_2O . A community with low NOS activity relative to the other reductases (i.e. NAR, NIR and NOR) will be a strong N_2O -source, while one with high relative NOS activity will emit less N_2O and may even be able to function as a net sink for N_2O produced during nitrification, as observed in microcosm experiments with Leca-particle biofilms in Mao et al. (2008).

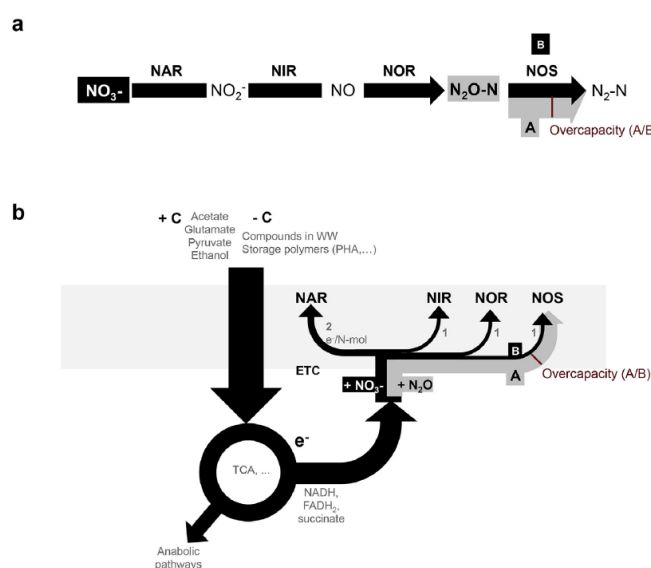


Figure 1.5: The denitrification pathway visualized in terms of (a) NO_x substrate or (b) electron flow distribution within the electron transport chain (ETC) (Conthe et al., 2019).

Heterotrophic denitrification can be found in different wastewater treatment systems. In a recent study, Conthe *et al.* (2019) showed that N_2O reduction rates was 2–5 times higher than NO_3^- reducing rates in activated sludge samples. Adding substrates into the previous samples demonstrated an overcapacity of N_2O reductase is widespread in denitrifying systems, which is more likely related to physiology than community composition.

N_2O emissions related to denitrification

In a very recent publication, Sabba *et al.* (2018) summarized the N_2O emission from a denitrifying biofilm process. Here we briefly selected the major contents from this review article.

- ✧ The N_2O formation in wastewater denitrification processes is often due to selective inhibition of the NOS enzyme (Guo *et al.*, 2017).
- ✧ The N_2O production and consumption in the heterotrophic catabolism occurred at the same time. Externally supplied N_2O can be reduced concurrently with NO_3^- and NO_2^- . While many denitrifying bacteria have a complete reduction pathway and can reduce NO_3^- and NO_2^- all the way to N_2 , less is known about bacteria that can grow with N_2O but not with NO_3^- or NO_2^- .
- ✧ The difference (or special) of the N_2O formation and reduction behavior can be due to the difference of the type of the denitrifying microorganisms. However, the actual contribution of DNRA to N_2O formation in these species remains uncertain (Butterbach-Bahl Klaus *et al.*, 2013)
- ✧ Behavior regarding N_2O emissions may also vary based on the type of electron donor. While the details on each of these donors are beyond the scope of this review, the kinetics for each donor can have important impacts on N_2O formation and consumption.

N_2O production models by heterotroph bacteria

Four-step denitrification models have been proposed to predict the accumulation of the intermediates during all denitrification process including the N_2O (Hiatt and Grady, 2008; Ni *et al.*, 2011; Pan *et al.*, 2013). To date, two distinct concepts have been proposed, which are represented by ASMN (Hiatt and Grady, 2008) and ASM-ICE (Pan *et al.*, 2013), respectively. Carbon oxidation and nitrogen reduction processes were directly coupled during 4 redox reactions in the ASMN model, while indirectly coupled during 5 redox reactions through electron carriers in the ASM-ICE model. However, more steps in the latter model allowed to describe the N_2O production under more diverse conditions than the former model.

N_2O model upgrade: Combining AOB and heterotrophic denitrification

Different approaches have been reported to integrate the N_2O production/consumption by both AOB and heterotrophic denitrifiers into a comprehensive N_2O model: i) ASM-type models that combine one of the single-pathway models of AOB with ASMN of heterotrophic denitrifiers (Ni *et al.*, 2011; Pocquet *et al.*, 2013; Guo and Vanrolleghem, 2014); ii) Electron balance-based model that integrate the electron carrier based two pathway model of AOB and ASMN (Ni *et al.*, 2015). Both modelling approaches have been successfully applied to describe N_2O emissions from mixed culture nitrification-denitrification systems and to identify the relative contributions between AOB and heterotrophic denitrifiers to total N_2O production (Ni *et al.*, 2011, 2013a, 2015).

In these integrative studies consumption of N_2O by heterotrophic denitrification (as a N_2O sink)

is noticed and reduces overall N₂O production under the conditions of high COD to N ratio and/or low DO level.

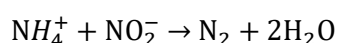
1.3 Anammox pathways

Anaerobic ammonium oxidation is a microbial process which release dinitrogen gas (N₂) (Figure 1.1). Bacteria catalysing this process oxidize NH₄⁺ to N₂ gas with NO₂⁻ as an electron acceptor. It was designated as anammox bacteria (AMX) or anaerobic ammonium oxidation bacteria (AnAOB). Mulder et al (1995) first experimentally confirmed this process in a denitrifying bioreactor operated in the Netherlands. Prior to this, theoretical chemist Engelbert Broda ever predicted the presence of a previously unknown lithotrophic microorganisms that can oxidize NH₄⁺ to N₂ gas with NO₂⁻ or NO₃⁻ as electron acceptors (Broda, 1977).

Multiple reactions and pathways

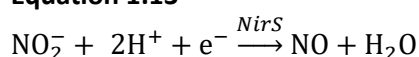
Overall catabolic process of AMX can be simplified by the following equation:

Equation 1.12

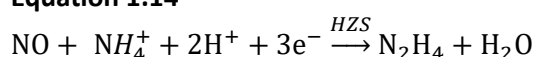


Based on our current understanding, the anammox catabolism is composed of three consecutive, coupled reactions with two intermediates, nitric oxide (NO), and hydrazine (N₂H₄). First, nitrite is reduced to NO with nitrite reductase (NirS) which is then, as we understand, condensed with ammonium to form hydrazine, via a multi-enzyme complex hydrazine synthase (HGS). Finally, hydrazine is oxidized to dinitrogen gas by hydrazine dehydrogenase (HDH) (Maalcke et al., 2014).

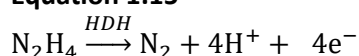
Equation 1.13



Equation 1.14

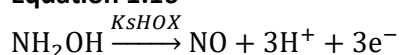


Equation 1.15



Maalcke et al. (2014) reported a novel pathway to make NO from NH₂OH using the purified *Kustc1061* enzyme from *K. stuttgartiensis* culture in MBR. The NH₂OH addition studies showed that, this HAO-like protein can share the same reaction specifically catalyze NH₂OH to NO releasing one less electron (Equation 1.16) than using the original HAO from AOB (Equation 1.5), the key protein in AOB. This new enzyme had a crystal structure and is related to HAO, a key protein in AOB. This pathway proposed a new way to detoxify the NH₂OH.

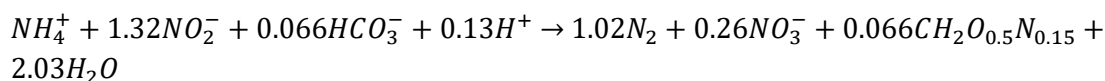
Equation 1.16



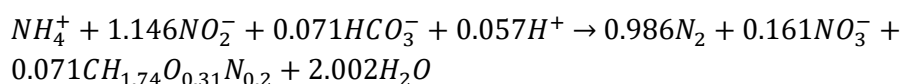
Stoichiometry considering the anabolism

The stoichiometry of the anammox was first systematically determined (Equation 1.17) with small AnAOB aggregates in a SBR bed reactor (Strous et al., 1998), and was recently revised (Equation 1.18) using a highly enriched culture of planktonic AnAOB cells (Lotti et al., 2014b). The difference between the nitrite and nitrate coefficients could be caused by the specific metabolic characteristics for different AnAOB species.

Equation 1.17(Strous et al., 1998)



Equation 1.18 (Lotti et al., 2014b)



Microbiology

Since its discovery in Delft, Anammox bacteria are ubiquitously distributed in a variety of ecosystems (Schmid et al., 2005), pilot plants for the ammonium removal (van Dongen et al., 2001; Fux et al., 2002), oxygen minimum zones (OMZs) of ocean (Kalvelage et al., 2011), brackish (Teixeira et al., 2012), freshwater systems (Penton et al., 2006), terrestrial environments (Shen et al., 2015), and marine sediments (Jensen et al., 2007) as well as the sub-oxic zone of the Black sea (Kuypers et al., 2003). In addition, anammox populations were also found in the extreme environments (Rysgaard and Glud, 2004; Borin et al., 2013; Russ et al., 2013; Oshiki et al., 2015).

The wide distribution of AnAOBs indicated the community diversity. Until now, all reported AnAOBs are affiliated with a monophyletic group in the phylum Planctomycetes, and can be further divided into five candidate genera: 'Ca. Kuenenia', 'Ca. Brocadia', 'Ca. Anammoxoglobus', 'Ca. Jettenia' and 'Ca. Scalindua' (Oshiki et al., 2015). 'Ca. Brocadia' and 'Ca. Kuenenia' are the most abundant in engineered anammox systems. 'Ca. Brocadia' prefers environments with high NH_4^+ and NO_2^- concentrations such as wastewater treatment plant, while 'Ca. Kuenenia' with lower affinity constants for NH_4^+ and NO_2^- is able to outcompete 'Ca. Brocadia' under the substrate-limited condition (Oshiki et al., 2015). 'Ca. Scalindua' prefers salty environments (Kuypers et al., 2003) and thrives at lower temperature ranges than other anammox bacteria (Awata et al., 2013). However, the information on the physiological characteristic for 'Ca. Anammoxoglobus' is scarce.

The microbial competitions for NO_2^- among three anammox species (i.e. 'Ca. Brocadia sinica', 'Ca. Jettenia caeni' and 'Ca. Kuenenia stuttgartiensis') were investigated under different nitrogen loading rates in MBRs. Results showed that 'Ca. Brocadia sinica' dominated at high NLRs and present throughout the gel beads and granules, while 'Ca. Jettenia caeni' dominated at low NLRs and distributed as spherical microclusters in the inner part (low NO_2^-) (Zhang et al., 2017). De Cocker et al. (2018) successfully enriched the anammox during the step-wise decreasing temperatures (from 30 to 20, 15, 12.5 and 10°C) in SBR for one year. AnAOB enrichment (increasing hzsA and 16S rDNA gene concentrations) and adaptation (shift from Ca. Brocadia to Ca. Kuenenia in SBR loweringT) contributed to the high specific ammonium removal rates (82.2 and 91.8 mg NH_4 -N gVSS⁻¹ d⁻¹ at 12.5 and 10 °C respectively) at the end.

The genomic studies expand our knowledge of AnAOB physiology. A comparison among three specific species belonged within different genera: 'Ca. Kuenenia stuttgartiensis', 'Ca. Scalindua profunda' and 'Ca. Jettenia caeni' was made (Figure 1.6). Results showed that nearly one third

of genes located in the genomes, including *nxrAB*, *hzsBGA*, *hds/hao* and *acsABCD*, were commonly shared. Interestingly, both the *nirS* and *nirK* orthologues were missing in the '*Ca. Brocadia fulgida*' and '*Ca. Brocadia sinica*' genomes. In addition, the genetic studies were able to predict the observation of the involvement of anammox bacteria *nirK* in NO_2^- reduction (Hira et al., 2012).

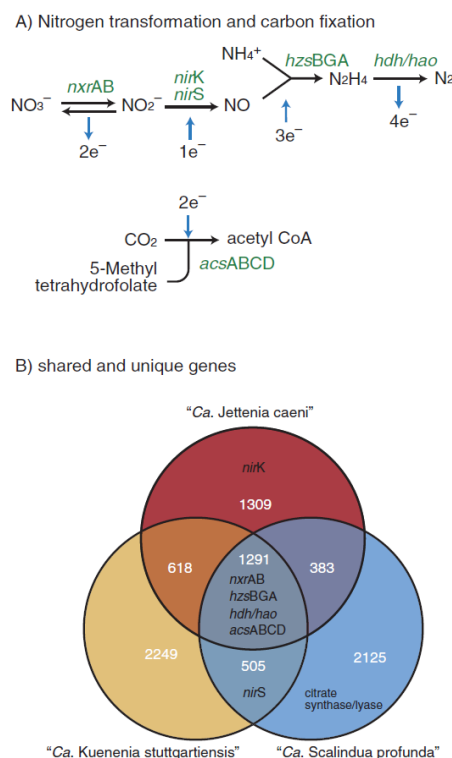


Figure 1.6: Venn diagram showing shared genes among three anammox bacterial genomes. (A. Nitrogen transformation and carbon fixation processes involved in anammox bacterial cells. *nxr*: nitrate/nitrite oxidoreductase, *nirK*: copper containing nitrite reductase, *nirS*: cytochrome cd1-type nitrite reductase, *hzs*: hydrazine synthase, *hds/hao*: hydrazine dehydrogenase/hydroxylamine dehydrogenase family protein, and *acs*: acetyl-CoA synthase/CO dehydrogenase. Electron flow is shown with blue arrows; B. Shared and unique genes among the '*Ca. Jettenia caeni*', '*Ca. Kuenenia stuttgartiensis*' and '*Ca. Scalindua profunda*' genomes were investigated using the BLAST search program) (Hira et al., 2012).

Oxygen inhibition

Oxygen inhibition has been described a lot for the marine and freshwater systems but this inhibition is reversible. The variability in the reported DO inhibitory levels can be due to the genera differences, potential microbial adaptation, testing procedure. The recovery and reversibility of activity following aerobic conditions was first investigated by Seuntjens et al. (2018). In this study, recurrent DO (0.5-8 mg O_2/L) was exposed into an anammox reactor (biomass diameter > 0.2 mm). Results showed that the first high-DO exposition resulted in the complete inhibition ($\text{IC}_{100} \leq 0.02 \text{ mg } \text{O}_2/\text{L}$) of AnAOB but recovered gradually after 5-37 hours without the oxygen exposure in order to reach a steady-state activity dependent on the perceived inhibition.

Potential N_2O emissions from anammox-related processes

Direct N_2O emission from PNA has not been demonstrated until now. Recently authors also reported the possible existence of unknown N_2O pathway based on the isotopic measurements during combined PNA system. Harris et al. (2015) observed that the N_2O

isotopic site preference (SP) was up to 40‰, which could not be explained with the current known N₂O pathways. Ali et al. (2016) also found around 30% of the N₂O emission was produced in the anammox-dominated anoxic zone. This observation indicated that in the combined PNA process, the potential role of anammox still need to be clarified. It can shift the conventional N₂O production pathways, especially during the rapidly changing experimental conditions.

1.4 Contribution of abiotic N₂O pathways

N₂O can also be produced also through the abiotic reactions by coupling NH₂OH oxidation with the reduction of NO₂⁻ (Harper et al., 2015), free nitrous acid (HNO₂) (Soler-Jofra et al., 2016), or NO (Spott et al., 2011). These are termed N-nitrosation hybrid reactions, or simply hybrid reactions (Spott et al., 2011). In addition, metals such as copper can catalyze abiotic N₂O production from NH₂OH via the hybrid reaction (Harper et al., 2015). Under some conditions, the hybrid reaction can become the predominant pathway for N₂O production in a partial nitrifying reactor (Terada et al., 2017; Soler-Jofra et al., 2018). N₂O production via the hybrid reaction is enhanced in the presence of AOB (Liu et al., 2017; Terada et al., 2017).

Abiotic N₂O emissions were investigated based on different kinetic studies. Chemical NO₂⁻ reduction by ferrous iron (Fe(II)) can lead to the formation of NO and N₂O without biomass in a 2 L reactor (Kampschreur et al., 2011), the rate of which is greatly influenced by pH, maximizing at 6.6. (NO₂⁻ of 600 mg N L⁻¹). In a partial nitrification, the chemical reaction between NH₂OH and NO₂⁻ (400 mg N L⁻¹) under the DO between 0.8 and 4.3 mg O₂ L⁻¹ is also reported in the study from Harper Jr. et al. (2015), however showing that N₂O from abiotic reaction increased with the decreased NH₂OH concentration, which can be higher than the biological contribution. The abiotic N₂O emission at 0.16 mg N L⁻¹ h⁻¹ of NH₂OH (0.3 mg N L⁻¹) with HNO₂ (0.04 mg N L⁻¹) was also investigated by Soler-Jofra et al. (2016), accounting one third of the N₂O emission rate in the SHARON reactor (NO₂⁻ of 650 mg N L⁻¹). Terada et al. (2017) also highlighted the importance of the NH₂OH reaction with nitrite at high AUR and NO₂⁻ (400 mg N L⁻¹) in a PN reactor. In a planktonic axenic *N.europaea* (ATCC 19718), Soler-Jofra et al. (2018) found that most of the biological N₂O emission could be explained by the chemical transformation during the transient anoxia. Considering high FNA (5*10⁻³ mg N L⁻¹) due to the high NO₂⁻ of 230 mg N L⁻¹ in this study, high pH and low NO₂⁻ was recommended to avoid the possible abiotic N₂O transformation.

In view of these recent studies on chemical N₂O pathways, the tests first contained high level of NO₂⁻ (over 200 mg N L⁻¹), which is typically observed in the PN reactor, as the NO₂⁻ accumulation is required. However, in other wastewater treatment system, the participation of NO₂⁻ consumers, such as the NOB in the SND system and Anammox in the PNA system, allowed the higher level of NO₂⁻ is an indicator of imbalanced process performance or unfavorable experimentation. Therefore, the huge difference might weaken the role of chemical N₂O production pathways.

Table 1.1. The putative abiotic N₂O production pathways

Reference	Biomass	Pathway note	Experimental conditions
(Soler-Jofra et al., 2018)	<i>Nitrosomonas europaea</i> (ATCC 19718)	Abiotic and biotic (by ammonia oxidizers) were very comparable. N ₂ O emission rates	a possible involvement of the cytochrome P460 from the HAO enzyme
(Terada et al., 2017)	Enriched AOB culture	Hybrid (biotic and abiotic N-nitrosation) N ₂ O production	NH ₂ OH and nitrite
(Liu et al., 2017)	AOB, AOA and Commamox	NH ₂ OH abiotic conversion rates, were 0.12%, 0.08% and 0.14% for AOB, AOA and <i>Ca. Nitrospira inopinata</i>	extracellular NH ₂ OH with nitrite
(Frame et al., 2017)	AOB	NH ₂ OH-dependent hybrid-N ₂ O production	Acidified conditions
(Soler-Jofra et al., 2016)	Partial nitrification reactor	0.06 mg N-NH ₂ OH/L, N ₂ O emission are produced from biotic or abiotic routes	NH ₂ OH and nitrite
(Kampschreur et al., 2011)	Without biomass	Chemical iron oxidation with nitrite	Nitrite and Fe (II) Nitrite and Fe (III)

N₂O model: integrating the abiotic reaction into the biological process, from suspended system to biofilm system

More recently, a consilient N₂O model was proposed (NDHA) that predicts three biological pathways and abiotic processes (Domingo-Félez and Smets, 2016). Potentially, the NDHA model describes N₂O production under a wide range of operational conditions.

The modified version of this model by Domingo-Félez et al. (2017) designed a delicate N₂O calibration procedure via extant respirometry. The NDHA model response was validated and described AOB-driven N₂O production at varying DO and HNO₂ concentrations. For the first time, the uncertainty of the calibrated parameters was propagated to the model outputs in a simulation case study, and compared to the uncertainty from a reference case. However, the model calibration experiences are not that much.

Actually, the current N₂O pathways cannot fundamentally differentiate the biological and chemical system sharing the same process biochemistry. During the chemical control experiments with biomass, the electron donor can still exist in other forms even after losing the biomass activity.

Another point is that all the published N₂O pathway models have not been performed to describe the N₂O emission from the biofilm-based PNA systems. Only very recently Wan et al. (2019) combined 3 pathways for modelling PNA process.

1.5 Isotopic fractionation technique for tracking N₂O pathways

1.5.1 Principles

It has been several decades since isotopic technology has been applied to identify N₂O sources from biosystems (Ritchie and Nicholas, 1972; Poth and Focht, 1985). Applications were concentrated on the biomass from the soil system (Wrage et al., 2005). During recent years, attentions have been also paid in the wastewater system including a wide biomass type (enzyme, pure culture, mixed culture and wastewater treatment) and multiple scale.

The development of the process-based pathway knowledge might help understand the effects of the operating conditions on N₂O production, ensure the transferability of outcomes from one system to another and support the N₂O mitigation strategy (Duan et al., 2017). Currently, three isotopic analysis methods were used based on conventional natural stable isotope, SP and ¹⁵N tracer respectively.

Differences between isotopes of the same element are so subtle that can be regarded as identical in general reactions. However, during kinetic reactions, when bonds are forged or broken, the slight difference in physical and chemical properties can lead to fractionation, altering the composition of natural isotopes in products. This variation in composition serves as the basis to monitor and trace the nitrogen conversion pathways during N₂O production (Duan et al., 2017).

Microbial nitrogen conversions leading to N₂O production can result in unique isotopic fractionation, thus making it possible to distinguish the sources of the emitted N₂O. In most cases, the enzymatic reactions preferentially convert lighter isotopes with smaller number of the neutrons, resulting in products isotopically lighter than in reactants, which is called kinetic isotope effects (Duan et al., 2017).

Quantitative analysis with SP and ¹⁵N tracer method

SP analysis enables the quantification of the relative contributions of N₂O production pathways and bulk $\delta^{15}\text{N}$ fractionations thus quantitatively reflecting the origin of N₂O. Unlike the inhibition approach or labelled isotope analysis which introduces inhibitors or artificially enriched ¹⁵N/¹⁸O, no foreign influences are introduced as SP analysis is based on natural ¹⁵N abundance, and SP analysis provides direct evidence investigating N₂O production pathways.

The bulk ¹⁵N isotopic composition refers to the average $\delta^{15}\text{N}$ at both positions (α and β).

Equation 1.19

$$\delta^{15}\text{N}^{bulk} = \frac{\delta^{15}\text{N}^{\alpha} + \delta^{15}\text{N}^{\beta}}{2}$$

The N₂O “site preference” (SP) refers to the difference in ¹⁵N isotopic composition of the central (α) position N compared to the terminal (β) position N. SP of N₂O, unlike $\delta^{15}\text{N}^{bulk}$, is independent of the substrate isotopic composition, and it is therefore a robust tool to differentiate between N₂O production pathways. The reliability of the SP signature value depends on the reliability of the determination method as well as its application range. Each N₂O pathway is characterized by one specific SP value.

Equation 1.20

$$SP = \delta^{15}\text{N}^{\alpha} - \delta^{15}\text{N}^{\beta}$$

The substrate separation is the common method for obtaining the SP value for single N₂O pathway, through providing substrates stimulating targeted pathway while eliminating its counterparts. Studies using the enzyme (Toyoda et al., 2005) can obtain accurate SP signature values especially for the enzyme-induced pathways than using pure- or mixed cultures, however whether these values can be applicable in the complex environmental system is still a problem. When the enriched pure culture are used (Peng et al., 2014), the reaction is closer to the practical case/situation considering that bacteria species share the similar SP values for the same pathway. The uncertainties of this method depend on the interference extent by the two targeted pathways due to the coexistence of two intermediates NH₂OH and nitrite, being not fully separated for two pathways.

According to the observed SP (Equation 1.20) and isotopomer mixing model (Equation 1.21), quantitative apportioning of ND and NN pathway have been achieved using full-scale activate sludge (Wunderlin et al., 2013) and lab-scale enriched nitrifying sludge (Peng et al., 2014).

Equation 1.21

$$F_{ND} = (1 - F_{NN}) = (SP_{tot} - SP_{NN}) / (SP_{ND} - SP_{NN})$$

Lab-scale experiments were conducted by adding different substrates (NO₂⁻, NH₂OH, NH₄⁺ and NO₃⁻) into the activated sludge taken from the nitrification reactor from the plant (Wunderlin et al., 2013). The NO₂⁻ addition and NH₂OH addition batch experiments respectively allowed to give an average SP value for ND (SP_{ND}: -2‰) and NN (SP_{NN}: 28.5‰), which was used as standard SP values for ND and NN pathway respectively. Consequently, according to Equation 1.21, increased SP value can be due to the stimulated NN pathway with the corresponding weakened ND pathway, if NN and ND pathway could be determined as two main N₂O production mechanisms:

1. During all NO₂⁻ oxidation experiments, ND pathway was considered as the sole N₂O pathway and the SP value decreased from the starting to the end.
2. During NH₂OH addition experiments, take 10 mg N-NH₂OH L⁻¹, DO of 1.1 mg/L as an example, the contribution of NN pathway decreased from 100% to 19% with decreased SP from 30.7‰ to 3.7‰. Simultaneous decrease of SP and NN pathway contribution is also observed in all the other NH₂OH addition experiments but to a lesser degree.
3. During both continuous and one-time NH₄⁺ addition experiments, at the beginning both NN and ND (over 75%) contributed to N₂O production. SP value decreased by 3‰ to 5‰ in all experiments, in company with the increased ND pathway contribution who dominated the overall N₂O production in the vast majority of batch experiments in the end.

The same quantification method was used by Peng et al. (2014) combining both SP and bulk ¹⁵N/¹⁴N ratios (d¹⁵N^{bulk}N₂O), in order to identify the contribution of NN and ND pathway to the overall N₂O production in an enriched nitrifying sludge. Assuming 28.5‰ and -2‰ were the standard SP value from N₂O produced from NN and ND, the influence of DO concentration on the pathway contribution was also identified in this study.

When DO increased from 0.2 to 3.0 mg O₂ L⁻¹, N₂O production due to the joint effect of both pathways was first confirmed by the obtained SP values (-0.5‰ and 6.4‰). Then, it was calculated that increased SP value upon increasing DO also demonstrated the increased NN pathway contribution from 5% to 27% with the corresponding decreased ND pathway contribution from 95% to 73%, which could be well predicted with the 2-pathway model.

However, two major differences existed when comparing the results between two studies (Wunderlin et al., 2013; Peng et al., 2014). One difference is the complete dominance of ND pathway in the first study unlike the second study; another difference is that NN pathway repression is found at either higher or lower DO concentration in the former study while only under lower DO concentration in the latter study. One possible explanation for the latter case is that NOB biomass was used to avoid the nitrite accumulation but also consumed oxygen, competing with AOB under the low DO condition, since ND pathway is facilitated under limiting-DO concentration compared with NN pathway.

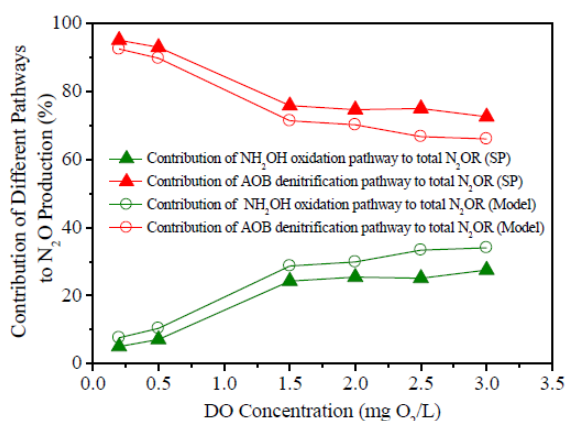


Figure 1.7: SP value and modelling enabling the N₂O pathway regulation in the partial nitrification process (Peng et al., 2014).

Measurement of $\delta^{15}\text{N}$ -N₂O value in emitted N₂O can qualitatively estimate the contribution from nitrification and denitrification in WWTS (Townsend-Small et al., 2011; Toyoda et al., 2011a). The difference in $\delta^{15}\text{N}$ -N₂O values between nitrification and denitrification is large enough to qualitatively estimate the contribution of nitrification and denitrification processes of emitted N₂O. However, $\delta^{15}\text{N}$ -N₂O is dependent on the substrate $\delta^{15}\text{N}$ -NH₄⁺ values and fractionations. The quantification of the contribution of nitrification and denitrification with $\delta^{15}\text{N}$ and $\delta^{18}\text{O}$ can only be possible if a set of universal enrichment factors are available for the N₂O production pathways. However non-enzymatic processes irrelevant to nitrogen conversion pathways might influence the overall isotope fractionation, reducing the accuracy and thus making this method can only in a qualitative analysis level.

Typical SP values for known N₂O pathways

In WWTS working with mixed culture there is no universally recognized and characterized SP value for each N₂O production pathway (Sutka et al., 2006; Toyoda et al., 2011b). Unlike heterotrophic bacteria with sole pathway, more studies concerning the pathway regulation are related with the AOB culture containing two pathways as NN and ND pathway.

In the investigated WWTS studies, the SP values for NN pathway varied from 28‰ to 33‰, while for the ND pathway from -14‰ to 0‰ (Toyoda et al., 2011a; Rathnayake et al., 2013; Wunderlin et al., 2013).

During the PNA processes, both N₂O production and consumption could happen. NH₂OH oxidation (NH₂OH→NO→N₂O) by AOB ranged from 30‰ to 36‰, while nitrifier denitrification (NO₂⁻→NO→N₂O) from -10‰~0‰; SP values of N₂O production from HET (NO₂⁻ to N₂O) ranged from -5‰~0‰ and consumption by HET (N₂O→N₂) from -16.4‰~-2.9‰. In addition, various chemical processes also lead the SP from 29.5‰~35‰ (Harris et al., 2015).

1.5.2 Experience on PNA process with isotopes analysis

For the first time, Harris et al. (2015) reported online measurements of N_2O off-gas isotopic composition from a continuously fed full-scale PNA reactor. Targeted conditions like increased Q_{air} , addition of NO_2^- under anoxic condition and the addition of NH_2OH were also tested to further follow the SP signature variation upon the changes. In this study, results were obtained under high and low NH_4^+ concentration.

First, increased SP (-1.0‰) and reduced N₂O (instant rate and emission factor) due to simultaneous increase of NH₄⁺ (20-50 mg L⁻¹) and DO (0.2-1.5 mg L⁻¹) cannot be explained. Then, the high SP value in both normal and targeted experiments cannot be explained with the current understanding of N₂O production and consumption, considering the accuracy. Next, the decreased SP (δ¹⁸O) and increased rNH₄⁺ due to the increased Q_{air} indicated the ND pathway leading to the N₂O spike with increased DO from lower than 0.05 mg O₂ L⁻¹ normally to over 0.2 mg O₂ L⁻¹. Finally, addition of NO₂⁻ led to the highest SP to 45.9‰ while addition of NH₂OH also lead to the increased SP up to 41.3‰. Based on the above observations an unknown N₂O is the most probable explanation pathway with the characteristic: 1). Low isotopic discrimination for d¹⁵N^{bulk}; 2) producing N₂O pathway anoxically enhanced by NO₂⁻ addition; 3). SP higher than all current known N₂O pathways.

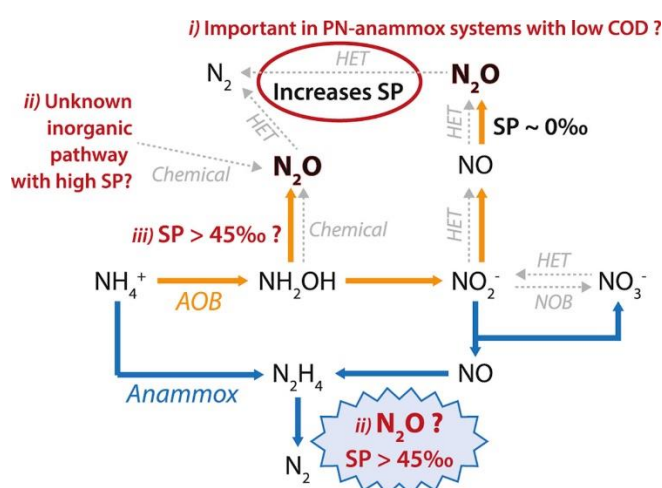


Figure 1.8: Online SP off-gas analysis enabling new N₂O pathway identification (Harris et al., 2015).

The second single stage PNA case study with isotopomers was conducted by Ali et al. (2016) in a 2 L SBR with 6 h cycle length. The N₂O isotopomer analysis was based on samples taken from three different SBR cycles. In order to quantify the different N₂O pathway contributions with the constant SP values (15‰-9‰), the effect of N₂O reduction by HET denitrification was first precluded by combined SP and ¹⁸O&¹⁵N^{bulk} analysis, and then the relative contribution from NN pathway and NO₂⁻ reduction was based on the estimation according to the chosen SP values for pure N₂O production via NN pathway of 33±4‰ and via NO₂⁻ reduction of -1±5.5‰ (including both ND and heterotrophic denitrification). N₂O isotopomer analysis revealed that NN pathway and NO₂⁻ reduction pathways contributed roughly equal in N₂O production. However, the results did not differentiate the N₂O contribution from nitrifier denitrification or ND, nor preclude the influence from N₂O reduction and/or anammox N₂O production. Furthermore, high abundance of NOB in this system might complicate the N₂O production by competing with anammox for NO₂⁻ and with AOB for oxygen.

N₂O microsensor combined with FISH analysis revealed that the major (70%) N₂O production area was the shallow surface area of a granule (0-0.5 mm) where nitrifiers mainly inhabited and DO rapidly decreased down to below 0.1 mg L⁻¹ at ca.0.1 mm from the surface of the granule. The rest of N₂O (around 30%) was produced in the anammox bacteria-dominated anoxic zone.

Different SP values and pathway contributions for N₂O in two single-stage PNA studies first revealed the efficiency of the SP technology in predicting the known and unknown pathways, but also indicated the complicated N₂O production mechanisms, which required the further investigation.

1.5.3. Convergence of SP and modelling for analyzing the N₂O pathway regulation

Recent studies also combined the SP analysis with other indirect methods such as modelling and enzyme mRNA transcription analysis.

Only with the SP, the relative contributions from more than two N₂O production pathways cannot be quantified. However, with the help of the mRNA analysis, the difference of *NorB* in AOB and heterotrophic denitrifiers allowed to differentiate the NO reduction activities of each group. Therefore, three pathways from the WWTS can be assessed (Ishii et al., 2014). However, the weakness of this technology is that the gene transcription might not reflect the real enzyme activity level, which can be further improved by selecting the perfect primer.

Ishii et al. (2014) use the combination of ¹⁵N stable isotope analysis, denitrification functional gene transcriptome analysis and microscale N₂O concentration measurements to identify the main N₂O producers in a PN aerobic granule reactor fed with ammonium and acetate. Results suggested that heterotrophic denitrification was the main contributor. Both NN and ND occurred, but their contribution to N₂O emission was relatively small (20–30%) compared with heterotrophic denitrification.

The simultaneous ¹⁵N and ¹⁸O labelling can improve the reliability of N₂O production pathways tracking. In a study conducted by Ma et al. (2017) the biofilm from a full-scale PNA reactor, was investigated the instantaneous effect of DO (from 0.2 to 45 mg O₂ L⁻¹), NO₂⁻ (from 0.7 to 11 mg N L⁻¹) and NH₄⁺ (from 15 to 480 mg N L⁻¹) on the N₂O pathways through independent ¹⁵N labelling of NH₄⁺, NO₂⁻, NO₃⁻ and ¹⁸O (labelling O₂). For the first time, ¹⁸O labelled O₂ was used to prove the process of NH₂OH oxidation taking advantage of oxygen exchange between NO₂⁻ and H₂O. Presence of heterotrophic denitrification is not distinguishable from ND through isotope labeling. However based on the very low net N₂O production rate observed at 0.2 mg O₂ L⁻¹ with only NO₂⁻ addition without NH₄⁺, the heterotrophic denitrification was a very minor source of N₂O production. Low oxygen concentration stimulates the ND pathway however, the stimulation of N₂O production from NN pathway was unexpected. NN pathway was also stimulated by the increased NH₄⁺ concentration.

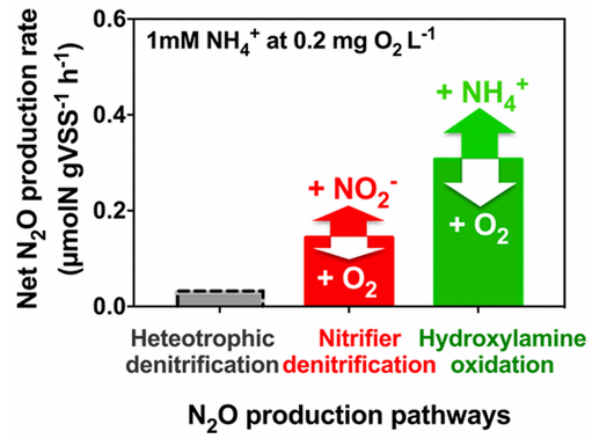


Figure 1.9: Influence of oxygen and ammonium load on three N_2O pathways from the PNA process (Ma et al., 2017).

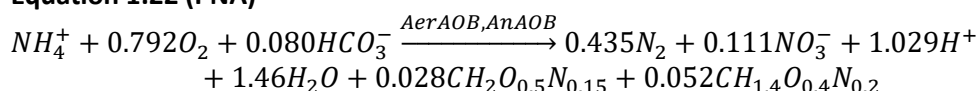
2. PNA control and operation

From the work of Vlaeminck et al. (2012) on PNA and microbial resource management three important challenges were pointed out: 1). maximizing the nitrogen removal efficiency; 2). minimizing the NO and N₂O emission and 3). obtaining through OLAND a plant-wide net energy gain from sewage treatment. This means that multi-objectives optimization and control strategies should be developed for reaching that objective. Aeration control is naturally in the center of such energy-GHG nexus preoccupation.

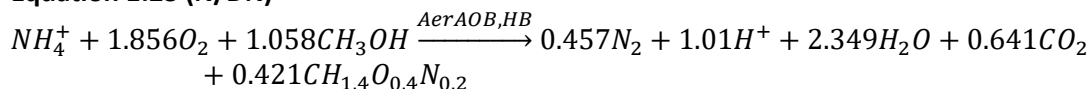
2.1 Global stoichiometry

The **PNA** stoichiometry is based on the equilibrated combination of the two consecutive processes: aerobic ammonia oxidation and the following anaerobic ammonium oxidation with the produced nitrite forming the harmless dinitrogen gas (Sliekers et al., 2002). Not only less oxygen and organic matter is required, but also less sludge is produced (Equation 1.22) for PNA than the conventional N/DN process (Equation 1.23). Obviously those stoichiometries do not take into account the possible NO or N₂O loss.

Equation 1.22 (PNA)



Equation 1.23 (N/DN)



2.2 Current operational and control strategies for PNA

A microbiology oriented control

The major challenge in PNA control is to repress durably the NOB activity, and to allow anammox to compete for space with sufficient specific retention time. This becomes tricky especially in non-optimal (but real) situation, in extension for mainstream treatment at low temperature, low concentration, or in presence of organic matter.

Five major groups are possibly involved in the real PNA system due to the mutual interactions among different microbial communities: AOB, NOB and AnAOB as autotroph bacteria while HB including aerobic and anaerobic bacteria also develop on both external and endogenous substrate (Table 2). Totally four main substrates are involved. Oxygen competitors are AOB, NOB and HB, while nitrite competitors are NOB, anammox and HB. The nitrite can only be produced by AOB and anoxic HB, while nitrate can only be produced by NOB and anammox. Besides, the substrate competition also related with the space competition within the granules or other aggregates.

The diverse reported parameters affecting the process overall performance included the inoculum (Agrawal et al., 2017), aggregate architecture (Wells et al., 2017), reactor configuration (Gilbert et al., 2015), feeding mode (Harris et al., 2015; Ali et al., 2016), aeration

pattern (Domingo-Félez et al., 2014; Castro-Barros et al., 2015; Corbalá-Robles et al., 2016), residual NH_4^+ concentration (Corbalá-Robles et al., 2016; Poot et al., 2016), dissolved oxygen (DO) concentration (Morales et al., 2016; Akaboci et al., 2018), Temperature (Lotti et al., 2014a).

Table 1.2: Potential consumer and producer for the main substrate in the PNA system (Adapted after Cao et al. 2017).

	Consumer (Neglecting biomass growth)	Producer
Ammonium (NH_4^+)	AOB, Anammox	-
Oxygen (DO)	AOB, NOB, Aerobic HB	-
Nitrite (NO_2^-)	NOB, Anammox, Aerobic HB, Anoxic HB	AOB, Anoxic HB
Nitrate (NO_3^-)	Anoxic HB, Aerobic HB	NOB, Anammox

Continuous or discontinuous operation?

As an example, in a floc-based PNA reactor, Sliekers et al. (2002) applied continuous feeding (over 95% of one SBR cycle) and continuous aeration with the constant air flow rate at 7.9 mL min^{-1} during one SBR cycle enabling the CANON with the NRR of $0.08 \text{ kg NH}_4^+ \text{ m}^{-3} \text{ d}^{-1}$ after 10 weeks. During the stable limiting-oxygen period, the undetectable DO level allowed the balanced activity between AOB and anammox ($\text{NO}_2^- \leq 0.6 \text{ mg N L}^{-1}$) in the flocs and the successful repression of NOB growth and heterotrophic activity, resulting that 15% and 85% of input ammonium was finally converted to NO_3^- and N_2 . However it is noticeable that N_2O production was not deeply investigated and only considered as negligible (less than 0.1%). While for an upflow membrane aerated biofilm reactor (UMABR), Li et al. (2016) reported that the process was operated under continuous feeding with synthetic wastewater (containing organic matter) at a NLR from 0.05 to $0.1 \text{ kg N m}^{-3} \text{ d}^{-1}$ and continuous aeration with pure oxygen with an online control system. The apparent DO at $0.6 \text{ mg O}_2 \text{ L}^{-1}$ did not lead to NO_2^- accumulation and 8% of the incoming NH_4^+ was finally produced as NO_3^- , indicating the high denitrification activity. Both sequencing and FISH analysis showed that the granular biomass harbored more balanced biomass composition for anammox and AOB (less NOB), while biofilm contained more surface-grown AOB and NOB content (5.4%) but much less anammox bacteria (4.8%).

In the SBR mode, the feeding action is commonly applied in a discontinuous way from a global view, called as semi-continuous, even it is fed continuously during single cycle. For one stage PNA system, a better reactor performance with less NOB activity is profitable at high NH_3 concentration with constant pH (7.8). Effect of the ammonium limitation on the CANON process was specifically investigated from saturation (12mM) to limitation level (5mM) in a continuously-fed SBR, with the length of feeding accounting for over 95% of an entire SBR cycle (Third et al., 2001). Switching from non-limiting NH_4^+ supply to limiting- NH_4^+ , directly resulted in the deteriorated nitrogen removal (0.08 to $0.04 \text{ kg m}^{-3} \text{ d}^{-1}$), reduced nitrogen removal efficiency (92% to 57%) and decreased biomass concentration from 1.0 to 0.75 g/L . As the growth of *Nitrospira sp.* was observed under ammonium limitation, a high NH_3 concentration is recommended for operating the one-stage PNA system.

On the other hand, alternated aeration in the SBR system were also conducted in different studies (Castro-Barros et al., 2015; Blum et al., 2018). In a full-scale SBR (Olburgen), the aeration flow rate alternated between 4041 and $1088 \text{ m}^3/\text{h}$ through a mixture of fresh air and recirculated gases, depending on the working capacity. The variation of NH_4^+ and NO_2^- is repeatable upon the duplicate transition between intense and low aerated periods. During

intense aeration after the decreased aeration periods, decreased NH_4^+ concentration 25 to 17 mg/L accompanied with increased NO_2^- concentration from 4.7 to 6.6 mg/L, reflecting more anammox inhibition, but at the same time indicating the less NOB activity. The simultaneous decreased NO_2^- and increased NH_4^+ concentration is observed after the switch to the low aerated period.

A more recent one-stage PNA study was conducted by Blum et al. (2018) applying the intermittent pattern while maintaining the constant stripping with same aeration flow rate at 2 L min^{-1} , using air and N_2 under the aeration and anoxic phase respectively. Meanwhile the balanced PNA system and efficient NOB repression was achieved under this strategy (Blum et al., 2018). Besides, the decreasing pH also substantially augmented the cycle-averaged N_2O emission from 1.1 % (standard pH from 8 to 7) to 2.7% (constant pH at 7), similar to the dependence of specific N_2O and NH_4^+ rates on both pH and NH_4^+ in an enriched AOB system (Law et al., 2012).

Therefore, the alternated aeration is profitable for NOB washout because the NOB recovered less easily than AOB during frequent anoxic period (Third et al., 2001; Ma et al., 2015).

The wide applications of the PNA process in the wastewater nitrogen removal systems brought us fruitful experiences on the operating strategies which has been summarized by Agrawal et al. (2018). The basic principle of the PNA strategy is to create the most favorable living environment for the enrichment of AerAOB and AnAOB while out-selecting their counterparts: NOB and heterotrophs, through two perspectives: ON/OFF and IN/OUT control.

On one hand from the perspective of substrates, ON/OFF control, oxygen and nitrogen can be supplied and maintained in different patterns. First, maintaining a low DO setpoint can help to suppress the NOB activity (see previous paragraphs), and at the same time promote the activity of AnAOB and AerAOB. However this optimal DO is not considered as unique and researchers also use higher DO setpoint to maximize the activity of AerAOB over NOB (Wett et al., 2013; Malovanyy et al., 2015).

Secondly, applying different reactor configuration (Agrawal et al., 2017), feeding mode and aeration pattern (Ma et al., 2015; Blum et al., 2018) can cause various temporal and spatial difference in the substrate levels and consumption rates. This difference can further produce particular (e.g. layer) distribution of each microbial group and various behaviors face to oxygen limitations or excess. For NOB the nitrite availability can be minimized for facilitating the repression considering that anammox have a very high affinity for nitrite. Additionally oxygen inhibition for AnAOB can be avoided in the biofilm when NH_4^+ is not absent maintaining a high specific consumption at the surface of the biofilm. Besides, FA or FNA can also directly and rapidly provide the inhibitory conditions to inhibit NOB (Q. Wang et al., 2017).

On the other hand from the perspective of sludge age, or "IN/OUT control", NOB and HB can be washed out by controlling the SRT in the condition where AerAOB and AnAOB can both be retained. Expecting AerAOB to prefer smaller flocs and AnAOB tending to grow in thick biofilm, the aggregates niches and growth condition could be fulfilled through a hybrid reactor or separation with hydrocyclones, sieves or by the control of hydrodynamic shear effect.

In summary, it is more advisable to consider both approaches for the NOB out-selection. The process can be operated via one- or two-stage, and floc-based, biofilm or granular system. Although the two-stage system is considered as easy to maintain (aerobic or anaerobic), lower GHG emissions and lower building costs have attracted people's attention to the single-stage

system, especially for full-scale system (Cao et al., 2017).

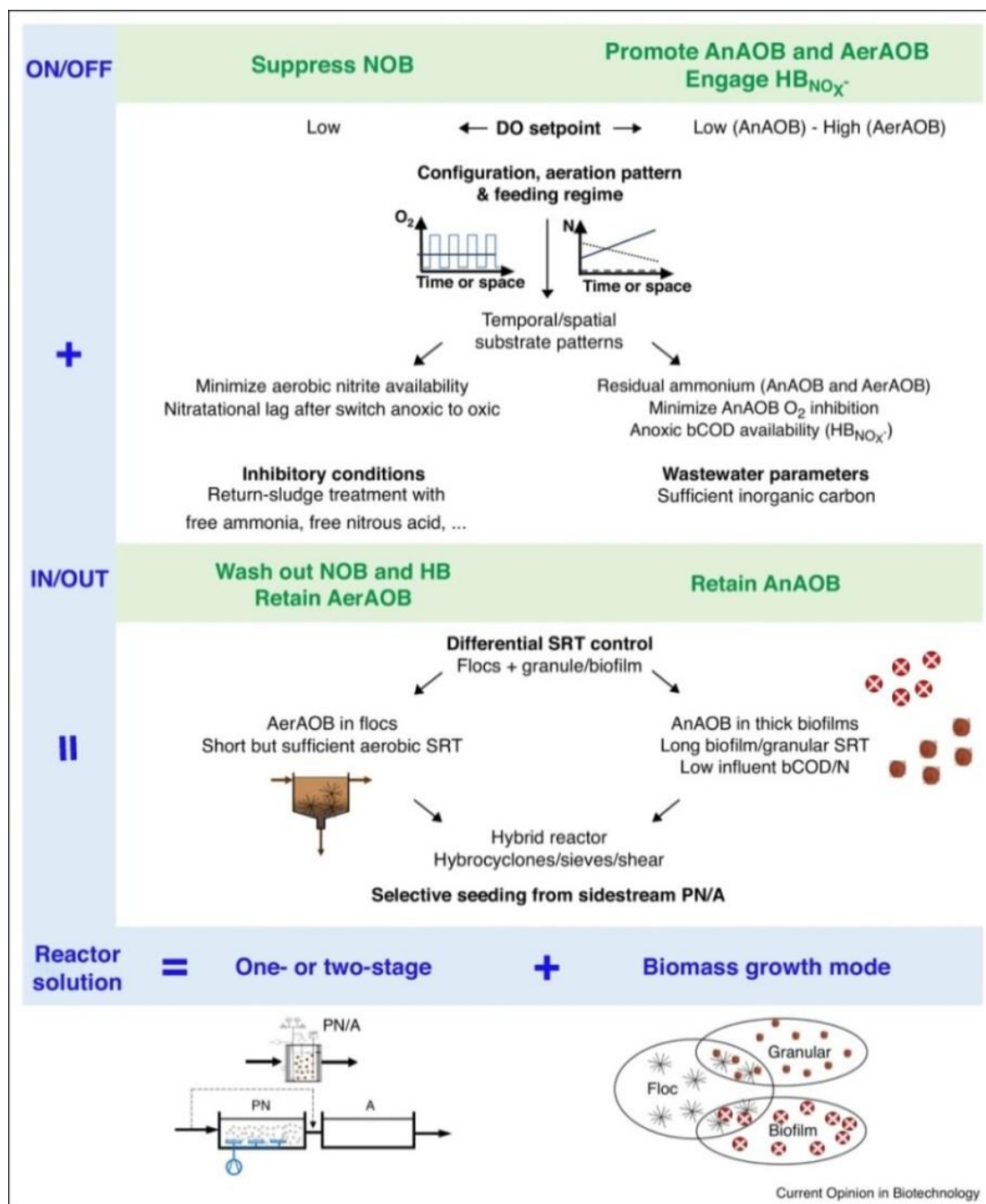


Figure 1.10: Strategies for the design and operation of a one-stage or two-stage partial nitrification/anammox (PNA) reactor (Agrawal et al., 2018).

2.3 Considering N_2O emission in the PNA process control?

As an important concern for an environmental evaluation index, N_2O emissions from the PNA process have been investigated during the last decade to reach optimal sustainability. More

applications into the single stage than two stage system can be found due to the prevalence of full-scale applications (Vlaeminck et al., 2012). Globally, N₂O emissions from two stage systems (Joss et al., 2009; Weissenbacher et al., 2010) are observed to be slightly higher than that obtained from single stage process (Kampschreur et al., 2008; Desloover et al., 2011) when the reactor was operated for a long period in full-scale application.

Table 3 collected the main results and operational conditions from existing studies on N₂O emissions in single stage PNA process.

The most reported influencing parameters includes biomass activity (AUR), aeration supply (DO, airflow rate, and intermittent vs continuous aeration), and nitrite concentration. According to previous studies and our actual knowledge on N₂O emissions, low DO and increased nitrite mainly increases the risk of N₂O emission in the nitrification reaction. But the accurate prediction of such combined effect of DO and nitrite was still controversial at the starting point of this PhD thesis. In addition, it is not that evident to say if our knowledge on nitrification is directly usable for predicting and understanding N₂O emission from PNA process in which several communities interfered symbiotically.

AUR (and Nitrogen load)

In the combined PNA process NH₄⁺ is simultaneously uptaken by AerAOB and by AnAOB.

In pure nitrification system a correlation exists between the biomass activity (specific AUR) and the N₂O production. Law et al. (2012) reported that N₂O production rate (N₂OR) is exponential to ammonium uptake rate (AUR) of an enriched AOB culture in a PN system fed with synthetic anaerobic digester liquor. This kind of exponential relationship is also observed in another enriched AOB culture by Ribera-Guardia and Pijuan. (2017). For the combined PNA system when applying intermittent aeration with varying intensity and frequency over six months, the correlation between N₂O production and extant ammonium oxidation in each cycle considering both aeration and non-aerated period is also reported by Domingo-Félez et al. (2014) in two SBRs. Besides, in this study, a more clear relationship is observed only considering the N₂O emission from the aeration phase.

Blum et al. (2018) found that aerobic N₂O production positively correlated with AUR when the intermittent aeration was applied to the combined PNA SBR, in contrast, no clear trend of N₂O production was observed during the non-aerated phases.

Therefore, observation in previous studies indicated the role of the biomass activity on the N₂O production rate. But the AUR in PNA system is generally controlled by oxygen limitation which means that it is almost impossible to differentiate the effect of increasing AUR and the effect of concomitant oxygen limitation (increasing with AUR).

Effect of the Air flow rate?

Air flow rate (Q_{air}) is the parameter generally used to control the oxygen transfer for adapting the biological rates in accordance with the nitrogen load and suitable performances (Domingo-Félez et al., 2014). Meanwhile, Q_{air} is also an important parameter affecting the N₂O emissions in the combined PNA process. However, different observations have been reported in the literature. M. J. Kampschreur et al. (2009) reported the short-term response of N₂O and NO

emissions upon the increased Q_{air} from 2000 to 3000 m³/h (40 to 46h, 67 to 68h) in a full-scale granular PNA process. The first two-step increase did not result in significant increase of N₂O emission (middle recovery) while the second increase resulted in nearly one order of magnitude higher N₂O emission rate. Also in the full-scale PNA granular system, Castro-Barros et al. (2015) found that increased Q_{air} from 1088 to 4041 m³/h resulted in increased N₂O formation as well as emission rate. In contrast, Domingo-Félez et al. (2014) found that N₂O emission ratio did not change significantly with varying Q_{air} (between 0.42 and 1.43 L/min) under the same oxygen loading rate in a lab-scale granular sludge system. In specific short term experiments, Harris et al. (2015) manually increased the Q_{air} from 20-750 L/h to 1500-3000 L/h under NH₄ concentration of 30 and 50 mg N/L respectively. The DO concentration increased (from 0.00064~0.054 mg/L to higher than 0.2 mg/L) corresponding to the increased Q_{air} . The instantaneous N₂O emission factor (N₂O/NH₄⁺) increased firstly and then decreased gradually under both low and high NH₄⁺ conditions, indicating a possible optimal DO around 0.02 mg/L.

But the recent simulation study from Wan et al. (2019) showed that the influence of parameters related to oxygen effect (aeration, DO) are non-monotonous, and severely interdependent with other parameters (granules size, presence of COD, temperature) as well as the nitrite accumulation.

Moreover the physical effect of flow rate almost instantaneous (by modifying the N₂O transfer coefficient or stripping rate) should be differentiated from effect of oxygen level on a short and long term on the microbial consortia activities and N₂O production. This last aspect is poorly considered in the literature.

Effect of NO₂⁻ accumulation?

Nitrite is known to stimulate the N₂O emission during both nitrification and denitrification process. Ma et al. (2017) showed the stimulating effect of nitrite on N₂O production under DO of 0.2 mgO₂/L using the biofilm from a PNA-based system. In the enriched AOB culture, Law et al. (2013) demonstrated the confounding effect of nitrite on the N₂O production that under low nitrite level between 10-50 mgN/L, N₂O was inhibited while higher NO₂⁻ level from 50 to 500 mgN/L inhibited the N₂O production depending on the DO level. In all batch tests conducted at DO concentration of 0.55 mg O₂/L, N₂O production rate increased rapidly at the start of the experiment and maintained a pseudo-steady N₂O production rate between NO₂⁻ of 10–50 mg N/L. A reproducible inhibitory effect of NO₂⁻ on the N₂O production rate of AOB was observed between NO₂⁻ concentrations of 50–500 mg N/L. This trend was observed independent of the way that the NO₂⁻ was introduced: produced through NH₃ oxidation, and NO₂⁻ dosing.

In a continuously aerated system, changing the aeration level changes the nitrite which is stabilized in the system. For instance, M. J. Kampschreur et al. (2009) increased the flow rate from 2000 to 3000 m³ h⁻¹ lead to the NO₂⁻ accumulation from 0 to 23 mg N/L, which clearly resulted in increased N₂O concentrations from 50 ppm to 720 ppm in the off-gas as well as increased emission rate from lower than 100 g h⁻¹ to higher than 1500 g h⁻¹. Similar observation was also obtained in a PNA granular sludge reactor (Castro-Barros et al., 2015) with online auto-adjusted aeration system based on the effluent quality (NO₂⁻ and NO₃⁻). Comparing the nitrite level between the normal SBR behavior under high aeration (4041 m³ h⁻¹) with and low aeration (1088 m³ h⁻¹) periods, the N₂O emission rates (0.051- 0.056 kg N m⁻³ d⁻¹) due to the increased nitrite concentration from 4.7 to 6.6 g N L⁻¹ under the high aeration is two times

higher than that obtained during the low aeration ($0.020\text{--}0.021 \text{ kg N m}^{-3} \text{ d}^{-1}$) with decreased nitrite from 6.6 to 4.7 g N L^{-1} .

Besides, the transition from prolonged period without fresh air addition to enhanced aeration resulted in the highest N_2O emissions.






Effect of intermittent anoxic phases?


As aeration intermittency was used for controlling oxygen transfer and NOB repression in some studies, effect on N_2O emission should be considered. Basically such effect can be related to complex regulation of the AOB metabolism respective to short term oxygen absence, but also to the possible contribution of heterotroph in consuming the N_2O in anoxic period.

Recently in a biofilm PNA process, the contribution of N_2O emission from aerated and non-aerated phase was respectively quantified by following the N_2O dynamic and showed that the aerated phase contributed 80% to the overall N_2O emission while 20% was attributed to the non-aerated phase (Blum et al., 2018). Globally the possible role in N_2O consumption or production of heterotrophic denitrifiers in PNA process needs more investigation. The recent modelling article of Wan et al. (2019) showed that our actual knowledge based models predict a significant consumption by heterotrophic denitrification as soon as biodegradable COD is present.

Domingo-Félez et al. (2014) demonstrated that significant decreases in N_2O emissions were obtained when the frequency of aeration (f_{redox}) was increased from 6 to 25 while maintaining a constant air flow rate (from >6 to $1.7\% \Delta\text{N}_2\text{O}/\Delta\text{TN}$) and oxygen loading rate ($0.81 \text{ g O}_2/\text{L/d}$). However, no significant effect on the emissions was noted when the duration of aeration (R_{on}) was increased from 53% to 93% while decreasing air flow rate ($10.9 \pm 3.2\% \Delta\text{N}_2\text{O}/\Delta\text{TN}$) under similar oxygen loading rate ($0.98\text{--}1.25 \text{ g O}_2/\text{L/d}$). Logically operating under conditions where anaerobic exceeds aerobic ammonium oxidation activity was proposed to minimize N_2O emissions from single-stage nitrification/anammox reactors. In intermittently aerated system, increasing the frequency of aeration cycling was considered as an efficient way of obtaining those conditions.

Table 1.3: Summary of recent studies on N₂O emissions from single-stage PNA process. (adapted after(Wan et al., 2019), N:nitrogen load; T:temperature)

No	Ref	Sampling position	Sludge	T (°C)	COD (g m ⁻³ d ⁻¹)	NH ₄ ⁺ load (g m ⁻³ d ⁻¹)	Feeding mode	Aeration pattern	Bulk DO (mg L ⁻¹)	N ₂ O-EF (% N-rem)	N ₂ O-EF (% N-load)	Main pathway	Influencing factor
1	(Blum et al., 2018)	4L SBR	Granule ~0.275mm	30	0	900	Batch feeding (2 min and 10 min)	Intermittent aeration Anoxic with and without N ₂	0.5-5(aerated) Decreasing to zero (Non-aerated)	1.1	0.979	ND or NN	N 
2	(X.-X. Wang et al., 2017)	15L SBBR	Biofilm (>0.75mm)	30		200	Batch feeding (5min)	Continuous aeration with O ₂ and N ₂	0.22- 0.28	5.6	5.6	ND and HD	
3	(Li et al., 2017)	30 L SBBR	Biofilm	30		70	Batch feeding (4min)	Intermittent Aeration (aerated:Non-aerated=1:1)	1.5-2.0 (aerated)		3.3 (1.6 under anaerobic condition)	HD	
4	(Ma et al., 2017)	250 mL serum bottle	Biofilm (20 g L ⁻¹)	30	0		Rapid injection	Continuous aeration with O ₂	0.2-45	0.6-12		NN	DO 
5	(Ali et al., 2016)	2L SBR	Granular (2.4±1.5 mm)	37	0	500-800	Batch feeding (5 min)	Continuous aeration (345min/cycle, air, 9.0 L h ⁻¹)	0.8-1.3	1.35	0.98	ND or NN	
6	(Yang et al., 2016)	200L MBBR	Biofilm (500 m ² /m ³)	25		850, 1250 and 1650	Continuous feeding	Intermittent aeration with air	1.5 aerated		0.51 1.29 1.12		N 
		700 m ³ MBBR	Biofilm	28		270	Continuous feeding	Intermittent aeration with air	3.0 aerated	0.62	0.51		
7	(Castro-Barros et al., 2015)	600m ³	Granular (1.5 mm)	37		1700	Continuous feeding	Continuous (air&cycled gas)	NG (Not given)	2.7	2		DO 
8	(Harris et al., 2015)	400L SBR	Biofilm	NG	-	24~360	'Intermittent feeding' including the semi-continuous addition of supernatant	Auto-regulation with air 250-400 L h ⁻¹	NG	0.1%~1.7%	NG	ND	DO 
						168~312		Auto-regulation with air 500-800 L h ⁻¹		0.6%~-1%			
9	(Staunton and Aitken, 2015)	20L SBR	Granular and activated sludge	35	61	52	Step feeding (10 min)	Continuous aeration with pure oxygen at 60 L h ⁻¹	<0.1	11.4	8.55		

10	(Domingo-Félez et al., 2014)	4L SBR	Granular	30	0	750	Step feeding (10 min)	Intermittent aeration with f_{redox} from 6 to 25	NG	1.6~6.4	1.3~6.0	ND or NN	
								Intermittent aeration with R_{on} from 53% to 93%		7.6~12.6	7.2~12.2		
11	(Clippeleir et al., 2013)	2.5 L Liq RBC	Biofilm (≤ 3 mm)	From 14 to 16	0-5436	From 585 To 2718	semi-continuous mode (pulse feeding)	Continuous aeration with air at 1800 L h^{-1}	From 2.9 to 4.0		From 3.0 to 6.4		T N 
12	(Hu et al., 2013)	5L SBR	Non-biofilm	12	0	28	Continuous feeding (11h)	Continuous aeration with oxygen	<0.05	2.4	2.28		
13	(Yang et al., 2013)	200 L MBBR	Biofilm	25	-	300-740	Continuous feeding	Both continuous aeration and intermittent aeration	1.5-2.5	0.51~1.29	0.4-2		
14	(Gilmore et al., 2012)	4 L MABR	Biofilm	30		Max of 140	Flow-through	Continuous aeration at 0.54 L h^{-1} with air or 80%argon/20% oxygen	From 0.2 to 0.8 in the surface		≤ 0.3		
15	(Weissenbacher et al., 2010)	500 m ³ SBR	Suspended	30	201	540	Continuous influent flow at 150 L min^{-1}	Intermittent aeration with maximum of $800 \text{ m}^3 \text{ h}^{-1}$ in normal aeration condition	0.3	1.46	1.3		
16	(Joss et al., 2009)	1400m ³ SBR	flocs	30	412	892	Batch feeding	Intermittent aeration	≤ 1	0.6 intermittent			
								Continuous aeration		0.4 continuous			
17	(M. J. Kampschreur et al., 2009)	600 m ³	granule $d=1.5 \text{ mm}$	37	-	1000	Continuous feeding	Continuous aeration at $2000 \text{ m}^3 \text{ h}^{-1}$	around 5	1.67	1.23		
18	(Sliekers et al., 2002)	2 L liq SBR	floc	30	0	131	Continuous feeding in each cycle (11.5h)	Continuous aeration with air at 0.47 L h^{-1}	<0.07		0.1		

3. Thesis objectives and chapter overview

This **first chapter** summarized our knowledge on microbial nitrification, denitrification, anammox processes, as well as the chemical nitrogen transformation pathways most likely to occur during the nitrogen conversion. A special attention was given to the applications of the isotopes techniques for tracking N_2O pathways in wastewater nitrogen removal systems.

The literature study has shown that N_2O emission from nitrification and PNA process is a major concern with highly variable emission factors. Maintaining the emission factor at acceptable level (at least lower than 2% and ideally lower than 1%) is definitively not evident. More studies are needed to find the best operational and control strategies for N_2O mitigation in the PNA system. Regarding this objective, this thesis was based on an integrated approach including experiments and simulations, successively or in parallel.

From literature it comes quite clearly that N_2O emissions from one stage PNA depends on parameters (DO, AUR, nitrite, gas transfer rate) which are highly correlated making difficult our understanding of specific effect of each single parameter. At the early stage of this PhD, regarding model development, the combined effect of nitrite and DO on N_2O emissions from AOB appeared to us as an important point to understand and predict. That is the reason why this work was first dedicated to the calibration of the most recently developed 2-pathway models: our model from Pocquet et al. (2016) and Ni et al. (2014) model.

Whereas DO limitation is considered as a possible method for repressing the NOB (mostly), it was not found any study on N_2O emission at extremely low DO level, especially on a long term. Indeed very recent work of Akaboci et al. (2018) showed the interest of such conditions for piloting PNA process but the N_2O emissions were not provided. This is actually the main focus of this thesis: to analyze and predict the performances and N_2O emission of one stage PNA process under DO limitation.

Hence the **second chapter** first evaluated the capability of the 2-pathway model combining nitrifier denitrification (ND) and hydroxylamine oxidation (NN) pathway for predicting N_2O productions by AOB in a wide range of DO and nitrite levels; confrontations in three microbial systems were then compared with another 2-pathway model based on the electron pool as the model concept; The calibration efforts were finally discussed for facilitating the future model applications.

In the **third chapter**, experiments with one stage PNA are presented. The PNA process was started up in a 11 L SBR and controlled with low air flux and terminal DO setpoint. The temperature was controlled at 26.6 °C in order to evaluate the possible application under sidestream and mainstream conditions. The evaluation of the process was in three different perspectives: 1) Chemical analysis and gas balance for monitoring long term performances and stoichiometry; 2) Physical characterization of the suspended solids and granular size distribution; 3) Microbial characterization using FISH and 16s rRNA. In the end, discussions were regarding to the possible links between the different aspects aiming to obtain a compressive understanding and deeper insights into the long-term operation of the PNA process under extremely low DO.

In the **fourth chapter**, N_2O emissions in the PNA process was analyzed from short- and long-term run. The emission pattern, long-term evolution and influencing parameters regarding to N_2O were identified. Additional tests included the isotopic analysis of specific kinetic cycle and

anoxic/aerobic batch tests with nitrite addition were conducted to further reveal the possible N₂O production mechanisms.

In the **fifth chapter**, a new biofilm model was developed on aquasim software to provide a global 1-D model for PNA process including N₂O emissions through 3 different pathways. The model is calibrated and its prediction capabilities are evaluated for oxygen limited environments. This is the first time such model is calibrated with real data. Then simulations are conducted to clarify the N₂O dynamic pattern observed in our study.

Finally the conclusion will be proposed in order to summarize the main new insights from that thesis and the possible perspectives.

References

- Agrawal, S., Karst, S.M., Gilbert, E.M., Horn, H., Nielsen, P.H., Lackner, S., 2017. The role of inoculum and reactor configuration for microbial community composition and dynamics in mainstream partial nitritation anammox reactors. *MicrobiologyOpen* 6. <https://doi.org/10.1002/mbo3.456>
- Agrawal, S., Seuntjens, D., Cocker, P.D., Lackner, S., Vlaeminck, S.E., 2018. Success of mainstream partial nitritation/anammox demands integration of engineering, microbiome and modeling insights. *Curr. Opin. Biotechnol., Energy biotechnology • Environmental biotechnology* 50, 214–221. <https://doi.org/10.1016/j.copbio.2018.01.013>
- Akaboci, T.R.V., Gich, F., Rusalleda, M., Balaguer, M.D., Colprim, J., 2018. Effects of extremely low bulk liquid DO on autotrophic nitrogen removal performance and NOB suppression in side- and mainstream one-stage PNA. *J. Chem. Technol. Biotechnol.* 0. <https://doi.org/10.1002/jctb.5649>
- Ali, M., Rathnayake, R.M.L.D., Zhang, L., Ishii, S., Kindaichi, T., Satoh, H., Toyoda, S., Yoshida, N., Okabe, S., 2016. Source identification of nitrous oxide emission pathways from a single-stage nitritation-anammox granular reactor. *Water Res.* 102, 147–157. <https://doi.org/10.1016/j.watres.2016.06.034>
- Annajhala, M.K., Kapoor, V., Santo-Domingo, J., Chandran, K., 2018. Comammox Functionality Identified in Diverse Engineered Biological Wastewater Treatment Systems. *Environ. Sci. Technol. Lett.* 5, 110–116. <https://doi.org/10.1021/acs.estlett.7b00577>
- Awata, T., Oshiki, M., Kindaichi, T., Ozaki, N., Ohashi, A., Okabe, S., 2013. Physiological Characterization of an Anaerobic Ammonium-Oxidizing Bacterium Belonging to the “*Candidatus Scalindua*” Group. *Appl. Env. Microbiol.* 79, 4145–4148. <https://doi.org/10.1128/AEM.00056-13>
- Baeten, J.E., Batstone, D.J., Schraa, O.J., van Loosdrecht, M.C.M., Volcke, E.I.P., 2019. Modelling anaerobic, aerobic and partial nitritation-anammox granular sludge reactors - A review. *Water Res.* 149, 322–341. <https://doi.org/10.1016/j.watres.2018.11.026>
- Beaumont, H.J.E., Lens, S.I., Reijnders, W.N.M., Westerhoff, H.V., van Spanning, R.J.M., 2004. Expression of nitrite reductase in *Nitrosomonas europaea* involves NsrR, a novel nitrite-sensitive transcription repressor. *Mol. Microbiol.* 54, 148–158. <https://doi.org/10.1111/j.1365-2958.2004.04248.x>
- Besson, M., Tiruta-Barna, L., Spérandio, M., 2017. Environmental Assessment of Anammox Process in Mainstream with WWTP Modeling Coupled to Life Cycle Assessment, in: *Lecture Notes in Civil Engineering. Presented at the Frontiers International Conference on Wastewater Treatment and Modelling*, Springer, Cham, pp. 392–397. https://doi.org/10.1007/978-3-319-58421-8_62
- Blackburne, R., Yuan, Z., Keller, J., 2008. Partial nitrification to nitrite using low dissolved oxygen concentration as the main selection factor. *Biodegradation* 19, 303–312. <https://doi.org/10.1007/s10532-007-9136-4>
- Blum, J.-M., Jensen, M.M., Smets, B.F., 2018. Nitrous oxide production in intermittently aerated Partial Nitritation-Anammox reactor: oxic N₂O production dominates and relates with ammonia removal rate. *Chem. Eng. J.* 335, 458–466. <https://doi.org/10.1016/j.cej.2017.10.146>
- Borin, S., Mapelli, F., Rolli, E., Song, B., Tobias, C., Schmid, M.C., De Lange, G.J., Reichart, G.J., Schouten, S., Jetten, M., Daffonchio, D., 2013. Anammox bacterial populations in deep marine hypersaline gradient systems. *Extrem. Life Extreme Cond.* 17, 289–299. <https://doi.org/10.1007/s00792-013-0516-x>
- Brock, T.D., 1999. *Milestones in Microbiology 1546 to 1940*. ASM Press.

- Broda, E., 1977. Two kinds of lithotrophs missing in nature. *Z. Für Allg. Mikrobiol.* 17, 491–493. <https://doi.org/10.1002/jobm.19770170611>
- Butterbach-Bahl Klaus, Baggs Elizabeth M., Dannenmann Michael, Kiese Ralf, Zechmeister-Boltenstern Sophie, 2013. Nitrous oxide emissions from soils: how well do we understand the processes and their controls? *Philos. Trans. R. Soc. B Biol. Sci.* 368, 20130122. <https://doi.org/10.1098/rstb.2013.0122>
- Camargo, J.A., Alonso, Á., 2006. Ecological and toxicological effects of inorganic nitrogen pollution in aquatic ecosystems: A global assessment. *Environ. Int.* 32, 831–849. <https://doi.org/10.1016/j.envint.2006.05.002>
- Cao, Y., Loosdrecht, M.C.M. van, Daigger, G.T., 2017. Mainstream partial nitrification–anammox in municipal wastewater treatment: status, bottlenecks, and further studies. *Appl. Microbiol. Biotechnol.* 101, 1365–1383. <https://doi.org/10.1007/s00253-016-8058-7>
- Caranto, J.D., Lancaster, K.M., 2017. Nitric oxide is an obligate bacterial nitrification intermediate produced by hydroxylamine oxidoreductase. *Proc. Natl. Acad. Sci.* 114, 8217–8222. <https://doi.org/10.1073/pnas.1704504114>
- Caranto, J.D., Vilbert, A.C., Lancaster, K.M., 2016. Nitrosomonas europaea cytochrome P460 is a direct link between nitrification and nitrous oxide emission. *Proc. Natl. Acad. Sci.* 113, 14704–14709. <https://doi.org/10.1073/pnas.1611051113>
- Castro-Barros, C.M., Daelman, M.R.J., Mampaey, K.E., van Loosdrecht, M.C.M., Volcke, E.I.P., 2015. Effect of aeration regime on N₂O emission from partial nitrification–anammox in a full-scale granular sludge reactor. *Water Res.* 68, 793–803. <https://doi.org/10.1016/j.watres.2014.10.056>
- Cervantes, F.J. (Ed.), 2009. Environmental Technologies to Treat Nitrogen Pollution: Principles and Engineering. IWA Publishing, London.
- Chandran, K., Stein, L.Y., Klotz, M.G., van Loosdrecht, M.C.M., 2011. Nitrous oxide production by lithotrophic ammonia-oxidizing bacteria and implications for engineered nitrogen-removal systems. *Biochem. Soc. Trans.* 39, 1832–1837. <https://doi.org/10.1042/BST20110717>
- Chen, H., Yue, Y., Jin, W., Zhou, X., Wang, Q., Gao, S., Xie, G., Du, S., Tu, R., Han, S., Guo, K., 2017. Enrichment and characteristics of ammonia-oxidizing archaea in wastewater treatment process. *Chem. Eng. J.* 323, 465–472. <https://doi.org/10.1016/j.cej.2017.04.130>
- Clippeleir, H.D., Vlaeminck, S.E., Wilde, F.D., Daeninck, K., Mosquera, M., Boeckx, P., Verstraete, W., Boon, N., 2013. One-stage partial nitrification/anammox at 15 °C on pretreated sewage: feasibility demonstration at lab-scale. *Appl. Microbiol. Biotechnol.* 97, 10199–10210. <https://doi.org/10.1007/s00253-013-4744-x>
- Colliver, B.B., Stephenson, T., 2000. Production of nitrogen oxide and dinitrogen oxide by autotrophic nitrifiers. *Biotechnol. Adv.* 18, 219–232. [https://doi.org/10.1016/S0734-9750\(00\)00035-5](https://doi.org/10.1016/S0734-9750(00)00035-5)
- Connan, R., Dabert, P., Moya-Espinosa, M., Bridoux, G., Béline, F., Magrí, A., 2018. Coupling of partial nitrification and anammox in two- and one-stage systems: Process operation, N₂O emission and microbial community. *J. Clean. Prod.* 203, 559–573. <https://doi.org/10.1016/j.jclepro.2018.08.258>
- Conthe, M., Lycus, P., Arntzen, M.Ø., Ramos da Silva, A., Frostegård, Å., Bakken, L.R., Kleerebezem, R., van Loosdrecht, M.C.M., 2019. Denitrification as an N₂O sink. *Water Res.* 151, 381–387. <https://doi.org/10.1016/j.watres.2018.11.087>
- Corbalá-Robles, L., Picioreanu, C., Loosdrecht, M.C.M. van, Pérez, J., 2016. Analysing the effects of the aeration pattern and residual ammonium concentration in a partial nitrification–anammox process. *Environ. Technol.* 37, 694–702. <https://doi.org/10.1080/09593330.2015.1077895>
- Costa, E., Pérez, J., Kreft, J.-U., 2006. Why is metabolic labour divided in nitrification? *Trends*

- Microbiol. 14, 213–219. <https://doi.org/10.1016/j.tim.2006.03.006>
- Courstens, E.N.P., Vandekerckhove, T., Prat, D., Vilchez-Vargas, R., Vital, M., Pieper, D.H., Meerbergen, K., Lievens, B., Boon, N., Vlaeminck, S.E., 2016. Empowering a mesophilic inoculum for thermophilic nitrification: Growth mode and temperature pattern as critical proliferation factors for archaeal ammonia oxidizers. *Water Res.* 92, 94–103. <https://doi.org/10.1016/j.watres.2016.01.022>
- Daims, H., Lebedeva, E.V., Pjevac, P., Han, P., Herbold, C., Albertsen, M., Jehmlich, N., Palatinszky, M., Vierheilig, J., Bulaev, A., Kirkegaard, R.H., Bergen, M. von, Rattei, T., Bendinger, B., Nielsen, P.H., Wagner, M., 2015. Complete nitrification by *Nitrospira* bacteria. *Nature* 528, 504–509. <https://doi.org/10.1038/nature16461>
- Daims, H., Wagner, M., 2018. *Nitrospira*. *Trends Microbiol.* 26, 462–463. <https://doi.org/10.1016/j.tim.2018.02.001>
- De Clippeleir, H., Vlaeminck, S.E., Carballa, M., Verstraete, W., 2009. A low volumetric exchange ratio allows high autotrophic nitrogen removal in a sequencing batch reactor. *Bioresour. Technol.* 100, 5010–5015. <https://doi.org/10.1016/j.biortech.2009.05.031>
- De Cocker, P., Bessiere, Y., Hernandez-Raquet, G., Dubos, S., Mozo, I., Gaval, G., Caligaris, M., Barillon, B., Vlaeminck, S.E., Sperandio, M., 2018. Enrichment and adaptation yield high anammox conversion rates under low temperatures. *Bioresour. Technol.* 250, 505–512. <https://doi.org/10.1016/j.biortech.2017.11.079>
- Desloover, J., De Clippeleir, H., Boeckx, P., Du Laing, G., Colsen, J., Verstraete, W., Vlaeminck, S.E., 2011. Floc-based sequential partial nitritation and anammox at full scale with contrasting N₂O emissions. *Water Res.* 45, 2811–2821. <https://doi.org/10.1016/j.watres.2011.02.028>
- Domingo-Félez, C., Calderó-Pascual, M., Sin, G., Plósz, B.G., Smets, B.F., 2017. Calibration of the comprehensive NDHA-N₂O dynamics model for nitrifier-enriched biomass using targeted respirometric assays. *Water Res.* 126, 29–39. <https://doi.org/10.1016/j.watres.2017.09.013>
- Domingo-Félez, C., Mutlu, A.G., Jensen, M.M., Smets, B.F., 2014. Aeration Strategies To Mitigate Nitrous Oxide Emissions from Single-Stage Nitritation/Anammox Reactors. *Environ. Sci. Technol.* 48, 8679–8687. <https://doi.org/10.1021/es501819n>
- Domingo-Félez, C., Smets, B.F., 2016. A consilience model to describe N₂O production during biological N removal. *Environ. Sci. Water Res. Technol.* 2, 923–930. <https://doi.org/10.1039/C6EW00179C>
- Duan, H., Ye, L., Erler, D., Ni, B.-J., Yuan, Z., 2017. Quantifying nitrous oxide production pathways in wastewater treatment systems using isotope technology – A critical review. *Water Res.* 122, 96–113. <https://doi.org/10.1016/j.watres.2017.05.054>
- Frame, C.H., Lau, E., Nolan, E.J.I., Goepfert, T.J., Lehmann, M.F., 2017. Acidification Enhances Hybrid N₂O Production Associated with Aquatic Ammonia-Oxidizing Microorganisms. *Front. Microbiol.* 7. <https://doi.org/10.3389/fmicb.2016.02104>
- Fux, C., Bohler, M., Huber, P., Brunner, I., Siegrist, H., 2002. Biological treatment of ammonium-rich wastewater by partial nitritation and subsequent anaerobic ammonium oxidation (anammox) in a pilot plant. *J. Biotechnol.* 99, 295–306.
- Gilbert, E.M., Agrawal, S., Schwartz, T., Horn, H., Lackner, S., 2015. Comparing different reactor configurations for Partial Nitritation/Anammox at low temperatures. *Water Res.* 81, 92–100. <https://doi.org/10.1016/j.watres.2015.05.022>
- Gilmore, K.R., Terada, A., Smets, B.F., Love, N.G., Garland, J.L., 2012. Autotrophic Nitrogen Removal in a Membrane-Aerated Biofilm Reactor Under Continuous Aeration: A Demonstration. *Environ. Eng. Sci.* 30, 38–45. <https://doi.org/10.1089/ees.2012.0222>
- Guo, G., Wang, Y., Hao, T., Wu, D., Chen, G.-H., 2017. Enzymatic nitrous oxide emissions from wastewater treatment. *Front. Environ. Sci. Eng.* 12, 10. <https://doi.org/10.1007/s11783-018-1021-3>

- Guo, L., Vanrolleghem, P.A., 2014. Calibration and validation of an activated sludge model for greenhouse gases no. 1 (ASMG1): prediction of temperature-dependent N₂O emission dynamics. *Bioprocess Biosyst. Eng.* 37, 151–163. <https://doi.org/10.1007/s00449-013-0978-3>
- Harper, W.F., Takeuchi, Y., Riya, S., Hosomi, M., Terada, A., 2015. Novel abiotic reactions increase nitrous oxide production during partial nitrification: Modeling and experiments. *Chem. Eng. J.* 281, 1017–1023. <https://doi.org/10.1016/j.cej.2015.06.109>
- Harris, E., Joss, A., Emmenegger, L., Kipf, M., Wolf, B., Mohn, J., Wunderlin, P., 2015. Isotopic evidence for nitrous oxide production pathways in a partial nitrification-anammox reactor. *Water Res.* 83, 258–270. <https://doi.org/10.1016/j.watres.2015.06.040>
- Hiatt, W.C., Grady, C.P.L., 2008. An Updated Process Model for Carbon Oxidation, Nitrification, and Denitrification. *Water Environ. Res.* 80, 2145–2156. <https://doi.org/10.2175/106143008X304776>
- Hira, D., Toh, H., Migita, C.T., Okubo, H., Nishiyama, T., Hattori, M., Furukawa, K., Fujii, T., 2012. Anammox organism KSU-1 expresses a NirK-type copper-containing nitrite reductase instead of a NirS-type with cytochrome cd1. *FEBS Lett.* 586, 1658–1663. <https://doi.org/10.1016/j.febslet.2012.04.041>
- Hu, Z., Lotti, T., Kreuk, M. de, Kleerebezem, R., Loosdrecht, M. van, Kruit, J., Jetten, M.S.M., Kartal, B., 2013. Nitrogen Removal by a Nitritation-Anammox Bioreactor at Low Temperature. *Appl. Environ. Microbiol.* 79, 2807–2812. <https://doi.org/10.1128/AEM.03987-12>
- IPCC, 2014. Climate Change 2014: Synthesis Report. Contribution of Working Groups I, II and III to the Fifth Assessment Report of the Intergovernmental Panel on Climate Change [Core Writing Team, R.K. Pachauri and L.A. Meyer (eds.)]. Geneva, Switzerland, p. 151.
- Ishii, S., Song, Y., Rathnayake, L., Tumendelger, A., Satoh, H., Toyoda, S., Yoshida, N., Okabe, S., 2014. Identification of key nitrous oxide production pathways in aerobic partial nitrifying granules. *Environ. Microbiol.* 16, 3168–3180. <https://doi.org/10.1111/1462-2920.12458>
- Jensen, M.M., Thamdrup, B., Dalsgaard, T., 2007. Effects of Specific Inhibitors on Anammox and Denitrification in Marine Sediments. *Appl. Environ. Microbiol.* 73, 3151–3158. <https://doi.org/10.1128/AEM.01898-06>
- Jetten, M.S.M., Horn, S.J., van Loosdrecht, M.C.M., 1997. Towards a more sustainable municipal wastewater treatment system. *Water Sci. Technol., Sustainable Sanitation* 35, 171–180. [https://doi.org/10.1016/S0273-1223\(97\)00195-9](https://doi.org/10.1016/S0273-1223(97)00195-9)
- Joss, A., Salzgeber, D., Eugster, J., König, R., Rottermann, K., Burger, S., Fabijan, P., Leumann, S., Mohn, J., Siegrist, H., 2009. Full-Scale Nitrogen Removal from Digester Liquid with Partial Nitritation and Anammox in One SBR. *Environ. Sci. Technol.* 43, 5301–5306. <https://doi.org/10.1021/es900107w>
- Junier, P., Molina, V., Dorador, C., Hadas, O., Kim, O.-S., Junier, T., Witzel, K.-P., Imhoff, J.F., 2010. Phylogenetic and functional marker genes to study ammonia-oxidizing microorganisms (AOM) in the environment. *Appl. Microbiol. Biotechnol.* 85, 425–440. <https://doi.org/10.1007/s00253-009-2228-9>
- Kalvelage, T., Jensen, M.M., Contreras, S., Revsbech, N.P., Lam, P., Günter, M., LaRoche, J., Lavik, G., Kuypers, M.M.M., 2011. Oxygen Sensitivity of Anammox and Coupled N-Cycle Processes in Oxygen Minimum Zones. *PLOS ONE* 6, e29299. <https://doi.org/10.1371/journal.pone.0029299>
- Kampschreur, M.J., Kleerebezem, R., de Vet, W.W.J.M., van Loosdrecht, M.C.M., 2011. Reduced iron induced nitric oxide and nitrous oxide emission. *Water Res.* 45, 5945–5952. <https://doi.org/10.1016/j.watres.2011.08.056>
- Kampschreur, M. J., Poldermans, R., Kleerebezem, R., van der Star, W.R.L., Haarhuis, R., Abma,

- W.R., Jetten, M.S.M., van Loosdrecht, M.C.M., 2009. Emission of nitrous oxide and nitric oxide from a full-scale single-stage nitritation-anammox reactor. *Water Sci. Technol.* 60, 3211–3217. <https://doi.org/10.2166/wst.2009.608>
- Kampschreur, Marlies J., Temmink, H., Kleerebezem, R., Jetten, M.S.M., van Loosdrecht, M.C.M., 2009. Nitrous oxide emission during wastewater treatment. *Water Res.* 43, 4093–4103. <https://doi.org/10.1016/j.watres.2009.03.001>
- Kampschreur, M.J., van der Star, W.R.L., Wielders, H.A., Mulder, J.W., Jetten, M.S.M., van Loosdrecht, M.C.M., 2008. Dynamics of nitric oxide and nitrous oxide emission during full-scale reject water treatment. *Water Res.* 42, 812–826. <https://doi.org/10.1016/j.watres.2007.08.022>
- Kanter, D.R., Wentz, J.A., Galloway, J.N., Moomaw, W.R., Winiwarter, W., 2017. Managing a forgotten greenhouse gas under existing U.S. law: An interdisciplinary analysis. *Environ. Sci. Policy* 67, 44–51. <https://doi.org/10.1016/j.envsci.2016.11.003>
- Kessel, M.A.H.J. van, Speth, D.R., Albertsen, M., Nielsen, P.H., Camp, H.J.M.O. den, Kartal, B., Jetten, M.S.M., Lücker, S., 2015. Complete nitrification by a single microorganism. *Nature* 528, 555–559. <https://doi.org/10.1038/nature16459>
- Kowalchuk, G.A., Stephen, J.R., 2001. Ammonia-Oxidizing Bacteria: A Model for Molecular Microbial Ecology. *Annu. Rev. Microbiol.* 55, 485–529. <https://doi.org/10.1146/annurev.micro.55.1.485>
- Kuypers, M.M.M., Sliekers, A.O., Lavik, G., Schmid, M., Jørgensen, B.B., Kuenen, J.G., Damsté, J.S.S., Strous, M., Jetten, M.S.M., 2003. Anaerobic ammonium oxidation by anammox bacteria in the Black Sea. *Nature* 422, 608–611. <https://doi.org/10.1038/nature01472>
- Lackner, S., Gilbert, E.M., Vlaeminck, S.E., Joss, A., Horn, H., van Loosdrecht, M.C.M., 2014. Full-scale partial nitritation/anammox experiences – An application survey. *Water Res.* 55, 292–303. <https://doi.org/10.1016/j.watres.2014.02.032>
- Law, Y., Lant, P., Yuan, Z., 2013. The Confounding Effect of Nitrite on N₂O Production by an Enriched Ammonia-Oxidizing Culture. *Environ. Sci. Technol.* 47, 7186–7194. <https://doi.org/10.1021/es4009689>
- Law, Y., Ni, B.-J., Lant, P., Yuan, Z., 2012. N₂O production rate of an enriched ammonia-oxidising bacteria culture exponentially correlates to its ammonia oxidation rate. *Water Res.* 46, 3409–3419. <https://doi.org/10.1016/j.watres.2012.03.043>
- Lawson, C.E., Lücker, S., 2018. Complete ammonia oxidation: an important control on nitrification in engineered ecosystems? *Curr. Opin. Biotechnol., Energy biotechnology • Environmental biotechnology* 50, 158–165. <https://doi.org/10.1016/j.copbio.2018.01.015>
- Lawton, T.J., Bowen, K.E., Sayavedra-Soto, L.A., Arp, D.J., Rosenzweig, A.C., 2013. Characterization of a Nitrite Reductase Involved in Nitrifier Denitrification. *J. Biol. Chem.* 288, 25575–25583. <https://doi.org/10.1074/jbc.M113.484543>
- Lebedeva, E.V., Off, S., Zumbärgel, S., Kruse, M., Shagzhina, A., Lücker, S., Maixner, F., Lipski, A., Daims, H., Spieck, E., 2011. Isolation and characterization of a moderately thermophilic nitrite-oxidizing bacterium from a geothermal spring. *FEMS Microbiol. Ecol.* 75, 195–204. <https://doi.org/10.1111/j.1574-6941.2010.01006.x>
- Li, K., Fang, F., Wang, H., Wang, C., Chen, Y., Guo, J., Wang, X., Jiang, F., 2017. Pathways of N removal and N₂O emission from a one-stage autotrophic N removal process under anaerobic conditions. *Sci. Rep.* 7. <https://doi.org/10.1038/srep42072>
- Li, X., Sun, S., Badgley, B.D., Sung, S., Zhang, H., He, Z., 2016. Nitrogen removal by granular nitritation–anammox in an upflow membrane-aerated biofilm reactor. *Water Res.* 94, 23–31. <https://doi.org/10.1016/j.watres.2016.02.031>
- Liu, S., Han, P., Hink, L., Prosser, J.I., Wagner, M., Brüggemann, N., 2017. Abiotic Conversion of Extracellular NH₂OH Contributes to N₂O Emission during Ammonia Oxidation. *Environ. Sci. Technol.* 51, 13122–13132. <https://doi.org/10.1021/acs.est.7b02360>

- Lotti, T., Kleerebezem, R., Hu, Z., Kartal, B., de Kreuk, M.K., van Erp Taalman Kip, C., Kruit, J., Hendrickx, T.L.G., van Loosdrecht, M.C.M., 2015. Pilot-scale evaluation of anammox-based mainstream nitrogen removal from municipal wastewater. *Environ. Technol.* 36, 1167–1177. <https://doi.org/10.1080/09593330.2014.982722>
- Lotti, T., Kleerebezem, R., Hu, Z., Kartal, B., Jetten, M.S.M., van Loosdrecht, M.C.M., 2014a. Simultaneous partial nitrification and anammox at low temperature with granular sludge. *Water Res.* 66, 111–121. <https://doi.org/10.1016/j.watres.2014.07.047>
- Lotti, T., Kleerebezem, R., Lubello, C., van Loosdrecht, M.C.M., 2014b. Physiological and kinetic characterization of a suspended cell anammox culture. *Water Res.* 60, 1–14. <https://doi.org/10.1016/j.watres.2014.04.017>
- Ma, B., Bao, P., Wei, Y., Zhu, G., Yuan, Z., Peng, Y., 2015. Suppressing Nitrite-oxidizing Bacteria Growth to Achieve Nitrogen Removal from Domestic Wastewater via Anammox Using Intermittent Aeration with Low Dissolved Oxygen. *Sci. Rep.* 5, 13048. <https://doi.org/10.1038/srep13048>
- Ma, C., Jensen, M.M., Smets, B.F., Thamdrup, B., 2017. Pathways and Controls of N₂O Production in Nitrification–Anammox Biomass. *Environ. Sci. Technol.* 51, 8981–8991. <https://doi.org/10.1021/acs.est.7b01225>
- Maalcke, W.J., Dietl, A., Marritt, S.J., Butt, J.N., Jetten, M.S.M., Keltjens, J.T., Barends, T.R.M., Kartal, B., 2014. Structural Basis of Biological NO Generation by Octaheme Oxidoreductases. *J. Biol. Chem.* 289, 1228–1242. <https://doi.org/10.1074/jbc.M113.525147>
- Malovanyy, A., Trela, J., Plaza, E., 2015. Mainstream wastewater treatment in integrated fixed film activated sludge (IFAS) reactor by partial nitrification/anammox process. *Bioresour. Technol.* 198, 478–487. <https://doi.org/10.1016/j.biortech.2015.08.123>
- Mampaey, K.E., Beuckels, B., Kampschreur, M.J., Kleerebezem, R., van Loosdrecht, M.C.M., Volcke, E.I.P., 2013. Modelling nitrous and nitric oxide emissions by autotrophic ammonia-oxidizing bacteria. *Environ. Technol.* 34, 1555–1566. <https://doi.org/10.1080/09593330.2012.758666>
- Manser, R., Gujer, W., Siegrist, H., 2005. Consequences of mass transfer effects on the kinetics of nitrifiers. *Water Res.* 39, 4633–4642. <https://doi.org/10.1016/j.watres.2005.09.020>
- Mao, Y., Bakken, L.R., Zhao, L., Frostegård, Å., 2008. Functional robustness and gene pools of a wastewater nitrification reactor: comparison of dispersed and intact biofilms when stressed by low oxygen and low pH. *FEMS Microbiol. Ecol.* 66, 167–180. <https://doi.org/10.1111/j.1574-6941.2008.00532.x>
- Morales, N., Val del Río, Á., Vázquez-Padín, J.R., Méndez, R., Campos, J.L., Mosquera-Corral, A., 2016. The granular biomass properties and the acclimation period affect the partial nitrification/anammox process stability at a low temperature and ammonium concentration. *Process Biochem.* 51, 2134–2142. <https://doi.org/10.1016/j.procbio.2016.08.029>
- Mulder, A., van de Graaf, A.A., Robertson, L.A., Kuenen, J.G., 1995. Anaerobic ammonium oxidation discovered in a denitrifying fluidized bed reactor. *FEMS Microbiol. Ecol.* 16, 177–183. [https://doi.org/10.1016/0168-6496\(94\)00081-7](https://doi.org/10.1016/0168-6496(94)00081-7)
- Ni, B.-J., Pan, Y., van den Akker, B., Ye, L., Yuan, Z., 2015. Full-Scale Modeling Explaining Large Spatial Variations of Nitrous Oxide Fluxes in a Step-Feed Plug-Flow Wastewater Treatment Reactor. *Environ. Sci. Technol.* 49, 9176–9184. <https://doi.org/10.1021/acs.est.5b02038>
- Ni, B.-J., Peng, L., Law, Y., Guo, J., Yuan, Z., 2014. Modeling of Nitrous Oxide Production by Autotrophic Ammonia-Oxidizing Bacteria with Multiple Production Pathways. *Environ. Sci. Technol.* 48, 3916–3924. <https://doi.org/10.1021/es405592h>
- Ni, B.-J., Rusalleda, M., Pellicer-Nàcher, C., Smets, B.F., 2011. Modeling Nitrous Oxide Production during Biological Nitrogen Removal via Nitrification and Denitrification:

- Extensions to the General ASM Models. *Environ. Sci. Technol.* 45, 7768–7776. <https://doi.org/10.1021/es201489n>
- Ni, B.-J., Ye, L., Law, Y., Byers, C., Yuan, Z., 2013a. Mathematical Modeling of Nitrous Oxide (N₂O) Emissions from Full-Scale Wastewater Treatment Plants. *Environ. Sci. Technol.* 47, 7795–7803. <https://doi.org/10.1021/es4005398>
- Ni, B.-J., Yuan, Z., 2015. Recent advances in mathematical modeling of nitrous oxides emissions from wastewater treatment processes. *Water Res.* 87, 336–346. <https://doi.org/10.1016/j.watres.2015.09.049>
- Ni, B.-J., Yuan, Z., Chandran, K., Vanrolleghem, P.A., Murthy, S., 2013b. Evaluating four mathematical models for nitrous oxide production by autotrophic ammonia-oxidizing bacteria. *Biotechnol. Bioeng.* 110, 153–163. <https://doi.org/10.1002/bit.24620>
- Okabe, S., Oshiki, M., Takahashi, Y., Satoh, H., 2011. N₂O emission from a partial nitrification–anammox process and identification of a key biological process of N₂O emission from anammox granules. *Water Res.* 45, 6461–6470. <https://doi.org/10.1016/j.watres.2011.09.040>
- Oshiki, M., Satoh, H., Okabe, S., 2015. Ecology and physiology of anaerobic ammonium oxidizing bacteria. *Environ. Microbiol.* 18, 2784–2796. <https://doi.org/10.1111/1462-2920.13134>
- Pan, Y., Ni, B.-J., Yuan, Z., 2013. Modeling Electron Competition among Nitrogen Oxides Reduction and N₂O Accumulation in Denitrification. *Environ. Sci. Technol.* 47, 11083–11091. <https://doi.org/10.1021/es402348n>
- Park, H.-D., Noguera, D.R., 2004. Evaluating the effect of dissolved oxygen on ammonia-oxidizing bacterial communities in activated sludge. *Water Res.* 38, 3275–3286. <https://doi.org/10.1016/j.watres.2004.04.047>
- Peng, L., Ni, B.-J., Erler, D., Ye, L., Yuan, Z., 2014. The effect of dissolved oxygen on N₂O production by ammonia-oxidizing bacteria in an enriched nitrifying sludge. *Water Res.* 66, 12–21. <https://doi.org/10.1016/j.watres.2014.08.009>
- Peng, L., Ni, B.-J., Law, Y., Yuan, Z., 2016. Modeling N₂O production by ammonia oxidizing bacteria at varying inorganic carbon concentrations by coupling the catabolic and anabolic processes. *Chem. Eng. Sci.* 144, 386–394. <https://doi.org/10.1016/j.ces.2016.01.033>
- Peng, L., Ni, B.-J., Ye, L., Yuan, Z., 2015. Selection of mathematical models for N₂O production by ammonia oxidizing bacteria under varying dissolved oxygen and nitrite concentrations. *Chem. Eng. J.* 281, 661–668. <https://doi.org/10.1016/j.cej.2015.07.015>
- Penton, C.R., Devol, A.H., Tiedje, J.M., 2006. Molecular Evidence for the Broad Distribution of Anaerobic Ammonium-Oxidizing Bacteria in Freshwater and Marine Sediments. *Appl. Environ. Microbiol.* 72, 6829–6832. <https://doi.org/10.1128/AEM.01254-06>
- Pérez, J., Lotti, T., Kleerebezem, R., Picioreanu, C., van Loosdrecht, M.C.M., 2014. Outcompeting nitrite-oxidizing bacteria in single-stage nitrogen removal in sewage treatment plants: A model-based study. *Water Res.* 66, 208–218. <https://doi.org/10.1016/j.watres.2014.08.028>
- Picioreanu, C., Pérez, J., van Loosdrecht, M.C.M., 2016. Impact of cell cluster size on apparent half-saturation coefficients for oxygen in nitrifying sludge and biofilms. *Water Res.* 106, 371–382. <https://doi.org/10.1016/j.watres.2016.10.017>
- Pocquet, M., Queinnec, I., Sperandio, M., 2013. Adaptation and identification of models for nitrous oxide (N₂O) production by autotrophic nitrite reduction, in: *Proceedings 11th IWA Conference on Instrumentation. Presented at the Control and Automation (ICA2013), Narbonne.*
- Pocquet, M., Wu, Z., Queinnec, I., Spérandio, M., 2016. A two pathway model for N₂O emissions by ammonium oxidizing bacteria supported by the NO/N₂O variation.

- Water Res. 88, 948–959. <https://doi.org/10.1016/j.watres.2015.11.029>
- Poot, V., Hoekstra, M., Geleijnse, M.A.A., van Loosdrecht, M.C.M., Pérez, J., 2016. Effects of the residual ammonium concentration on NOB repression during partial nitrification with granular sludge. *Water Res.* 106, 518–530. <https://doi.org/10.1016/j.watres.2016.10.028>
- Poth, M., Focht, D.D., 1985. ¹⁵N Kinetic Analysis of N₂O Production by *Nitrosomonas europaea*: an Examination of Nitrifier Denitrification. *Appl. Environ. Microbiol.* 49, 1134–1141.
- Poughon, L., Dussap, C.-G., Gros, J.-B., 2001. Energy model and metabolic flux analysis for autotrophic nitrifiers. *Biotechnol. Bioeng.* 72, 416–433. [https://doi.org/10.1002/1097-0290\(20000220\)72:4<416::AID-BIT1004>3.0.CO;2-D](https://doi.org/10.1002/1097-0290(20000220)72:4<416::AID-BIT1004>3.0.CO;2-D)
- Purkhold, U., Pommerening-Röser, A., Juretschko, S., Schmid, M.C., Koops, H.-P., Wagner, M., 2000. Phylogeny of All Recognized Species of Ammonia Oxidizers Based on Comparative 16S rRNA and amoA Sequence Analysis: Implications for Molecular Diversity Surveys. *Appl. Environ. Microbiol.* 66, 5368–5382.
- Rathnayake, R.M.L.D., Song, Y., Tumendelger, A., Oshiki, M., Ishii, S., Satoh, H., Toyoda, S., Yoshida, N., Okabe, S., 2013. Source identification of nitrous oxide on autotrophic partial nitrification in a granular sludge reactor. *Water Res., Microbial ecology of drinking water and wastewater treatment* 47, 7078–7086. <https://doi.org/10.1016/j.watres.2013.07.055>
- Ravishankara, A.R., Daniel, J.S., Portmann, R.W., 2009. Nitrous Oxide (N₂O): The Dominant Ozone-Depleting Substance Emitted in the 21st Century. *Science* 326, 123–125. <https://doi.org/10.1126/science.1176985>
- Regmi, P., Miller, M.W., Holgate, B., Bunce, R., Park, H., Chandran, K., Wett, B., Murthy, S., Bott, C.B., 2014. Control of aeration, aerobic SRT and COD input for mainstream nitrification/denitrification. *Water Res.* 57, 162–171. <https://doi.org/10.1016/j.watres.2014.03.035>
- Ribera-Guardia, A., Pijuan, M., 2017. Distinctive NO and N₂O emission patterns in ammonia oxidizing bacteria: Effect of ammonia oxidation rate, DO and pH. *Chem. Eng. J.* 321, 358–365. <https://doi.org/10.1016/j.cej.2017.03.122>
- Richardson, D., Felgate, H., Watmough, N., Thomson, A., Baggs, E., 2009. Mitigating release of the potent greenhouse gas N₂O from the nitrogen cycle – could enzymic regulation hold the key? *Trends Biotechnol.* 27, 388–397. <https://doi.org/10.1016/j.tibtech.2009.03.009>
- Ritchie, G. a. F., Nicholas, D.J.D., 1972. Identification of the sources of nitrous oxide produced by oxidative and reductive processes in *Nitrosomonas europaea*. *Biochem. J.* 126, 1181–1191. <https://doi.org/10.1042/bj1261181>
- Russ, L., Kartal, B., Op den Camp, H.J.M., Sollai, M., Le Bruchec, J., Caprais, J.-C., Godfroy, A., Sinninghe Damsté, J.S., Jetten, M.S.M., 2013. Presence and diversity of anammox bacteria in cold hydrocarbon-rich seeps and hydrothermal vent sediments of the Guaymas Basin. *Front. Microbiol.* 4, 219. <https://doi.org/10.3389/fmicb.2013.00219>
- Rysgaard, S., Glud, R.N., 2004. Anaerobic N₂ production in Arctic sea ice. *Limnol. Oceanogr.* 49, 86–94. <https://doi.org/10.4319/lo.2004.49.1.0086>
- Sabba, F., Terada, A., Wells, G., Smets, B.F., Nerenberg, R., 2018. Nitrous oxide emissions from biofilm processes for wastewater treatment. *Appl. Microbiol. Biotechnol.* <https://doi.org/10.1007/s00253-018-9332-7>
- Schmid, M.C., Maas, B., Dapena, A., van de Pas-Schoonen, K., van de Vossenberg, J., Kartal, B., van Niftrik, L., Schmidt, I., Cirpus, I., Kuenen, J.G., Wagner, M., Sinninghe Damsté, J.S., Kuypers, M., Revsbech, N.P., Mendez, R., Jetten, M.S.M., Strous, M., 2005. Biomarkers for In Situ Detection of Anaerobic Ammonium-Oxidizing (Anammox) Bacteria. *Appl. Environ. Microbiol.* 71, 1677–1684. <https://doi.org/10.1128/AEM.71.4.1677-1684.2005>

- Seuntjens, D., Carvajal-Arroyo, J.M., Ruopp, M., Bunse, P., De Mulder, C.P., Lochmatter, S., Agrawal, S., Boon, N., Lackner, S., Vlaeminck, S.E., 2018. High-resolution mapping and modeling of anammox recovery from recurrent oxygen exposure. *Water Res.* <https://doi.org/10.1016/j.watres.2018.07.024>
- Shaw, L.J., Nicol, G.W., Smith, Z., Fear, J., Prosser, J.I., Baggs, E.M., 2006. *Nitrosospira* spp. can produce nitrous oxide via a nitrifier denitrification pathway. *Environ. Microbiol.* 8, 214–222. <https://doi.org/10.1111/j.1462-2920.2005.00882.x>
- Shen, L., Wu, H., Gao, Z., Xu, X., Chen, T., Liu, S., Cheng, H., 2015. Occurrence and importance of anaerobic ammonium-oxidising bacteria in vegetable soils. *Appl. Microbiol. Biotechnol.* 99, 5709–5718. <https://doi.org/10.1007/s00253-015-6454-z>
- Sliekers, A.O., Derwort, N., Gomez, J.L.C., Strous, M., Kuenen, J.G., Jetten, M.S.M., 2002. Completely autotrophic nitrogen removal over nitrite in one single reactor. *Water Res.* 36, 2475–2482. [https://doi.org/10.1016/S0043-1354\(01\)00476-6](https://doi.org/10.1016/S0043-1354(01)00476-6)
- Sliekers, A.O., Haaijer, S.C.M., Stafsnes, M.H., Kuenen, J.G., Jetten, M.S.M., 2005. Competition and coexistence of aerobic ammonium- and nitrite-oxidizing bacteria at low oxygen concentrations. *Appl. Microbiol. Biotechnol.* 68, 808–817. <https://doi.org/10.1007/s00253-005-1974-6>
- Smil, V., 2001. *Enriching the Earth: Fritz Haber, Carl Bosch, and the Transformation of World Food Production*. MIT Press.
- Soler-Jofra, A., Picioreanu, C., Yu, R., Chandran, K., van Loosdrecht, M.C.M., Pérez, J., 2018. Importance of hydroxylamine in abiotic N₂O production during transient anoxia in planktonic axenic *Nitrosomonas* cultures. *Chem. Eng. J.* 335, 756–762. <https://doi.org/10.1016/j.cej.2017.10.141>
- Soler-Jofra, A., Stevens, B., Hoekstra, M., Picioreanu, C., Sorokin, D., van Loosdrecht, M.C.M., Pérez, J., 2016. Importance of abiotic hydroxylamine conversion on nitrous oxide emissions during nitrification of reject water. *Chem. Eng. J.* 287, 720–726. <https://doi.org/10.1016/j.cej.2015.11.073>
- Soliman, M., Eldyasti, A., 2018. Ammonia-Oxidizing Bacteria (AOB): opportunities and applications—a review. *Rev. Environ. Sci. Biotechnol.* 17, 285–321. <https://doi.org/10.1007/s11157-018-9463-4>
- Sorokin, D.Y., Lückner, S., Vejmekova, D., Kostrikina, N.A., Kleerebezem, R., Rijpstra, W.I.C., Damsté, J.S.S., Le Paslier, D., Muyzer, G., Wagner, M., van Loosdrecht, M.C.M., Daims, H., 2012. Nitrification expanded: discovery, physiology and genomics of a nitrite-oxidizing bacterium from the phylum Chloroflexi. *ISME J.* 6, 2245–2256. <https://doi.org/10.1038/ismej.2012.70>
- Spérandio, M., Pocquet, M., Guo, L., Ni, B.-J., Vanrolleghem, P.A., Yuan, Z., 2016. Evaluation of different nitrous oxide production models with four continuous long-term wastewater treatment process data series. *Bioprocess Biosyst. Eng.* 39, 493–510. <https://doi.org/10.1007/s00449-015-1532-2>
- Spott, O., Russow, R., Stange, C.F., 2011. Formation of hybrid N₂O and hybrid N₂ due to codenitrification: First review of a barely considered process of microbially mediated N-nitrosation. *Soil Biol. Biochem.* 43, 1995–2011. <https://doi.org/10.1016/j.soilbio.2011.06.014>
- Staunton, E.T., Aitken, M.D., 2015. Coupling Nitrogen Removal and Anaerobic Digestion for Energy Recovery from Swine Waste: 2 Nitritation/Anammox. *Environ. Eng. Sci.* 32, 750–760. <https://doi.org/10.1089/ees.2015.0063>
- Stein, L.Y., Klotz, M.G., 2016. The nitrogen cycle. *Curr. Biol.* 26, R94–R98. <https://doi.org/10.1016/j.cub.2015.12.021>
- Strous, M., Heijnen, J.J., Kuenen, J.G., Jetten, M.S.M., 1998. The sequencing batch reactor as a powerful tool for the study of slowly growing anaerobic ammonium-oxidizing microorganisms. *Appl. Microbiol. Biotechnol.* 50, 589–596.

- <https://doi.org/10.1007/s002530051340>
- Sutka, R.L., Ostrom, N.E., Ostrom, P.H., Breznak, J.A., Gandhi, H., Pitt, A.J., Li, F., 2006. Distinguishing Nitrous Oxide Production from Nitrification and Denitrification on the Basis of Isotopomer Abundances. *Appl. Environ. Microbiol.* 72, 638–644. <https://doi.org/10.1128/AEM.72.1.638-644.2006>
- Suzuki, I., Dular, U., Kwok, S.C., 1974. Ammonia or Ammonium Ion as Substrate for Oxidation by *Nitrosomonas europaea* Cells and Extracts. *J. Bacteriol.* 120, 556–558.
- Teixeira, C., Magalhães, C., Joye, S.B., Bordalo, A.A., 2012. Potential rates and environmental controls of anaerobic ammonium oxidation in estuarine sediments. *Aquat. Microb. Ecol.* 66, 23–32. <https://doi.org/10.3354/ame01548>
- Terada, A., Sugawara, S., Hojo, K., Takeuchi, Y., Riya, S., Harper, W.F., Yamamoto, T., Kuroiwa, M., Isobe, K., Katsuyama, C., Suwa, Y., Koba, K., Hosomi, M., 2017. Hybrid Nitrous Oxide Production from a Partial Nitrifying Bioreactor: Hydroxylamine Interactions with Nitrite. *Environ. Sci. Technol.* 51, 2748–2756. <https://doi.org/10.1021/acs.est.6b05521>
- Terada, A., Sugawara, S., Yamamoto, T., Zhou, S., Koba, K., Hosomi, M., 2013. Physiological characteristics of predominant ammonia-oxidizing bacteria enriched from bioreactors with different influent supply regimes. *Biochem. Eng. J.* 79, 153–161. <https://doi.org/10.1016/j.bej.2013.07.012>
- Third, K.A., Sliekers, A.O., Kuenen, J.G., Jetten, M.S.M., 2001. The CANON System (Completely Autotrophic Nitrogen-removal Over Nitrite) under Ammonium Limitation: Interaction and Competition between Three Groups of Bacteria. *Syst. Appl. Microbiol.* 24, 588–596. <https://doi.org/10.1078/0723-2020-00077>
- Thorndycroft, F.H., Butland, G., Richardson, D.J., Watmough, N.J., 2007. A new assay for nitric oxide reductase reveals two conserved glutamate residues form the entrance to a proton-conducting channel in the bacterial enzyme. *Biochem. J.* 401, 111–119. <https://doi.org/10.1042/BJ20060856>
- Torre, J.R.D.L., Walker, C.B., Ingalls, A.E., Könneke, M., Stahl, D.A., 2008. Cultivation of a thermophilic ammonia oxidizing archaeon synthesizing crenarchaeol. *Environ. Microbiol.* 10, 810–818. <https://doi.org/10.1111/j.1462-2920.2007.01506.x>
- Townsend-Small, A., Pataki, D.E., Tseng, L.Y., Tsai, C.-Y., Rosso, D., 2011. Nitrous oxide emissions from wastewater treatment and water reclamation plants in southern California. *J. Environ. Qual.* 40, 1542–1550. <https://doi.org/10.2134/jeq2011.0059>
- Toyoda, S., Mutoke, H., Yamagishi, H., Yoshida, N., Tanji, Y., 2005. Fractionation of N₂O isotopomers during production by denitrifier. *Soil Biol. Biochem.* 37, 1535–1545. <https://doi.org/10.1016/j.soilbio.2005.01.009>
- Toyoda, S., Suzuki, Y., Hattori, S., Yamada, K., Fujii, A., Yoshida, N., Kouno, R., Murayama, K., Shiomi, H., 2011a. Isotopomer Analysis of Production and Consumption Mechanisms of N₂O and CH₄ in an Advanced Wastewater Treatment System. *Environ. Sci. Technol.* 45, 917–922. <https://doi.org/10.1021/es102985u>
- Toyoda, S., Yano, M., Nishimura, S., Akiyama, H., Hayakawa, A., Koba, K., Sudo, S., Yagi, K., Makabe, A., Tobari, Y., Ogawa, N.O., Ohkouchi, N., Yamada, K., Yoshida, N., 2011b. Characterization and production and consumption processes of N₂O emitted from temperate agricultural soils determined via isotopomer ratio analysis. *Glob. Biogeochem. Cycles* 25. <https://doi.org/10.1029/2009GB003769>
- Upadhyay, A.K., Hooper, A.B., Hendrich, M.P., 2006. NO Reductase Activity of the Tetraheme Cytochrome c₅₅₄ of *Nitrosomonas europaea*. *J. Am. Chem. Soc.* 128, 4330–4337. <https://doi.org/10.1021/ja055183+>
- van Dongen, U., Jetten, M.S., van Loosdrecht, M.C., 2001. The SHARON-Anammox process for treatment of ammonium rich wastewater. *Water Sci. Technol. J. Int. Assoc. Water Pollut. Res.* 44, 153–160.

- Vannecke, T.P.W., Volcke, E.I.P., 2015. Modelling microbial competition in nitrifying biofilm reactors. *Biotechnol. Bioeng.* 112, 2550–2561. <https://doi.org/10.1002/bit.25680>
- Vázquez-Padín, J.R., Pozo, M.J., Jarpa, M., Figueroa, M., Franco, A., Mosquera-Corral, A., Campos, J.L., Méndez, R., 2009. Treatment of anaerobic sludge digester effluents by the CANON process in an air pulsing SBR. *J. Hazard. Mater.* 166, 336–341. <https://doi.org/10.1016/j.jhazmat.2008.11.055>
- Vlaeminck, S.E., De Clippeleir, H., Verstraete, W., 2012. Microbial resource management of one-stage partial nitritation/anammox. *Microb. Biotechnol.* 5, 433–448. <https://doi.org/10.1111/j.1751-7915.2012.00341.x>
- Wan, X., Baeten, J.E., Volcke, E.I.P., 2019. Effect of operating conditions on N₂O emissions from one-stage partial nitritation-anammox reactors. *Biochem. Eng. J.* 143, 24–33. <https://doi.org/10.1016/j.bej.2018.12.004>
- Wang, Q., Duan, H., Wei, W., Ni, B.-J., Laloo, A., Yuan, Z., 2017. Achieving Stable Mainstream Nitrogen Removal via the Nitrite Pathway by Sludge Treatment Using Free Ammonia. *Environ. Sci. Technol.* 51, 9800–9807. <https://doi.org/10.1021/acs.est.7b02776>
- Wang, X.-X., Fang, F., Chen, Y.-P., Guo, J.-S., Li, K., Wang, H., 2017. N₂O micro-profiles in biofilm from a one-stage autotrophic nitrogen removal system by microelectrode. *Chemosphere* 175, 482–489. <https://doi.org/10.1016/j.chemosphere.2017.02.026>
- Weissenbacher, N., Takacs, I., Murthy, S., Fuerhacker, M., Wett, B., 2010. Gaseous nitrogen and carbon emissions from a full-scale deammonification plant. *Water Environ. Res. Res. Publ. Water Environ. Fed.* 82, 169–175.
- Wells, G.F., Shi, Y., Laurenzi, M., Rosenthal, A., Szivák, I., Weissbrodt, D.G., Joss, A., Buerghmann, H., Johnson, D.R., Morgenroth, E., 2017. Comparing the Resistance, Resilience, and Stability of Replicate Moving Bed Biofilm and Suspended Growth Combined Nitritation–Anammox Reactors. *Environ. Sci. Technol.* 51, 5108–5117. <https://doi.org/10.1021/acs.est.6b05878>
- Wett, B., 2007. Development and implementation of a robust deammonification process. *Water Sci. Technol.* 56, 81–88. <https://doi.org/10.2166/wst.2007.611>
- Wett, B., Omari, A., Podmirseg, S.M., Han, M., Akintayo, O., Brandón, M.G., Murthy, S., Bott, C., Hell, M., Takács, I., Nyhuis, G., O’Shaughnessy, M., 2013. Going for mainstream deammonification from bench to full scale for maximized resource efficiency. *Water Sci. Technol.* 68, 283–289. <https://doi.org/10.2166/wst.2013.150>
- Woese, C.R., Weisburg, W.G., Paster, B.J., Hahn, C.M., Tanner, R.S., Krieg, N.R., Koops, H.-P., Harms, H., Stackebrandt, E., 1984. The phylogeny of purple bacteria: The beta subdivision. *Syst. Appl. Microbiol.* 5, 327–336. [https://doi.org/10.1016/S0723-2020\(84\)80035-1](https://doi.org/10.1016/S0723-2020(84)80035-1)
- Wrage, N., van Groenigen, J.W., Oenema, O., Baggs, E.M., 2005. A novel dual-isotope labelling method for distinguishing between soil sources of N₂O. *Rapid Commun. Mass Spectrom.* RCM 19, 3298–3306. <https://doi.org/10.1002/rcm.2191>
- Wrage, N., Velthof, G.L., van Beusichem, M.L., Oenema, O., 2001. Role of nitrifier denitrification in the production of nitrous oxide. *Soil Biol. Biochem.* 33, 1723–1732. [https://doi.org/10.1016/S0038-0717\(01\)00096-7](https://doi.org/10.1016/S0038-0717(01)00096-7)
- Wunderlin, P., Lehmann, M.F., Siegrist, H., Tuzson, B., Joss, A., Emmenegger, L., Mohn, J., 2013. Isotope Signatures of N₂O in a Mixed Microbial Population System: Constraints on N₂O Producing Pathways in Wastewater Treatment. *Environ. Sci. Technol.* 47, 1339–1348. <https://doi.org/10.1021/es303174x>
- Wunderlin, P., Mohn, J., Joss, A., Emmenegger, L., Siegrist, H., 2012. Mechanisms of N₂O production in biological wastewater treatment under nitrifying and denitrifying conditions. *Water Res.* 46, 1027–1037. <https://doi.org/10.1016/j.watres.2011.11.080>
- Yang, J., Trela, J., Plaza, E., 2016. Nitrous oxide emissions from one-step partial nitritation/anammox processes. *Water Sci. Technol.* 74, 2870–2878.

<https://doi.org/10.2166/wst.2016.454>

- Yang, J., Trela, J., Plaza, E., Tjus, K., 2013. N₂O emissions from a one stage partial nitrification/anammox process in moving bed biofilm reactors. *Water Sci. Technol.* 68, 144–152. <https://doi.org/10.2166/wst.2013.232>
- Zhang, L., Narita, Y., Gao, L., Ali, M., Oshiki, M., Ishii, S., Okabe, S., 2017. Microbial competition among anammox bacteria in nitrite-limited bioreactors. *Water Res.* 125, 249–258. <https://doi.org/10.1016/j.watres.2017.08.052>
- Zhang, T., Ye, L., Tong, A.H.Y., Shao, M.-F., Lok, S., 2011. Ammonia-oxidizing archaea and ammonia-oxidizing bacteria in six full-scale wastewater treatment bioreactors. *Appl. Microbiol. Biotechnol.* 91, 1215–1225. <https://doi.org/10.1007/s00253-011-3408-y>

Chapter 2: Comparison of different two-pathway models for describing the combined effect of DO and nitrite on the nitrous oxide production by ammonia-oxidizing bacteria

1. Introduction

Mathematical modeling of nitrous oxide (N_2O) emitted from biological wastewater treatment is one of the major challenges for minimizing greenhouse gas emissions (Ni *et al.*, 2011, 2013a; Pan *et al.*, 2013; Harper Jr. *et al.*, 2015). Several studies were dedicated to the development of new models describing N_2O emission during nitrification and denitrification, with the mechanisms being still under review (Ni *et al.*, 2011, 2013b, 2014, 2015; Law *et al.*, 2012; Harper Jr. *et al.*, 2015; Pocquet *et al.*, 2016). N_2O production associated to nitrification by autotrophic ammonia-oxidizing bacteria (AOB) was proven to contribute significantly to overall emissions (Kampschreur *et al.*, 2011; Wunderlin *et al.*, 2013; Wang *et al.*, 2014; Harper Jr. *et al.*, 2015), and mainly through two pathways: i) the nitrifier denitrification (ND) pathway (N_2O as the terminal product of nitrite reduction) (Law *et al.*, 2012; Wunderlin *et al.*, 2012; Ni *et al.*, 2013b); ii) the incomplete hydroxylamine oxidation (NN) pathway (N_2O as the side-product of NH_2OH oxidation) (Wunderlin *et al.*, 2012; Ni *et al.*, 2013b; Pocquet *et al.*, 2016). Previous work showed that single-pathway models, either based on ND or NN pathway, cannot reproduce all the N_2O production data including both short-term and long-term process monitoring (Ni *et al.*, 2013b; Sperandio *et al.*, 2014; Peng *et al.*, 2015a). Those conclusions indicated that both pathways are involved and a unified model was urgently required to incorporate both pathways in order to increase the genericity of the N_2O production model (Ni *et al.*, 2013b; Ni and Yuan, 2015; Mannina *et al.*, 2016; Pocquet *et al.*, 2016).

The first innovative 2-pathway model (marked Model I) was proposed by Ni *et al.* (2014) linking all biochemical oxidation and reduction processes through introducing a pool of electron carriers as new model components. This model has been able to describe the individual effect of dissolved oxygen (DO) on N_2O productions, and the simulated contribution of each pathway was consistent with the isotope measurements (Peng *et al.*, 2014). In addition, considering higher NO_2^- levels (from 3 to 50 mg N/L), the model was also calibrated to experiments with the combined effect of DO and nitrite (NO_2^-), and was capable of reproducing the batch experiment results (Peng *et al.*, 2015b). However, further calibration and validation of this 2-pathway model based on more varied experimental data and long-term monitoring are now necessary.

In parallel with a different model structure, another 2-pathway model (marked Model II) including five successive enzymatic reactions was developed by Pocquet *et al.* (2016). Unlike Model I, all the consumptions of electron donor and acceptor are connected without considering electron carriers. This model was calibrated, and was shown to well describe not only the data from batch experiments with various accumulated levels of nitrite, especially the trends observed for the $\text{NO}/\text{N}_2\text{O}$ ratio as well as N_2O emission factors ($\text{N}_2\text{O}_{\text{EF}}$), but also the long term N_2O emission data from a SBR process with variations of nitrite, pH and DO (Pocquet *et al.*, 2016). However, intrinsic assumptions due to the case study contained in this model should be further extended and more calibration and validation efforts from varying experimental observations are also required (Mannina *et al.*, 2016).

Side-by-side comparison of N₂O modeling by AOB is an effective method to examine both the capability and the applicability of models (Ni *et al.*, 2013b; Sperandio *et al.*, 2014; Peng *et al.*, 2015a; Pocquet *et al.*, 2016). Up to now, several studies were focused on the N₂O production model comparison work (Guo and Vanrolleghem, 2013; Mampaey *et al.*, 2013; Peng *et al.*, 2015a; Mannina *et al.*, 2016; Pocquet *et al.*, 2016). Ni *et al.* (2013b) compared the abilities of four different single-pathway models to predict N₂O dynamics in three case studies, and results showed that for each case, but not all, could be described by one single-pathway model. Spérandio *et al.* (2016) compared five activated sludge models describing N₂O production by AOB with four different long-term process data sets and the satisfactory calibration was obtained but none of the models was able to describe all the N₂O data obtained in the different systems with a similar parameter set. Peng *et al.* (2015a) compared two single-pathway models with Model I and identified the practical application conditions for each model in terms of DO and NO₂⁻. Furthermore, the comparison between Model II with other existing models was recently studied by Pocquet *et al.* (2016) which showed that NN pathway model was capable of describing the NO emissions but did not match the N₂O emission. However, the comparison between the two newly-developed 2-pathway models has not been done until now.

The first purpose of this study was to test and then compare the capabilities of the recently-developed 2-pathway models in describing the combined effect of DO and nitrite on the N₂O production by AOB from three different case studies (Peng *et al.*, 2014, 2015b; Pocquet *et al.*, 2016). The second is to provide insights into the applicability and the future calibration of these 2-pathway models of N₂O production by AOB.

2. Materials and methods

2.1 Experimental Data

As shown in Table 2.1, N₂O measurements (43 data sets in total) from three series of kinetic experiments with different types of microbial culture containing AOB were used for model evaluation. Conditions were chosen for testing the predictive abilities of two models respecting the combined effect of DO and NO₂⁻. Different influent feeding modes were used: continuous step-feeding for Case 1 and 2, batch feeding for Case 3 (Peng *et al.*, 2014, 2015b; Pocquet *et al.*, 2016) .

Table 2.1: Summary of the experimental data and operating conditions for three study cases.

	Case 1 (Peng <i>et al.</i> , 2015b): Batch DO and NO₂⁻ effect	Case 2 (Peng <i>et al.</i> , 2014): Batch DO effect	Case 3 (Pocquet <i>et al.</i> , 2016): Batch NO₂⁻ effect
Data	30 * (N ₂ OR _{sp})	7 * (N ₂ OR _{sp}) and SP measurements	6 * (N ₂ O _{EF})
DO (mg O₂/L)	Five levels: from 0.35 to 3.5	Seven levels: from 0.2 to 3.0	Similar level, dynamic Average at 4.5
NO₂⁻ (mg N/L)	Six levels: from 3.0 to 50	Low levels: from 1 to 1.5	Six levels: from 20 to 123
Feeding mode	Continuous feeding	Continuous feeding	Batch feeding
NH₄⁺ (mg N/L)	Around 20	Around 18	Initial of 10.5
pH	7.5	7.5	8.5 ± 0.1
Temperature (°C)	22	22	28
Biomass	I ^a : Enriched AOB+NOB	I ^a : Enriched AOB+NOB II: Another enriched NOB	I ^b : Enriched AOB II ^c : OHO

^a: With NOB activity; ^b: Without NOB activity; ^c: Ordinary Heterotrophic Organism

DO in Case 1 and 2 was controlled at desired level by a gas mixture of N₂ and air with a constant total flow rate (Peng *et al.*, 2014, 2015b). Comparatively, for Case 3, air flow rate was constant and DO showed dynamic profile similar for all the tests (Figure 2.S1). Average DO (4.5 mg O₂/L) is reported but the real dynamic DO data was used as the input for simulation. The NO₂⁻ concentrations remained constant for Case 1 and Case 2, but accumulated gradually during the batch test for Case 3. All the details of the experimental data and operating conditions could be found in the corresponding articles (Peng *et al.*, 2014, 2015b; Pocquet *et al.*, 2016). For the case 1 and 2, the total gas flow rate was controlled constantly at 0.5 L/min. For each change in altering DO concentration, the change in the air flow rate was compensated for by an equivalent opposite change in the N₂ flow rate. Consequently the effect of the change in DO on N₂O emission was only due to a biological effect rather than a modification of the N₂O stripping.

Biomass specific ammonia oxidation rate (AOR_{sp}), biomass specific N_2O production rate (N_2OR_{sp}) and the ratio between N_2O nitrogen emitted and the ammonium nitrogen converted (N_2O emission factor or N_2O_{EF}) were determined for each test. N_2O emission rate (N_2OR) was calculated by multiplying the measured gas phase N_2O concentration and the known gas flow rate. For case 1 and 2, as continuous feeding was maintained during several hours the emission rate stabilized and it was considered that the emission rate was equal to the formation rate. The average rate over each testing period (with constant conditions applied) was calculated by averaging the measured N_2OR over the period (relatively constant in all cases). N_2OR_{sp} ($mgN_2O-N/hr/g$ VSS) and AOR_{sp} ($mgNH_4^+-N/hr/g$ VSS) were calculated by normalizing the N_2OR and AOR data with the MLVSS concentration. The N_2O emission factor was calculated based on the ratio between the total N_2O emitted (mg N_2O-N) and the total NH_4^+ converted (mg NH_4^+-N) during each test. Comparatively for the case 3, as batch feeding was performed a dynamic emission of N_2O was obtained. The N_2O emission rate was then integrated in order to estimate the total N_2O emitted (mg N_2O-N) and calculate the N_2O emission factor.

2.2 Mathematical Models

The kinetic and stoichiometric matrices for the two 2-pathway models describing the N_2O productions are provided in the appendix (Tables 2.S1, S2) and detailed in published articles (Ni *et al.*, 2014; Pocquet *et al.*, 2016).

Table 2.2: Major differences between Model I and Model II.

	Model I (Ni <i>et al.</i> , 2014)	Model II (Pocquet <i>et al.</i> , 2016)
One-step simplification for ND pathway	Yes	Yes
Intracellular electron carrier (reduced and oxidized form)	Yes	No
True substrate for NH_4^+ oxidation	NH_4^+	NH_3
True substrate for NO_2^- reduction	NO_2^-	HNO_2
pH dependency	No	Yes
AOB growth	No	Yes
Effect of DO on the ND pathway	Electron competition	Inhibition

Both Model I and Model II considered the incorporation of NN and ND pathways and the simplification of ND by reducing the two-step nitrite reduction into one-step for avoiding the NO loop (Table 2.2). The main differences between those two models are the introduction of the electron carrier and the oxygen reduction as a separate process in Model I, while Model II does not. A recent study (Guo and Vanrolleghem, 2013) showed that the role of DO is still a controversial aspect regarding to N_2O modelling. For this consideration, in Model II inhibition of ND by oxygen was introduced into the ND pathway with a modified Haldane term which

decreases that process under high DO level, but also limits it at very low level. pH influence was included in Model II but not in Model I.

2.3 Model Calibration

Models were calibrated with three data series (Table 2.1) obtained from three different cultures (Ni *et al.*, 2014; Pocquet *et al.*, 2016). Model was initialized by inputting all the parameter values obtained originally from one specific data series (Ni *et al.*, 2014; Pocquet *et al.*, 2016). Simulation results were obtained or calculated, sensitivity analysis was then performed (based on an absolute/absolute deviation function) followed by a systematic analysis of the differences between the simulations and calibration targets (based on the root mean square deviation). Subsequently, a limited number of key parameters were chosen according to the sensitivity analysis and expert human knowledge in order to find the best-fitted values by continuing multiple calibration steps. Before prediction of N₂O emissions, the ammonium uptake rate and the profile of NH₄⁺, DO and nitrite should be properly captured. Hence the calibration was performed in two steps: First some parameters were calibrated to predict accurately the ammonium uptake rate and oxygen uptake rate (as for conventional nitrification models): $r_{NH_3,ox}$, K_{NH_3} and K_{O_2,NH_3} for model I; $\mu_{AOB,HAO}$, $K_{O_2,AOB,1}$, $K_{O_2,AOB,2}$ for Model II. Then regarding the N₂O prediction specifically the most important parameters to be adapted were those related to the maximum production rate of each pathway: $r_{NO_2,red}$, $r_{NO_2,red}$ for Model I, $\eta_{N_2O,ND}$, $\eta_{N_2O,NN}$ for Model II. Additionally the affinity constant for nitrite or free nitrous acid (Model I or II), the oxygen inhibition constant (Model II), the affinity constants for M_{red,3} & M_{red,4} and for M_{ox} (Model I) were adapted if necessary.

Parameter values were estimated by minimizing the root mean square deviation between measured data and model predictions for all the three cases. All simulations were performed with AQUASIM software.

3. Results

Case 1: Combined DO and NO_2^- effect on culture 1

Figures 2.1-3 showed all the simulation results of Case 1 with Model I and Model II including the $\text{N}_2\text{O}_{\text{sp}}$ (specific N_2O production rate) and the contributions of ND and NN pathway.

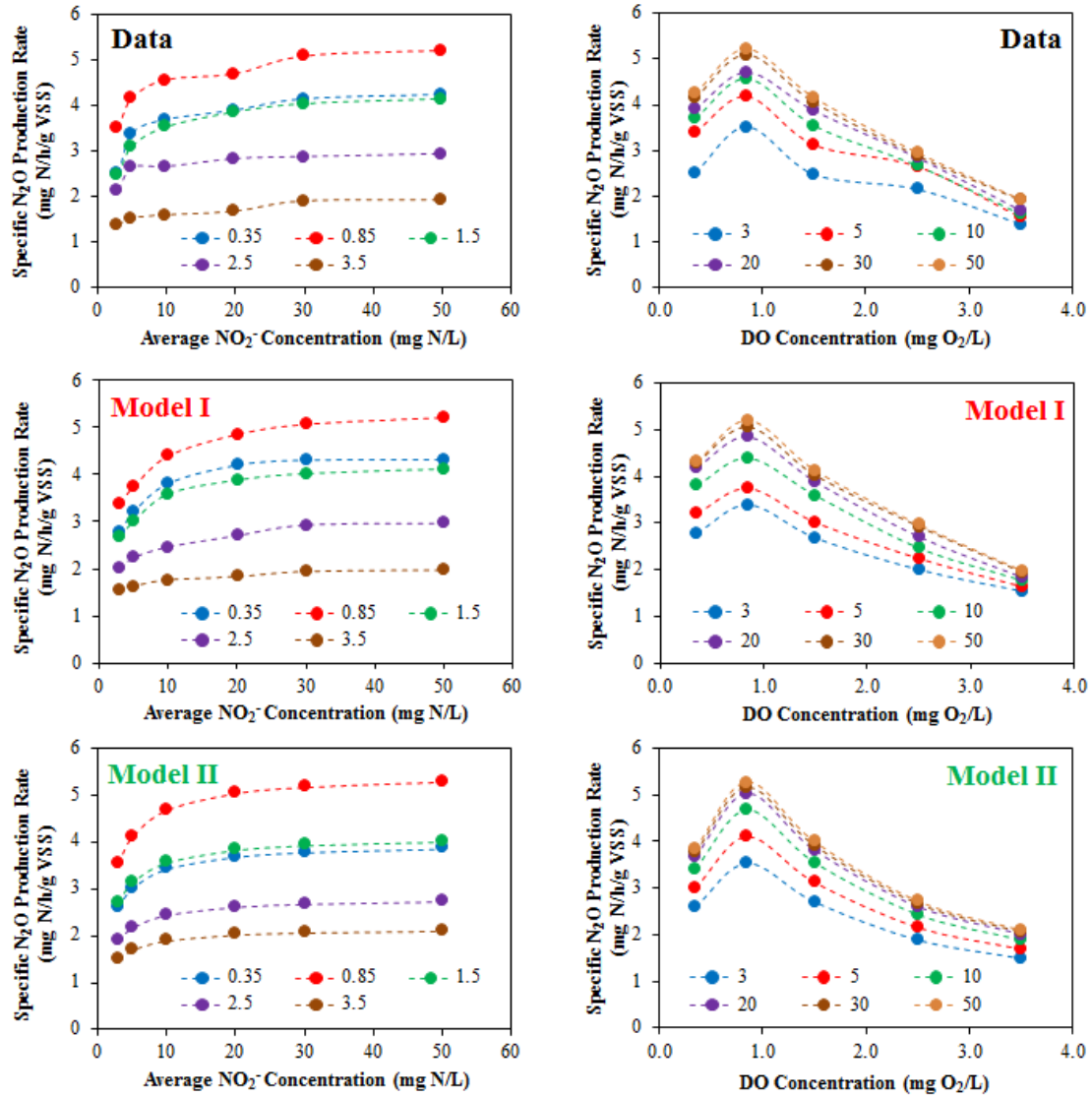


Figure 2.1: Experimental and simulated $\text{N}_2\text{O}_{\text{sp}}$ in function of DO and NO_2^- concentrations in Case 1 (Peng *et al.*, 2015b): The value of mark from the left figures represent the values for DO, for the right figures NO_2^- .

As shown in Figure 2.1 and Figure 2.2, both Model I and Model II are able to describe the tendency of experimental $\text{N}_2\text{O}_{\text{sp}}$ concerning the effect of NO_2^- and DO as well as the values. Simulations results showed that under each investigated DO level, $\text{N}_2\text{O}_{\text{sp}}$ increased as the NO_2^- increased from 3 to 50 mg N/L, while for each NO_2^- level, the maximum $\text{N}_2\text{O}_{\text{sp}}$ occurred at DO

of 0.85 mg O₂/L (Figure 2.1). Even with a small difference, the simulated N₂O_{sp} of two models matched the experimental data very well (Figure 2.2).

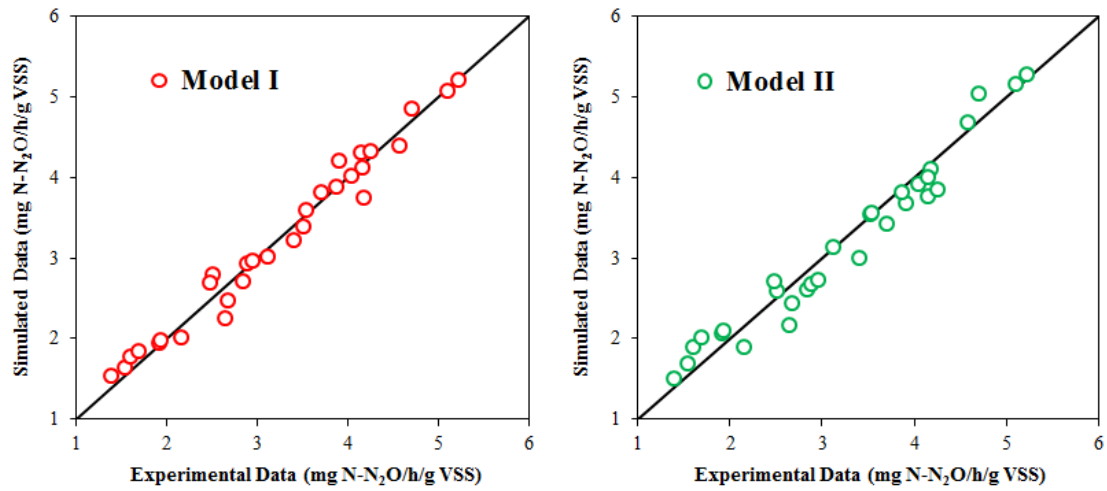


Figure 2.2: Comparison of simulated N₂O_{sp} between Model I and Model II against the experimental data in Case 1.

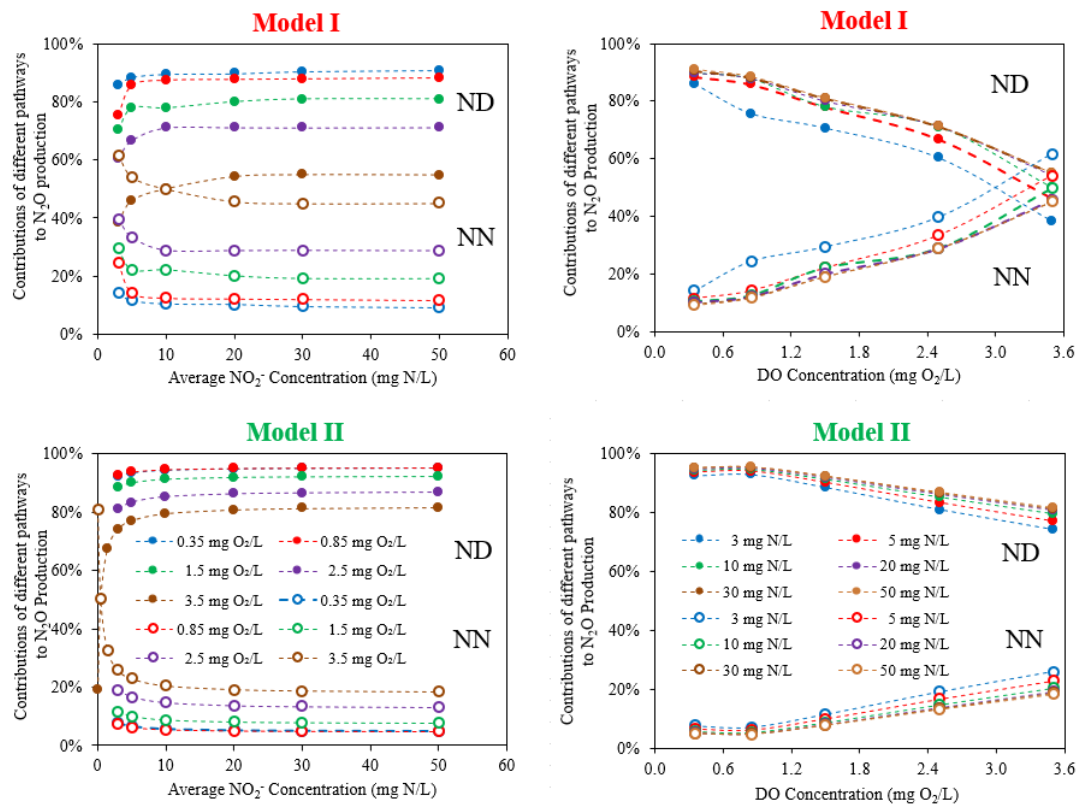


Figure 2.3: Model-predicted contributions of ND and NN pathways with Model I and Model II under various DO and NO₂⁻ concentrations in Case 1.

As to the predictions of the ND pathway by two models, the result from Model I was slightly lower than that in Model II, which is even stronger at higher DO levels. Simulations with Model

II showed that the ND pathway dominated over NN during the whole DO and nitrite levels, which is not the case for Model I where the contribution of NN pathway was higher than 50% under the DO of 3.5 mg O₂/L and NO₂⁻ of 3 and 5 mg N/L.

In order to see whether NN pathway could be the dominant pathway over ND with the further decrease of the NO₂⁻ concentration by Model II, additional simulations were performed under three even lower NO₂⁻ levels (0.1, 0.5 and 1.5 mg N/L) and the highest DO of 3.5 mg O₂/L. The simulation results (Figure 2.3) showed that, with the continued decreasing of NO₂⁻ concentration, the contribution of ND pathway decreased and reached almost half at NO₂⁻ of 0.5 mg N/L and declined to no more than one fifth, in accompany with the NN pathway becoming the major contributor. Figures 2. S2- S4 showed other simulation results in terms of N₂O_{EF} and an example of the dynamic for the batch test with Model II.

In summary, for the investigated DO (from 0.35 to 3.5 mg O₂/L) and NO₂⁻ (from 3 to 50 mg N/L), both Model I and Model II could well describe all the experimental N₂O_{sp}. Similar tendency of the predicted contributions for ND and NN pathway was obtained by two models but contributions of ND predicted with Model I are lower than that obtained with Model II. By decreasing NO₂⁻ level, further predictions by Model II showed the contribution of NN pathway will gradually increase and exceeding the ND pathway.

Case 2: DO effect at low NO₂⁻ level with culture 2

Figures 2.4-6 showed all the simulation results of Case 2 with Model I and Model II in terms of N₂O_{sp}, contributions of ND and NN pathway and N₂O_{EF}.

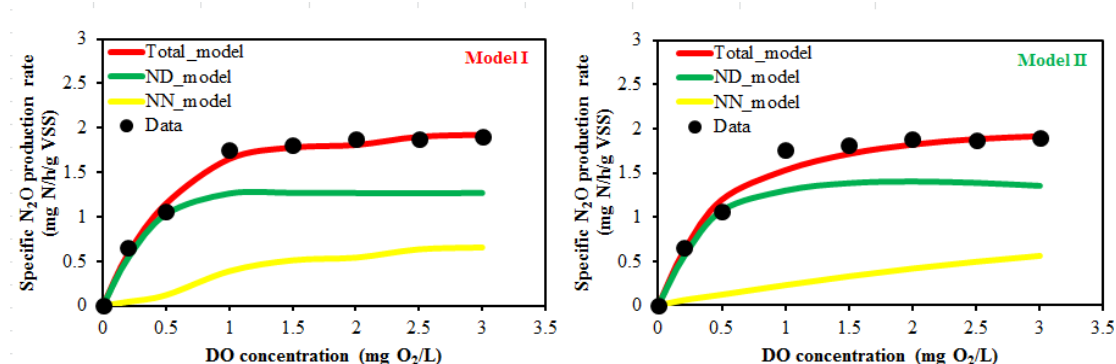


Figure 2.4: Comparison of experimental and simulated N₂O_{sp} with Model I and Model II in Case 2 (Peng *et al.*, 2014).

As shown in Figure 2.4, both models enable to capture the tendency and value of experimental observed N₂O_{sp} very well during the investigated DO range from 0 to 3 mg O₂/L. Specifically, both model predictions showed that N₂O_{sp} increased as the DO increased from 0 to 1 mg O₂/L and remained almost constant for further increase.

Meanwhile, the predicted contributions for the ND and NN pathway by two models are also in agreement with that obtained by the isotopic measurements (Figure 2.5), both of which

showed that the contribution of ND pathway decreases when DO increases from 0.2 to 3 mg O₂/L, and that for NN increases accordingly.

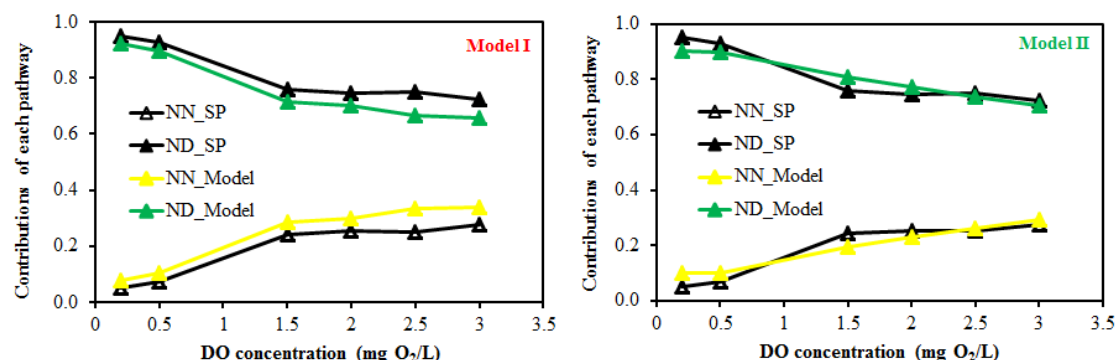


Figure 2.5: Comparison of the model-predicted contributions between Model I and Model II in Case 2. SP: Site-specific measurements.

For further analysis, both simulated AOR and calculated N₂O_{EF} (emission factor estimated by averaging simulated N₂O_{sp} with simulated AOR) against the experimental data were displayed in Figure 2.6.

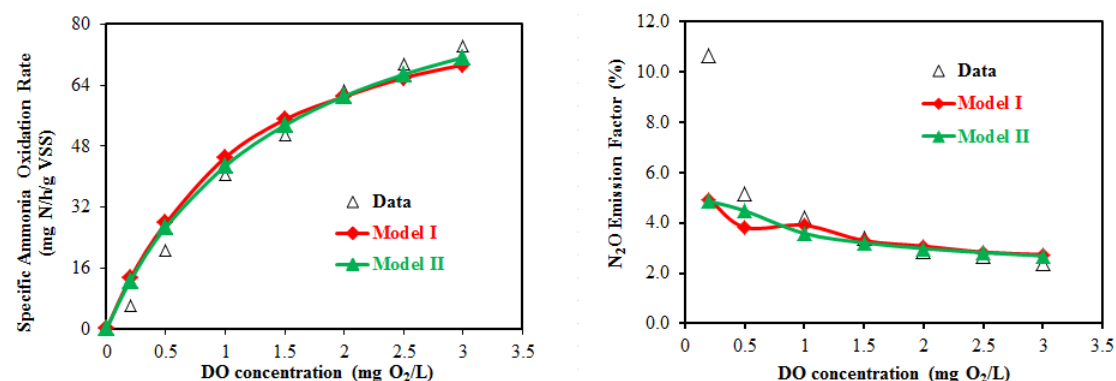


Figure 2.6: Comparison of simulated and experimental data for AOR and N₂O_{EF} between Model I and Model II in Case 2.

In terms of AOR, the simulation results of the AORs matched well with the experimental observed AOR, except for lower rates at DO equal or lower than 0.5 mg O₂/L. Regarding the N₂O_{EF}, both models showed similar predictions and described the decrease tendency of the N₂O_{EF} during the whole DO levels from 0.2 to 3 mg O₂/L, except for the lowest DO level (0.2 mg O₂/L), both model simulations were under-estimated over the experimental data. But this was related to the difficulty for predicting low DO effect on AOR, the N₂O production rate being correctly predicted.

To summarize, both Model I and Model II could well describe the experimentally observed N₂O_{sp} during this investigated range for DO (from 0.2 to 3 mg O₂/L) and nitrite (lower than 2 mg N/L). Both model predictions and SP measurements showed the similar contributions for both ND and the NN pathway. The simulated AOR and N₂O_{EF} matched quite well with the experimental data, but N₂O_{EF} was underestimated when DO was lower than 0.5 mg O₂/L.

Case 3: Nitrite effect in culture 3

Figure 2.7 showed the simulation results of N_2O_{EF} in Case 3 with Model I and Model II in terms of nitrite and HNO_2 .

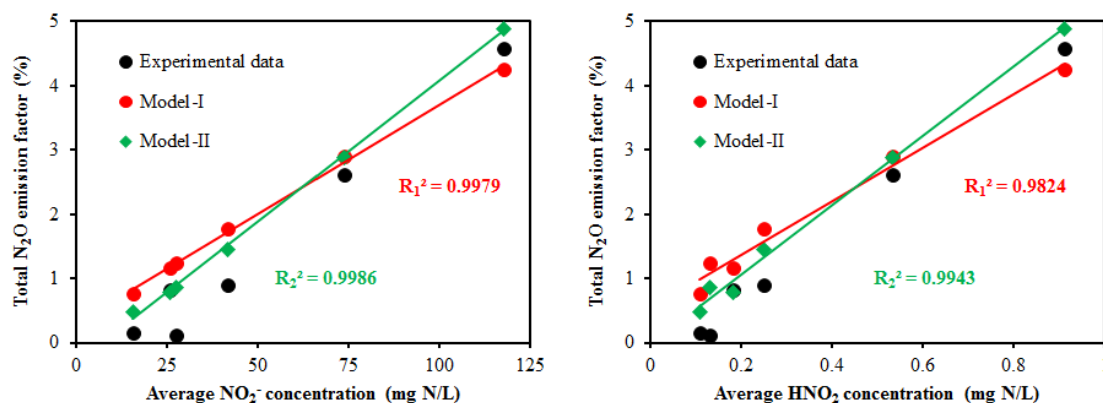


Figure 2.7: Comparison of experimental and simulated N_2O_{EF} with Model I and Model II in function of NO_2^- and HNO_2 respectively in Case 3.

As shown in Figure 2.7, the two 2-pathway models were both able to reproduce the experimental N_2O_{EF} in this case study. For the relation with NO_2^- , the total N_2O_{EF} increased with the increase of average NO_2^- concentration almost linearly and the models could generally describe the experimental data. From the perspective of HNO_2 , which consider the effect of pH, the simulation results is even closer to the experimental data compared with that obtained by the nitrite., with a slight advantage of model II, which takes into account the pH effect by considering FA and FNA as substrate in kinetics. However, only the small pH difference (≤ 0.2) was observed among those experiments.

To summarize, both Model I and Model II could well describe the experimental observed N_2O_{EF} in this case during investigated NO_2^- concentration (20-123 mg N/L). A better simulation could be obtained in consideration of the HNO_2 instead of NO_2^- with Model II.

4. Discussion

In this work, we selected three different cases including 43 kinetic experiments considering a large range for both DO and nitrite concentrations (Table 2.1), and the two models were compared for the first time based on their capabilities to predict the observed N_2O data including both N_2O_{sp} and N_2O_{EF} (Ni *et al.*, 2014; Peng *et al.*, 2014, 2015b; Pocquet *et al.*, 2016). Overall, the two different two-pathway models with different mathematical structures could be calibrated to describe similarly the experimental N_2O emissions collected in the different experimental systems.

Peng *et al.* (2015b) investigated the combined effect of DO (0.35 to 3.5 mg O_2 /L) and NO_2^- (3 to 50 mg N/L) on N_2O production by AOB as well as the corresponding mechanisms and the experimental data were well captured with Model I at all conditions (case 1). For Model II, by adjusting only three parameters ($\eta_{N_2O,ND}$, $K_{NO_2,AOB,Nor}$, $K_{HNO_2,AOB}$) compared with the original model (Pocquet *et al.*, 2016) (Tables 2.S2 and S4), the model was also able to well describe the data. As to the individual effect of DO and nitrite on N_2O emissions for case 2 (Peng *et al.*, 2014) and case 3 (Pocquet *et al.*, 2016), both models also showed a good prediction of the N_2O_{sp} (case 2: Figure 2.4) and N_2O_{EF} (case 3: Figure 2.7) as well as the predicted contributions of the ND and NN pathway (case 2, Figure 2.5) which were in accordance with the isotopic measurements. For the effect of DO on the N_2O emission factor, both the two different model structures allowed to predict the observed tendencies. It should be notice that both models can describe a contradictory effect of oxygen depending on the preponderant pathway. At low nitrite the N_2O emission can increase with DO due to importance of NN pathway whereas at high nitrite level the N_2O emission decreases with DO due to preponderance of ND pathway (Figure 2.1). In both models the DO increase limits the ND pathway due to either electron acceptor competition (Model I) or inhibition (Model II), while it favors the NN pathway contribution. This is in accordance with the studies based on isotopes signature measurements (Peng *et al.*, 2014).

Concerning the predicted contribution of each pathway the same variations and tendencies were obtained but quantitative contribution of each pathway can slightly differ. For the contributions of each pathway considering the effect of NO_2^- at higher levels (case 1: from 3 to 50 mg N/L) and lower levels (case 2: lower than 2 mg N/L), predictions by both models showed the same stimulating effect of NO_2^- on the contribution of the ND pathway (NN: inhibiting) but with slightly different values (case 1: Figure 2.3 and case 2: Figure 2.5). The same result was also obtained by a further simulation with Model II considering even lower NO_2^- (0.1, 0.5 and 1.5 mg N/L) which showed that NN pathway could become dominant pathway with enough lower NO_2^- level (Figure 2.3 and Table 2.3). This positive correlation between the ND contribution and NO_2^- concentration is also consistent with the simulation results obtained by Peng *et al.* (2015a). It should be noted that, the similar observation found by Wunderlin *et al.* (2013) showed the same contribution of the ND pathway around 75% to 100%, which is closer to the results obtained by Model II than in Model I. Therefore, the difference between the simulated contributions of two pathways by two models should be further confirmed with diverse situations and new isotopic measurements.

Regarding the choice of considering HNO_2 in Model II compared with NO_2^- in Model I, the model II could predict slightly better result of $\text{N}_2\text{O}_{\text{EF}}$ than in model I with culture 3 for which slight pH change were observed (Figure 2.7). One possible explanation is that model II considers as the true substrate HNO_2 instead of nitrite in Model I. As a consequence Model II predicts a stimulating effect of pH decrease on the ND pathway. Law *et al.* (2011) found pH can influence both the $\text{N}_2\text{O}_{\text{sp}}$ and AOR but future work will be needed to confirm how the pH should be taken into account. This could be achieved by combining pH models with Model II and confrontation with experiments in an extended range of pH.

Table 2.3: Comparison of simulation results with Model I and Model II

	Model I	Model II
Predict the contradictory effect of DO depending on nitrite level and the preponderant pathway	Yes	Yes
Predict the stimulating effect of NO_2^- on the ND pathway contribution	Yes	Yes
Predict the stimulating effect of DO on the NN pathway contribution (validated by isotope signature)	Yes	Yes
Total number of parameters	19	12 (+2 for growth)
Number of parameters to be calibrated for the different cultures	5 to 10	3 to 8
Predict the stimulating effect of pH decrease on ND pathway (through HNO_2)	No	Yes

Regarding the calibration (see parameter values on Table 2.S2-S4) the same set of parameters was used for each culture but some parameters should be calibrated depending on the culture case. Small parameter modifications (only 3 parameters) were necessary with the model II from the case 3 (nitrite variation) to case 1 (nitrite and DO variation), but higher effort (8 parameters) was needed for case 2 (DO variation at low nitrite level). In comparison 5 parameters were modified with Model I for case 1 and 2, but higher effort was necessary for case 3 (10 parameters). Hence the effort was slightly higher with model I but not that significant. On one hand, Model I seems easier to fit to the data obtained at low nitrite with different DO, as in that condition the ND contribution was initially overestimated by Model II and the total production was practically poorly inhibited by DO. By considering the competition between nitrite and oxygen for electron carrier S_{Mred} the Model I probably describe in a more realistic mechanism than inhibition. On the other hand the calibration of model I in case 3 with dynamic variation of ammonium and nitrite was quite complicated due to important modifications needed on affinity constant on species which are not measurable ($K_{\text{NO}_2, \text{ox}}$, $K_{\text{Mred}, 3}$, $K_{\text{Mred}, 4}$). In contrast for Model II, all parameters are related to variables which can be directly measured or calculated. Finally the Table 2.3 gives an overview of the models comparison. Electron transport included in Model I increases the model complexity but makes it closer to the real metabolic processes, leading to a perfect model for a better understanding. This could be also useful in practice if the model would describe more accurately some observations or if the calibration effort would be reduced. However our comparison did not show a real advantage of model I on the used data series as the model II was also able to describe similarly the observations without needing more calibration effort. But this should not be considered as a definitive conclusion. For instance it should be

remarked that suspended biomass only were simulated in this work, and a future comparison for biofilm systems would be also necessary (Sabba *et al.*, 2015). Finally further work should be devoted to obtain parameters with different experiments and cultures, which should be compared and synthesized, aiming to form a consistent pattern for the implementation in the improvement/simplification of the 2-pathway models.

5. Conclusion

This study has validated the two different 2-pathway models with extensive sets of experiments under different DO and/or nitrite conditions with different cultures. Despite their different mathematical structures both models were able to describe accurately the synergetic effect of DO and nitrite on the N₂O emissions. The results did not demonstrate strong difference in their application ranges (e.g. higher NO₂⁻ or lower NO₂⁻). The model I describes in detail the metabolic electron transport and is more appropriate for understanding whereas the model II is simpler but sufficiently accurate for capturing the combined effect of nitrite and oxygen on N₂O emissions.. Work is now recommended with data from full scale systems in which the medium complexity and the combination with other biochemical reactions could reveal stronger difference between these two models.

6. Acknowledge

This work was supported by the French National Research Agency (ANR) and the China Scholarship Council (CSC).

References

- Guo L, Vanrolleghem PA. 2013. Calibration and validation of an activated sludge model for greenhouse gases no. 1 (ASMG1): prediction of temperature-dependent N₂O emission dynamics. *Bioprocess and Biosystems Engineering* **37**: 151–163.
- Harper Jr. WF, Takeuchi Y, Riya S, Hosomi M, Terada A. 2015. Novel abiotic reactions increase nitrous oxide production during partial nitrification: Modeling and experiments. *Chemical Engineering Journal* **281**: 1017–1023.
- Kampschreur MJ, Kleerebezem R, de Vet WWJM, van Loosdrecht MCM. 2011. Reduced iron induced nitric oxide and nitrous oxide emission. *Water Research* **45**: 5945–5952.
- Law Y, Lant P, Yuan Z. 2011. The effect of pH on N₂O production under aerobic conditions in a partial nitrification system. *Water Research* **45**: 5934–5944.
- Law Y, Ni B-J, Lant P, Yuan Z. 2012. N₂O production rate of an enriched ammonia-oxidizing bacteria culture exponentially correlates to its ammonia oxidation rate. *Water Research* **46**: 3409–3419.
- Mampaey KE, Beuckels B, Kampschreur MJ, Kleerebezem R, van Loosdrecht MCM, Volcke EIP. 2013. Modelling nitrous and nitric oxide emissions by autotrophic ammonia-oxidizing bacteria. *Environmental Technology* **34**: 1555–1566.
- Mannina G, Ekama G, Caniani D, Cosenza A, Esposito G, Gori R, Garrido-Baserba M, Rosso D, Olsson G. 2016. Greenhouse gases from wastewater treatment — A review of modelling tools. *Science of The Total Environment* **551–552**: 254–270.
- Ni B-J, Yuan Z. 2015. Recent advances in mathematical modeling of nitrous oxides emissions from wastewater treatment processes. *Water Research* **87**: 336–346.
- Ni B-J, Rusalleda M, Pellicer-Nàcher C, Smets BF. 2011. Modeling Nitrous Oxide Production during Biological Nitrogen Removal via Nitrification and Denitrification: Extensions to the General ASM Models. *Environmental Science & Technology* **45**: 7768–7776.
- Ni B-J, Ye L, Law Y, Byers C, Yuan Z. 2013a. Mathematical Modeling of Nitrous Oxide (N₂O) Emissions from Full-Scale Wastewater Treatment Plants. *Environmental Science & Technology* **47**: 7795–7803.
- Ni B-J, Yuan Z, Chandran K, Vanrolleghem PA, Murthy S. 2013b. Evaluating four mathematical models for nitrous oxide production by autotrophic ammonia-oxidizing bacteria. *Biotechnology and Bioengineering* **110**: 153–163.
- Ni B-J, Peng L, Law Y, Guo J, Yuan Z. 2014. Modeling of Nitrous Oxide Production by Autotrophic Ammonia-Oxidizing Bacteria with Multiple Production Pathways. *Environmental Science & Technology* **48**: 3916–3924.
- Ni B-J, Pan Y, van den Akker B, Ye L, Yuan Z. 2015. Full-Scale Modeling Explaining Large Spatial Variations of Nitrous Oxide Fluxes in a Step-Feed Plug-Flow Wastewater Treatment Reactor. *Environmental Science & Technology* **49**: 9176–9184.
- Pan Y, Ni B-J, Yuan Z. 2013. Modeling Electron Competition among Nitrogen Oxides Reduction and N₂O Accumulation in Denitrification. *Environmental Science & Technology* **47**: 11083–11091.
- Peng L, Ni B-J, Erler D, Ye L, Yuan Z. 2014. The effect of dissolved oxygen on N₂O production by ammonia-oxidizing bacteria in an enriched nitrifying sludge. *Water Research* **66**: 12–21.
- Peng L, Ni B-J, Ye L, Yuan Z. 2015a. Selection of mathematical models for N₂O production by ammonia oxidizing bacteria under varying dissolved oxygen and nitrite concentrations. *Chemical Engineering Journal* **281**: 661–668.
- Peng L, Ni B-J, Ye L, Yuan Z. 2015b. The combined effect of dissolved oxygen and nitrite on N₂O production by ammonia oxidizing bacteria in an enriched nitrifying sludge. *Water Research* **73**: 29–36.

- Pocquet M, Wu Z, Queinnec I, Spérandio M. 2016. A two pathway model for N₂O emissions by ammonium oxidizing bacteria supported by the NO/N₂O variation. *Water Research* **88**: 948–959.
- Sabba F, Picioreanu C, Pérez J, Nerenberg R. 2015. Hydroxylamine diffusion can enhance N₂O emissions in nitrifying biofilms: a modeling study. *Environ Sci Technol.* **49**(3):1486-1494.
- Spérandio M, Pocquet M, Guo L, Vanrolleghem PA, Ni B-J, Yuan Z. 2014. Calibration of nitrous oxide production models with continuous long-term process data. In *The 4th IWA/WEF Wastewater Treatment Modelling Seminar(WWTmod2014)* Spa, Belgium; 99–121.
- Spérandio M, Pocquet M, Guo L, Ni B-J, Vanrolleghem PA, Yuan Z. 2016. Evaluation of different nitrous oxide production models with four continuous long-term wastewater treatment process data series. *Bioprocess and Biosystems Engineering* **39**: 493–510.
- Wang Q, Jiang G, Ye L, Pijuan M, Yuan Z. 2014. Heterotrophic denitrification plays an important role in N₂O production from nitrification reactors treating anaerobic sludge digestion liquor. *Water Research* **62**: 202–210.
- Wunderlin P, Mohn J, Joss A, Emmenegger L, Siegrist H. 2012. Mechanisms of N₂O production in biological wastewater treatment under nitrifying and denitrifying conditions. *Water Research* **46**: 1027–1037.
- Wunderlin P, Lehmann MF, Siegrist H, Tuzson B, Joss A, Emmenegger L, Mohn J. 2013. Isotope Signatures of N₂O in a Mixed Microbial Population System: Constraints on N₂O Producing Pathways in Wastewater Treatment. *Environmental Science & Technology* **47**: 1339–1348.

SUPPLEMENTARY DATA:

Table 2.S1: Process matrices for the two 2-pathway models evaluated in this study

Model components										Kinetic rate expressions
Processes	S_{N_2O}	S_{NO_2}	S_{NO}	S_{NH_2OH}	S_{NH}	S_{O_2}	S_{Max}	S_{Mred}	X_{AOB}	
s										
Model I										
R-1				1	-1	-1	1	-1		$R1 = r_{NH_2OH,ox} \frac{S_{O_2}}{S_{O_2} + K_{O_2,NH_2}} \frac{S_{NH}}{S_{NH} + K_{NH_2}} \frac{S_{Mred}}{S_{Mred} + K_{Mred,1}} X_{AOB}$
R-2			1	-1			-	3/2		$R2 = r_{NH_2OH,ox} \frac{S_{NH_2OH}}{S_{NH_2OH} + K_{NH_2OH}} \frac{S_{Max}}{S_{Max} + K_{Max}} X_{AOB}$
R-3		1	-1				-	1/2		$R3 = r_{NO,ox} \frac{S_{NO}}{S_{NO} + K_{NO,ox}} \frac{S_{Max}}{S_{Max} + K_{Max}} X_{AOB}$
R-4	1/2		-1					1/2	-	$R4 = r_{NO,red} \frac{S_{NO}}{S_{NO} + K_{NO,red}} \frac{S_{Mred}}{S_{Mred} + K_{Mred,2}} X_{AOB}$
R-5						-1/2	1	-1		$R5 = r_{O_2,red} \frac{S_{O_2}}{S_{O_2} + K_{O_2,red}} \frac{S_{Mred}}{S_{Mred} + K_{Mred,3}} X_{AOB}$
R-6	1/2	-1					1	-1		$R6 = r_{NO_2,red} \frac{S_{NO_2}}{S_{NO_2} + K_{NO_2}} \frac{S_{Mred}}{S_{Mred} + K_{Mred,4}} X_{AOB}$
R-7										$S_{Mred} + S_{Max} = C_{tot}$
Model II										
A-1				1	-1	-1.14				$R1 = q_{AOB,AMO} \frac{S_{O_2}}{S_{O_2} + K_{O_2,AOB,1}} \frac{S_{NH_2}}{S_{NH_2} + K_{NH_2,AOB}} X_{AOB}$
A-2		$\frac{1}{Y_{AOB}}$	$-\frac{1}{Y_{AOB}}$	$-i_{N,BM}$	$-\frac{1.71 - Y_{AOB}}{Y_{AOB}}$			1		$R2 = \mu_{AOB,HAO} \frac{S_{O_2}}{S_{O_2} + K_{O_2,AOB,2}} \frac{S_{NH_2OH}}{S_{NH_2OH} + K_{NH_2OH,AOB}} \frac{S_{NH}}{S_{NH} + 10^{-12}} X_{AOB}$
A-3		1	-1			-0.57				$R3 = q_{AOB,HAO} \frac{S_{O_2}}{S_{O_2} + K_{O_2,AOB,2}} \frac{S_{NO}}{S_{NO} + K_{NO,AOB,HAO}} X_{AOB}$
A-4	4	1	-4	-1						$R4 = q_{AOB,HAO} \eta_{N_2O,NN} \frac{S_{NH_2OH}}{S_{NH_2OH} + K_{NH_2OH,AOB}} \frac{S_{NO}}{S_{NO} + K_{NO,AOB,Nor}} X_{AOB}$
A-5	2	-1		-1						$R5 = q_{AOB,HAO} \eta_{N_2O,ND} \frac{S_{NH_2OH}}{S_{NH_2OH} + K_{NH_2OH,AOB}} \frac{S_{HNO_2}}{S_{HNO_2} + K_{HNO_2,AOB}} DO_{Holdane} X_{AOB}$
										$DO_{Holdane} = \frac{S_{O_2}}{K_{O_2,AOB,ND} + (1 - 2 \cdot \sqrt{K_{O_2,AOB,ND} / K_{1,O_2,AOB}}) \cdot S_{O_2} + S_{O_2}^2 / K_{1,O_2,AOB}}$

Table 2.S2: All calibrated parameters of Model I in three cases

Name	Description	Unit	Case1(Peng <i>et al.</i> , 2015b)	Case 2(Peng <i>et al.</i> , 2014)	Case 3(Pocquet <i>et al.</i> , 2016)
Model I					
$r_{NH_3,ox}$	Maximum ammonia oxidation rate	mmol/(g VSS*h)	19.17	17.7	35
$r_{NH_2OH,ox}$	Maximum NH ₂ OH oxidation rate	mmol/(g VSS*h)	22.86	22.86	22.86
$r_{NO,ox}$	Maximum NO oxidation rate	mmol/(g VSS*h)	22.86	22.86	22.86
$r_{O_2,red}$	Maximum oxygen reduction rate	mmol/(g VSS*h)	48.02	38.5	48.02
$r_{NO_2,red}$	Maximum nitrite reduction rate	mmol/(g VSS*h)	3.06	3.92	5.5
$r_{NO,red}$	Maximum NO reduction rate	mmol/(g VSS*h)	0.016	0.012	0.03
K_{O_2,NH_3}	Oxygen affinity constant for ammonia oxidation	mmol O ₂ /L	0.066	0.047	0.03125
K_{NH_3}	Ammonia affinity constant for ammonia oxidation	mmol N/L	0.17	0.17	0.01429
K_{NH_2OH}	NH ₂ OH affinity constant for NH ₂ OH oxidation	mmol N/L	0.05	0.05	0.05
$K_{NO,ox}$	NO affinity constant for NO oxidation	mmol N/L	0.0006	0.0006	0.00002143
$K_{O_2,red}$	Oxygen affinity constant for oxygen reduction	mmol O ₂ /L	0.0019	0.0019	0.0019
K_{NO_2}	Nitrite affinity constant for nitrite reduction	mmol N/L	0.2	0.01	43
$K_{NO,red}$	NO affinity constant for NO reduction	mmol N/L	0.0006	0.0006	0.0005714
K_{Mox}	S _{Mox} affinity constant for NH ₂ OH and NO oxidation	mmol/g VSS	0.028	0.01*C _{tot}	0.01*C _{tot}
$K_{Mred,1}$	S _{Mred} affinity constant for ammonia oxidation	mmol/g VSS	0.001*C _{tot}	0.001*C _{tot}	0.001*C _{tot}
$K_{Mred,2}$	S _{Mred} affinity constant for NO reduction	mmol/g VSS	0.001*C _{tot}	0.001*C _{tot}	0.001*C _{tot}
$K_{Mred,3}$	S _{Mred} affinity constant for oxygen reduction	mmol/g VSS	0.069	0.069	0.012
$K_{Mred,4}$	S _{Mred} affinity constant for nitrite reduction	mmol/g VSS	0.013	0.19	0.002
C_{tot}	The constant sum of S _{Mred} and S _{max}	mmol/g VSS	0.01	0.01	0.01

Table 2.S3: All calibrated parameters of Model II in three cases

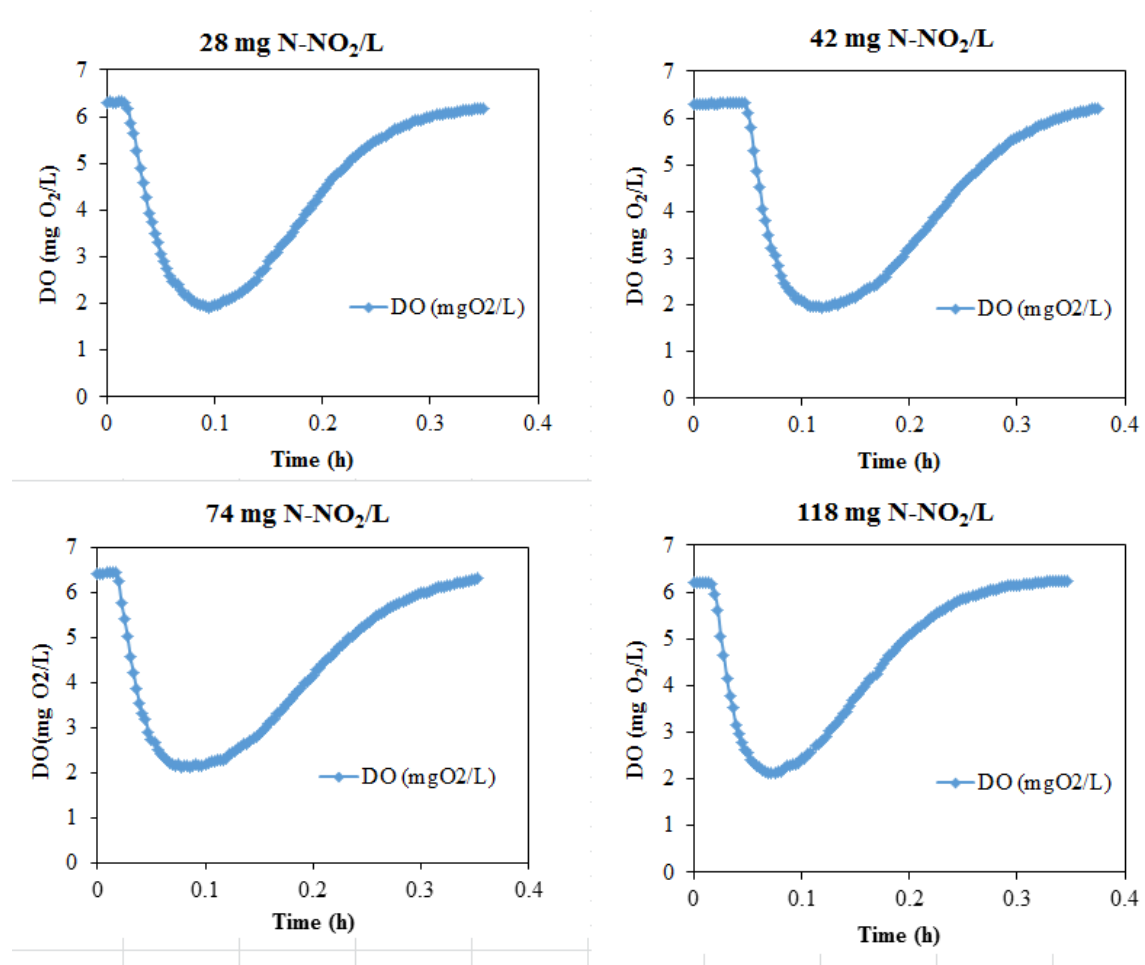
Name	Description	Unit	Case1	Case 2	Case 3
Model II					
$\eta_{N_2O,ND}$	Reduction factor applied for the ND pathway	dimensionless	0.0250	0.1056	0.250
$\eta_{N_2O,NN}$	Reduction factor applied for the NN pathway	dimensionless	0.0015	0.07693	0.0015
$\mu_{AOB,HAO}$	Maximum AOB growth rate during HAO reaction	1/h	0.0325	0.019944	0.0325
$K_{O_2,AOB,1}$	AOB affinity constant for O ₂ AMO reaction	mg-O ₂ /L	1	1.5000	1
$K_{NH_3,AOB}$	AOB affinity constant for NH ₃	mg-N/L	0.2	0.2	0.2
$K_{O_2,AOB,2}$	AOB affinity constant for O ₂ (HAO)	mg-O ₂ /L	0.6	0.3	0.6
$K_{NH_2OH,AOB}$	AOB affinity constant for NH ₂ OH	mg-N/L	0.9	0.9	0.9
$K_{NO,AOB,HAO}$	AOB affinity constant for NO from (HAO)	mg-N/L	0.0003	0.0003	0.0003
$K_{NO,AOB,Nor}$	AOB affinity constant for NO from NirK	mg-N/L	0.0004	0.0080	0.008
$K_{HNO_2,AOB}$	AOB affinity constant for HNO ₂	mg-N/L	0.00014	0.00073	0.004
$K_{O_2,AOB,ND}$	Haldane constant from ND by Haldane	mg-O ₂ /L	0.5	0.0190	0.5
$K_{I,O_2,AOB}$	Haldane constant from ND	mg-O ₂ /L	0.8	4.5	0.8
$i_{N,BM}$	Fration of NH in biomass	mg-N/mg-CODX	0.07	0.07	0.07
Y_{AOB}	AOB growth yield	mg-CODX/mg-N	0.15	0.15	0.15
$q_{AOB,AMO}$	Maxiumum rate for AMO reaction	mg N / (mg-COD*h)	0.2167	0.1330	0.2167
$q_{AOB,HAO}$	Maximum AOB kinetic coefficient for HAO reaction	mg-N / (mg-COD*h)	0.2167	0.1330	0.2167

Note: $q_{AOB,AMO} = q_{AOB,HAO} = \mu_{AOB,HAO} / Y_{AOB}$

Table 2.S4: Summary of the calibrated parameters (Original: Model I of culture I(Ni *et al.*, 2014) and Model II(Pocquet *et al.*, 2016))

	Model I			Model II		
	Case 1	Case 2	Case 3	Case 1	Case 2	Case 3
Process reaction rate or related parameters		$r_{NH_3,ox}$				
			$r_{NH_3,ox}$		$\eta_{N_2O,ND}$	
	$r_{NH_3,ox}$	$r_{O_2,red}$	$r_{NO_2,red}$	$\eta_{N_2O,ND}$	$\eta_{N_2O,NN}$	-
		$r_{NO_2,red}$			$\mu_{AOB,HAO}$	
		$r_{NO,red}$	$r_{NO,red}$			
Affinity constant parameters			K_{O_2,NH_3}			
			K_{NH_3}			
	K_{O_2,NH_3}				$K_{O_2,AOB,1}$	
	K_{NO_2}		$K_{NO,ox}$			
		K_{O_2,NH_3}	K_{NO_2}	$K_{NO,AOB,Nor}$	$K_{O_2,AOB,2}$	-
	K_{Max}			$K_{HNO_2,AOB}$	$K_{HNO_2,AOB}$	
	$K_{Mred,4}$		$K_{NO,red}$			
Other parameters			$K_{Mred,3}$			
			$K_{Mred,4}$			
	-	-	-	-	$K_{O_2,AOB,ND}$	-
					$K_{I,O_2,AOB}$	

Figure 2.S1: Experimental DO variation during the batch test for Case 3 under different NO_2^- levels^a.



Note: Value of the NO_2^- concentration is the average value which was calculated as half of the sum of the start and the end concentration

Figure 2.S2: Comparison between simulated (constant period) and experimental (whole period) N_2O_{EF} in Case 1

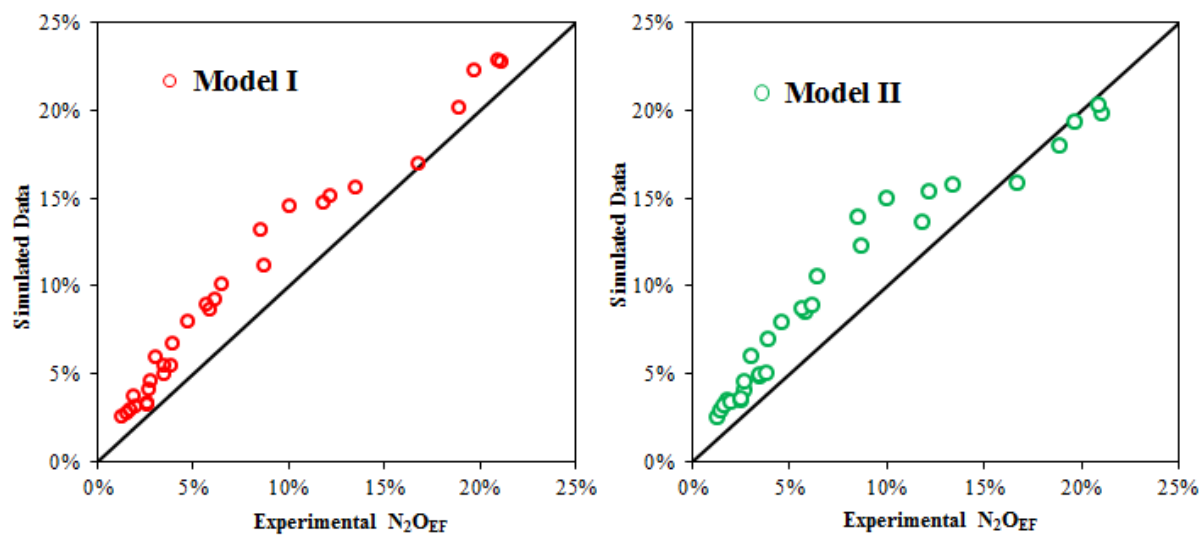


Figure 2.S3: Correlations between Model I-predicted and Model II-predicted N_2O_{EF} in Case 1.

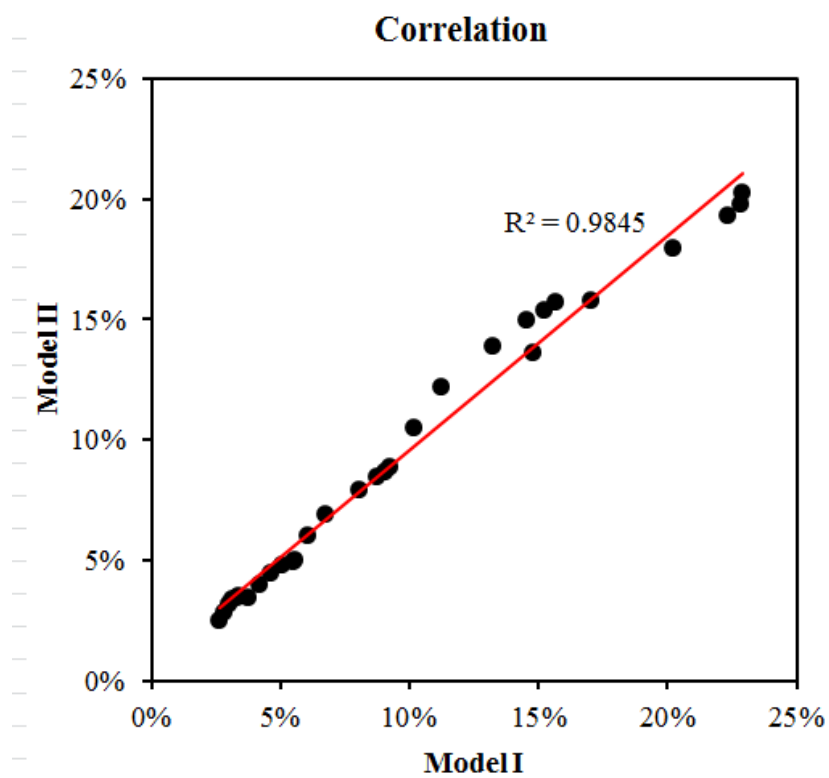
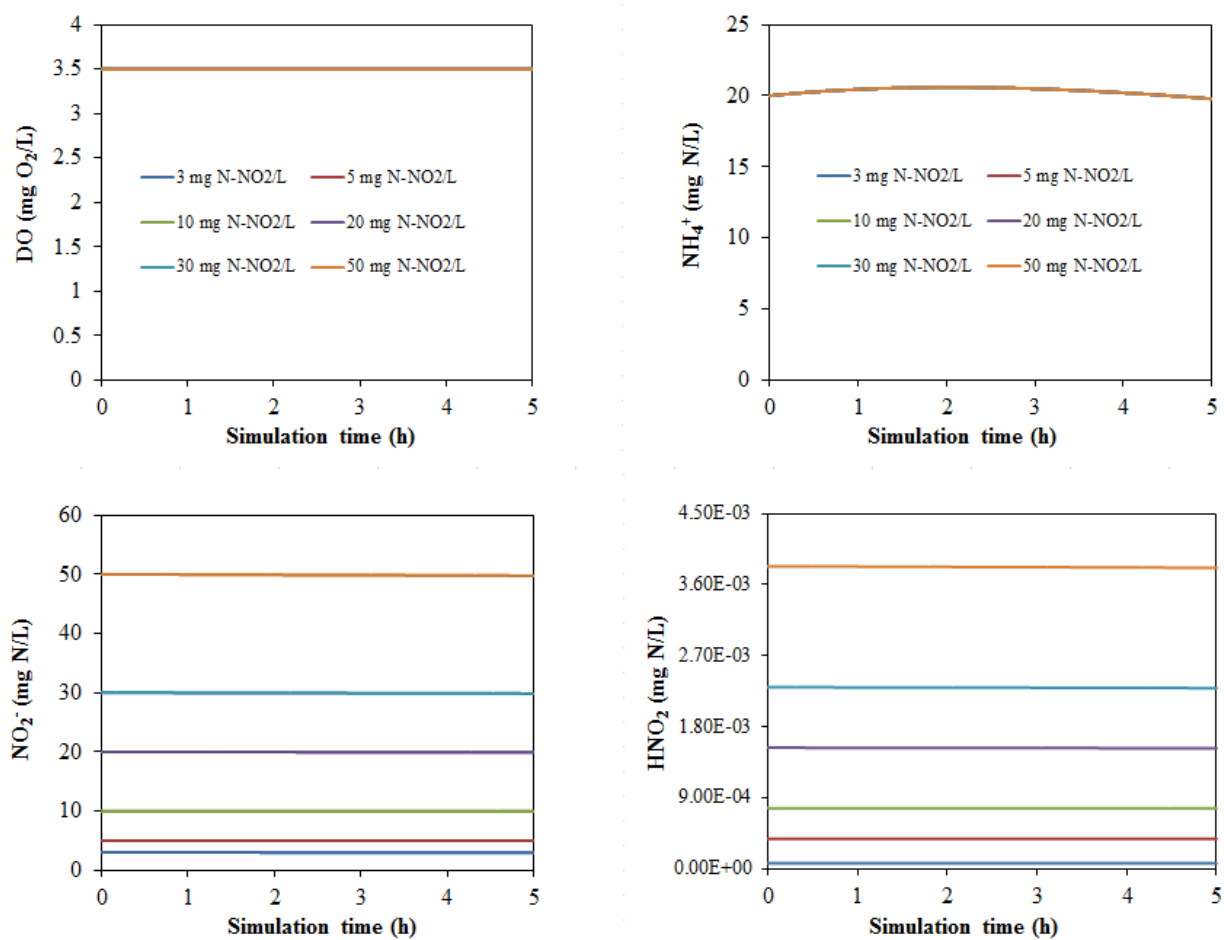


Figure 2.S4: Simulated levels of NH_4^+ , DO and NO_2^- as well as HNO_2 in a series of batch tests by Model I. (DO at 3.5 mg O_2/L ; NO_2^- from 3 to 50 mg N/L) in Case 1



Chapter 3: One-stage partial nitrification anammox under oxygen limitation: performance, stoichiometry, N₂O emission and microbial segregation

1. Introduction

In the last decade, autotrophic conversion of ammonium into dinitrogen by partial nitrification coupled to anammox process (PNA) has been developed with successful applications at full scale. The process is today applicable for treating high strength rejection water coming from anaerobic digestion (Lackner et al., 2014), whereas research is very active for investigating application at lower temperature on the main stream for sewage treatment (Lotti et al., 2014a; Gilbert et al., 2014; Laureni et al., 2016; Agrawal et al., 2017; De Cocker et al., 2018).

Researching robust operating conditions and control strategies for single stage PNA process is still very important to cope with simultaneous and possibly contradictory objectives: (1) maximizing the nitrogen removal efficiency, (2) minimizing the energy needs and (3) reducing N₂O emission (greenhouse gas). Indeed the relatively high emission factor of N₂O can be considered as a major risk and drawback of such new process.

Without appropriate control, up to $10.9 \pm 3.2\%$ of the removed nitrogen (Domingo-Félez et al., 2014) can be emitted when we know that an increase by only 1% of the emission factor can offset the benefit of PNA in term of global carbon footprint (Besson et al., 2017).

Lackner et al. (2014) surveyed over 100 full-scale PNA plants with 88% being operated as single-stage system, revealing some operational difficulties as the incoming solids, the aeration control and nitrate built up. Recent reviews (Cao et al., 2017; Agrawal et al., 2018; Baeten et al., 2019) all reveals the needs for mechanistic understanding of these autotrophic communities in such granular sludge systems and highlighted the importance of guiding methods for accurate control. Ideally such control system should maintain the aerobic ammonium oxidation (AOB) at a sufficiently high rate but not higher than the maximal capacity of anammox to anaerobically consume the produced nitrite with excess of ammonium. And obviously limiting the NOB growth is systematically considered as the major challenge of such control to maximize the performance of the system.

Aeration and feeding strategies are the most generally considered parameters for such control. Continuous feeding (Sliekers et al., 2002; Morales et al., 2016; Connan et al., 2018), successive batch feeding (Domingo-Félez et al., 2014; Gilbert et al., 2015, Castro-Barros et al., 2015), as well as intermittent feeding mode can be successfully applied (Harris et al., 2015). Generally it appears that maintaining high ammonium concentration or significant residual ammonium concentration help to repress the NOB (through FA inhibition notably) and anammox species to growth. Indeed anammox takes advantage to work without ammonium limitation for better competing for nitrite with NOB. Finally regarding the N₂O emissions it is still difficult to find a consensus in literature about the effect of feeding mode and pattern.

Controlling simultaneously the air flow rate and the aeration time is generally used to control the equilibrium between the activity of both aerobic and anaerobic oxidizing bacteria (Akaboci et al. 2018). By controlling the reaction with oxygen transfer rate (OTR) it is possible to adapt the rate of the process to both the biomass capacity and the nitrogen loading rate (NLR). This leads to the question about effect of low DO concentration on both nitrification rate (NRR), energy and N₂O emissions. Very recently Akaboci et al. (2018) reported that working at extremely low DO (under the detection limit) did not compromise the PNA process and

allowed to maintain at 25°C a NRR of 0.3-0.4 kg m⁻³ d⁻¹, when in comparison Ali et al. (2016) observed the granular sludge PNA with NRR of 0.4-0.6 kg m⁻³ d⁻¹ under a DO level of 1.0 mg O₂ L⁻¹. Even higher NRR can be reached (1.1 kg m⁻³ d⁻¹) in a study by De Clippeleir et al. (2009) under the DO between 0.3 and 0.7 mg O₂ L⁻¹.

Advantage of working at low DO is naturally the low energy requirements, because the gradient between saturated oxygen concentration and DO is maximal (Fan et al., 2017), this allows to transfer more with the same transfer coefficient. However the microbial genus diversity and the adaptation of autotrophic species in granular sludge at such low DO condition was poorly studied. Effect of oxygen limitation on competition between aerobic AOB, Anaerobic AOB (Anammox) and NOB is still controversial. It was reported that regarding the affinity constant for oxygen, low oxygen was not completely detrimental for nitrite oxidizing organisms (Akaboci et al., 2018). Low DO combined with high ammonium concentration allowed repressing efficiently NOB at least in sidestream configuration, but low DO as a single parameter did not permit to repress NOB in mainstream condition. Basically an indirect effect of lowering DO is to limit the nitrification rate and limiting nitrite accumulation in the bulk liquid which influences the competition between anammox and NOB.

Concerning the direct effect of dissolved oxygen and oxygen transfer rate on N₂O emissions contradictory observations have been reported in literature (Kampschreur et al., 2009; Domingo-Félez et al., 2014; Castro-Barros et al., 2015; Harris et al., 2015). On the one hand N₂O production by AOB is considered to be encouraged when lowering DO through the nitrifiers denitrification pathway: nitrite becoming an alternative electron acceptor is reduced into NO and N₂O (Peng et al., 2014, 2015). But on the other hand high air flow rate also increases the gas/liquid transfer coefficient for all the gases encouraging NO and N₂O loss. Moreover increasing the air flow rate can result in higher nitrite accumulation and possibly higher N₂O emission through the same nitrifiers denitrification pathway. Using alternating aeration, Domingo-Félez et al. (2014) showed that significant decreases in N₂O emissions were obtained when the frequency of aeration was increased while maintaining a constant air flow rate (from >6 to 1.7% ΔN₂O/ΔTN). However, no significant effect on the emissions was noted when the duration of aeration was increased while decreasing air flow rate (10.9 ± 3.2% ΔN₂O/ΔTN). Operating under conditions where anaerobic exceeds aerobic ammonium oxidation activity was proposed to minimize N₂O emissions from single-stage nitrification/anammox reactors. In contrast, Ma et al. (2017) recently showed that the DO concentration exerted the strongest control on net N₂O production, production pathways being stimulated by low O₂ independently of NO₂⁻ concentrations. Through mathematical modelling of a granular sludge reactor Wan et al. (2019) shows that individual changes of operating parameters led to large and often non-monotonic changes in the N₂O emissions. For this author this could explain the large variety of emissions factors and some apparent contradictions found in literature. The dissolved oxygen (DO) concentration that allows simultaneous low N₂O emissions and high nitrogen removal appeared to be very site-specific, depending on the granule size. This last question regarding the possible role of granule size distribution and biomass segregation on N₂O emission has been poorly investigated until now due to the difficulty in controlling this parameter in practice.

The objective of this study is thus to investigate the long term behavior of a single stage granular sludge PNA process operated under DO limitation. With a control system based on oxygen transfer rate (OTR) and aeration time, the process has been operated during more than 300 days at a relatively low temperature (26.6°C) for exploring possible application under sidestream and mainstream application. Removal efficiencies and rates were monitored, overall stoichiometry was analysed with long term evolution of N₂O emissions, microbial communities and particle size were characterized revealing significant biomass segregation.

2. Materials and methods

2.1 SBR operational mode

The experiment was conducted in a laboratory-scale reactor with a working volume of 11 L and a headspace volume of 3 L. The reactor was equipped with mechanical stirring and gas diffuser. Air flow rate was imposed by a mass flowmeter (Bronkorst). The pH (H8481 HD, SI Analytics), temperature and dissolved oxygen (DO) with (VisifermTM, Hamilton), dissolved CO₂ (Membrane Kit InPro5000 3.1B, Mettler Toledo) as well as Oxidation-Reduction Potential (PL89225Pt, SI Analytics) probes were continuously monitored with online-equipped sensors in the liquid phase. The off-gas was continuously sampled from the top of the reactor at a constant flow rate of 0.06 L/min and measured with online devices for N₂O (X-STREAM X2GP, Emerson) and NO (NGA 2000 CLD, Emerson) concentrations. To prevent from the moisture, a condenser and hydrophobic gas filter (0.2µm) were installed before gas analyzers. The N₂O and NO gas analyzers were calibrated monthly. Data were logged every 1-2 min by an online software. The temperature was maintained at 26.6 ± 0.6 °C using a water jacket. pH was maintained (6.9-7.5) through dosing 1 M NaHCO₃ or injecting CO₂ gas.

The reactor was inoculated with granular sludge (0.87±0.03 g VSS L⁻¹) taken from a single stage PNA process, and stored at 4°C during transport. For recovering anammox activity it was first operated in anoxic condition with supplying ammonium and nitrite for 36 days (details in supplementary information). At the end of this period maximal anammox activity was 9.4 mg N-NH₄⁺ g VSS⁻¹ h⁻¹. Then the reactor was operated in SBR mode with continuous aeration during reaction phase during 293 days with a synthetic influent containing ammonium as sole nitrogen source.

The cycle consisted in the following sequence: anoxic feeding (8 min), aerated reaction phase (variable), settling (2 min), and withdraw (8 min). 1L of liquid was added or removed during feeding or decanting period, resulting in a volumetric exchange ratio (VER) of 9.1%.

The synthetic influent mimicked a high strength wastewater with high level of ammonium (500 mgN L⁻¹) without organic matter. The composition was adapted from van de Graaf et al. (1996): 2.36 g/L (NH₄)₂SO₄ (0.5 g/LNH₄-N), 3.00 g/L NaHCO₃, 0.025 g/L KH₂PO₄, 0.2 g/L MgSO₄·7H₂O, 0.147 g/L CaCl₂·2H₂O and 2 mL of trace element solutions I and II. Trace element solution I contained 3 g/L EDTA and 3.93 g/L FeCl₂·4H₂O; And trace element solution II contained 15 g/L EDTA, 0.43 g/L ZnSO₄·7H₂O, 0.24 g/L CoCl₂·6H₂O, 1.21 g/L MnCl₂·4H₂O, 0.25 g/L CuSO₄·5H₂O; 0.24 g/L Na₂MoO₄·2H₂O, 0.32 g/L NiSO₄·7H₂O, 0.16g/L Na₂SeO₃·5H₂O, 0.01

g/L H_3BO_3 , 0.05 g/L $\text{Na}_2\text{WO}_4 \cdot 2\text{H}_2\text{O}$. This feeding solution had a pH of 8.2 and a molar ratio of ammonium to bicarbonate of 1:1. It was stored at 4°C and changed every week.

Table 3.1: Operational conditions during the study.

Phase	A1 (Days1-101)	B1 (Days102-106)	A2 (Days107-145)	B2 (Days146-293)
Air flow rate (L h^{-1})	4.5	11.7	4.5	11.7
Maximum DO set point ($\text{mg O}_2 \text{ L}^{-1}$)	0.3, 1.0 and 2.0 ^{II}	0.3	0.3	0.3
T ($^{\circ}\text{C}$) ^I	26.6±0.6	26.6±0.4	26.5±0.5	26.7±0.3
pH	7.2±0.3	7.4±0.1	7.4±0.1	7.4±0.1
VER (%)	9.1	9.1	9.1	9.1
Bulk DO ($\text{mg O}_2 \text{ L}^{-1}$) ^I	0.065±0.057 (101)	0.011±0.002 (5)	0.00±0.00 (62)	0.00±0.00 (434)
Q (L d^{-1}) ^I	1.4±0.3 (101)	2.8±0.1 (5)	1.9±0.2 (62)	3.2±0.3 (434)
HRT (d) ^I	8.1±1.6 (101)	3.9±0.2 (5)	6.0±0.6 (62)	3.4±0.3 (434)
Cycle length (h) ^I	17.7±3.4 (101)	8.5±0.3 (5)	13.0±1.4 (62)	7.5±0.7 (434)
Aeration (h) ^I	17.5±3.4 (101)	8.2±0.3 (5)	12.8±1.4 (62)	7.2±0.7 (434)
Feed (min)	8	8	8	8
Settling (min)	2	2	2	2
Discharging (min)	8 ^{III} and 5	5	5	5

I: Parameter value: average value ± standard deviation (n), n indicates the measurement times;

II: The value was increased from 0.3 to 2.0 $\text{mg O}_2 \text{ L}^{-1}$ on Day39, decreased to 1.0 $\text{mg O}_2 \text{ L}^{-1}$ on Day96, and decreased to 0.3 $\text{mg O}_2 \text{ L}^{-1}$ on Day100.

III: The length of discharging decreased from 8 to 5 min on Day39.

2.2 Aeration control and oxygen transfer rate

Air flow rate was imposed for limiting the dissolved oxygen to a very low value ($<0.2 \text{ mg.L}^{-1}$) controlling the ammonium oxidation rate by oxygen transfer rate (OTR):

Equation 3.1

$$\text{OTR} = K_L a \cdot (\text{DO}^* - \text{DO})$$

The DO concentration measured in the bulk during reaction phase was initially between 0.02-0.2 $\text{mg O}_2 \text{ L}^{-1}$ decreasing during almost 100 days (phase A1), was still detectable in phase B1, but became completely undetectable after Day 107 (Table 3.1).

Reaction phase duration was automatically controlled by detecting the end of the ammonium oxidation. Aeration was switched off and settling started as soon as a maximal DO setpoint was reached. Indeed DO rapidly increased at the end of nitrification due to ammonium depletion and lower oxygen demand. After testing different setpoints (0.3, 1.0 and 2.0 $\text{mg O}_2 \text{ L}^{-1}$) during phase A1, it was fixed at 0.3 $\text{mg O}_2 \text{ L}^{-1}$ during the entire period. As the duration of reaction time was automatically controlled, the nitrogen loading rate was close to the ammonium uptake rate and finally also imposed by the OTR.

Dynamic method was used to determine periodically the oxygen transfer coefficient for oxygen (K_La) (Garcia-Ochoa and Gomez, 2009). Measurements were performed with effluent from SBR cycles without biomass but with the mineral medium. Stripping with N_2 and oxygenating were performed successively for different airflow rates (0, 1.1, 3.9, 10.7, 27.8, 45 $L\ h^{-1}$). See details in SI. Measurements were done in duplicates. Linear correlation was obtained between coefficient and air flow rate ($K_La=0.076.Q_{air}+0.2075$; $R^2= 0.9871$). This experiment was also conducted during the study to quantify the slight evolution of the correlation (at days 160: $K_La=0.076.Q_{air}+0.3755$; $R^2=0.9671$) which is assumed to be related to diffuser properties (fouling can reduce the bubble size for instance).

The influence of aeration intensity on reactor performance was studied by imposing two different levels of air flow rates (periods A and B). Initially the imposed air flow rate (Q_{air}) was chosen (level A: 4.5 $L\ h^{-1}$) for maintaining an ammonium uptake rate of about 25% of maximal anoxic anammox rate. The correlation between air flow rate and transfer coefficient (K_La) was first determined. Then air flow rate was chosen in order to maintain oxygen-limiting conditions during the reaction period (DO close to 0.1 mg/L). After 100 days, air flow rate was increased to level B during one week, before reducing to level A for 40 days. Level B was definitively imposed at Day 145 until the end of the study (300 days). The level B (11.7 $L.h^{-1}$) was chosen in order to adapt the oxygen transfer rate to the increase of nitrification rate. It was also fixed in order to not observe any nitrite accumulation in the reactor (meaning that nitrite production rate by AOB was lower than the maximal nitrite consumption rate by anammox). Finally regarding the applied air flow rate, the operating period could be further divided into four phases: A1, A2 (low air flow rate), B1 and B2 (high air flow rate). This protocol allowed evaluating both the short term and long term effect of a change in the aeration rate to the nitrogen removal rate.

2.3 Chemical analysis

Mixed liquor samples were taken periodically for NH_4^+ , NO_2^- and NO_3^- analyses. For the effluent with low content of granules, the liquid sample was immediately filtrated through 0.2 μm milipore filters and was stored at 4°C for further chemical analysis. While for batch samples, in order to prevent the loss of granular sludge, the centrifuge at 4°C for 2 min was performed before the filtration and the concentrated sludge was collected and returned back to the reactor at the feeding phase of next cycle.

Ammonium was measured using spectrophotometric method with the Nessler standard method (AFNOR NFT 90-015). Nitrite and nitrate concentrations were quantified using spectrophotometric methods, using a continuous flow analyzer SMARTCHEM200 (AMS, Italy). Total suspended solids (TSS), ash content and volatile suspended solids (VSS) were measured according to standard methods (APHA et al., 1998).

2.4 Particle size distribution (PSD), sieving and microbial analysis

Granules were harvested from the reactor during the aeration phase for microscopic observation and particle size determination. Stirring rate was slightly increased (twice) during the sampling for improving the homogeneity in the reactor. Samples were diluted with distilled water, placed on a plastic transparent plate, ensuring the clear dispersion of granules without attaching each other. Images were captured with a NIKON DS-U2 digital microscope camera. At least 50 pictures were taken for representative image analysis. The image treatment first consisted of a conversion to greyscale using Irfan View software (v.4.10). Next, using Visilog software (v.6.7), the pixel-scale values were converted by a scaling factor. Each grey-scale image underwent a binarization step after which the surface of each particle was quantified and used to estimate the sphere-equivalent diameter. The used script was made so that particles touching the edge of the photo or with a diameter smaller than 15 μm would not be detected. The obtained data was then treated in Excel with a visual basic macro to obtain the number, surface and volume weighted PSD, and mean diameters.

For analyzing the community developed in different granules categories, the biomass was fractionated using two stainless sieves with mesh size of 315 μm and 1000 μm ; resulting in three categories: < 315 μm , between 315 and 1000 μm , and > 1000 μm . Sieving protocol was adapted from Laguna et al. (1999).

The sequencing analysis was conducted twice before the reactor was operated in limiting-oxygen condition and when it had been operated for 193 days. For all the samples (day 1 and day 193), one sample of 1.5 mL mixed liquor were taken from the reactor, and separated with varying diameters or not. It was used for microbial community analyses. After centrifugation (20 min at 19,000g), supernatant was removed and the remaining biomass was immediately frozen in liquid nitrogen. DNA extraction of these samples was performed using the FastDNA spinkit™ from MP biomedical following the provided Fastprep® protocol. The extracted DNA was stored at $-20\text{ }^{\circ}\text{C}$ until further use.

For the first analysis, in order to map AnAOB enrichment, qPCR was used to quantify the AnAOB based on phylogenetic primers (16S rRNA) and functional primers (hzsA). Also, to follow up the composition of the overall community, the analysis was performed twice. For the first time, the MiSeq illumine sequencing was performed by the Geno ToulGenomics and Transcriptomics facility (GeT-PlaGe, Auzerville, France). Sequencing data was performed using the pipeline FROGS, one of the tools proposed on Galaxy, an open web-based platform for genomic research. For the second analysis, the DNA from samples S1, S2 and S3 were assayed with Qubit (Qubit™ dsDNA BR Assay Kit). The libraries were created from 3ng of DNA. The variable regions of the 16S rDNA of the bacteria were amplified using ThermoFisher's Ion 16S Metagenomics kit. The libraries were created using the Ion Plus Fragment Library kit and Ion Xpress™ Barcode Adapters according to the manufacturer's recommendations (ThermoFisher). The libraries obtained were quantified using the Qubit™ dsDNA HS Assay Kit and the bioanalyzer 2100 (Agilent-DNA1000 kit). 8pg/ μl of each library were pooled together, amplified on beads by emulsion PCR and enriched on the Ion OneTouch™ 2 System (ThermoFisher) using the Ion 520 & 530 OT2 kit. The template was sequenced (400pb oriented

single end) on the Ion Torrent S5 using an Ion 520 chip. The data obtained were analyzed using Ion Reporter V5.

Fluorescent in-situ hybridization (FISH) was performed to identify and visualize some microbial species. The harvested biomass samples were fixed with 4% paraformaldehyde solution. After cleaning 10 times with the PBS (phosphate buffered saline), the sample was then conserved at -20°C in the mixture of PBS and ethane (50/50). Entire granules were embedded in OCT (Cryo Embedding Medium) reagent for 24 to 48 h prior to their cryosectioning. Slides with a thickness of 16 µm were cut and each single section was placed on the surface of hole of hydrophobic microscope slides (electron microscopy sciences Cat 63421-10). Hybridization was performed at 46 °C adjusting the formamide concentrations at the percentages from the nature of the probes. The used probes for in situ hybridization were 5' labelled with the fluorochromes FITC or Cy3. The epi-fluorescent microscope Leica, equipped with different cubes to observed FITC, Cy3 or Cy5. Images were processed using Leica FW4000 view software. Only qualitative analysis were performed as a weak point of the FISH method is that the auto-fluorescent signals can in some cases generate over hybridization results which make quantification poorly accurate (Ge et al., 2015).

Table 3.2: Oligonucleotide probes used for FISH analysis.

Probe	Probe	Targeted organisms	Probe sequence (5'-3')	Reference
General	EUB 338	Domain bacteria	GCT GCC TCC CGT AGG AGT	(Vázquez-Padín et al., 2010)
	Amx368	All anammox bacteria	CCT TTC GGG CAT TGC GAA	(Loy et al., 2007)
Anammox	Amx820	Ca. Brocadia anammoxidans	AAA ACC CCT CTA	(Loy et al., 2007)
		Ca. Kuenenia stuttgartiensis	CTT AGT GCCC	
	Apr820	Ca. Anammoxoglobus propionicus	AAA CCC CTC TAC CGA GTG CCC	(Loy et al., 2007)
	Amx1240	Ca. Brocadia anammoxidans	TTT AGC ATC CCT TTG TAC CAA CC	(Schmid et al., 2005)
	Bfu613	Ca. Brocadia fulgida	GGA TGC CGT TCT TCC GTT AAG CGG	(Loy et al., 2007)
	Kst157	Ca. Kuenenia stuttgartiensis	GTT CCG ATT GCT CGA AAC	(Loy et al., 2007)
	Nse1472	Nitrosomonas europaea,	ACC CCA GTC ATG ACC CCC	(Loy et al., 2007)
		N. halophila,		
		N. eutropha,		
AOB	Nso1225	Kraftisried-Isolat Nm103	CGC CAT TGT ATT ACG TGT GA	(Loy et al., 2007)
		β-Subdivision of AOB		
	Nsv443	Nitrosolobus multiformis	CCG TGA CCG TTT	(Loy et al., 2007)
		Nitrosolobus multiformis Nitrosovibrio tenuis	CGT TCC G	

2.5 Calculation and stoichiometry analysis

For each cycle, the volumetric ammonium uptake rate (AUR, $\text{mgN L}^{-1} \text{h}^{-1}$) was calculated with the input ammonium and the reaction time. Complete kinetics were followed 26 times during the study (every 2 weeks), and indicated that ammonium consumption was almost linear within reaction phase. The specific ammonium uptake rate (SAUR, $\text{mgN g-VSS}^{-1} \text{h}^{-1}$) was calculated with biomass concentration (VSS) measured or interpolated between two measurements.

For each cycle, the NO and N₂O emission rate (NO_{ER} and N₂O_{ER}, $\text{mgN L}^{-1} \text{d}^{-1}$) were calculated by multiplying the measured gas concentration and the gas flow rate. The emission factors (N₂O_{EF} and NO_{EF}, %) were calculated as the ratio between the total N_xO emitted as nitrogen (obtained by integrating the rates) and the total ammonia-nitrogen removed during each cycle. Average concentration and emission rate were also calculated.

Stoichiometry analysis and mass balance were especially performed during two stable periods at the end of period A (low flow rate) and B (high flow rate) as shown in Table 3.3.

Nitrogen conversion into NO₃⁻, NO, N₂O, N₂ (by difference) and N assimilated into the biomass were considered. Residual nitrite and ammonium were negligible during the entire study. Dissolved NO and N₂O_{EF} were assumed negligible at the end of SBR cycle and in the effluent. Calculation were reported to 100 g N-NH₄⁺ converted. Oxygen uptake was obtained by integrating oxygen transfer rate. Biomass formula were assumed for AOB ($\text{CH}_{1.4}\text{O}_{0.4}\text{N}_{0.2}$) and anammox ($\text{CH}_{1.74}\text{O}_{0.31}\text{N}_{0.2}$) leading to nitrogen content of 12.4% and 13% respectively, or 12.6% of VSS in average assuming a ratio of 1.51. Biomass production rate was estimated based on increase in concentration (ΔVSS) in the reactor and solids loss.

3. Results

3.1 Process performances

The PNA process was operated over a time period of 293 days (Table 3.3, Figure 3.1). The whole period included 20 weeks at low aeration level (4.5 L h^{-1} , A1 and A2) and 22 weeks at high aeration level (11.7 L h^{-1} , B1 and B2).

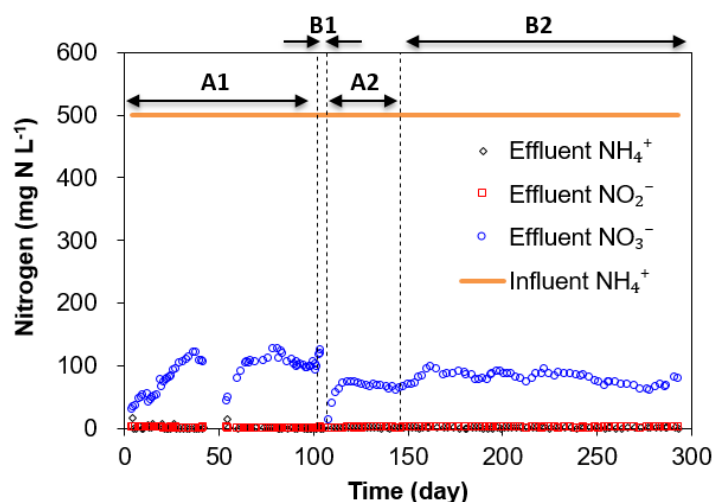


Figure 3.1: Evolution of reactor performance during the study (NH_4^+ , NO_2^- , NO_3^- concentrations). A1 and A2 correspond to low aeration level (4.5 L h^{-1}), B1 and B2 high aeration level (11.7 L h^{-1}). See details in Table 3.1 and SI (Table 3.S2)

Very good nitrogen removal was observed throughout the entire study (Figure 3.1). Ammonium was almost totally removed and effluent nitrite concentration was also very low ($< 0.3 \text{ mg N L}^{-1}$). During the first months, nitrate accumulated up to 100 mgN L^{-1} (25 % of the inlet ammonium) but progressively decreased and stabilized at $65.9 \pm 2.0 \text{ mgN L}^{-1}$ representing $12.9 \pm 0.5 \%$ of the ammonium removed (Table 3.3 phase A2S, days 130-140). It is noticeable that the process was stopped during several days (days 45-51, sludge was stored at 4°C) and performances were rapidly recovered within three days after restarting. After increasing the air flow rate (phases B1 and B2) the nitrate first accumulated, revealing a probable increase of nitrite oxidizing bacteria activity. However during the following months (period B2), as the new aeration level was imposed on a long term the nitrate again stabilized, and reached $73.5 \pm 4.3 \text{ mgN L}^{-1}$ at the end of the study, which corresponded to 14.7% of the ammonium removed. Therefore, total nitrogen removal was stabilized at 87% and 85% respectively at the end of each period (A and B).

Table 3.3: Reactor performance in the whole and stable period. The value in the bracket indicated the number of calculations.

Whole phase	A1 (Days1-101)	B1 (Days102-106)	A2 (Days107-145)	B2 (Days146-293)
AUR (mg N L ⁻¹ h ⁻¹)	2.7±0.5 (101)	5.4±0.2 (5)	3.5±0.3 (62)	6.1±0.6 (434)
SAUR (mg N g VSS ⁻¹ h ⁻¹)	2.9±0.6 (101)	5.9±0.2 (5)	3.9±0.4 (62)	5.4±0.5 (434)
Effluent NH ₄ ⁺ (mg N L ⁻¹)	1.21±2.9 (63)	0.07±0.02 (3)	0.16±0.06 (20)	0.21±0.11 (61)
Effluent NO ₃ ⁻ (mg N L ⁻¹)	87.1±27.4 (63)	119.6±3.6 (3)	62.6±13.7 (20)	79.2±9.1 (61)
Effluent NO ₂ ⁻ (mg N L ⁻¹)	0.21±0.35 (63)	0.17±0.23 (3)	0.14±0.05 (20)	0.23±0.10 (61)
TN removal efficiency (%)	82.3±5.3 (63)	76.0±0.8 (3)	87.4±2.7 (20)	84.1±1.8(61)
N ₂ O-EF (%)	1.5±0.9 (100)	3.1±0.5 (5)	5.1±1.1 (62)	2.7±1.2 (434)
N ₂ O-ER (mg N L ⁻¹ d ⁻¹)	1.0±0.7 (100)	4.0±0.7 (5)	4.4±1.1 (62)	4.0±1.5 (434)
N ₂ O (ppm)	84.2±57.9 (100)	125.5±21.3 (5)	356.3±90.9 (62)	123.4±48.0 (434)
NO-EF (%)	0.027±0.004 (60)	0.032±0.004 (5)	0.042±0.010 (62)	0.029±0.010 (374)
NO-ER (mg N L ⁻¹ d ⁻¹)	0.019±0.006 (60)	0.041±0.005 (5)	0.036±0.009 (62)	0.041±0.013 (374)
NO (ppm)	3.0±0.9 (60)	2.5±0.3 (5)	5.8±1.5 (62)	2.6±0.9 (374)
Stable period	-	-	A2S (Days130-140)	B2S (Days246-256)
AUR (mg N L ⁻¹ h ⁻¹)	-	-	3.8±0.1 (20)	6.5±0.3 (34)
SAUR (mg N g VSS ⁻¹ h ⁻¹)	-	-	4.2±0.2 (20)	5.4±0.2 (34)
Effluent NO ₃ ⁻ (mg N L ⁻¹)	-	-	65.9±2.0 (6)	73.5±4.3 (5)
ΔNO ₃ ⁻ /ΔNH ₄ ⁺ (%)	-	-	12.9±0.5 (6)	14.3±0.5 (5)
N ₂ O-EF (%)	-	-	5.8±0.4 (20)	2.1±0.2 (34)
N ₂ O-ER (mg N L ⁻¹ d ⁻¹)	-	-	5.3±0.3 (20)	3.2±0.3 (34)
N ₂ O (ppm)	-	-	424.6±27.4 (20)	99.4±9.5 (34)
NO-EF (%)	-	-	0.043±0.002 (20)	0.023±0.004 (34)
NO-ER (mg N L ⁻¹ d ⁻¹)	-	-	0.039±0.002 (20)	0.036±0.006 (34)
NO (ppm)	-	-	6.3±0.2 (20)	2.2±0.4 (34)

3.2 Activity and biomass growth

Volumetric and specific ammonium uptake rate were monitored for the entire study (Figure 3.2). On a long term, it is clear that the AUR progressively increased for each period with a constant air flow rate (A or B). When the air flow rate was maintained at 4.5 L h⁻¹, AUR was initially around 2.4±0.3 mg N L⁻¹ h⁻¹ and reached 3.8±0.1 mg N L⁻¹ h⁻¹ at the end of phase A2. Similarly during the phase B, when the air flow rate was maintained at 11.7 L h⁻¹, AUR continuously increased up to 6.5±0.3 mg N L⁻¹ h⁻¹ at the end of phase B2. In addition as the system operated under oxygen limitation, AUR was controlled by OTR, and both increased suddenly each time the air flow rate increased (step A1 to B1, step A2 to B2).

SAUR increased continuously during period A (first 150 days) from 2.7±0.4 mgN g-VSS⁻¹ h⁻¹ to 4.2±0.2 mgN g-VSS⁻¹ h⁻¹. After increasing to 6.5 mgN g-VSS⁻¹ h⁻¹ it finally stabilized at 5.4±0.2 mgN g-VSS⁻¹ h⁻¹ during period B2.

This increase of activity can be explained by both biomass growth and microbial adaptation to low dissolved oxygen level. This confirmed the recent study of Akaboci et al. (2018) indicating that very low dissolved oxygen was not detrimental to PNA process. Besides, the biomass specific activity increased faster (34.4%) than the volumetric rate (29.6%) during the first period (A1-A2), during which biomass concentration was almost constant in the reactor (Figure 3.3). This suggests an adaptation of aerobic AOB to the stringent DO limitation. In contrast, during period B, both VSS and AUR accumulated, resulting in a relatively stable SAUR.

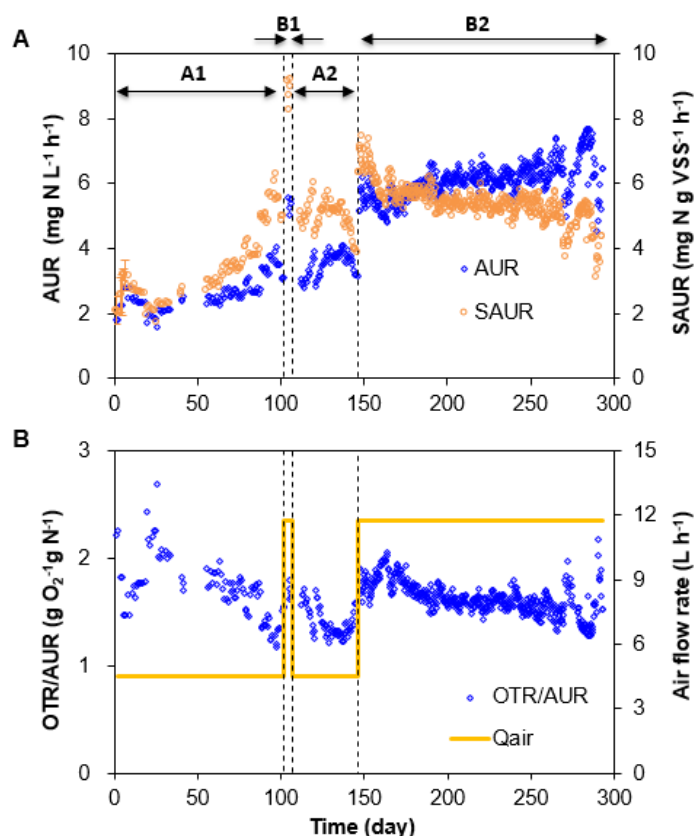


Figure 3.2: Evolution of the ammonium uptake rate and oxygen demand during the study. **A)** Volumetric ammonium uptake rate (AUR) and specific ammonium uptake rate (SAUR); **B)** Ratio of the oxygen transfer rate to ammonium uptake rate (OTR/AUR) and air flow rate (Q_{air}).

As oxygen transfer rate was measured, it was compared to ammonium uptake rate for estimating the ratio OTR:AUR. Initially during the first month the value of this ratio was $2 \pm 0.2 \text{ gO}_2 \text{ gN}^{-1}$ but progressively decreased down to $1.40 \pm 0.2 \text{ gO}_2 \text{ gN}^{-1}$ after 100 days. It should be also pointed that the ratio also increased rapidly following each sudden increase of air flow rate (B1 and B2), and progressively decreased as the AUR increased. This oxygen demand was surprisingly very low compared to the theoretical oxygen demand for pure PNA process (see discussion). The fact that this ratio increased each time the oxygen transfer rate was increased suggests that some processes were regulated by the oxygen availability. Low oxygen demand and low level of nitrate both indicate an efficient repression of nitrite oxidizing bacteria (NOB). However NOBs were likely to be less repressed after an OTR increase, explaining either the observed increase of nitrate and increase of oxygen demand. But finally it should be noted

that on a long term even with the higher air flow rate (period B2) the oxygen demand progressively decreased down to $1.50 \pm 0.2 \text{ gO}_2 \text{ gN}^{-1}$.

TSS and VSS measurements confirmed that biomass grew during the entire study but more intensively during period B (Figure 3.3). This seems logical as the nitrogen load increased during this second period due to the increased OTR. Both the biomass concentrations in the reactor and in the effluent were followed (Figure 3.3A and 3B). Concentration in the reactor increased from $0.87 \pm 0.03 \text{ g VSS L}^{-1}$ to $1.46 \pm 0.04 \text{ g VSS L}^{-1}$, despite an unexplained drop at the beginning of phase A2 (Day110). VSS:TSS ratio remained stable at $89.2 \pm 1.4\%$ throughout the study (conventional for pure bacterial biomass) indicating that no precipitation occurred.

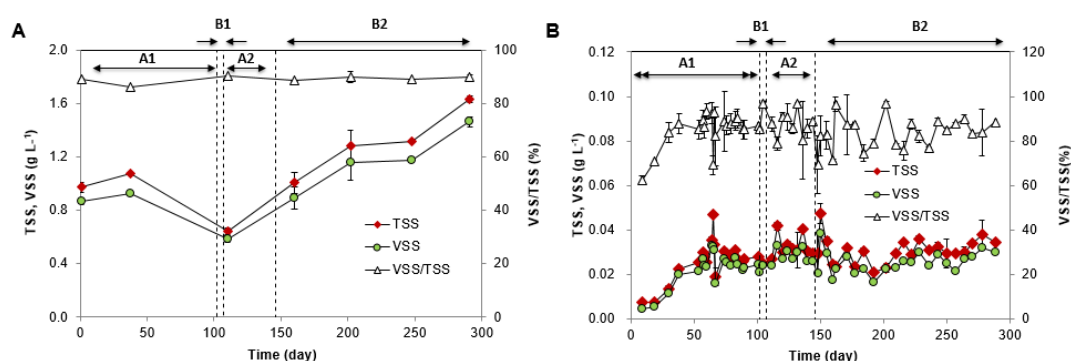


Figure 3.3: Evolution of the suspended solids during the study.

Solids in the effluent were initially quite low ($4.5 \pm 0.2 \text{ mg VSS L}^{-1}$ in the first days), gradually increased up to $33 \pm 1.6 \text{ mg VSS L}^{-1}$ in 50 days, and then remained almost constant until the end of this study. This indicated that biomass loss was relatively stable and well quantified, this data will be used for mass balance analysis. The average VSS/TSS of the effluent biomass ($84.8 \pm 7.3\%$) was not significantly different from mixed liquor. From this measurement average sludge retention time (SRT) can be estimated to 170 days. Obviously in reality the retention time of granules is much higher whereas the biomass growing in suspension likely has a lower retention time.

3.3 Typical batch cycles

Figure 3.4 shows typical dynamics monitored in the SBR reactor during the different operating periods: initial startup period A1 (low flow rate: 4.5 L h^{-1}), stable period of period A2 (low flow rate: 4.5 L h^{-1}) and stable period B2 (high flow rate: 11.7 L h^{-1}). The profiles were reproducible during consecutive cycles for all those periods.

The dissolved oxygen (DO) concentration systematically showed a stable and extremely low value during the reaction time and a sharp increase at the end of the reaction when ammonia was depleted. The DO level during reaction was detectable at $0.02\text{-}0.05 \text{ mg O}_2 \text{ L}^{-1}$ during the period A1 (Figure 3.4B1), but decreased down to unmeasurable limit in the stable periods A2 and B2 (Figures 3.4B2 and B3). This decreased DO level with operation time was concomitant

with the AUR increase. Additionally the time for DO increasing to $0.30 \text{ mg O}_2 \text{ L}^{-1}$ (setpoint stopping the cycle) was gradually shortened from 3 h on Day 11 down to 9 min after 18 weeks (stable low Q_{air}) and further down to than 5 min after 16 weeks (stable high Q_{air}). DO decreased rapidly during the settling and discharging whereas influent DO provoked a very small peak ($0.1 \text{ mg O}_2 \text{ L}^{-1}$) during feeding before a drop to the stable low level.

During each cycle ammonium concentration in the reactor (starting around 50 mgN L^{-1}) was consumed almost linearly during the reaction period. The time needed for depleting ammonium progressively has decreased by 36 % during phase A (from A1 to end of A2) and by 61% during phase B (end of B2) compared to initial cycle, due to increase in AUR. Nitrite concentration was always maintained very low ($<1 \text{ mg N L}^{-1}$) with typical and reproducible pattern observed for each cycle. A first small peak during the first 8 minutes of feeding for the time when the dissolved oxygen was still present provoking rapid ammonium oxidation (Figures 3.5C2 and C3). Once oxygen was depleted nitrite decreased and stabilized at a low but constant level due to the balanced activity between aerobic AOB and AnAOB (Anammox). This stable level was lowest during the initial cycles ($0.3\text{-}0.5 \text{ mg N L}^{-1}$), higher at the end of period A2 ($0.6\text{-}0.8 \text{ mg N L}^{-1}$) (low Q_{air}) while in between ($0.4\text{-}0.5 \text{ mg N L}^{-1}$) at the end of period B (high Q_{air}). Whereas nitrate was slightly consumed during the first cycle (probably due to residual organic matter provoking denitrification), it finally showed very reproducible linear increase during reaction time.

NO and N_2O were continuously measured in the gas phase (Fig 5). Initially emissions were extremely low: NO was not detectable, N_2O emission factor at 0.34% for day 11. Emissions progressively increased concomitantly with AUR during the first months (details in next chapter). Then typical patterns were observed during each cycle. N_2O concentration increased during the first hour, reached a plateau, and decreased one hour before the end of ammonium oxidation. For some cases (example day 243), a peak of N_2O was observed during the first hour before decreasing to the plateau. This peak was correlated to high nitrification rate during the first minutes of the cycle as oxygen was not yet limiting. A small NO peak was also generally observed after feeding before those of N_2O . NO concentration was less than 10 ppm but showed reproducible patterns. NO emission varied proportionally with N_2O but was 50 times lower than N_2O .

The highest N_2O emissions was observed at the end of period A for a low air flow rate. The N_2O concentration was around 500 ppm and emission factor at $5.8 \pm 0.4\%$ (6.1% on example Fig 5). After increasing air flow rate emission slowly decreased and stabilized at the end of period B. Emission factor was then at $2.1 \pm 0.2 \%$.

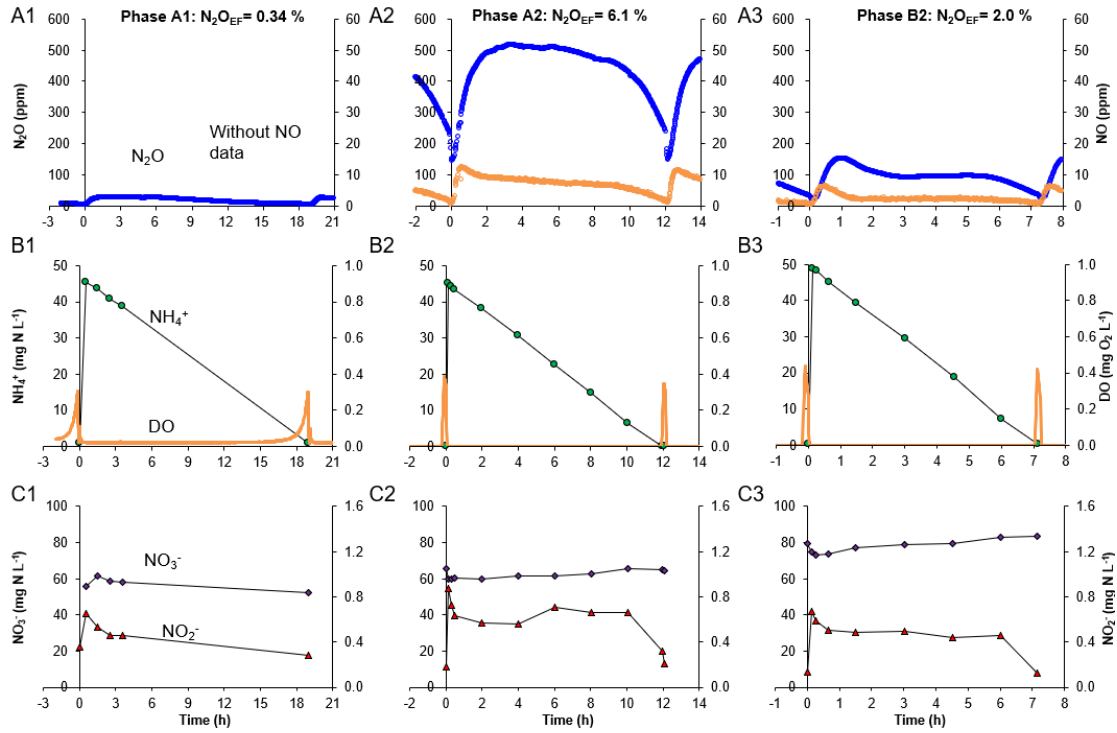


Figure 3.4: Three typical batch cycles on period A1 Day 11 (A1-C1), end of period A2 Day 134 (A2-C2) and end of period B2 day 243 (A3-C3) respectively.

3.4 Granular sludge size distribution

Based on image analysis volumetric particle size distribution was determined (Figures 3.6, 7 Table 3.4). An increase of granules size was observed during the study, min-max diameters increased from [79.4;1660] μm to [277;2198] μm within 172 days. This was likely due to both biomass growth and particle selection due to the short retention time (2 minutes).

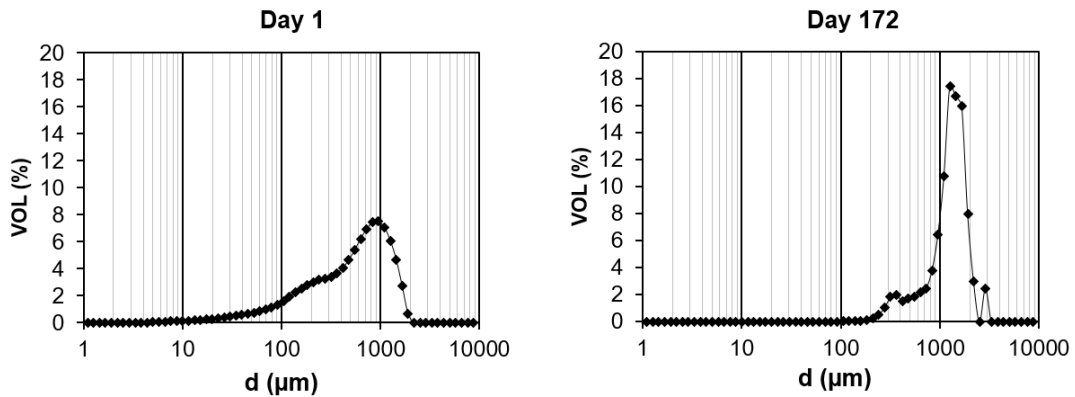


Figure 3.5: Evolution of the volumetric particle size distribution on day 1 and day 172.

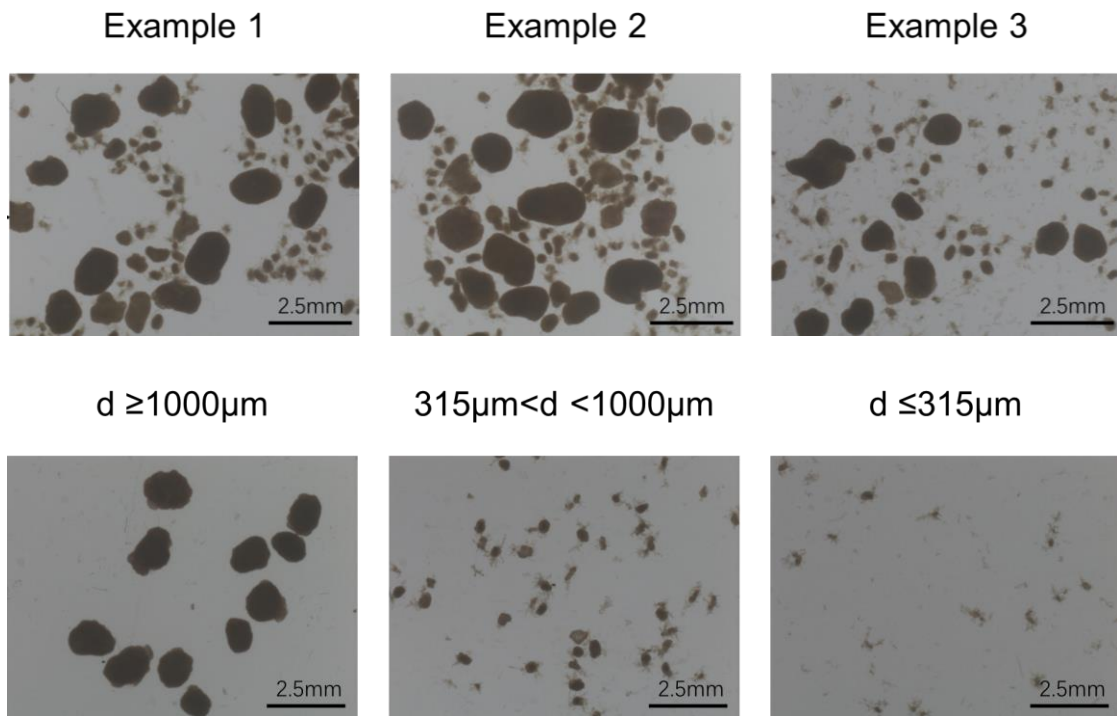


Figure 3.6: Granular sludge morphology. Three pictures taken on day 172 (up). Separated granules after the screening on Day 239 (down).

More surprisingly microscope observations and PSD showed a clear bimodal distribution of the granular sludge (Figure 3.5). Indeed a strong segregation into two ranges of particle size was observed. This segregation was less visible in the initial biomass seed but was extremely pronounced in the sample collected in the middle (day 172) and at the end of the study (day 239). The distribution showed two peaks for a diameter of about 1250-1300 μm for the big granules ($>1000\mu\text{m}$) and about 350-400 μm for smaller granules ($<1000\mu\text{m}$).

Table 3.4. A summary of the global and peak size distribution on Day 1 and Day 172.

Global	Parameters	Day 1	Day 172	
Distribution ($\geq 1\%$)	V_{tot} (%)	92.7	96.6	
	d_{min} (μm)	79.4	277	
	d_{max} (μm)	1660	2198	
	d (0.1) (μm)	118	557	
	d (0.5) (μm)	616	1300	
	d (0.9) (μm)	1367	1880	
Peak		Peak	Peak1	peak 2
Distribution (3-step sizes)	V_{tot} (%)	22.0	5.3	44.9
	d_{min} (μm)	832	318	1102
	d_{max} (μm)	1096	419	1452

A physical sieving method was used to separate aggregates into three categories with two mesh sizes (315 μm and 1000 μm). The differences between big and small granules were even more evident when fractions were observed separately (Figure 3.6, down). The big spheroid particles ($d \geq 1000 \mu\text{m}$) are dark, dense and compact granules, while small particles ($315 \mu\text{m} < d < 1000 \mu\text{m}$) are bright orange-yellow and loose granules with a fluffy biofilm on the surface. The smallest particles ($d \leq 315 \mu\text{m}$) looked like a mixture of flocs and very small granules.

3.5 Microbial community identification: 16 sRNA and FISH

Figure 3.7 shows the results of 16S rRNA sequencing for initial biomass and over a period of 192 days of operation (absolute abundance value). Analysis was performed on a global sample initially but on the three fractions separated by sieving on the final sample (S1: $>1\text{mm}$, S2: $0.315\text{mm}-1\text{mm}$, S3: $<0.315\text{mm}$).

Initially, the biomass was characterized by the high abundance (75%) of anammox genera *Candidatus Kuenenia*, while AOB and NOB were seldomly observed (Figure 3.7A). After the reactor was operated for 192 days, the main anammox genera did not change but has significantly decreased in relative abundance (less than 40%) compared to AOB, NOB and heterotroph bacteria which appeared in all categories of aggregates (Figure 3.7B). *Nitrosomonas* was the main AOB found whereas *nitrospira* was the only NOB genera detected in a much smaller amount. A high diversity of heterotrophs was detected with a significant amount of *dechloromonas*.

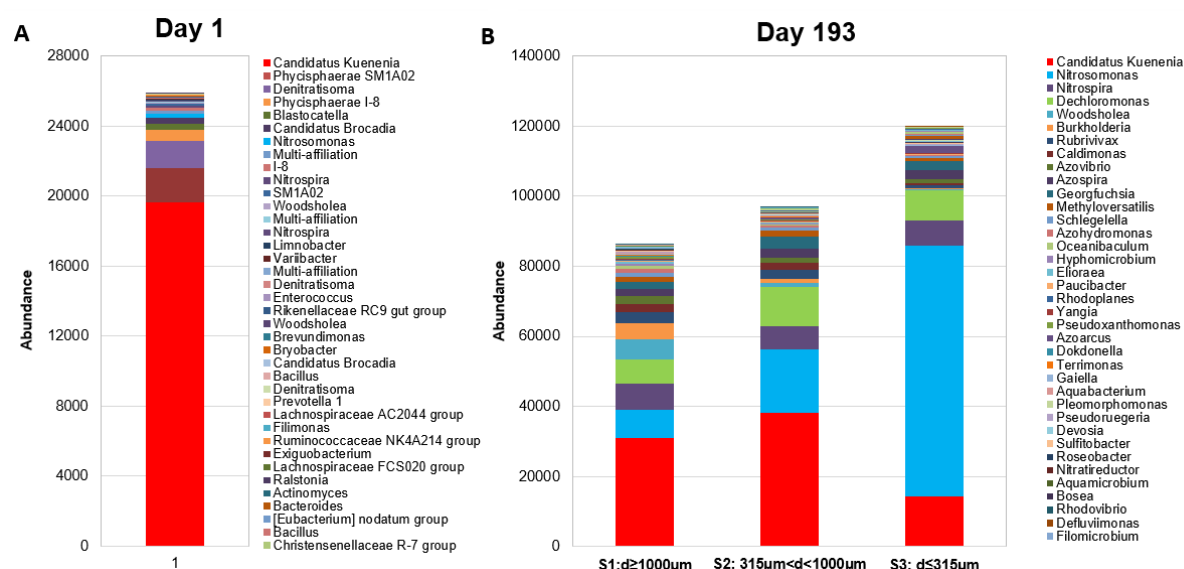


Figure 3.7: Microbial community analysis by 16S rRNA sequencing on day 1 (A) and day 193 (B).

Figure 3.7B clearly demonstrated a heterogeneous distribution of anammox and AOB species within the different categories of granules. Anammox showed comparable relative abundance in S1 and S2 but was much less present in small aggregates (S3). In contrast AOB (*Nitrosomonas*) was in much higher abundance in the small aggregates (S3), much less in medium size (S2) and really minor in big granules (S1). Interestingly no segregation was observed for NOB (*Nitrospira*) which was observed in similar abundance in all kinds of particles.

Figure 3.8 and Figure 3.9 showed the FISH results performed on Day 38 and Day 180 respectively. Both AOB and Anammox microbial species were investigated. First, the hybridization of the sliced granules with *Amx368* probe (all anammox bacteria) using EUB 338 (green in Figure 3.8A1) as the background, showed that all anammox bacteria (red, Figure 3.8A1) distributed throughout the granules, outer and the inner parts. The response of the *Amx 820* probe further confirmed the presence of *Ca. Brocadia* and/or *Ca. Kuenenia*. Finally, the combination of light responses of *Apr1240* (*Ca. Brocadia*) and higher response of *Kst157* further identified the main genera was *Ca. Kuenenia*, which is in accordance with the 16s rRNA sequencing. For AOB identification, the overlapping responses of *Nse1472* probe (*Nitrosomonas europaea*, *N. halophila*, *N. eutropha*, *Kraftisried-Isolat Nm103*) and the *Nso 1225* (Betaproteobacterial AOB) indicated the presence of lineage of AOB and the genus level of *Nitrosomonas*, which is also in agreement with the sequencing result. Figure 3.8B3 showed that the AOB distributed around the granules surface.

Furthermore, combining the FISH and 16 rRNA analysis of the coexistence of *Ca. Kuenenia* and *Nitrosomonas europaea*, Figure 3.7C1 showed the relative distribution of *Ca. Kuenenia* with the background of *Nitrosomonas europaea* as the main AOB ammonia-oxidizing bacteria. The overlapped area focused more in the outer parts of the granular sludge.

After 142 days, the overlapping probes with *Amx368*, *Amx820* and *Kst 157* showed the main anammox bacteria remained the same as obtained before. No response of the *Amx 1240* occurred again showed the absence of *Ca. Brocadia anammoxidans*. Similarly, the simultaneous response of the probe *Nse 1472* and *Nso 1225* showed that the presence of *Nitrosomonas* in the granular biomass, which also agree with 16s rRNA analysis result showing the presence of *Nitrosomonas europaea* on Day 193 (Figure 3.7B).

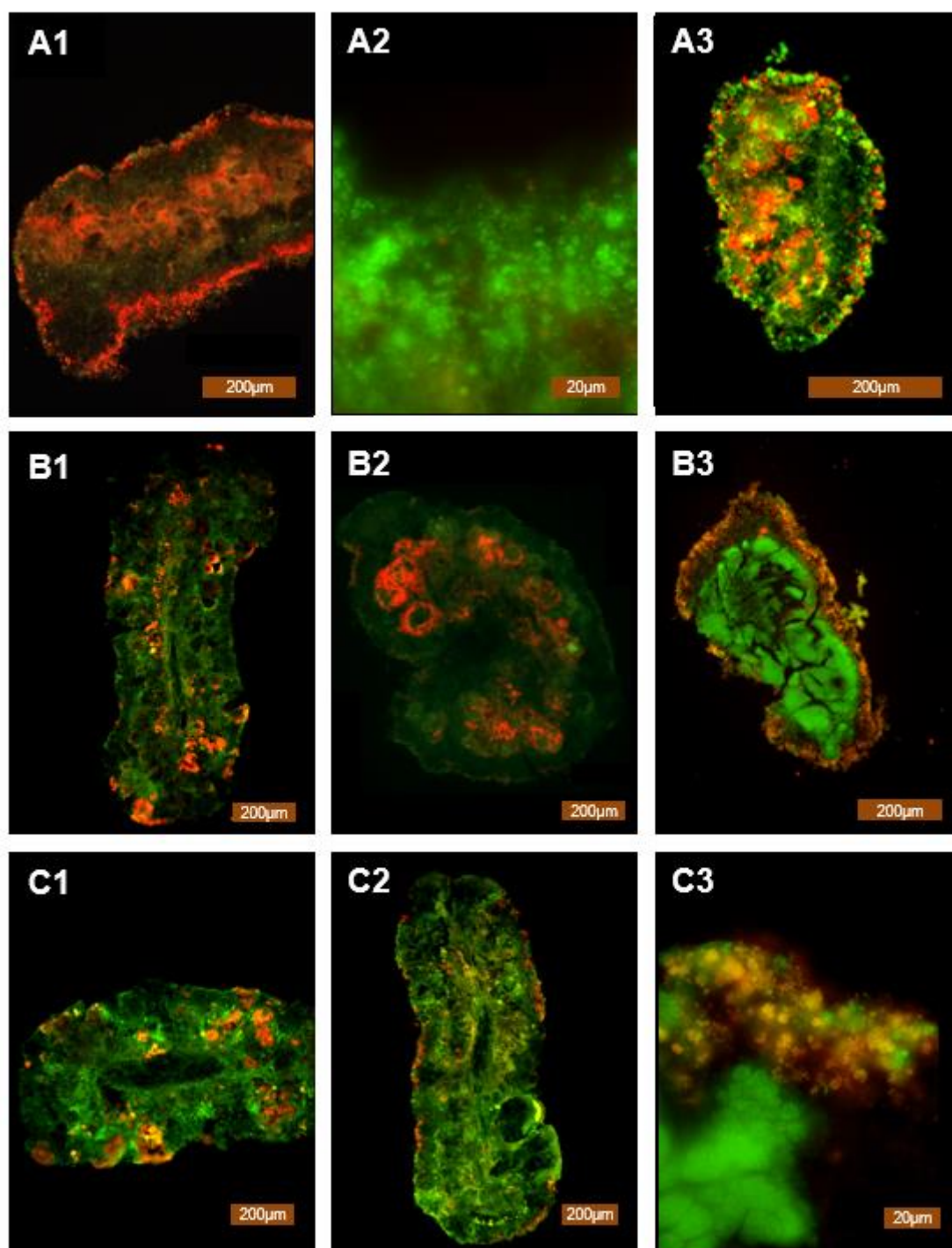


Figure 3.8: Hybridization result on Day 38.

A1: Amx368-Cy3 EUB338-FITC; **B1:** Amx820 Cy3 EUB338 FITC; **C1:** Amx820 Cy3 NSO1225 FITC;

A2: Amx1240 Cy3 EUB338 FITC; **B2:** Kst157 Cy3 EUB338 FITC **C2:** NSO1225 Cy3 EUB338 FITC;

A3: NSO1225 Cy3 EUB338 FITC; **B3:** Nse1472 Cy3 EUB338 FITC; **C3:** Nse1472 Cy3 EUB338 FITC

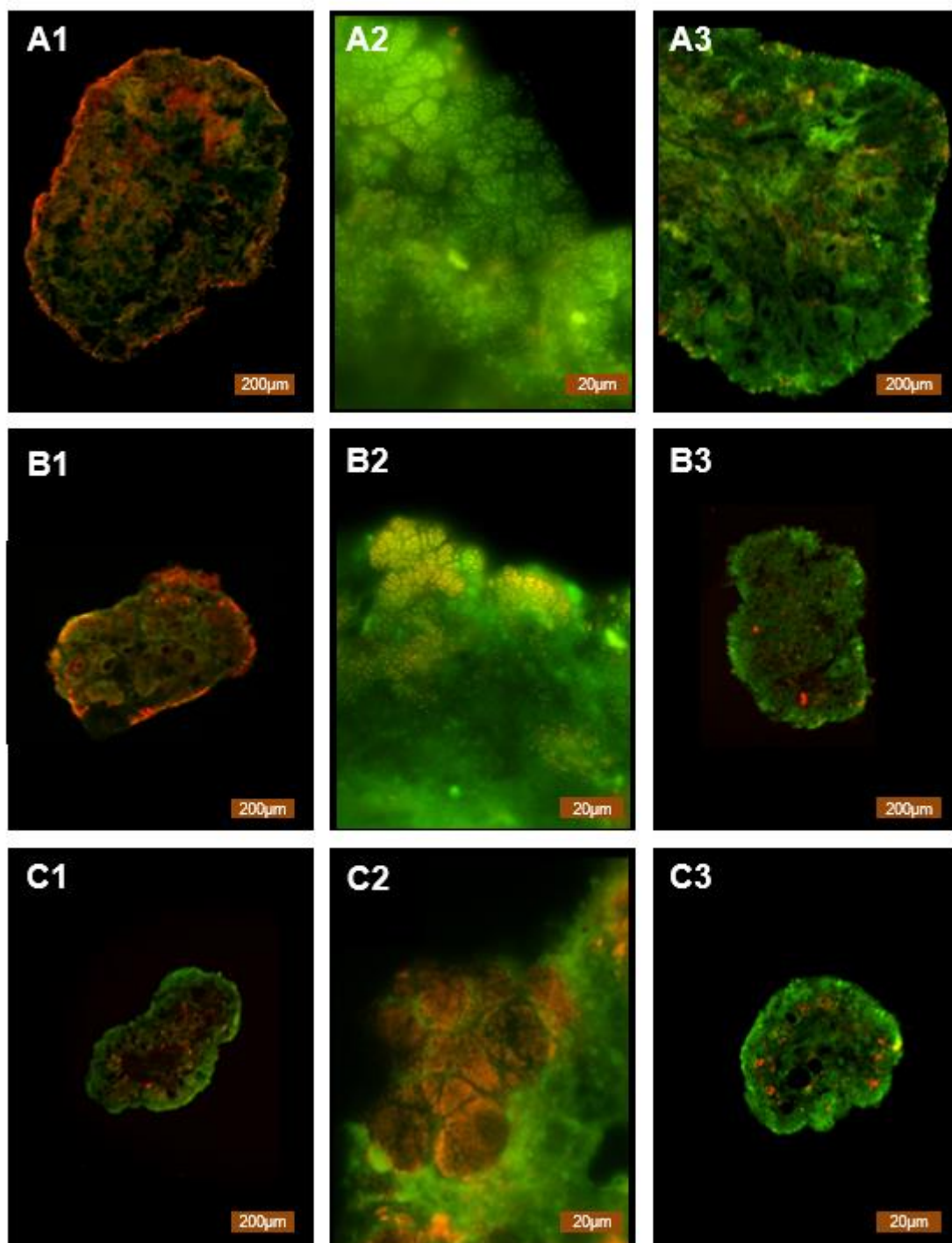


Figure 3.9: Hybridization result on Day 180.

A1: Amx368 Cy3 EUB338 FITC; **B1:** Amx820 Cy3 NSO1225 FITC; **C1:** Amx368 Cy3 EUB FITC;

A2: Amx1240 Cy3 EUB338 FITC; **B2:** Bfu613 Cy3 EUB338; **C2:** Amx820 Cy3 NSO1225 FITC;

A3: Kst157 Cy3 EUB338 FITC; **B3:** Nse1472 Cy3 EUB FITC; **C3:** Nso1225 Cy3 EUB FITC.

4. Discussion

4.1 PNA performances and stoichiometry under oxygen limitation

In this study, granular sludge PNA process achieved with very good performances during 300 days at 26.5°C. The system was successfully operated under DO limitation, ammonium oxidation rate being controlled by oxygen transfer rate (OTR) and reaction time being controlled by a maximal DO setpoint. SAUR of 130 mg N g VSS⁻¹ d⁻¹ was stabilized at the end of our running period. The oxygen demand was very low and a limited amount of nitrates was produced. Considering the theoretical nitrate production by anammox (Table 3.5), we can estimate that only 2 to 7% of total nitrogen was likely converted by NOB during the experience, depending on the value of the yield for AOB and anammox. *Nitrospira* was the only AOB genus found in our medium by 16S rRNA sequencing technique. It can be noticed that *nitrospira* genera includes different clades, including the newly discovered *commamox* pathway (full oxidation of ammonium to nitrate). But our sequencing technique was not able to differentiate such clade from normal NOB-*nitrospira*.

Globally this shows that working at extremely low DO is not detrimental to aerobic ammonium oxidation by AOB and allows good repression of NOB on a long term. This was confirmed by the very recent work of Akaboci et al. (2018). Our results also demonstrated that AUR and SAUR progressively increased on a long term which suggests a possible adaptation of AOB to the very strict oxygen limitation (as also assumed by the previous author). Our first modelling approach (chapter 2) indicates that half-saturation constant for AOB for oxygen of about 0.05 mgO₂ L⁻¹ should be assumed to predict such a nitrification rate. A literature review by Vannecke and Volcke (2015) showed that AOB affinity constant with O₂ ranged from 0.07 to 3 mg O₂/L. Low value as 0.03 mg L⁻¹ was considered as the intrinsic constant by Picioreanu et al. (2016) for AOB whereas apparent values were calculated from 0.25 to 0.4 mgO₂ L⁻¹. Our estimation is in the lower range of the K_{O2} values reported for *nitrosomonas* supporting a possible adaption of AOB to very low oxygen level. Low DO is reported to favor the proliferation of members of *N. europaea* lineage in full-scale and in lab-scale reactors (Park and Noguera, 2004), which was also confirmed by our microbial characterisation.

A physical explanation can be the modification of AOB distribution within the granules surface. Indeed in this work, 16S RNA sequencing results demonstrated that AOB were found in majority on small granules and suspended biomass. As small aggregates have a higher specific surface area, mass-transfer rates of all substrate and especially oxygen are facilitated. In other words this AOB segregation could be seen as a response to very strict oxygen limitation. Indeed distributing bacteria on small granules and bulk aggregates should consequently decrease apparent half-saturation coefficient for oxygen.

On Table 3.5 the global stoichiometry observed in this study (phase A2S and B2S) is compared with the theoretical ones estimated by combining anammox and aerobic AOB stoichiometry's obtained by previous authors (Equation 1.8 and Equation 1.17). First, the estimated amount of assimilated nitrogen (biomass) was in the same range as the theoretical. As mentioned previously, the experimental NO₃⁻ production (13.2 g and 14.7 g) in both low and high flow

rate were higher than the stoichiometric ones (11.1 g and 7.4 g). The nitrate production rate during phase A2S was closer to the theoretical probably because NOB were more repressed at low air flow rate condition.

The experimental oxygen demand (OTR:AUR) decreased to unexpected low level during our study. Table 3.5 shows the literature stoichiometry's, combining the nitrification (Equation 1.8) (Cervantes, 2009) and the primary anammox (Strous et al., 1998) stoichiometries, yields the first overall OLAND stoichiometry (Equation 1.22) (Vlaeminck et al., 2012), with an oxygen consumption of 1.81 g O₂ g N⁻¹. More recently Lotti et al. (2014b) re-calculated the anammox stoichiometry (Equation 1.18) with free cells by using a highly enriched anammox microbial community. In the new stoichiometry of anammox, less nitrite being consumed, a lower theoretical oxygen demand of 1.70 g O₂ g N⁻¹ (Equation 1.18 and Equation 1.8) is obtained for PNA system.

Indeed our experimental values of 0.130 and 0.152 g O₂ g N⁻¹ observed respectively at low and high flow rate were significantly lower than theoretical values. If experimental errors in measuring the oxygen transfer are excluded, the only assumption we found was a possible NO short-cut. This would mean that NO produced by AOB would be directly consumed by anammox reducing the oxygen demand compared to nitrite short-cut. It is indeed demonstrated that anammox can directly consumed NO (Kartal et al., 2010), which is an intermediate in the nitrite reduction metabolism. If the nitrogen oxidation was stopped to NO, instead of nitrite, this would theoretically reduce the oxygen demand by 17%. But this is without considering all the consequences on anammox metabolism which are difficult to predict (production of nitrate, growth...).

Table 3.5. Experimental and theoretical stoichiometric analysis of nitrogen source and sink as well as oxygen consumption.

	Produced NO ₃ ⁻	Produced Biomass-N	Consumed O ₂	Produced NO	Produced N ₂ O
For 100 g NH ₄ ⁺ -N	gN	gN-VSS	gO ₂	gN	gN
Experimental PNA process in the stable phase A2	13.2	1.51	130.2	0.043	5.75
Experimental PNA process in the stable Phase B2	14.7	1.06	152.7	0.023	2.06
Theoretical AOB & Anammox (Strous et al., 1998)	11.1	1.46	181.03	-	-
Theoretical AOB & Anammox (Lotti et al., 2014b)	7.4	1.64	170.06	-	-

4.2 Biomass segregation: consequence on N₂O emissions?

N₂O and NO emission dynamics will be evaluated in details in the next chapter. Globally during the study NO emission was detectable but small (about 0.023-0.043%), and much lower than N₂O emissions. N₂O emission (initially limited) increase up to 6.1% at low air flow rate and decrease to 2.0% after increasing the flow rate until the end of the study. Both results were

obtained with undetectable DO in the reactor, showing that the dissolved oxygen can be hardly used for discriminating such emission. The high N₂O emission period (A2) was concomitant with the lowest oxygen demand (OTR:AUR) which leads us to think that for such system at extremely low DO, this parameter is probably better than DO to indicate the level of oxygen limitation and the risk of high emission. As the nitrite denitrification pathway is likely to be the major pathway in PNA (Wan et al., 2018) (and demonstrated in the next chapter), an increase of such mechanism is expected under strong DO limitation despite controversial literature. However the studies on the effect of oxygen on ND pathway have been done for measurable DO and this is still unknown at unmeasurable DO.

Finally a strong segregation of particle size was here demonstrated in a PNA system. Such phenomenon is not explained here from a mechanical point of view. In a previous study, the relationship between the microbial activity of AOB and anammox and the aggregate size were demonstrated based on three suspended-growth oxygen-limited autotrophic nitrification-denitrification reactors (Vlaeminck et al., 2010). Results showed that AOB activity was improved due to the aggregation to small granules in this study. Meanwhile, the possible interaction among granules in terms of the exchange of solutes between granules of different sizes cannot be neglected (Volcke et al., 2012). But regarding N₂O emissions, the possible links between N₂O emission and AOB segregation in small particles is an interesting question which can be investigated in the future.

In the last modelling work of Wan et al. (2019) the highest N₂O emission was obtained for relatively small granules (emission factor of 11% for radius of 300 µm). But dependency of N₂O emissions with granule size was not linear. N₂O emission factor was lower in smaller aggregates (radius<0.2mm) but also for big granules (emission factor of 2% for radius of 1.2mm). However this was calculated for single size granular sludge. It is thus difficult to predict the possible effect of heterogeneous distribution of AOB in a bimodal granular sludge. Future simulations may help to scrutinize this assumption.

5. Conclusions

- PNA process was successfully controlled by oxygen transfer rate at extremely low DO during 300 days at 26.5°C.
- Specific N removal rate of 0.096-0.014 g N⁻¹ g VSS d⁻¹ was obtained at 26°C with a very limited contribution of NOB, confirming that DO limitation was not detrimental for ammonium oxidation by AOB and allows limiting the NOB growth.
- Oxygen demand progressively decreased under DO limitation, stabilized around 1.3-1.5 gO₂/gN, i.e. value slightly lower than theoretical stoichiometry. This was correlated to low NO emission but significant N₂O emissions (maximal N₂OER of 6% limited to 2% after adapting the air flow rate).
- Granular sludge was naturally segregated into two categories of sizes (300-400 µm, 1100-1400 µm). AOB (*Nitrosomonas Europaea*) were found mainly on the surface of small granules, whereas anammox (*Candidatus Kuenenia*) were in majority in big granules (300-400 µm), and NOB and OHO were homogeneously distributed.

6. Appendix

6.1 Recovery period

The reactor was inoculated with granular sludge (0.87 ± 0.03 g VSS L^{-1}) taken from a single stage PNA process after the storage at 4°C. Sludge was first fed with NH_4^+ and NO_2^- in complete anoxic condition for 36 days in the SBR mode to recover the anammox activity. In the reaction phase (over 90%), anoxic condition (≤ 0.1 mg O_2 L^{-1}) was ensured by nitrogen gas injection at 21 $L\ h^{-1}$. Temperature was maintained at 26.6 ± 0.6 °C using a water jacket; while pH was maintained at 7.8 ± 0.1 with N_2 (base) and CO_2 gas (acid).

Table 3.S1: SBR configuration in sludge recovery period

	Part 1	Part 2	Transition	Part 3
Starting time (h)	2.8	168.9	210.9	376.7
End time (h)	164.8	210.9	376.7	664.7
No. cycle	27	7	7	24
Cycle length(h)	6	6	13-34	12
Feeding (min)	15	15	8-15	8
Aeration (min)	330	330	700-2000	700
Settling (min)	5	5	5	7
Discharging (min)	10	10	10	5

The initial 6-h cycle comprised of 15 min anoxic feeding, 330 min anoxic phase, 5 min settling and 10 min effluent withdrawal. The increase of the influent nitrogen load (ALR) from 0.6 mg $N-NH_4$ $L^{-1}\ h^{-1}$ to 3.8 mg $N-NH_4$ $L^{-1}\ h^{-1}$ was realized by stepwise increasing NH_4^+ concentration from 14 to 500 mg $N\ L^{-1}$ while fixing the NH_4^+/NO_2^- ratio. Increased cycle length up to 13-34 h for about one week overcame the nitrite accumulation due to sudden increased TN load on Day 8. The final cycle length was fixed at 12 h. The volumetric (AUR) and specific ammonium uptake rates (SAUR) were increased from 1.6 mg $N-NH_4^+$ $L^{-1}\ h^{-1}$ to 8.2 mg $N-NH_4^+$ $L^{-1}\ h^{-1}$ and 1.8 mg $N-NH_4^+$ g VSS $^{-1}\ h^{-1}$ to 9.4 mg $N-NH_4^+$ g VSS $^{-1}\ h^{-1}$ after 36 days.

Table 3.S2: Technical events and disturbances during the study.

Type	Time	Description
Excess feeding	Day 50 and 53	The influent was fed 9 times in less than 5 hours, therefore, the supernatant of liquid was removed twice at an exchange ratio of 45% after settling on Day 51
Insufficient feeding	Day 60	0.5L influent remained in the feeding tank
Two-time feeding	Day 158	0.25L and 0.75L manually for the 1st and 2nd time
Frequent DO saturation	Day 102-104	DO reached saturation ≥ 7 mg $O_2\ L^{-1}$ four times due to the loss of the sensor signal
Electricity stop	Day 18	Electricity stop for 1h
Electricity stop	Day 276	Electricity stop for 10.5h
Biofilm attachment	Day 282	Remove biofilms in the reactor

6.2 Transfer coefficient measurements

Integration between two different times containing a linear area was used to calculate the K_{La} , and the obtained values at all flow rates were fitted to a linear function between Q_{air} and K_{La} . The first results had a good linearity ($R^2=0.99$) and was used to maintain K_{La} at 0.5 h^{-1} in phase A which corresponds to Q_{air} at 4.5 L h^{-1} (Figure 3.S1A). Then 2 times increase of K_{La} to 1.0 h^{-1} was achieved by increasing the Q_{air} up to 11.7 L h^{-1} in phase B.

Equation 3.S1

$$\ln \frac{C^* - C_2}{C^* - C_1} = -k_L a \cdot (t_2 - t_1)$$

Where, $k_L a$ is the volumetric mass transfer coefficient for oxygen (h^{-1}); t_1 and t_2 is the initial and final time point of linear area of DO evolution with time (h); C^* is the saturated DO concentration during the measurement ($\text{mg O}_2 \text{ L}^{-1}$); C_1 and C_2 is the DO concentration at time t_1 and t_2 ($\text{mg O}_2 \text{ L}^{-1}$).

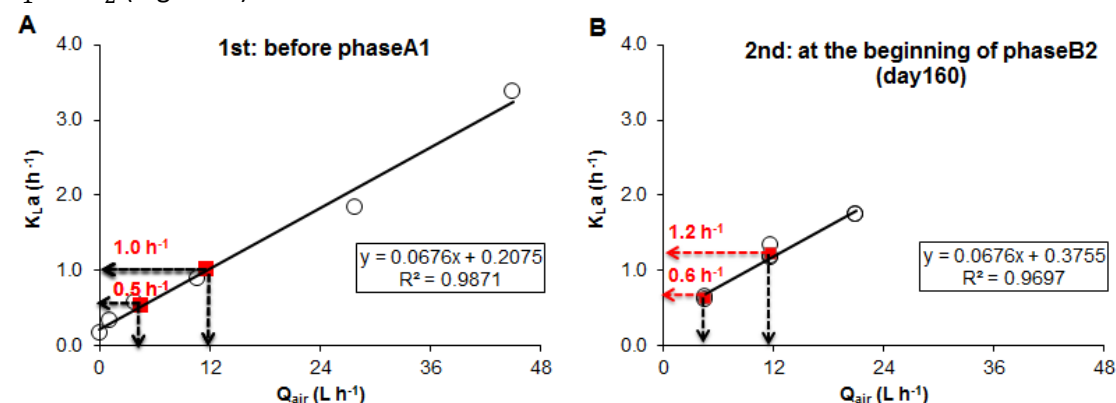
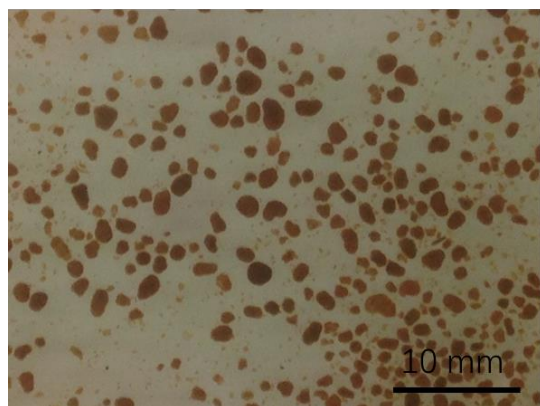


Figure 3.S1: Oxygen transfer results before phaseA1 (A) and at the beginning of phaseB2 (B: Day 160)

Day 20



Day 276

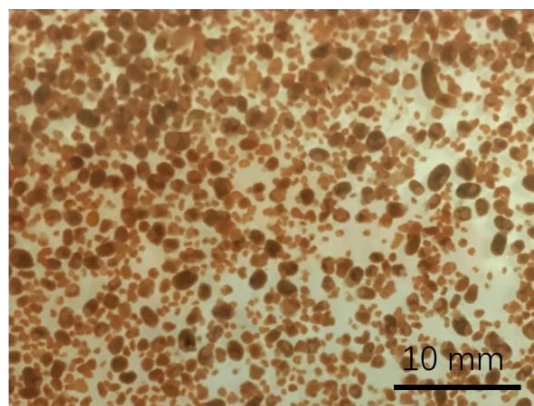


Figure 3.S2: Comparison of the granule morphology between Day 20 and Day 276.

References

- Agrawal, S., Karst, S.M., Gilbert, E.M., Horn, H., Nielsen, P.H., Lackner, S., 2017. The role of inoculum and reactor configuration for microbial community composition and dynamics in mainstream partial nitritation anammox reactors. *MicrobiologyOpen* 6. <https://doi.org/10.1002/mbo3.456>
- Agrawal, S., Seuntjens, D., Cocker, P.D., Lackner, S., Vlaeminck, S.E., 2018. Success of mainstream partial nitritation/anammox demands integration of engineering, microbiome and modeling insights. *Curr. Opin. Biotechnol., Energy biotechnology • Environmental biotechnology* 50, 214–221. <https://doi.org/10.1016/j.copbio.2018.01.013>
- Akaboci, T.R.V., Gich, F., Rusalleda, M., Balaguer, M.D., Colprim, J., 2018. Effects of extremely low bulk liquid DO on autotrophic nitrogen removal performance and NOB suppression in side- and mainstream one-stage PNA. *J. Chem. Technol. Biotechnol. O.* <https://doi.org/10.1002/jctb.5649>
- Ali, M., Rathnayake, R.M.L.D., Zhang, L., Ishii, S., Kindaichi, T., Satoh, H., Toyoda, S., Yoshida, N., Okabe, S., 2016. Source identification of nitrous oxide emission pathways from a single-stage nitritation-anammox granular reactor. *Water Res.* 102, 147–157. <https://doi.org/10.1016/j.watres.2016.06.034>
- APHA, AWWA, WEF, 1998. Standard methods for the examination of water and wastewater. American Public Health Association, Washington, DC, US.
- Baeten, J.E., Batstone, D.J., Schraa, O.J., van Loosdrecht, M.C.M., Volcke, E.I.P., 2019. Modelling anaerobic, aerobic and partial nitritation-anammox granular sludge reactors - A review. *Water Res.* 149, 322–341. <https://doi.org/10.1016/j.watres.2018.11.026>
- Besson, M., Tiruta-Barna, L., Spérandio, M., 2017. Environmental Assessment of Anammox Process in Mainstream with WWTP Modeling Coupled to Life Cycle Assessment, in: *Lecture Notes in Civil Engineering. Presented at the Frontiers International Conference on Wastewater Treatment and Modelling*, Springer, Cham, pp. 392–397. https://doi.org/10.1007/978-3-319-58421-8_62
- Cao, Y., Loosdrecht, M.C.M. van, Daigger, G.T., 2017. Mainstream partial nitritation–anammox in municipal wastewater treatment: status, bottlenecks, and further studies. *Appl. Microbiol. Biotechnol.* 101, 1365–1383. <https://doi.org/10.1007/s00253-016-8058-7>
- Castro-Barros, C.M., Daelman, M.R.J., Mampaey, K.E., van Loosdrecht, M.C.M., Volcke, E.I.P., 2015. Effect of aeration regime on N₂O emission from partial nitritation-anammox in a full-scale granular sludge reactor. *Water Res.* 68, 793–803. <https://doi.org/10.1016/j.watres.2014.10.056>
- Cervantes, F.J. (Ed.), 2009. *Environmental Technologies to Treat Nitrogen Pollution: Principles and Engineering*. IWA Publishing, London.
- Connan, R., Dabert, P., Moya-Espinosa, M., Bridoux, G., Béline, F., Magrí, A., 2018. Coupling of partial nitritation and anammox in two- and one-stage systems: Process operation, N₂O emission and microbial community. *J. Clean. Prod.* 203, 559–573. <https://doi.org/10.1016/j.jclepro.2018.08.258>
- De Clippeleir, H., Vlaeminck, S.E., Carballa, M., Verstraete, W., 2009. A low volumetric exchange ratio allows high autotrophic nitrogen removal in a sequencing batch reactor. *Bioresour. Technol.* 100, 5010–5015. <https://doi.org/10.1016/j.biortech.2009.05.031>
- De Cocker, P., Bessiere, Y., Hernandez-Raquet, G., Dubos, S., Mozo, I., Gaval, G., Caligaris, M., Barillon, B., Vlaeminck, S.E., Sperandio, M., 2018. Enrichment and adaptation yield

- high anammox conversion rates under low temperatures. *Bioresour. Technol.* 250, 505–512. <https://doi.org/10.1016/j.biortech.2017.11.079>
- Domingo-Félez, C., Mutlu, A.G., Jensen, M.M., Smets, B.F., 2014. Aeration Strategies To Mitigate Nitrous Oxide Emissions from Single-Stage Nitritation/Anammox Reactors. *Environ. Sci. Technol.* 48, 8679–8687. <https://doi.org/10.1021/es501819n>
- Fan, H., Liu, X., Wang, Hao, Han, Y., Qi, L., Wang, Hongchen, 2017. Oxygen transfer dynamics and activated sludge floc structure under different sludge retention times at low dissolved oxygen concentrations. *Chemosphere* 169, 586–595. <https://doi.org/10.1016/j.chemosphere.2016.10.137>
- Garcia-Ochoa, F., Gomez, E., 2009. Bioreactor scale-up and oxygen transfer rate in microbial processes: An overview. *Biotechnol. Adv.* 27, 153–176. <http://dx.doi.org/10.1016/j.biotechadv.2008.10.006>
- Ge, S., Wang, S., Yang, X., Qiu, S., Li, B., Peng, Y., 2015. Detection of nitrifiers and evaluation of partial nitrification for wastewater treatment: A review. *Chemosphere, Wastewater-Energy Nexus: Towards Sustainable Wastewater Reclamation* 140, 85–98. <https://doi.org/10.1016/j.chemosphere.2015.02.004>
- Gilbert, E.M., Agrawal, S., Karst, S.M., Horn, H., Nielsen, P.H., Lackner, S., 2014. Low Temperature Partial Nitritation/Anammox in a Moving Bed Biofilm Reactor Treating Low Strength Wastewater. *Environ. Sci. Technol.* 48, 8784–8792. <https://doi.org/10.1021/es501649m>
- Gilbert, E.M., Agrawal, S., Schwartz, T., Horn, H., Lackner, S., 2015. Comparing different reactor configurations for Partial Nitritation/Anammox at low temperatures. *Water Res.* 81, 92–100. <https://doi.org/10.1016/j.watres.2015.05.022>
- Harris, E., Joss, A., Emmenegger, L., Kipf, M., Wolf, B., Mohn, J., Wunderlin, P., 2015. Isotopic evidence for nitrous oxide production pathways in a partial nitritation-anammox reactor. *Water Res.* 83, 258–270. <https://doi.org/10.1016/j.watres.2015.06.040>
- Kampschreur, M.J., Poldermans, R., Kleerebezem, R., van der Star, W.R.L., Haarhuis, R., Abma, W.R., Jetten, M.S.M., Jetten, M.S.M., van Loosdrecht, M.C.M., 2009. Emission of nitrous oxide and nitric oxide from a full-scale single-stage nitritation-anammox reactor. *Water Sci. Technol. J. Int. Assoc. Water Pollut. Res.* 60, 3211–3217. <https://doi.org/10.2166/wst.2009.608>
- Kartal, B., Tan, N.C.G., Biezen, E.V. de, Kampschreur, M.J., Loosdrecht, M.C.M.V., Jetten, M.S.M., 2010. Effect of Nitric Oxide on Anammox Bacteria. *Appl. Environ. Microbiol.* 76, 6304–6306. <https://doi.org/10.1128/AEM.00991-10>
- Lackner, S., Gilbert, E.M., Vlaeminck, S.E., Joss, A., Horn, H., van Loosdrecht, M.C.M., 2014. Full-scale partial nitritation/anammox experiences – An application survey. *Water Res.* 55, 292–303. <https://doi.org/10.1016/j.watres.2014.02.032>
- Laguna, A., Ouattara, A., Gonzalez, R.O., Baron, O., Famá, G., El Mamouni, R., Guiot, S., Monroy, O., Macarie, H., 1999. A simple and low cost technique for determining the granulometry of upflow anaerobic sludge blanket reactor sludge. *Water Sci. Technol., Wastewater Anaerobic Treatment* 40, 1–8. [https://doi.org/10.1016/S0273-1223\(99\)00602-2](https://doi.org/10.1016/S0273-1223(99)00602-2)
- Laureni, M., Falås, P., Robin, O., Wick, A., Weissbrodt, D.G., Nielsen, J.L., Ternes, T.A., Morgenroth, E., Joss, A., 2016. Mainstream partial nitritation and anammox: long-term process stability and effluent quality at low temperatures. *Water Res.* 101, 628–639. <https://doi.org/10.1016/j.watres.2016.05.005>
- Lotti, T., Kleerebezem, R., Hu, Z., Kartal, B., Jetten, M.S.M., van Loosdrecht, M.C.M., 2014a. Simultaneous partial nitritation and anammox at low temperature with granular sludge. *Water Res.* 66, 111–121. <https://doi.org/10.1016/j.watres.2014.07.047>

- Lotti, T., Kleerebezem, R., Lubello, C., van Loosdrecht, M.C.M., 2014b. Physiological and kinetic characterization of a suspended cell anammox culture. *Water Res.* 60, 1–14. <https://doi.org/10.1016/j.watres.2014.04.017>
- Loy, A., Maixner, F., Wagner, M., Horn, M., 2007. probeBase—an online resource for rRNA-targeted oligonucleotide probes: new features 2007. *Nucleic Acids Res.* 35, D800–D804. <https://doi.org/10.1093/nar/gkl856>
- Ma, C., Jensen, M.M., Smets, B.F., Thamdrup, B., 2017. Pathways and Controls of N₂O Production in Nitritation–Anammox Biomass. *Environ. Sci. Technol.* 51, 8981–8991. <https://doi.org/10.1021/acs.est.7b01225>
- Morales, N., Val del Río, Á., Vázquez-Padín, J.R., Méndez, R., Campos, J.L., Mosquera-Corral, A., 2016. The granular biomass properties and the acclimation period affect the partial nitritation/anammox process stability at a low temperature and ammonium concentration. *Process Biochem.* 51, 2134–2142. <https://doi.org/10.1016/j.procbio.2016.08.029>
- Park, H.-D., Noguera, D.R., 2004. Evaluating the effect of dissolved oxygen on ammonia-oxidizing bacterial communities in activated sludge. *Water Res.* 38, 3275–3286. <https://doi.org/10.1016/j.watres.2004.04.047>
- Peng, L., Ni, B.-J., Erler, D., Ye, L., Yuan, Z., 2014. The effect of dissolved oxygen on N₂O production by ammonia-oxidizing bacteria in an enriched nitrifying sludge. *Water Res.* 66, 12–21. <https://doi.org/10.1016/j.watres.2014.08.009>
- Peng, L., Ni, B.-J., Ye, L., Yuan, Z., 2015. The combined effect of dissolved oxygen and nitrite on N₂O production by ammonia oxidizing bacteria in an enriched nitrifying sludge. *Water Res.* 73, 29–36. <https://doi.org/10.1016/j.watres.2015.01.021>
- Piciooreanu, C., Pérez, J., van Loosdrecht, M.C.M., 2016. Impact of cell cluster size on apparent half-saturation coefficients for oxygen in nitrifying sludge and biofilms. *Water Res.* 106, 371–382. <https://doi.org/10.1016/j.watres.2016.10.017>
- Schmid, M.C., Maas, B., Dapena, A., van de Pas-Schoonen, K., van de Vossenberg, J., Kartal, B., van Niftrik, L., Schmidt, I., Cirpus, I., Kuenen, J.G., Wagner, M., Sinnighe Damsté, J.S., Kuypers, M., Revsbech, N.P., Méndez, R., Jetten, M.S.M., Strous, M., 2005. Biomarkers for In Situ Detection of Anaerobic Ammonium-Oxidizing (Anammox) Bacteria. *Appl. Environ. Microbiol.* 71, 1677–1684. <https://doi.org/10.1128/AEM.71.4.1677-1684.2005>
- Sliekers, A.O., Derwort, N., Gomez, J.L.C., Strous, M., Kuenen, J.G., Jetten, M.S.M., 2002. Completely autotrophic nitrogen removal over nitrite in one single reactor. *Water Res.* 36, 2475–2482. [https://doi.org/10.1016/S0043-1354\(01\)00476-6](https://doi.org/10.1016/S0043-1354(01)00476-6)
- Strous, M., Heijnen, J.J., Kuenen, J.G., Jetten, M.S.M., 1998. The sequencing batch reactor as a powerful tool for the study of slowly growing anaerobic ammonium-oxidizing microorganisms. *Appl. Microbiol. Biotechnol.* 50, 589–596. <https://doi.org/10.1007/s002530051340>
- van de Graaf, A.A., de Bruijn, P., Robertson, L.A., Jetten, M.S.M., Kuenen, J.G., 1996. Autotrophic growth of anaerobic ammonium-oxidizing micro-organisms in a fluidized bed reactor. *Microbiology* 142, 2187–2196. <https://doi.org/10.1099/13500872-142-8-2187>
- Vannecke, T.P.W., Volcke, E.I.P., 2015. Modelling microbial competition in nitrifying biofilm reactors. *Biotechnol. Bioeng.* 112, 2550–2561. <https://doi.org/10.1002/bit.25680>
- Vázquez-Padín, J., Mosquera-Corral, A., Campos, J.L., Méndez, R., Revsbech, N.P., 2010. Microbial community distribution and activity dynamics of granular biomass in a CANON reactor. *Water Res.* 44, 4359–4370. <https://doi.org/10.1016/j.watres.2010.05.041>

- Vlaeminck, S.E., De Clippeleir, H., Verstraete, W., 2012. Microbial resource management of one-stage partial nitrification/anammox. *Microb. Biotechnol.* 5, 433–448.
<https://doi.org/10.1111/j.1751-7915.2012.00341.x>
- Vlaeminck, S.E., Terada, A., Smets, B.F., Clippeleir, H.D., Schaubroeck, T., Bolca, S., Demeestere, L., Mast, J., Boon, N., Carballa, M., Verstraete, W., 2010. Aggregate Size and Architecture Determine Microbial Activity Balance for One-Stage Partial Nitrification and Anammox. *Appl. Environ. Microbiol.* 76, 900–909.
<https://doi.org/10.1128/AEM.02337-09>
- Volcke, E.I.P., Picioreanu, C., Baets, B.D., Loosdrecht, M.C.M. van, 2012. The granule size distribution in an anammox-based granular sludge reactor affects the conversion—Implications for modeling. *Biotechnol. Bioeng.* 109, 1629–1636.
<https://doi.org/10.1002/bit.24443>
- Wan, X., Baeten, J.E., Volcke, E.I.P., 2019. Effect of operating conditions on N₂O emissions from one-stage partial nitrification-anammox reactors. *Biochem. Eng. J.* 143, 24–33.
<https://doi.org/10.1016/j.bej.2018.12.004>

Chapter 4: Long-term and short-term dynamics of N₂O emission in PNA process under oxygen limitation

1. Introduction

The partial nitrification anammox (PNA) process is the conversion of a part of ammonium into nitrite combined with anaerobic conversion of ammonia and nitrite into dinitrogen with anammoxidans type bacteria. This process is considered as an environmental friendly operation due to low aeration needs allowing water resource recovery facilities to tend to energy neutrality (Cao et al., 2017). Consequently over 100 full-scale wastewater treatment plants have been installed worldwide for treating reject water from anaerobic digestion which contain a high concentration of ammonium (Lackner et al., 2014). However this process, or more accurately the partial nitrification, can emit significant amount of N_2O in the atmosphere, which might compensate its overall benefit. Indeed nitrous oxide (N_2O) is a potent greenhouse gas with 300 times higher radiative forcing than carbon dioxide (IPCC, 2014) and predicted to be the dominant tropospheric ozone depleting substance emitted in the 21st century (Ravishankara et al., 2009). Additionally, N_2O can easily react with multiple chemical N-forms in the lifecycle threatening the human health, and therefore unwanted even at trace levels (Kanter et al., 2017).

N_2O emissions from PNA or anammox reactors have been studied with suspended culture (Sliekers et al., 2002; Lotti et al., 2014), granular sludge (Kampschreur et al., 2009; Castro-Barros et al., 2015) and attached biofilm (Ma et al., 2017; Kampschreur et al., 2008). The reported N_2O emission factor from the single-stage PNA process ranged from less than 0.1% up to more than 20% of the nitrogen removed (Sliekers et al., 2002; Harris et al., 2015; Wan et al., 2019). Fundamentally, the current identified microbial N_2O pathways include nitrifier denitrification (Nitrite as terminal electron acceptor) and incomplete NH_2OH oxidation by AOB (ammonium oxidizing bacteria), as well as incomplete denitrification by heterotrophic denitrifiers (Chandran et al., 2011; Law et al., 2012; Wang et al., 2014). Although the abiotic pathways have also been reported to contribute the N_2O production, e.g. iron (III) with nitrite (Kampschreur et al., 2011), NH_2OH with HNO_2 (Soler-Jofra et al., 2016, 2018), abiotic role is normally insignificant due to the strict reaction condition (low pH) and/or extreme substrate conditions needed for such reaction. Using natural stable isotopes measurement for nitrogen and oxygen, conversion pathways and processes impacting N_2O production were traced (Ma et al., 2017). In addition N_2O isotopomers analysis is an efficient tool to distinguish N_2O pathways through the SP signature (Harris et al., 2015; Sutka et al., 2006; Wunderlin et al., 2013), each pathway being characterized by one specific site preference (SP) range (Wunderlin et al., 2013; Ali et al., 2016; Terada et al., 2017). For the NH_2OH oxidation pathway, the experimental N_2O SP values from pure culture and mixed culture studies are generally from 28.4‰ to 36.6‰. For the nitrifier denitrification pathway SP values range from -1.7‰ to 0.1‰. SP values measured in pure culture experiments for the heterotrophic denitrification pathway are mostly from -5.1‰ to -0.5‰ (Duan et al., 2017). SP values for abiotic reactions are also relatively constant, ranging from 29.5‰ to 35.2‰ (Duan et al., 2017). This technique was recently applied to investigate the N_2O production pathways in PNA systems. In a lab-scale continuously fed PNA reactor, an unexpectedly-high SP value up to 40‰ was reported during the normal operating condition which cannot be explained by neither of identified N_2O pathways (Harris et al., 2015). More recently in a granular PNA system, the isotopomer analysis during the normal operation cycles quantified the comparative contribution of NH_2OH

oxidation and nitrite reduction but cannot exclude the possible role of the N_2O production by the anammox bacteria (Ali et al., 2016). This possibility was also consistent with the further batch analysis with both N_2O microsensor measurements and FISH analysis that about 30% of N_2O was produced inside the anammox-dominated anoxic zone. Although nitrous oxide (N_2O) is not present in the anammox molecular metabolism (Kartal et al., 2011), whether anammox bacteria is able to produce N_2O is disputable. For the pure culture system, Lotti et al. (2014) reported that a highly enriched anammox free-cells (over 98%) emit 0.20% of the removed nitrogen as N_2O , and further increased N-load resulted in the increased N_2O emissions. In another study anammox granules from a two-stage PNA process can emit 0.14% of the removed nitrogen but the most probable contributor was the putative heterotrophic bacteria but not anammox bacteria (Okabe et al., 2011). In the single-stage PNA process, the participation of anammox bacteria might complicate the original AOB and heterotroph pathways. Given that NO is the same intermediate for AOB, heterotrophic bacteria and anammox, anammox bacteria might also act as N_2O influencing species in the PNA process (Ali et al., 2016; Harris et al., 2015).

Different aeration strategies have been used in the single-stage PNA system such as non-limiting to limiting DO, high frequency to low frequency alternated aeration and non-aeration, pure anoxic to enhanced aeration (Castro-Barros et al., 2015; Domingo-Félez et al., 2014; Kampschreur et al., 2009). Operation of PNA under extremely low DO with oxygen transfer rate control was successfully applied (Akaboci et al., 2018). First efficient aeration control is critically important for repressing nitrite oxidizing bacteria (NOB) and enriching objective ammonium oxidizing bacteria (AnAOB and AerAOB) in a single-stage PNA reactor. In addition oxygen diffusion and limitation possibly affect the N_2O production based on full-scale (Kampschreur et al., 2009; Domingo-Félez et al., 2014; Castro-Barros et al., 2015). However the effect of oxygen limitation on the N_2O emissions in PNA system is still controversial. A short-term measurement campaign conducted by M. J. Kampschreur et al., (2009) showed that oxygen limitation intend to decrease the N_2O emission ($0\text{--}2\text{ mg O}_2\text{ L}^{-1}$). In the same direction Castros Barros et al. (2015) reported that increasing aeration stimulated N_2O emissions temporarily. However Ma et al. (2017) observed an increase of N_2O emission at lower dissolved oxygen ($0.2\text{ to }2\text{ mg L}^{-1}$) with a stimulation of both NN and ND pathway at low DO. Using intermittent aeration, higher frequency of transition between aerated and non-aerated periods led to higher N_2O emission (Domingo-Félez et al., 2014). The recent work of Wan et al. (2019) showed that the effect of oxygen on N_2O emission is highly non monotonous, showing a peak of emission close to the optimal DO zone for maximizing nitrogen removal efficiency. But this dependency was significantly influenced by other factors like granules radius or presence of influent organics.

Previous studies concerning N_2O production in PNA process focused mainly on short term response of the system to oxygen limitation (Kampschreur et al., 2009) or to rapidly changing aeration mode (intermittency and intensity) (Domingo-Félez et al., 2014; Castro-Barros et al., 2015; Ma et al., 2017). However, the characteristic of N_2O emission under constant and long term oxygen limitation is relatively unknown. Meanwhile, the short term and long term responses of N_2O emission after increasing or decreasing the aeration rate while maintaining limiting-oxygen condition is also unexplored yet.

The objective of this study was to comprehensively characterize emission of nitrogen oxides (N_2O and NO) from a lab-scale single-stage PNA reactor under constant aeration and highly limiting oxygen conditions ($\text{DO} < 0.2 \text{ mg L}^{-1}$), with the following expectations: 1) summarize the main N_2O emission pattern and the parameters influencing those patterns; 2) identify/confirm the possible N_2O production pathways with nitrogen isotopes and specific batch tests, 4) compare short-term and long-term responses to change in air flow rate exploring various levels of oxygen limitation.

2. Materials and methods

2.1 Reactor operation

The experiment was conducted in a laboratory-scale reactor with a working volume of 11 L and a headspace volume of 3 L. The reactor was equipped with mechanical stirring and gas diffuser. Air flow rate was imposed by a mass flowmeter (Bronkorst). The pH (H8481 HD, SI Analytics), temperature and dissolved oxygen (DO) with (VisifermTM, Hamilton), dissolved CO_2 (Membrane Kit InPro5000 3.1B, Mettler Toledo) as well as Oxidation-Reduction Potential (PL89225Pt, SI Analytics) probes were continuously monitored with online-equipped sensors in the liquid phase. The off-gas was continuously sampled from the top of the reactor at a constant flow rate of 0.06 L/min and measured with online devices for N_2O (X-STREAM X2GP, Emerson) and NO (NGA 2000 CLD, Emerson) concentrations. To prevent from the moisture, a condenser and hydrophobic gas filter ($0.2 \mu\text{m}$) were installed before gas analyzers. The N_2O and NO gas analyzers were calibrated monthly. Data were logged every 1-2 min by an online software. The temperature was maintained at $26.6 \pm 0.6 \text{ }^\circ\text{C}$ using a water jacket. pH was maintained (6.9-7.5) through dosing 1 M NaHCO_3 or injecting CO_2 gas.

The reactor was inoculated with granular sludge ($0.87 \pm 0.03 \text{ g VSS L}^{-1}$) taken from an industrial single stage PNA process, and stored at 4°C during transport. For recovering anammox activity it was first operated in anoxic condition with supplying ammonium and nitrite for 36 days (details in supplementary information). At the end of this period maximal anammox activity was $9.4 \text{ mg N-NH}_4^+ \text{ g VSS}^{-1} \text{ h}^{-1}$. Then the reactor was operated in SBR mode with continuous aeration during reaction phase for 293 days with a synthetic influent containing ammonium as sole nitrogen source.

The cycle consisted in the following sequence: feeding (8 min), aerated reaction phase (variable), settling (2 min), and withdraw (8 min). 1L of liquid was added or removed during feeding or decanting period, resulting in a volumetric exchange ratio (VER) of 9.1%. During normal feeding phase, aeration was turned off. For testing this effect aeration was imposed during feeding for a specific period of 5 days (Days 255-260).

The synthetic influent mimicked a high strength wastewater with high level of ammonium (500 mg N L^{-1}) without organic matter. The wastewater composition was modified from van de Graaf et al. (1996): $2.36 \text{ g/L } (\text{NH}_4)_2\text{SO}_4$ ($0.5 \text{ g/L NH}_4\text{-N}$), 3.00 g/L NaHCO_3 , $0.025 \text{ g/L KH}_2\text{PO}_4$, $0.2 \text{ g/L MgSO}_4 \cdot 7\text{H}_2\text{O}$, $0.147 \text{ g/L CaCl}_2 \cdot 2\text{H}_2\text{O}$ and 2 mL of trace element solutions I and II per liter of feed. The trace element solution I contained (g/L): 3.0 EDTA and $3.93 \text{ FeCl}_2 \cdot 4\text{H}_2\text{O}$; trace

element solution II contained (g/L) 15 EDTA, 0.43 ZnSO₄·7H₂O, 0.24 CoCl₂·6H₂O, 1.21 MnCl₂·4H₂O, 0.25 CuSO₄·5H₂O, 0.24 Na₂MoO₄·2H₂O, 0.32 NiSO₄·7H₂O, 0.16 Na₂SeO₃·5H₂O, 0.01 H₃BO₃, 0.05 Na₂WO₄·2H₂O. This feeding solution had a pH of 8.2 and a molar ratio of ammonium to bicarbonate of 1:1. It was stored at 4°C and changed every week.

2.2 Aeration control and oxygen transfer rate

Air flow rate was imposed for limiting the DO to a very low value (<0.2 mg O₂ L⁻¹) controlling the ammonium oxidation rate by oxygen transfer rate (OTR):

Equation 4.1

$$OTR = K_L a \cdot (DO^* - DO)$$

Reaction phase duration was automatically controlled by detecting the end of the ammonium oxidation. Aeration was switched off and settling started as soon as a maximal DO setpoint was reached. Indeed DO rapidly increased at the end of nitrification due to ammonium depletion and lower oxygen demand. As the duration of reaction time was automatically controlled, the nitrogen loading rate was closed to the ammonium uptake rate and finally also imposed by the OTR. The effect of maximum DO setpoint value was studied during the first period: it was increased from 0.3 to 2.0 mg O₂ L⁻¹ on Day 39, decreased to 1.0 mg O₂ L⁻¹ on Day 96, and decreased to 0.3 mg O₂ L⁻¹ on Day 100 until the end of the study.

Dynamic method was used to determine periodically the transfer coefficient for oxygen (K_La) (Garcia-Ochoa and Gomez, 2009). Measurements were performed with effluent from SBR cycles without biomass but with the mineral medium. Stripping with N₂ and oxygenating were performed successively for different airflow rates (0, 1.1, 3.9, 10.7, 27.8, 45 L h⁻¹). See details in the previous chapter. Measurements were done in duplicates. Linear correlation was obtained between coefficient and air flow rate (K_La=0.076.Q_{air}+0.2075; R²= 0.9871). This experiment was also conducted during the study to check regularly possible change of the evolution of the correlation (at days 160: K_La=0.076.Q_{air}+0.3755; R²=0.9671).

The influence of aeration intensity on reactor performance was studied by imposing two different levels of air flow rates (periods A and B). Initially the imposed air flow rate (Q_{air}) was chosen (level A: 4.5 L h⁻¹) for maintaining DO concentration lower than 0.2 mg L⁻¹; resulting in an initial ammonium uptake rate of about 25% of maximal anoxic anammox rate. After 100 days, air flow rate was increased to level B during one week to study short term effect, before reducing to level A for 40 days. Level B was definitively imposed at Day 145 until the end of the study (300 days). The level B (11.7 L.h⁻¹) was chosen in order to adapt the oxygen transfer rate to the increase of nitrification rate. It was also fixed in order to not observe any nitrite accumulation in the reactor (nitrite production rate by AOB being the limiting step compared to nitrite consumption rate by anammox). The DO concentration measured in the bulk during reaction phase was initially in a range 0.02-0.2 mg O₂ L⁻¹ decreasing during almost 100 days (phase A1), was still detectable in phase B1, but became completely undetectable after Day 107.

Regarding the applied Q_{air} , the operating period was considered divided into four phases: A1, A2 (low air flow rate), B1 and B2 (high air flow rate). This protocol allowed evaluating both the short term and long term effect of the change in the aeration rate total nitrogen removal rate.

2.3 Chemicals analysis and specific batch tests

Effluent samples and mixed liquor samples were taken periodically for chemical analysis. Effluent samples were immediately filtrated through 0.2 μm millipore filters and was stored at 4°C for further chemical analysis. For sludge samples, in order to prevent the loss of biomass, centrifugation at 4°C for 2 min was performed before the filtration, and the separated sludge was returned back to the reactor at the feeding phase of next cycle.

Ammonium was measured using spectrophotometric method with the Nessler standard method (AFNOR NFT 90-015). Nitrite and nitrate were determined by spectrophotometry (Griess method) using a continuous flow analyzer Smartchem 200 (AMS, Italy). Total suspended solids (TSS), ash content and volatile suspended solids (VSS) were measured according to standard methods (APHA et al., 1998).

Regularly kinetic studies were carried out in the reactor during SBR cycle. Samples were taken along the cycle and immediately filtered through Millipore filter units (0.2 μm pore size) for measurements of NH_4^+ , NO_2^- and NO_3^- .

During the last weeks of the study, specific batch tests were performed for exploring the possible N_2O pathways. In order to test the contribution of heterotrophic denitrification on the total N_2O emission, anoxic experiment was performed (Day 289). For such experience nitrogen gas was blown through the liquid and headspace (50.3 L h^{-1}). Additional nitrite was provided to the system for measuring both nitrate and nitrite utilization rates under non limiting condition, as well as N_2O emission rate. Another series of tests were realized under aerobic condition but with increasing nitrite level on Day 290-291. DO level was below the detection limit ($<0.05 \text{ mg L}^{-1}$) of the DO sensor during all those tests. Three levels of average nitrite concentration were used: 0.45 mg N L^{-1} , 4.4 mg N L^{-1} , 14.5 mg N L^{-1} .

2.4 Isotopes analysis

During the period of maximal N_2O emission, a batch cycle was also characterized using isotopic measurements. Isotope measurements were analyzed in IEES Laboratory (Sorbonne Université, Paris, France) using an isotope ratio mass spectrometer (IRMS, DeltaVplus; Thermo Scientific, Bremen, Germany) in continuous-flow with a purge-and-trap system and coupled with a Finnigan GasBench II system (Thermo Scientific). Oxygen and nitrogen isotope data are expressed in the usual delta notation ($\delta^{15}\text{N}$ and $\delta^{18}\text{O}$), defined as:

Equation 4.2

$$\delta_{\text{sample}} (\text{‰}) = \left(\frac{R_{\text{sample}}}{R_{\text{standard}}} - 1 \right) \times 1000 \quad ,$$

where R is the isotopic ratio $^{15}\text{N}/^{14}\text{N}$ or $^{18}\text{O}/^{16}\text{O}$.

Nitrogen and oxygen isotope ratios of nitrate and nitrite were determined separately following a modified protocol of McIlvin and Altabet (Semaoune et al. 2012). Nitrogen isotope ratios were determined following the protocol of Zhang et al (2007). These methods consist in the conversion of the substrate (ammonium or nitrite or nitrate) into dissolved N_2O .

The GasBench II allows to sampling of the gases and removal of the water contained in the liquid samples, and finally separation of the interfering gases of N_2O using a chromatographic column (CP-poraPLOT U; Thermo Scientific). The N_2O -SP ($\delta^{15}\text{N}_\alpha - \delta^{15}\text{N}_\beta$) values were calculated based on the raw values of $\delta^{15}\text{N}$ -bulk and $\delta^{31}\text{NO}$ ($\delta^{15}\text{N}^\alpha\text{-N}_2\text{O}$), which were measured by the IRMS from the same N_2O reference gas. $\delta^{15}\text{N}$ - N_2O of the reference gas was calibrated in the laboratory of the Tokyo Institute of Technology using calibration procedures reported previously (Toyoda and Yoshida, 1999). Ammonium and nitrate standards were used to calibrate the isotopic composition of N_2O (USGS-25, $\delta^{15}\text{N} = -30.43\text{‰}$, IAEA N1, $\delta^{15}\text{N} = 0.4\text{‰}$, IAEA N2, $\delta^{15}\text{N} = 20.3\text{‰}$, IAEA 305, $\delta^{15}\text{N} = 39.8\text{‰}$, USGS34, $\delta^{15}\text{N} = 1.8\text{‰}$, $\delta^{18}\text{O} = 27.9\text{‰}$ and USGS35, $\delta^{15}\text{N} = 2.7\text{‰}$, $\delta^{18}\text{O} = 57.5\text{‰}$). The precision of the measurement is 0.5‰ for $\delta^{15}\text{N}$ and 1‰ for $\delta^{18}\text{O}$.

2.5 Calculations

In addition to regular kinetic measurements, for each SBR cycle, volumetric ammonium uptake rate (AUR, $\text{mgN L}^{-1} \text{h}^{-1}$) was estimated with the input ammonium and the reaction time (assuming ammonium consumption almost constant within reaction phase). The specific ammonium uptake rate (SAUR, $\text{mgN g-VSS}^{-1} \text{h}^{-1}$) was calculated with biomass concentration (VSS) measured or interpolated between two measurements.

For each cycle, the NO and N_2O emission rate (NO_{ER} and $\text{N}_2\text{O}_{\text{ER}}$, $\text{mgN L}^{-1} \text{d}^{-1}$) were calculated by multiplying the measured gas concentration and the gas flow rate. The emission factors ($\text{N}_2\text{O}_{\text{EF}}$ and NO_{EF} , %) were calculated as the ratio between the total N_xO emitted as nitrogen (obtained by integrating the rates) and the total ammonia-nitrogen removed during each cycle. Average concentration and emission rate were also calculated.

The average NO_2^- concentration during reaction phase was calculated based on the cycles when the kinetic study was performed by excluding initial and latter one hour from each SBR cycle, to conserve stable nitrite concentration observed over 70% of the SBR cycle.

3. Results

3.1 Typical N₂O patterns during batch cycles

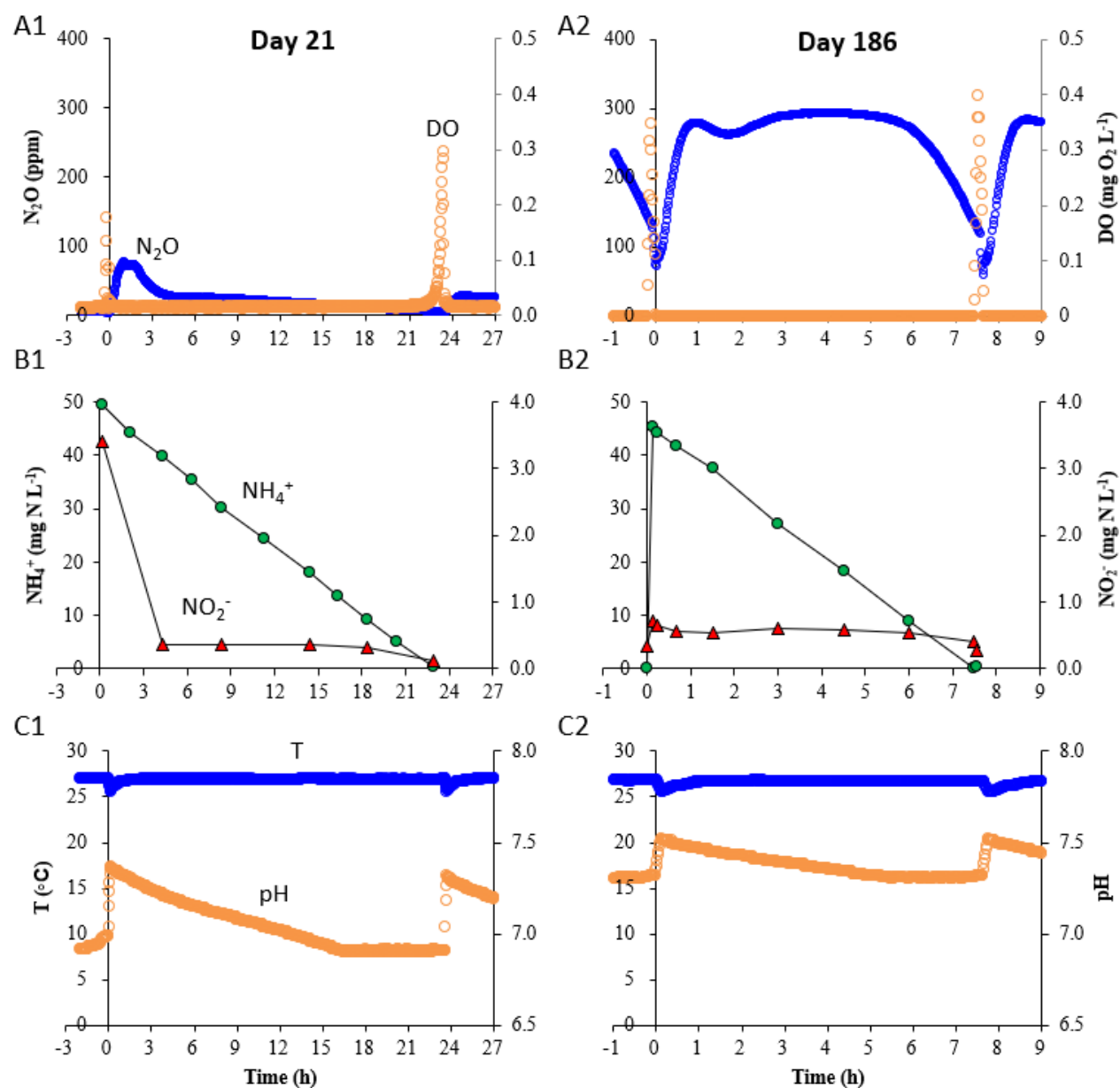


Figure 4.1: Example of kinetics for two SBR cycles on Day 21 (left: A1, B1 and C1) and Day 186 (right: A2, B2 and C2).

Figure 4.1 showed two examples of data profiles collected during batch cycle at the start (Day 21) and the last period (Day 186) of the study. Globally ammonium was consumed linearly indicating a constant AUR during the cycle without ammonium limitation effect.

Regularly (like in Figure 4.1A1) the N₂O emission profile showed a dual pattern with two different phases: (1) a transient period after feeding during which a N₂O peak can be observed; and (2) a second period with more stable emission associated to the constant ammonium

uptake rate. Operating parameters influencing each phase will be discussed later. But as a first observation, the Figure 4.1A1 showed that the initial peak of N₂O was generally associated to a nitrite peak measured after feeding period (3.6 mg N L⁻¹ .on the example of Figure 4.1A1). Then after one to three hours the nitrite level was stabilized to a value ranging from 0.3 to 1 mgN L⁻¹ which corresponds to equilibrium between production rate by AOB and consumption rate by Anammox.

While the contribution of transient peak was significant (41% of total N₂O emission) during the start-up period with relatively low emission (Figure 4.1A1), the stable N₂O emission played a dominating role (80% of total N₂O emission) during the period with high emission corresponding to high ammonium uptake rate (Figure 4.1A2). From the mathematical point of view, this quantification method serves as a useful feedback on the changes of the N₂O evolution in successive cycles.

3.2 Long term evolution of N₂O emission during intensification period

Figure 4.2 showed the responses of N₂O dynamic during the first 5 months (up to Day 143) as both AUR and nitrogen loading rate increased (phase A). Among this intensification period AUR did increase over time cycle by cycle, from 1.9 to 3.9 mg L⁻¹ h⁻¹, and the reaction time decreased from 24h to 12h as a consequence.

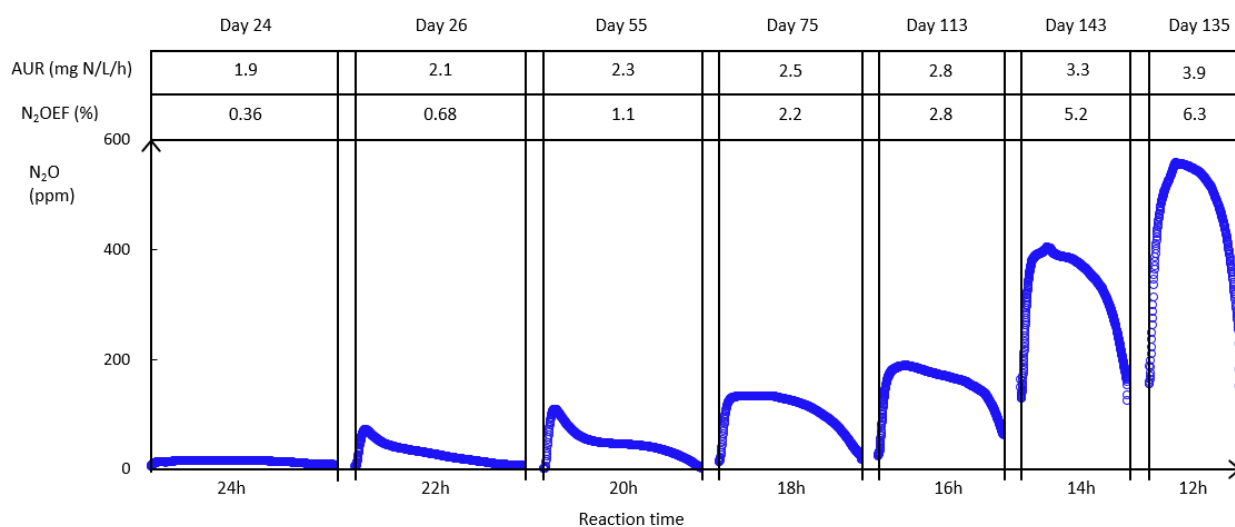


Figure 4.2: Batch tests conducted just after (Day 148, N₂OEF=5.6%) and one week (Day 156, N₂OEF=2.2%) after increasing the air flow rate to 11.7 L h⁻¹.

For the first cycles N₂O emission rate remained quite low, with an emission factor of 0.36% for Day 24. This was observed during more than one month. Then N₂OEF started to increase and was two times higher (0.63%) as the AUR increase by 10%. Finally N₂O emission increased almost exponentially during 5 months, reaching about 6.3% of the removed nitrogen at the end of the phase A. During this period a linear relationship was found between AUR and N₂O_{EF} (with R² = 0.98). In addition, given the constant biomass concentration throughout this study, nitrate production rate (not shown, see previous chapter 2) progressively decreased during the same period indicating that NOB were progressively repressed.

Figures 4.3A and B shows respectively the calculated N₂O and NO concentration and emission factor profiles for each single cycle during the entire study. While Figure 4.3C shows the evolution of the average nitrite concentration (average value measured during stable emission). First the results again illustrates the increasing emissions (N₂O and NO) observed during the first 135 days. The maximum N₂O_{EF} at 7.2% in this period was observed on Day 122, while for the maximum NO_{EF} at 0.068%. After the increase of air flow rate (Day 145) the data show the long term mitigation of both N₂O and NO emissions, despite some oscillations were provoked by disturbances due to specific tests. Notably during this period, oxygen transfer tests (K_{la}) were conducted before Day 161 for 5 days, (not accounted in the operation time). The electricity was also stopped for 33 hours without agitation on Day 212 maintaining anoxic situation for 33 hours. Alternating increase and decrease of N₂O emissions resulted in four peaks and four valleys (Day 160 at 1.3%, Day 196 at 1.4%, Day 216 at 1.8% and Day 237 at 1.3%), while NO_{EF} ranged between 0.02% and 0.07%.

The evolution of nitrite concentration (Figure 4.3C) under the low air flow rate was first a continuous decrease from 0.90 to 0.27 mg N L⁻¹ during the beginning 20 days. Then it gradually increased until the end of phase A1, up to 0.63 mg N L⁻¹ (Day 134) before the air flow rate was increased. After the air flow rate was increased to 11.7 L h⁻¹ on Day 146, this value first increased rapidly up to 0.94±0.10 mg N L⁻¹ and decreased for 10 days like N₂O, reaching down to 0.48±0.08 mg N L⁻¹, and finally remained stable between 0.4 and 0.6 mg N L⁻¹.

Globally if a correlation between nitrite and N₂O emissions is somehow observed, the long term data showed that a unique correlation is impossible to find, indicating a multiple parameter phenomenon. For a given period like the initial phase of period B, emission mitigation correlated well with nitrite lowering. But on the other hand, variable N₂O oscillations during the rest of phase B were uncorrelated to nitrite (stable).

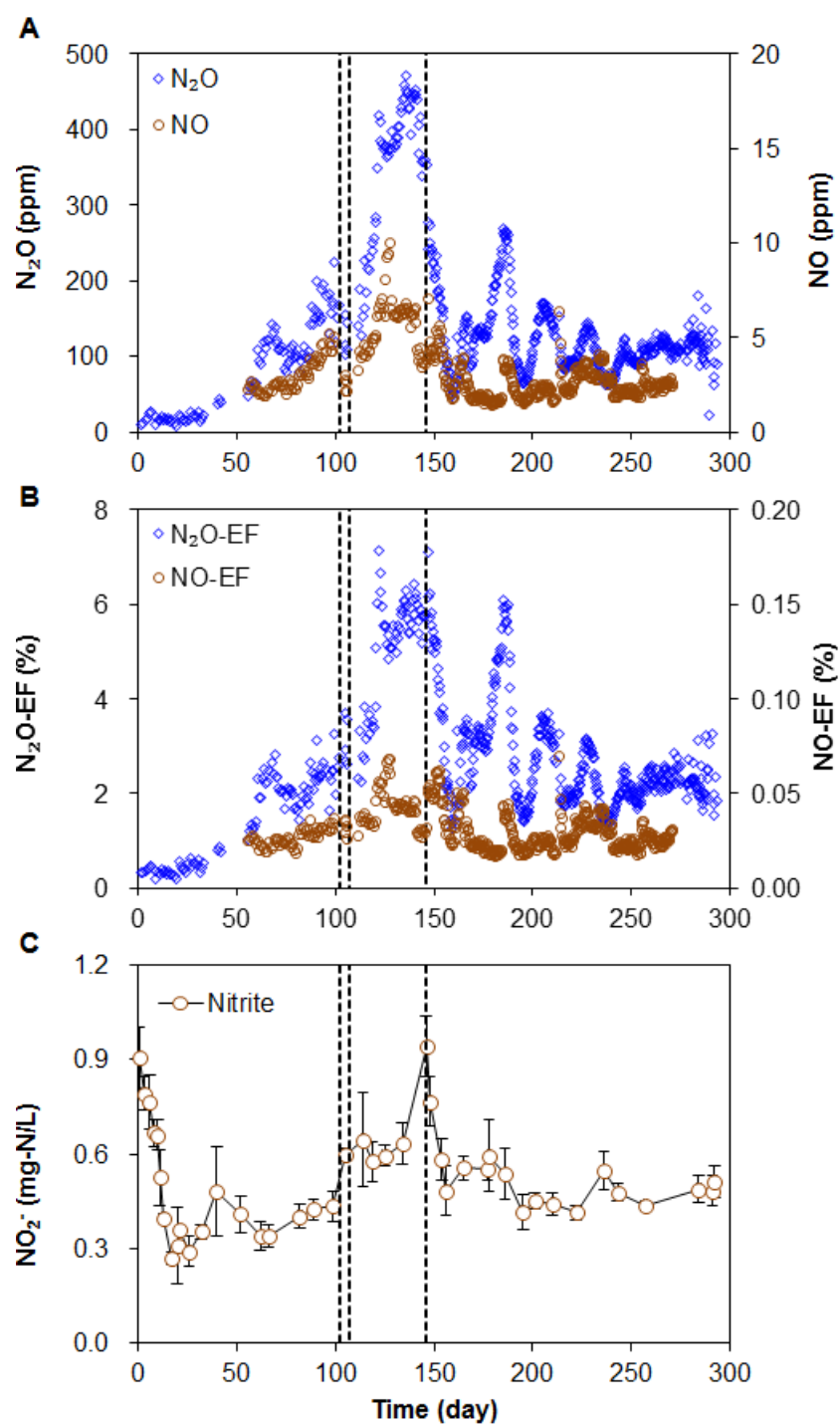


Figure 4.3: The evolution of concentration (A) and emission factor (B) for N_2O and NO gases, as well as the average nitrite (C) concentration calculated as an average without considering initial peaks.

3.3 Operational parameters influencing initial N₂O peak: DO setpoint, aeration during feeding

Transition between two cycles was a source of disturbance causing initial N₂O peaks at varying levels. Among operational parameters which were observed to influence this peak were the maximal dissolved oxygen (reached at the end of the reaction period) and the aeration during feeding. And more globally this peak was encouraged each time nitrite was accumulated during transition phase.

The maximal DO setpoint permitted the automatic controller to stop aeration and start settling and a new cycle. In a system operated at extremely low DO, this value was reached after depletion of ammonium and a time lag (this time during which oxygen rises due to lower oxygen uptake rate with constant oxygen transfer rate). Effect of this DO set point level was evaluated during phase A. It was initially set at 0.3 mg O₂ L⁻¹ but first increased to 1.0 mg O₂ L⁻¹ for 16 days and later to 2.0 mg O₂ L⁻¹ for 20 days, before being adjusted back to 1.0 mg O₂ L⁻¹ for 5 days and then set constantly at 0.3 mg O₂ L⁻¹ until the end. As illustrated on the Figure 4.2 (day 55), the initial N₂O peak was higher for such high DO. However fixing the DO setpoint to a very low level was risking errors in detection due to some noise in the signal. Therefore, the value of 0.3 mg L⁻¹ was a good compromise.

While feeding phase was unaerated for most of the study, aeration was maintained during the feeding for a given week at the end of the running period. For both periods, successive cycles showed very high reproducibility (Figure 4.5). As shown in Figure 4.4, the kinetics were very similar except for nitrite, NO and N₂O. Aeration during feeding induced more nitrite accumulation during first minutes of the cycle, as well as higher NO, and N₂O peaks. Quantitatively the N₂O peak was two times higher whereas the global emission factor gained 15% (2.0 to 2.3 %, see Table 4.1). Interestingly this was also accompanied by a NO peak (small but detectable) which confirmed to be the intermediate precursor of N₂O (Figure 4.4).

For summarizing, during the transient phase between two cycles, oxygen rising or aeration were observed to provoke a sudden high nitrification rate during the first minutes of reaction phase with unbalanced anammox activity which led to nitrite peak and finally undesired N₂O emission.

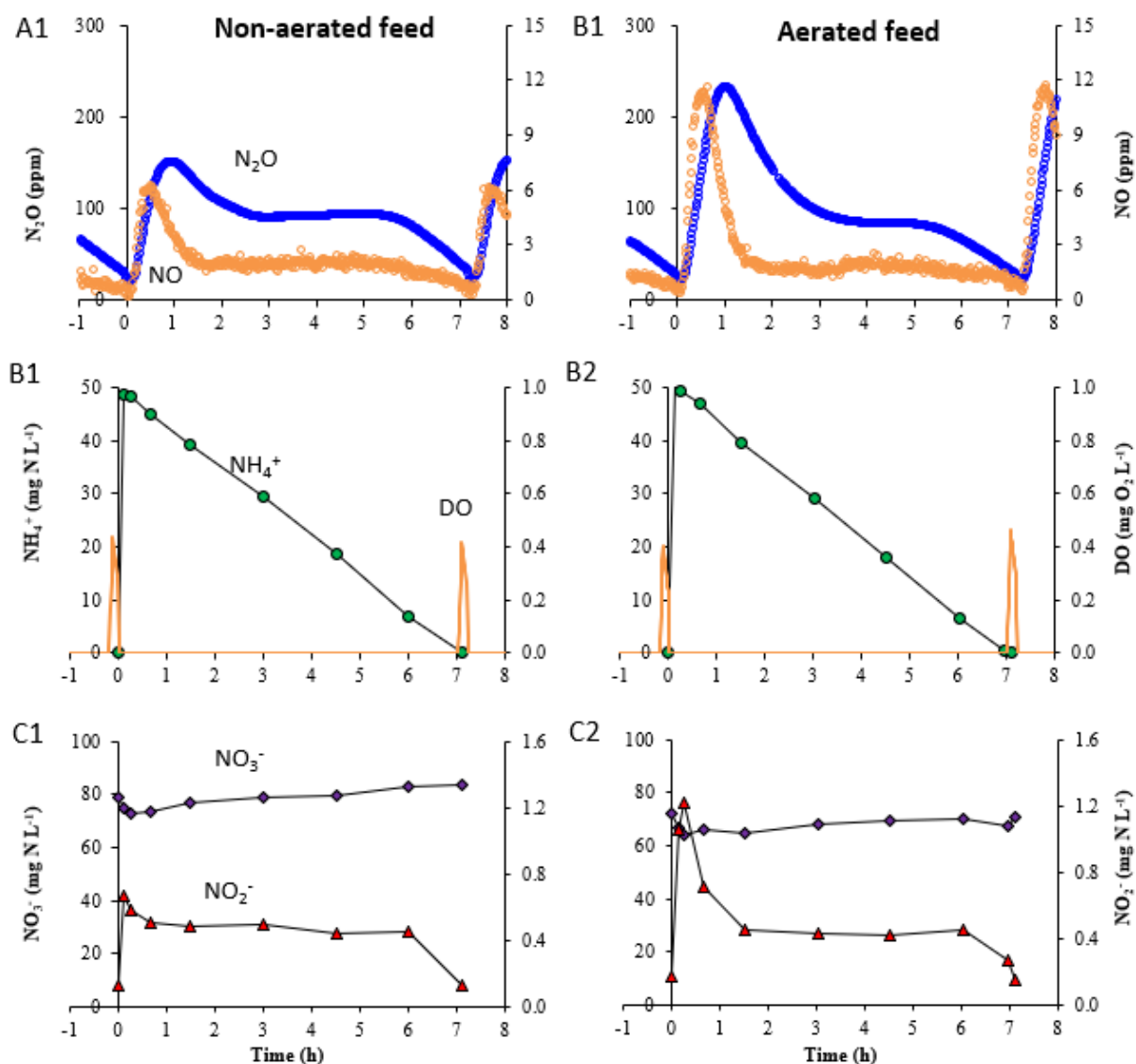


Figure 4.4: Comparison of the SBR cycles with unaerated (A1, B1, C1) and aerated feeding (A2, B2, C2). Nitrous oxide and nitric oxide concentrations (A1 and A2), ammonium and DO (B1 and B2), nitrite and nitrate concentration (C1 and C2); day 243 and 257.

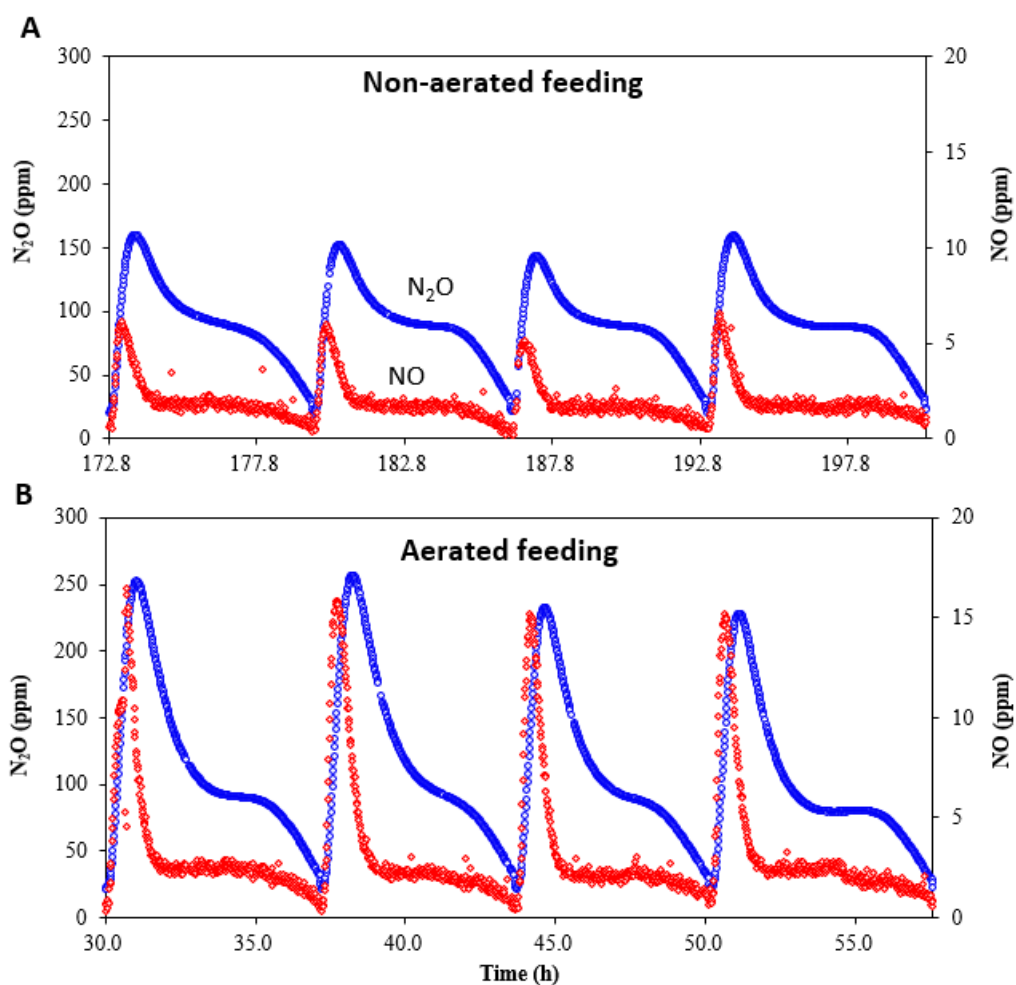


Figure 4.5: The repeatable cyclic NO and N_2O emissions between the aerated and non-aerated feeding.

Table 4.1: A statistical summary of the NO and N_2O emissions during the selective operation periods with aerated and non-aerated feeding.

	Non-aerated feeding	Aerated feeding
Operating time (days)	248 - 253	255 - 260
N_2O peak (ppm)	144-195	193-257
NO peak (ppm)	4.9-8.1	10.2-20.1
N_2OEF (%)	2.0 ± 0.1	2.3 ± 0.2
$NOEF$ (%)	0.022 ± 0.0022	0.029 ± 0.003

3.4 Influence of air flow rate on N₂O emission (short and long term)

Air flow rate was first increased from 4.5 L h⁻¹ to 11.7 L h⁻¹ at Day 102 for only one week for studying short term effect (before returning to the initial rate). Then it was increased again at Day 146 and maintained for the rest of the study to study long term effect. On Figure 4.6, each point corresponds to a SBR cycle during which AUR, N₂O_{ER} and N₂OEF were measured.

N₂O_{ER} and AUR were relatively stable before flow rate increase. For each time the air flow was increased both AUR and N₂O_{ER} increased instantaneously and proportionally during the following cycles. For the first experiment this situation was stable during the following 5 days. After reestablishing the initial flow rate value, both N₂O_{ER} and AUR returned to the initial values. The emission factor did not change significantly during this experiment ranging from 2.5% to 3%.

For the second experiment, high air flow level being maintained on a long term, both N₂O emission rate and emission factor finally decreased progressively days after days. Whereas ammonium uptake rate was maintained relatively high ($5.6 \pm 0.3 \text{ mg N L}^{-1} \text{ h}^{-1}$), N₂O_{ER} went down from $7.5 \pm 0.7 \text{ mg N L}^{-1} \text{ d}^{-1}$ to $1.5 \text{ mg N L}^{-1} \text{ d}^{-1}$ and the emission factor decreased from 5.8% to 1.3% within 15 days.

Figure 4.7 showed two batch tests respectively 2 days and 10 days after following air flow increase. Comparing the batch test, the N₂O gas concentration has decreased by a factor 3, and NO concentration (much smaller) by a factor 2. Another difference is the nitrite level: the peak after feeding went from 1.8 to 0.6 mg N L⁻¹ and the constant nitrite level during ammonium uptake decrease from 0.75 mg N L⁻¹ to 0.5 mg N L⁻¹.

Overall, these observations clearly demonstrated a different effect at short and long term of the air flow rate increase. Under DO limitation, increase of OTR first increases both ammonium oxidation rate and N₂O emission rate but on a long term the system adapted and finally emitted much less N₂O even with a higher nitrogen loading rate.

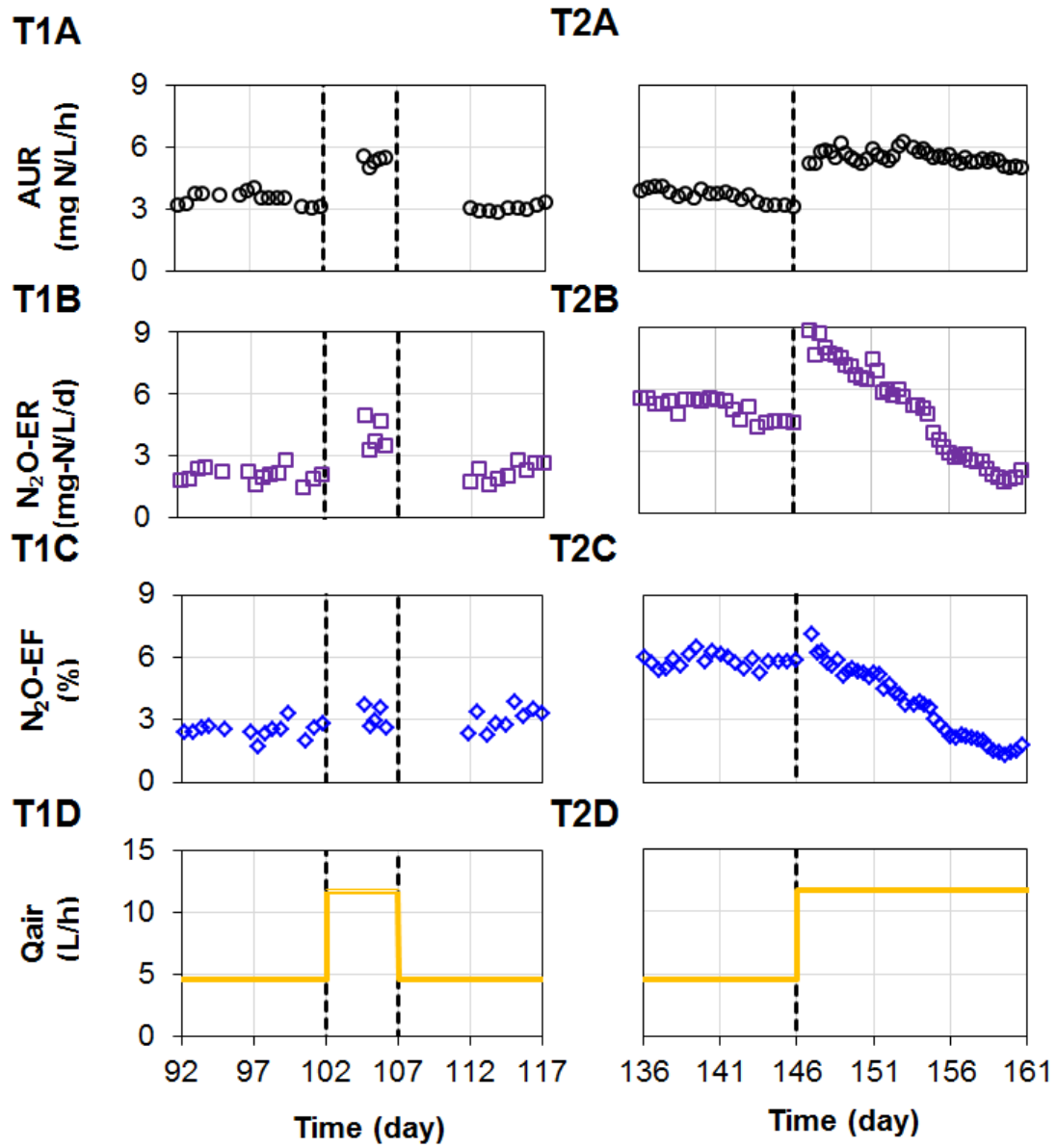


Figure 4.6: Responses of AUR (A), N₂OER (B), N₂O_{EF} (C) and Q_{air} (D) to air flow rate modification. T1 and T2 represent the first and the second transition periods. Each point corresponds to one SBR cycle.

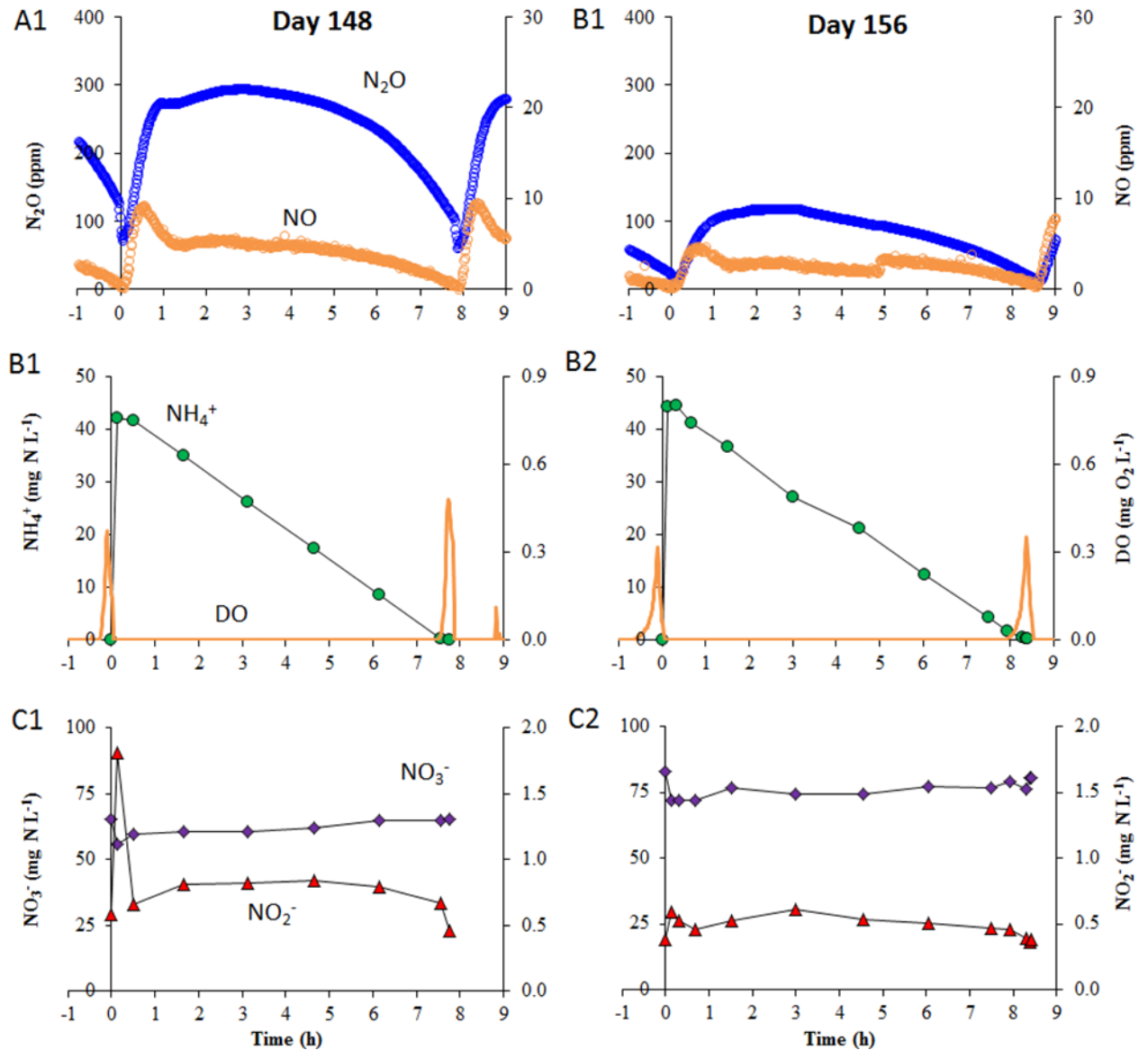


Figure 4.7: Batch tests conducted just after (Day 148, $\text{N}_2\text{OEF}=5.6\%$) and one week (Day 156, $\text{N}_2\text{OEF}=2.2\%$) after increasing the air flow rate to 11.7 L h^{-1} .

3.5 Isotopes analysis

The $\delta^{15}\text{N}$ with ammonium, nitrite and nitrate as substrates and the SPs of the emitted N_2O were determined during the period when the N_2O emission factor was stabilized at the highest value (Figures 4.8A and B). For each feeding, the same range of the initial and final $\delta^{15}\text{N}$ value for all substrates showed that the nitrogen evolution remained relatively stable during successive cycles. During the cycle a clear tendency over time is observed for $\delta^{15}\text{N}-\text{NO}_2^-$: a rapid decline of the initial value from 91.4‰ to -23.9‰ after the feeding followed by the progressive increase up to 90.7‰ at the end of the cycle. The gradual increase of $\delta^{15}\text{N}-\text{NH}_4^+$ (1.9‰ , 0.9 h) just after feeding to 57.5‰ (10 h) is in company with the constant $\delta^{15}\text{N}-\text{NO}_3^-$

averaging at 42.8‰ from the start to the end (Figure 4.8A). For N_2O , the $\delta^{15}N$ - N_2O results showed a first decrease trend after feeding from 5.6‰ to -24.7‰ (similar value as for nitrite) and subsequently it gradually increased to the initial level (5.5‰) at the end of the cycle (Figure 4.8B). This indicates that the nitrite is first produced with a lower content of ^{15}N but is also progressively consumed (by Anammox and possibly denitrification) which makes its ^{15}N content increase. N_2O as a final product logically showed a low ^{15}N content. But the fact that this content increased a little during the cycle can indicate that some processes (possibly heterotroph denitrification) slightly consumed it.

The N_2O -SP measurement showed a rapid increase from -2.6‰ to 5.5‰ during the initial 20 min followed by the subsequent level stabilizing at 0.7 ± 1.5 ‰ from 0.5 h until the end of this cycle (Figure 4.8.B). This range of SP value was theoretically associated to the nitrite denitrification pathway.

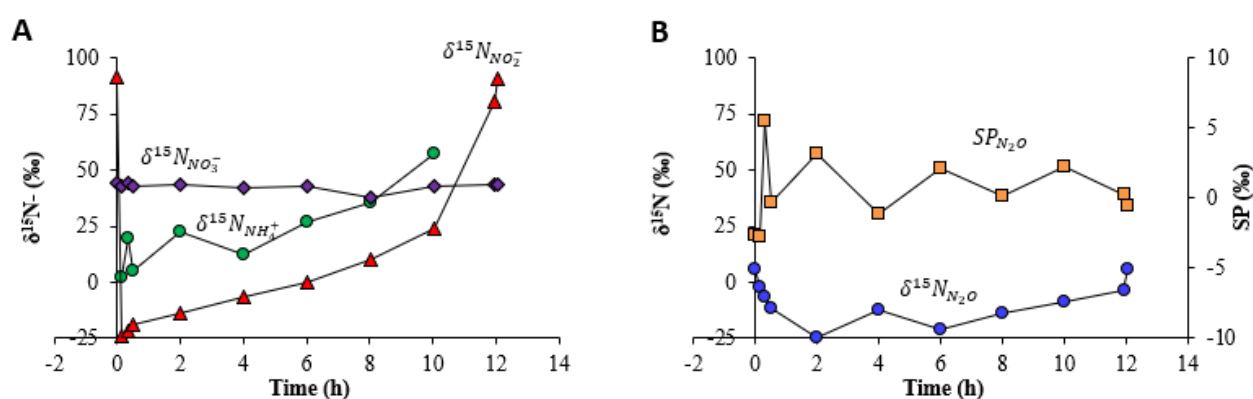


Figure 4.8: $\delta^{15}N$ of NH_4^+ , NO_2^- , NO_3^- in the liquid (A) phase and N_2O in the gas phase (B), as well as the N_2O -SP at each sampling time over one cycle on Day 134.

3.6 N_2O emission rate during specific batch tests

Series of batch tests were performed to investigate the N_2O emission at varying nitrite levels, under aerobic and anoxic conditions (Table 4.2 and Figure 4.S1).

At the end of phase B, for typical batch test under aeration, the N_2O ER was $2.38 \text{ mg N L}^{-1} \text{ h}^{-1}$ and N_2O EF was 1.8%, for a nitrite level around 0.45 mg N L^{-1} . Then a test was performed under aerated condition with high level of nitrite (15.5 mg N L^{-1}). Whereas AUR was comparable to a normal batch, the average nitrite consumption rate was $0.23 \text{ mg N L}^{-1} \text{ d}^{-1}$ (linear zone) and the average nitrate production rate (NAUR) was $0.61 \text{ mg N L}^{-1} \text{ d}^{-1}$. It was like if only the nitrite provided by ammonium oxidation was (locally) consumed but not significantly the additional nitrite. The N_2O emission during that test was 4 times higher than in normal condition ($10.5 \text{ mg N L}^{-1} \text{ d}^{-1}$), and N_2O EF was 9.0%, i.e. 5 times higher than in normal test at the same period. This illustrates the strong stimulating effect of nitrite on N_2O emission.

Anoxic test was performed also with additional nitrite (6.6 mg N L^{-1}) in order to estimate the N_2O emission from heterotrophic denitrification at the maximal denitrifying rate. During that test both nitrite and nitrate were consumed at rate of $0.29 \text{ mg N L}^{-1} \text{ h}^{-1}$ and $0.59 \text{ mg N L}^{-1} \text{ h}^{-1}$ respectively during 8 hours, illustrating the denitrifying capacity. The average N_2O emission rate was $0.80 \text{ mg N L}^{-1} \text{ d}^{-1}$. While it corresponds to 3.8% of the nitrite and nitrate reduced in the test, this rate is 3 times lower than the emission rate measured during normal cycle under aeration and low nitrite level. This supports the idea that heterotroph denitrifying activity was not the major pathway under normal aerated SBR operation.

Table 4.2: Batch tests under specific conditions. Ammonium uptake rate (AUR), nitrite uptake rate (NIUR), nitrate uptake rate (NAUR), nitrate production rate (NAPR), N_2O emission rate (N_2OER) and N_2O emission factor (N_2OEF).

Condition	NH_4^+	NO_2^-	NO_3^-	AUR	NIUR	NAUR	NAPR	N_2OER	N_2OEF
	mg N L^{-1}			$\text{mg N L}^{-1} \text{ h}^{-1}$				$\text{mg N L}^{-1} \text{ h}^{-1}$	%
Anoxic with nitrite (Day 289)	0	Mean: 4.40 Max: 6.60 Min: 3.53	Mean: 76.1 Max: 81.3 Min: 73.9	0	0.16	1.02	-	0.033	-
Aerobic – no nitrite (Day 291)	Max: 46.6 Min: 0	Mean: 0.45 Max: 0.73 Min: 0.21	Mean: 77.8 Max: 82.8 Min: 73.6	5.83	0.012	-	1.14	0.099	1.8
Aerobic – with nitrite (Day 290)	Max: 43.0 Min: 0	Mean: 14.51 Max: 15.48 Min: 13.36	Mean: 73.9 Max: 79.9 Min: 70.6	4.83	0.23	-	0.77	0.44	9.0

4. Discussion

4.1 Dynamic and range of N_2O emission under O_2 limitation

In this study dynamic pattern of N_2O emissions from PNA process operated under DO limitation was monitored on a long term. N_2O emission profile shows two contributions during SBR cycle: a peak following each feeding and a plateau during the reaction time. The first was enhanced by aeration during feeding or any excess of oxygen due to too high DO setpoint, both provoking small accumulation of nitrite due to unbalanced nitrification and anammox activities. During the first months the emission factor and rate (plateau) were observed to increase exponentially with the specific ammonium uptake rate, following the progressive growth of AOB and the concomitant repression of NOB. Comparable correlation between AUR and N_2OER has been already observed for nitrifying culture (Law et al., 2012, Ribera-Guardia and Pijuan, 2018) but this is the first time for the PNA system under oxygen limitation. This was also associated to a decrease of the OTR:AUR ratio which can be explained by an increasing repression of NOB which decrease the oxygen need. This led to high N_2O emission (stabilized around 5.8 % at the end of period A2) and a very low oxygen consumed per amount of ammonium removed. Although it is positive from an energetic point of view, this is dramatic in term of global warming potential.

Finally the range of N₂O emission factor measured throughout the study (0.3 to 7.2 %) was relatively comparable to previous studies on single stage PNA systems with various levels of aeration (Table 4.S2). After increasing the air flow rate, emission factor stabilized around 2.0 ±0.1 % at the end of the study. This value is on the average of emission factors reported in literature, suggesting that low DO system does not systematically lead to higher emission factor. As a comparison higher values were observed by Domingo-Félez et al. (2014) (1.6 % to 12%) working under low DO with alternated aeration. Recently Connan et al. (2018) measured emissions yield ranging from 0.5 to 6.3% of the removed nitrogen in a PNA system running in SBR mode at a DO of . Ma et al. (2017) measured emissions factors varying from 0.6 to 2% for various DO level from 2.8 to 0.2 mg O₂ L⁻¹, confirming the stimulating effect of low DO on N₂O emission during short term experiments (single batch for each level). Our study shows that significant changes can be observed on a long term at very low DO level without measurable variation of the DO (<0.2 mg L⁻¹). These variations are likely to be related to small variation of nitrite concentration (Figure 4.6), but also related to DO limitation at local scale which are hardly measurable. The N₂O emission of the PNA system operating at very low DO is finally controllable but very sensitive to the nitrite level.

4.2 Dominance of ND pathway and nitrite stimulating effect

The measurement of natural isotopes and the isotopic signature (SP) indicates that the N₂O was produced in majority by nitrite denitrification pathway when the highest N₂O emission was reached. Indeed SP-N₂O measurement (between -2.7‰ and 5.5‰) is typical of ND pathway and clearly excluded hydroxylamine pathway. Nitrifier denitrification and heterotrophic denitrification are not distinguishable through site preference analysis, the two pathways involving the same nitrite enzymatic reduction. However based on the very low emission rate observed under anoxic condition in presence of both nitrate and nitrite (Table 4.2), we can assume that heterotrophic denitrification was a very minor source of N₂O (and even lower in presence of oxygen).

Transient accumulation of nitrite after feeding (Figure 4.3) or external addition of nitrite (Table 4.2) both provoke a strong increase of N₂O emission. This is perfectly in line with ND pathway which is expected to be stimulated by high nitrite level in this range of concentration (0.5 to 15 mg N L⁻¹) (Lang et al., 2016; Ma et al., 2017). The stimulating effect of nitrite is even more important under O₂ limitation, as previously demonstrated in this thesis (Lang et al., 2016), due to competition for electron between oxygen and nitrite in the catabolism of nitrifiers. This is also in accordance with previous studies dedicated to nitrifying culture (Peng et al., 2015) or mixed nitrifier-anammox culture (Ma et al., 2017).

In nitrifier denitrification pathway, NO₂⁻ is converted into NO by NirK enzyme, and NO is reduced into N₂O by NOR enzyme. This matched well with the gas analysis during typical batch cycle (Figure 4.3): peak of NO (stimulated by initial nitrite presence) was observed before the maximum of N₂O emission. Ratio of NO to N₂O emission factor were very low (ranging from 0.004 to 0.03) which confirms previous observation of Pocquet et al. (2016) with nitrifying culture: very low NO:N₂O ratio are observed when ND pathway was installed in majority.

Whereas for nitrifying culture it was demonstrated that ND pathway dominated at low DO under constant NO_2^- level (Peng et al., 2014) results are more controversial for PNA process (Ali et al., 2016; Harris et al., 2015; Ma et al., 2017). Harris et al. (2015) reported that N_2O emission was likely due to the nitrifier denitrification with SP measurements, in agreement with our observation. However an equilibrium contribution of the hydroxylamine oxidation and nitrifier denitrification was estimated by Ma et al. (2017) and higher rate of hydroxylamine oxidation related N_2O production was found at low DO with short experiments. However, hydraulic and operating condition (DO and nitrite) were quite different from the parent reactor (Ali et al., 2016; Ma et al., 2017). In our study similar conditions were maintained during months and response were probably more representative for long term operation in given conditions. Finally, possibly due to enzymatic pool adaptation, it seems that on a long term under oxygen limitation the nitrite denitrification pathway becomes the major contributor to the N_2O emission in PNA process.

For all that reasons a control strategy allowing to minimize the nitrite accumulation in both transient and stable phases of the cycle is highly recommended for mitigating N_2O emissions from PNA system under oxygen limitation.

4.3 Long term vs short term effects of aeration

In this work it was demonstrated that the effect of a change in air flow rate on short term and long term differs significantly. When the N_2O emission were maximal ($\text{EF}=5.8\%$), the increase of air flow rate (and oxygen transfer rate) first provokes an instantaneous proportional increase of both AUR and N_2O emission rate during several days. However on a long term, N_2O emission rate progressively decreased and N_2O emission factor finally stabilized at 2.1%.

This behavior can be analyzed regarding transient behavior of intermediate NO and NO_2^- . The system being operated under DO limitation, the sudden increase of oxygen transfer rate first implies a sudden increase of ammonium oxidizing rate with a consequent jump of intermediates. Indeed, both NO and nitrite increase during the reaction phase just after this sudden increase of air flow rate (Figure 4.7) from 0.6 to 1 mg N L^{-1} . This logically stimulates N_2O emission rate on a short term. Moreover, higher gas liquid transfer coefficient stimulates N_2O stripping. But after several days the system adapts in a way that both NO , nitrite, and finally N_2O emission are reduced (Figure 4.6). This could be related to enzymatic adaptation of the nitrifier metabolism. Indeed an adaptation of the catabolic system in a way to consume more efficiently the excess of electron produced by HAO enzymes was reported by Chandran et al. (2011). But this could be also explained by a growth of nitrite oxidizing bacteria (NOB) which consumed nitrite more rapidly and limit its N_2O emission stimulation. A small increase of nitrate production rate was observed supporting this hypothesis. Change in physical distribution of the ammonium oxidizing species growing more synergetically with the anammox species in the biofilm could be also imagined, anammox being also able to consume both NO_2^- and NO . However these assumptions are difficult to demonstrated practically and modelling study could help to go more in depth in such mechanisms (chapter 5).

Such difference between short and long term dynamic dynamics reported here clearly shows the complexity of regulation of N₂O production. This is possibly the origin of some contradictory results about the effect of aeration on emission from PNA system. Finally this also indicates that any aeration optimization for N₂O mitigation should be considered on a long term horizon and not only based on short term experiments in future studies.

5. Conclusions

- Long term and short term dynamics of N₂O emissions from a PNA process operated under oxygen limitation were studied during 300 days.
- The first N₂O peak observed after feeding can be limited by anaerobically feeding, lowering the level of oxygen reached at the end of the reaction phase, and finally avoiding any temporarily accumulation of nitrite.
- N₂O emission factor progressively increased from 0.4±0.1% up to 5.8±0.3% within 5 months, but was finally stabilized at 2±0.1% after increasing the air flow rate on a long term. This indicates that emission from PNA operated under very low oxygen level is not far from PNA system working under higher level of oxygen.
- Analysis of nitrogen isotopes and site preference tends to show that the main emission pathway was the nitrite reduction and heterotroph poorly contribute.
- Short term and long term effect of increase of air flow rate were different. Optimization for N₂O mitigation should be considered on a long term horizon and not only with short term assays.

6. Appendix

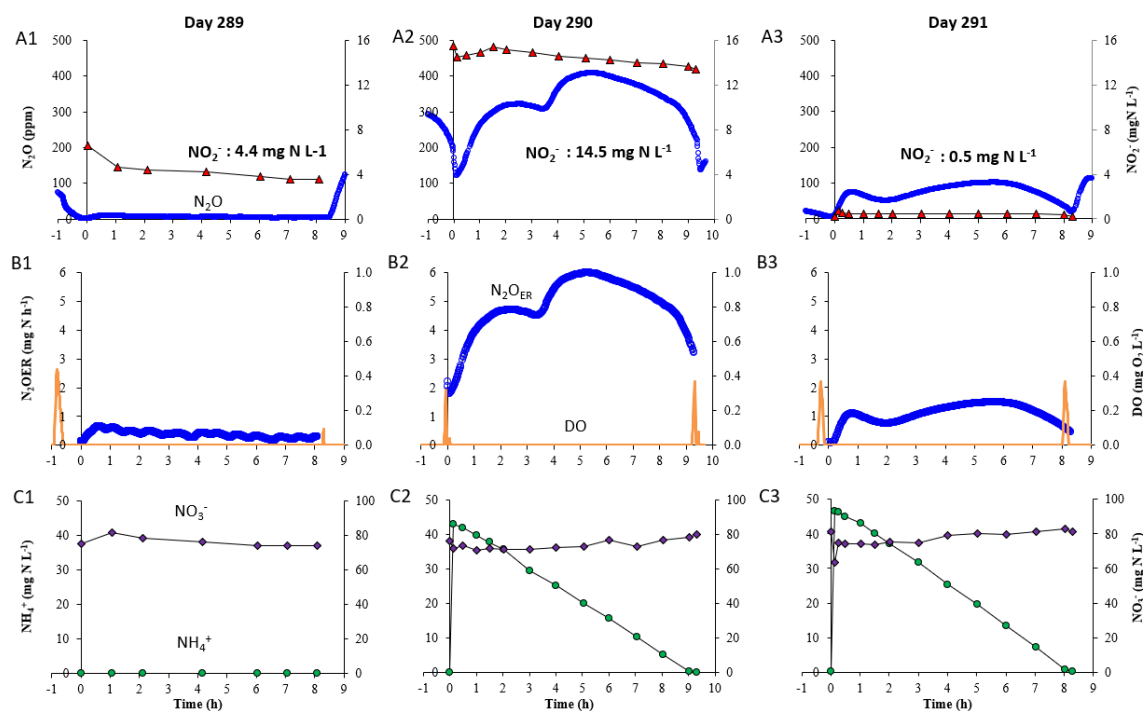
Table 4. S1: SP, $\delta^{15}\text{N}$ and NO_2^- values.

NO.	Time (h)	NO_2^- (mg L^{-1})	SP- N_2O (‰)	$\delta^{15}\text{N-NO}_3$ (‰)	$\delta^{15}\text{N-NH}_4$ (‰)	$\delta^{15}\text{N-NO}_2$ (‰)	$\delta^{15}\text{N-N}_2\text{O}$ (‰)
1	0.0	0.19	-2.6	44.4	-	91.4	5.6
2	0.1	0.86	-2.7	43.1	1.9	-23.9	-2.0
3	0.3	0.71	5.5	44.3	19.9	-22.0	-6.8
4	0.5	0.62	-0.4	43.2	5.2	-18.8	-11.8
5	2.0	0.56	3.2	43.4	22.2	-13.9	-24.7
6	4.0	0.56	-1.2	42.3	12.4	-6.9	-12.6
7	6.0	0.70	2.1	42.6	26.5	-0.1	-21.0
8	8.0	0.65	0.1	37.6	35.2	10.0	-14.1
9	10.0	0.65	2.2	42.5	57.5	24.1	-9.1
10	11.9	0.32	0.3	43.5	-	80.6	-3.7
11	12.1	0.21	-0.5	43.4	-	90.7	5.5

Table 4.S2: Summary of studies on the aeration strategy, ammonium removal and N₂O emissions from the one-stage PNA processes.

References	Feeding mode Biomass origin Reactor	Oxygen control (air flow rate, DO concentration....)	AUR (mg NH ₄ ⁺ -N L ⁻¹ h ⁻¹)		SAUR mg NH ₄ ⁺ -N g-VSS ⁻¹ h ⁻¹		N ₂ OEF (%)
Sliekers et al. (2002)	<ul style="list-style-type: none">• Lab-scale (2 L)• Suspended biomass• Continuous feeding	Air flow rate was fixed at Q _{air} =7.9 mL/min in normal operation, resulting in DO lower than 0.07mg/L	0.1 normally		3.1 normally		~0.05 normally
Kampschreur et al. (2009)	<ul style="list-style-type: none">• Full scale (600m3)• Granular sludge• Continuous feeding	Air was introduced at the bottom of the riser tubes at 2000 m ³ /h in normal operation, resulting in the DO at 5 mgO ₂ /L	41.3 - 41.5		-		1.7 normally
Joss et al. (2009)	<ul style="list-style-type: none">• Pilot scale (400L)• Suspended sludge• Continuous feeding	Q _{air} was set manually to control the net activity of the reactor and adjust it to the incoming supernatant load to be treated; DO higher than 1.0 mg/L resulted in immediate shutdown of the aeration followed by the automatic switch-on at DO lower than 0.5 mg/L.	20.8		-		0.6 (intermittent aeration) 0.4 (continuous aeration)
Domingo-Félez et al. (2014)	<ul style="list-style-type: none">• Lab scale (4L)• Suspended sludge• Continuous feeding	OLR and HRT was remained constant in both tests, resulting in the apparent DO <0.01% at 30°C; During the 1 st test, number of redox cycling periods was increased from 6 to 25 and Q _{air} was fixed at 2.22 L/min; during the 2 nd test, aeration fraction was increased from 53% to 93% by fixing 3 sub-cycles, resulting in a concomitant decrease of Q _{air} from 1.17 to 0.93 L/min	f _{redox} =6	31.1	f _{redox} =6	11.5	5.5
			f _{redox} =8	29.1	f _{redox} =8	10.8	6.4
			f _{redox} =10	29.0	f _{redox} =10	10.7	5.9
			f _{redox} =16	26.5	f _{redox} =16	9.8	2.7
			f _{redox} =25	25.8	f _{redox} =25	9.6	1.6
			R _{on} =53%	31.2	R _{on} =53%	11.1	9.2
			R _{on} =63%	30.2	R _{on} =63%	10.8	12.6
			R _{on} =72%	29.0	R _{on} =72%	10.4	11.6
			R _{on} =81%	32.2	R _{on} =81%	11.5	9.5
R _{on} =93%	29.8	R _{on} =93%	10.6	7.6			
Ma et al. (2017)	<ul style="list-style-type: none">• Incubation test• biofilm from cylindrical plastic carriers• 250 mL serum bottles with 150 mL headspace	<ul style="list-style-type: none">• Manual injection of O2• DO1=0.2 mg/L• (VSS = 20 g/L)	22		1.1		0.6
		<ul style="list-style-type: none">• DO2=2.8 mg/L	31		1.6		0.03

Figure 4.S1: Specific tests with different levels of nitrite and aeration conditions. Three tests were conducted on Day 289 (A1-C1) under the N_2 flow rate of 50.3 L h^{-1} , Day 290 (A2-C2) with the air flow rate of 11.7 L h^{-1} and Day 291 (A3-C3) with air flow rate of 11.7 L h^{-1} respectively.



References

- Ali, M., Rathnayake, R.M.L.D., Zhang, L., Ishii, S., Kindaichi, T., Satoh, H., Toyoda, S., Yoshida, N., Okabe, S., 2016. Source identification of nitrous oxide emission pathways from a single-stage nitrification-anammox granular reactor. *Water Res.* 102, 147–157. <https://doi.org/10.1016/j.watres.2016.06.034>
- APHA, AWWA, WEF, 1998. Standard methods for the examination of water and wastewater. American Public Health Association, Washington, DC, US.
- Cao, Y., van Loosdrecht, M.C.M., Daigger, G.T., 2017. Mainstream partial nitrification–anammox in municipal wastewater treatment: status, bottlenecks, and further studies. *Appl. Microbiol. Biotechnol.* 101, 1365–1383. <https://doi.org/10.1007/s00253-016-8058-7>
- Castro-Barros, C.M., Daelman, M.R.J., Mampaey, K.E., van Loosdrecht, M.C.M., Volcke, E.I.P., 2015. Effect of aeration regime on N₂O emission from partial nitrification-anammox in a full-scale granular sludge reactor. *Water Res.* 68, 793–803. <https://doi.org/10.1016/j.watres.2014.10.056>
- Chandran, K., Stein, L.Y., Klotz, M.G., van Loosdrecht, M.C.M., 2011. Nitrous oxide production by lithotrophic ammonia-oxidizing bacteria and implications for engineered nitrogen-removal systems. *Biochem. Soc. Trans.* 39, 1832–1837. <https://doi.org/10.1042/BST20110717>
- Domingo-Félez, C., Mutlu, A.G., Jensen, M.M., Smets, B.F., 2014. Aeration Strategies To Mitigate Nitrous Oxide Emissions from Single-Stage Nitrification/Anammox Reactors. *Environ. Sci. Technol.* 48, 8679–8687. <https://doi.org/10.1021/es501819n>
- Duan, H., Ye, L., Erler, D., Ni, B.-J., Yuan, Z., 2017. Quantifying nitrous oxide production pathways in wastewater treatment systems using isotope technology – A critical review. *Water Res.* 122, 96–113. <https://doi.org/10.1016/j.watres.2017.05.054>
- Harris, E., Joss, A., Emmenegger, L., Kipf, M., Wolf, B., Mohn, J., Wunderlin, P., 2015. Isotopic evidence for nitrous oxide production pathways in a partial nitrification-anammox reactor. *Water Res.* 83, 258–270. <https://doi.org/10.1016/j.watres.2015.06.040>
- IPCC, 2014. Climate Change 2014: Synthesis Report. Contribution of Working Groups I, II and III to the Fifth Assessment Report of the Intergovernmental Panel on Climate Change [Core Writing Team, R.K. Pachauri and L.A. Meyer (eds.)]. Geneva, Switzerland, p. 151.
- Joss, A., Salzgeber, D., Eugster, J., König, R., Rottermann, K., Burger, S., Fabijan, P., Leumann, S., Mohn, J., Siegrist, H., 2009. Full-Scale Nitrogen Removal from Digester Liquid with Partial Nitrification and Anammox in One SBR. *Environ. Sci. Technol.* 43, 5301–5306. <https://doi.org/10.1021/es900107w>
- Kampschreur, M.J., Kleerebezem, R., de Vet, W.W.J.M., van Loosdrecht, M.C.M., 2011. Reduced iron induced nitric oxide and nitrous oxide emission. *Water Res.* 45, 5945–5952. <https://doi.org/10.1016/j.watres.2011.08.056>
- Kampschreur, M.J., Poldermans, R., Kleerebezem, R., Star, W.R.L. van der, Haarhuis, R., Abma, W.R., Jetten, M.S.M., Loosdrecht, M.C.M. van, 2009. Emission of nitrous oxide and nitric oxide from a full-scale single-stage nitrification-anammox reactor. *Water Sci. Technol.* 60, 3211–3217. <https://doi.org/10.2166/wst.2009.608>
- Kampschreur, M.J., van der Star, W.R.L., Wielders, H.A., Mulder, J.W., Jetten, M.S.M., van Loosdrecht, M.C.M., 2008. Dynamics of nitric oxide and nitrous oxide emission during full-scale reject water treatment. *Water Res.* 42, 812–826. <https://doi.org/10.1016/j.watres.2007.08.022>
- Kanter, D.R., Wentz, J.A., Galloway, J.N., Moomaw, W.R., Winiwarter, W., 2017. Managing a forgotten greenhouse gas under existing U.S. law: An interdisciplinary analysis. *Environ. Sci. Policy* 67, 44–51. <https://doi.org/10.1016/j.envsci.2016.11.003>
- Kartal, B., Maalcke, W.J., de Almeida, N.M., Cirpus, I., Gloerich, J., Geerts, W., Op den Camp, H.J.M., Harhangi, H.R., Janssen-Megens, E.M., Francoijs, K.-J., Stunnenberg, H.G.,

- Keltjens, J.T., Jetten, M.S.M., Strous, M., 2011. Molecular mechanism of anaerobic ammonium oxidation. *Nature* 479, 127–130. <https://doi.org/10.1038/nature10453>
- Lackner, S., Gilbert, E.M., Vlaeminck, S.E., Joss, A., Horn, H., van Loosdrecht, M.C.M., 2014. Full-scale partial nitrification/anammox experiences – An application survey. *Water Res.* 55, 292–303. <https://doi.org/10.1016/j.watres.2014.02.032>
- Lang, L., Pocquet, M., Ni, B.-J., Yuan, Z., Spérandio, M., 2016. Comparison of different 2-pathway models for describing the combined effect of DO and nitrite on the nitrous oxide production by ammonia-oxidizing bacteria. *Water Sci. Technol.* wst2016389. <https://doi.org/10.2166/wst.2016.389>
- Law, Y., Ni, B.-J., Lant, P., Yuan, Z., 2012. N₂O production rate of an enriched ammonia-oxidizing bacteria culture exponentially correlates to its ammonia oxidation rate. *Water Res.* 46, 3409–3419. <https://doi.org/10.1016/j.watres.2012.03.043>
- Lotti, T., Kleerebezem, R., Lubello, C., van Loosdrecht, M.C.M., 2014. Physiological and kinetic characterization of a suspended cell anammox culture. *Water Res.* 60, 1–14. <https://doi.org/10.1016/j.watres.2014.04.017>
- Ma, C., Jensen, M.M., Smets, B.F., Thamdrup, B., 2017. Pathways and Controls of N₂O Production in Nitrification–Anammox Biomass. *Environ. Sci. Technol.* 51, 8981–8991. <https://doi.org/10.1021/acs.est.7b01225>
- Okabe, S., Oshiki, M., Takahashi, Y., Satoh, H., 2011. N₂O emission from a partial nitrification–anammox process and identification of a key biological process of N₂O emission from anammox granules. *Water Res.* 45, 6461–6470. <https://doi.org/10.1016/j.watres.2011.09.040>
- Peng, L., Ni, B.-J., Erler, D., Ye, L., Yuan, Z., 2014. The effect of dissolved oxygen on N₂O production by ammonia-oxidizing bacteria in an enriched nitrifying sludge. *Water Res.* 66, 12–21. <https://doi.org/10.1016/j.watres.2014.08.009>
- Peng, L., Ni, B.-J., Ye, L., Yuan, Z., 2015. The combined effect of dissolved oxygen and nitrite on N₂O production by ammonia oxidizing bacteria in an enriched nitrifying sludge. *Water Res.* 73, 29–36. <https://doi.org/10.1016/j.watres.2015.01.021>
- Pocquet, M., Wu, Z., Queinnec, I., Spérandio, M., 2016. A two pathway model for N₂O emissions by ammonium oxidizing bacteria supported by the NO/N₂O variation. *Water Res.* 88, 948–959. <https://doi.org/10.1016/j.watres.2015.11.029>
- Ravishankara, A.R., Daniel, J.S., Portmann, R.W., 2009. Nitrous Oxide (N₂O): The Dominant Ozone-Depleting Substance Emitted in the 21st Century. *Science* 326, 123–125. <https://doi.org/10.1126/science.1176985>
- Semaoune, P., Sebilo, M., Templier, J., Derenne, S., 2012. Isotopic fractionation of nitrate associated to diffusion and advection. *Environmental Chemistry*. 9, 158–162.
- Sliekers, A.O., Derwort, N., Gomez, J.L.C., Strous, M., Kuenen, J.G., Jetten, M.S.M., 2002. Completely autotrophic nitrogen removal over nitrite in one single reactor. *Water Res.* 36, 2475–2482. [https://doi.org/10.1016/S0043-1354\(01\)00476-6](https://doi.org/10.1016/S0043-1354(01)00476-6)
- Soler-Jofra, A., Picioreanu, C., Yu, R., Chandran, K., van Loosdrecht, M.C.M., Pérez, J., 2018. Importance of hydroxylamine in abiotic N₂O production during transient anoxia in planktonic axenic *Nitrosomonas* cultures. *Chem. Eng. J.* 335, 756–762. <https://doi.org/10.1016/j.cej.2017.10.141>
- Soler-Jofra, A., Stevens, B., Hoekstra, M., Picioreanu, C., Sorokin, D., van Loosdrecht, M.C.M., Pérez, J., 2016. Importance of abiotic hydroxylamine conversion on nitrous oxide emissions during nitrification of reject water. *Chem. Eng. J.* 287, 720–726. <https://doi.org/10.1016/j.cej.2015.11.073>
- Sutka, R.L., Ostrom, N.E., Ostrom, P.H., Breznak, J.A., Gandhi, H., Pitt, A.J., Li, F., 2006. Distinguishing Nitrous Oxide Production from Nitrification and Denitrification on the Basis of Isotopomer Abundances. *Appl. Environ. Microbiol.* 72, 638–644. <https://doi.org/10.1128/AEM.72.1.638-644.2006>

- Terada, A., Sugawara, S., Hojo, K., Takeuchi, Y., Riya, S., Harper, W.F., Yamamoto, T., Kuroiwa, M., Isobe, K., Katsuyama, C., Suwa, Y., Koba, K., Hosomi, M., 2017. Hybrid Nitrous Oxide Production from a Partial Nitrifying Bioreactor: Hydroxylamine Interactions with Nitrite. *Environ. Sci. Technol.* 51, 2748–2756. <https://doi.org/10.1021/acs.est.6b05521>
- Toyoda, S., Yoshida, N., 1999. Determination of Nitrogen Isotopomers of Nitrous Oxide on a Modified Isotope Ratio Mass Spectrometer. *Anal. Chem.* 71, 4711–4718. <https://doi.org/10.1021/ac9904563>
- van de Graaf, A.A., de Bruijn, P., Robertson, L.A., Jetten, M.S.M., Kuenen, J.G., 1996. Autotrophic growth of anaerobic ammonium-oxidizing micro-organisms in a fluidized bed reactor. *Microbiology* 142, 2187–2196. <https://doi.org/10.1099/13500872-142-8-2187>
- Wang, Q., Jiang, G., Ye, L., Pijuan, M., Yuan, Z., 2014. Heterotrophic denitrification plays an important role in N₂O production from nitrification reactors treating anaerobic sludge digestion liquor. *Water Res.* 62, 202–210. <https://doi.org/10.1016/j.watres.2014.06.003>
- Wunderlin, P., Lehmann, M.F., Siegrist, H., Tuzson, B., Joss, A., Emmenegger, L., Mohn, J., 2013. Isotope Signatures of N₂O in a Mixed Microbial Population System: Constraints on N₂O Producing Pathways in Wastewater Treatment. *Environ. Sci. Technol.* 47, 1339–1348. <https://doi.org/10.1021/es303174x>
- Zhang, L., Altabet, M.A., WU, T., Hadas, O., 2007. Sensitive measurement of NH₄⁺ ¹⁵N/¹⁴N (δ¹⁵NH₄⁺) at natural abundance levels in fresh and saltwaters. *Anal. Chem.* 79, 5297–5303.

Chapter 5: Modelling N₂O emission from PNA process under oxygen limitation: Preliminary results and prospects

1. Introduction

Numerical simulation is very useful for analyzing and predicting dynamic behavior of biofilm reactor in order to improve performances. This approach can be applied for describing granular sludge reactors using 1D models considering granules as spherical particles. N₂O emissions from nitrifying and denitrifying systems were previously investigated (Sabba et al., 2015) but only three simulation studies on N₂O emissions from one-stage partial nitrification-anammox reactors have been published yet (Van Hulle et al., 2012 ; Peng et al., 2016; Wan et al., 2019). Hulle et al. (2012) evaluated the N₂O emissions in a granular sludge reactor, by considering the nitrifier denitrification (ND) pathway. The simulation indicated that emission maxima for NO and N₂O coincide with the region for optimal Anammox conversion. Peng et al. (2016) studied the N₂O formation via both ND and NN from a biofilm reactor. The main conclusion was that significant amount of N₂O was produced at low DO level with a maximum around 0.4-0.6 mg O₂ L⁻¹, and that lowering the ammonium concentration could reduce N₂O production. The heterotrophic denitrification pathway was not included in either of these studies. Very recently, Wan et al. (2019) included the contribution of heterotrophs and scrutinized influence of operating conditions including DO, nitrogen load, granule size, temperature and influent organics. Individual operating conditions had non-monotonic effects on N₂O emissions. The most important conclusion of those simulations was that heterotroph bacteria was a major sink of N₂O in presence of influent COD, and can play a major role in mitigating the emissions. Until now these simulation works have never been confronted to real observation nor calibrated with experimental data.

The present work aims to evaluate the N₂O production from one stage PNA running under DO limitation at extremely low DO (DO<0.2 mg/L). Such condition has been poorly evaluated in previous studies. The model is first confronted to experimental data after calibrating the most sensitive parameters. Then N₂O emissions pathways and effect of operating parameters impacting the N₂O emissions are assessed and discussed.

2. Model description

The model is developed and solved on Aquasim. Growth of AOB with 2-pathway N₂O model (Pocquet et al., 2016), growth of heterotroph with the four step denitrification model (Hiatt and Grady, 2008), NOB and anammox growth are included. Granules were described as spherical biofilm with a mean diameter of 500 µm, divided in 100 layers for numerical resolution. The model structure is similar to Wan et al. 2019, except the AOB growth which was related to the hydroxylamine oxidation as in the original model of Pocquet et al. (2016) whereas Wan et al. (2019) distributed growth on both hydroxylamine and NO oxidation. The mass and numbers of granules were calculated with the measured MLVSS, the mean diameter (500 µm) and assuming density and porosity of the biofilm. The gas transfer is predicted through K_{La}, measured for oxygen and calculated for NO and N₂O with diffusivity ratios. Simulation was performed on a long term (1000 days) for the reference condition (phase B of the experimental study) to obtain steady state results and stable biomass profiles in the biofilm.

The short term effect of additional nitrite, the effect of NOB repression, and the effect of air flow rate was then evaluated.

3. Results and discussion

3.1. Model calibration for PNA at extremely low DO

The data of the last period of the experimental study (chapter 4) was considered for the calibration. The process had been operated for more than 250 days, and with the same operating condition for 100 days. After a manual sensitivity analysis, the calibration was performed in two steps: first adapting the parameters influencing the nitrogen removal rate, then adapting the parameters to predict the N_2O emission rate and dynamics. The parameters which were chosen for calibration were the affinity constant, especially those for oxygen. Indeed it was impossible to predict the observed ammonium removal rate at the low DO imposed in the process ($<0.05 \text{ mg L}^{-1}$) with the values used in the original calibration of Pocquet et al. (2016), Pocquet et al. (2016) and Wan et al. (2019). The affinity constants for oxygen were set at $0.045 \text{ mgO}_2/\text{L}$ for AOB ($K_{O_2, AOB1}$, $K_{O_2, AOB1}$). As discussed in the chapter 3, this is possibly due to acclimatization of nitrifiers to very low DO on a long term. But such low values are also possibly due to the preferred colonization of smallest particles by AOB which is not taken into account in the model. Following the reduction of affinity constant for oxygen and due to high accumulation of hydroxylamine, affinity constant of AOB for hydroxylamine had also to be reduced. As the presence of NOB was observed in practice, the affinity constant of NOB was also calibrated to make possible the growth of NOB at low level of DO. The value of $K_{O_2, NOB}$ was set at $0.12 \text{ mgO}_2/\text{L}$ in order to predict the observed nitrate produced (see Figure 5.1). This calibration pointed out the very sensitivity of N_2O emission to the NOB growth (discussed below). After calibration ammonium, nitrate, nitrite, oxygen and N_2O profiles were described correctly for the reference cycle (Figure 5.1).

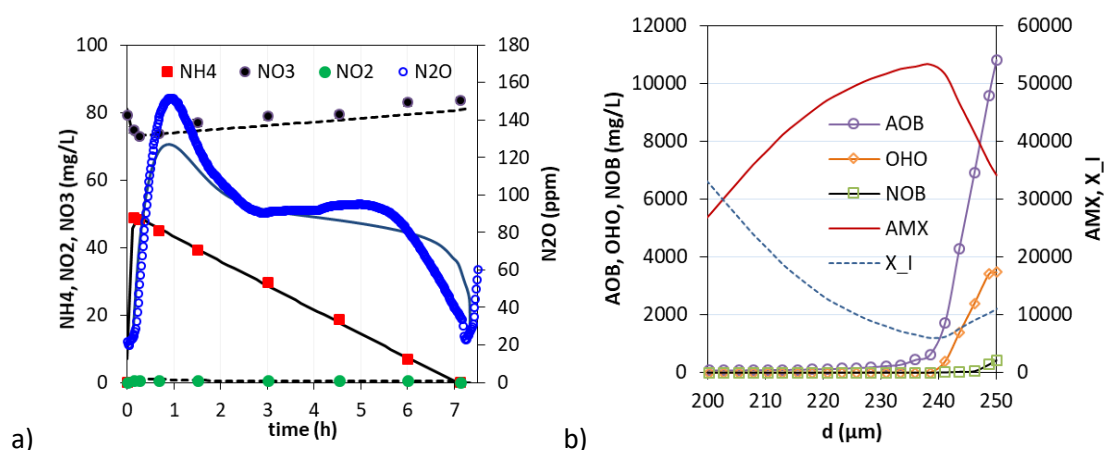


Figure 5.1: Modelled and simulated data for reference cycle (SBR Day 243). a) Nitrogen concentrations; b) distribution of biomass in the biofilm.

As a validation step, the model was evaluated to simulate two batch tests performed with different levels of nitrite (Table 5.1). The model was able to predict the stimulating effect of nitrite on N₂O emission rate and emission factor with an acceptable error ranging from 3% to 9% (increasing from 1.80% to 9.0 % for nitrite concentration pulsed from 0.73 to 15.5 mgN L⁻¹).

Table 5.1: Modelling the stimulating effect of nitrite on the production and emission of N₂O.

Condition	NO ₂ ⁻ mg N L ⁻¹	AUR mg N L ⁻¹ h ⁻¹		N ₂ OER mg N L ⁻¹ d ⁻¹		N ₂ OEF %	
	Level	exp	mod	exp.	mod.	Exp.	Mod.
Batch Aerobic NH ₄ ⁺ =50MgN/L	0.73	5.83	5.24	2.38	2.47	1.80	1.96
	15.5	4.83	5.28	10.54	11.05	9.0	8.7

3.2 Effect of NOB repression on the N₂O emission

Under oxygen limitation the nitrogen removal rate is controlled by the oxygen transfer rate. By imposing a limiting oxygen transfer rate the oxidation of nitrite into nitrate is limited and NOB are progressively repressed. As illustrated by Figure 5.2, the impact of NOB concentration on the N₂O emission rate is very important. Indeed for a variation of NOB from 15 to 0 mg L⁻¹, the N₂O emission rate increased severely from 1 to 10 mg/L.d and the emission factor from 1% to 5.7%. It is noticeable that it is exactly the range of variation observed during our experimental study. This is due to local nitrite level which is modified by the NOB activity, and stimulates N₂O production rate by ND pathway.

Therefore NOB repression have dramatic impact on N₂O emission if the nitrite consumption by NOB is not compensated by any increase of anammox activity in the biofilm, such phenomenon occurring on a long term. This can explain why the long term dynamic observed experimentally showed first a slow but very important increase of the N₂O emission (even without significant observable DO and NO₂⁻ change) but also slow regulation on a long term (see also the effect of aeration).

Despite the calibration was not performed to predict exactly the first 5 months of experience the simulations support our mechanistic explanation. During this period the AUR increased without measurable change in the dissolved oxygen, whereas the N₂O emission factor increased from 0.35% to 6%. As the nitrate production rate decreases progressively as well as the oxygen demand, it can be assumed that the NOB activity was progressively repressed during this period, generating local nitrite accumulation and increase of N₂O production rate. After increasing the air flow rate, a first increase of both nitrite and N₂O emission was observed but after several days it decreased. This may be due to higher NOB activity (nitrate production rate has significantly increased). As shown on Figure 5.2, a modification of NOB concentration in the system (here from 1 to 15 mgCOD/L) provokes strong variation of N₂O emission rate without significant DO variation and for nitrite variation on a small range varying from 0.1 to 1 mgN L⁻¹.

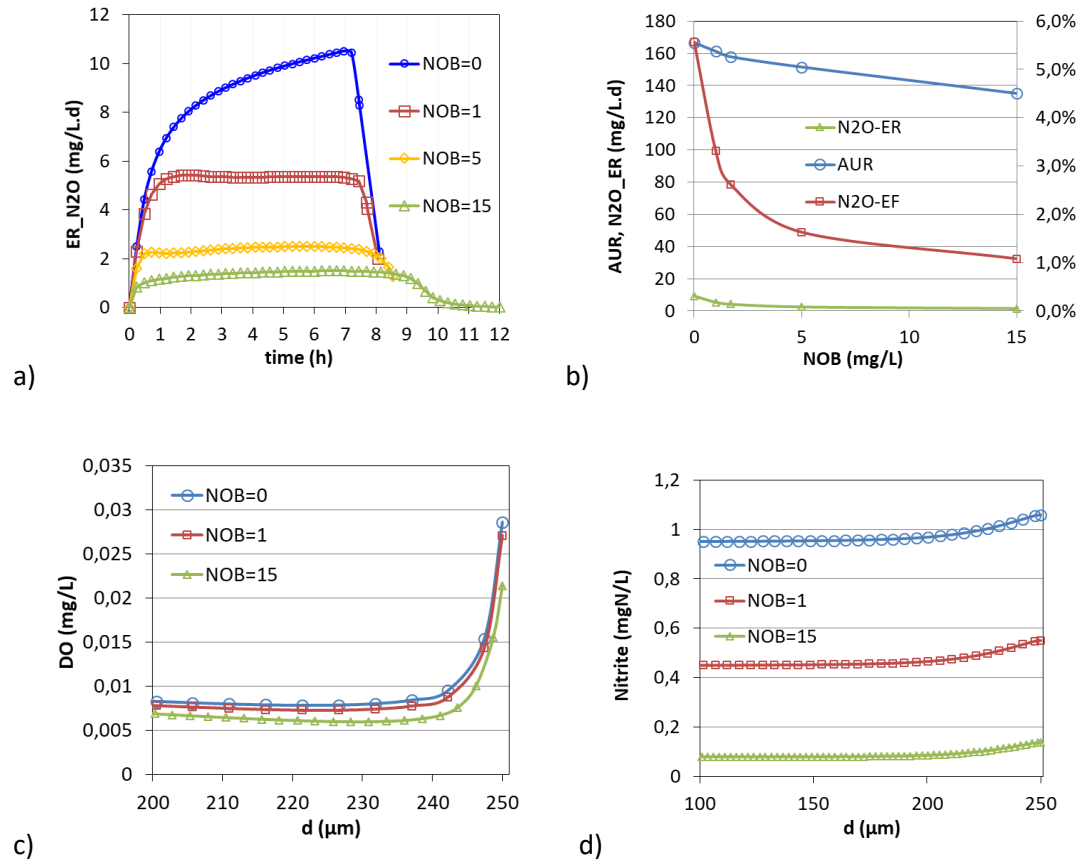


Figure 5.2: Effect of NOB on the N₂O emissions from PNA in SBR process (X_NOB=0-15 mg/L)

3.3 Effect of air flow rate (K_{La} variation)

Modification of air flow rate influences both AUR and N₂O emission by means of K_{La} and oxygen transfer rate (Figure 5.3). As an example compared to the reference situation variations from -50% to +30% of air flow rate lead to N₂O-ER ranging in average from 0.5 to 8.5 mgN-NO₂/L.d (2 mgN/L.d for reference) corresponding to a variation of N₂O emission factor from 0.48% to 3.45% of ammonium removed. Here simulations were performed by assuming a complete wash out of the NOB, according to the result of long term simulation with the model (this situation being not reached during our experimental study). Hence increasing the air flow rate on a short term increases the rate of N₂O emission and the emission factor.

On a long term maintaining higher air flow rate allows to maintain higher nitrogen loading rate (NLR), as we did during the experimental study. As AOB growth is stimulated, AOB concentration increased at the surface of the biofilm. For instance at the highest air flow rate ($K_{La}+30\%$), AOB concentration in the surface layer progressively increased by 32% and N₂O decreases by 37% reaching an emission factor of 2.16%. This AOB densification generates sharper oxygen gradient at the surface of the biofilm and lower dissolved oxygen in the deeper layer, which allow anammox to be less inhibited by oxygen. Consequently nitrite are better

consumed and the N_2O emission decreased. This phenomenon is in very good agreement with the experimental observations described in this thesis (period B2).

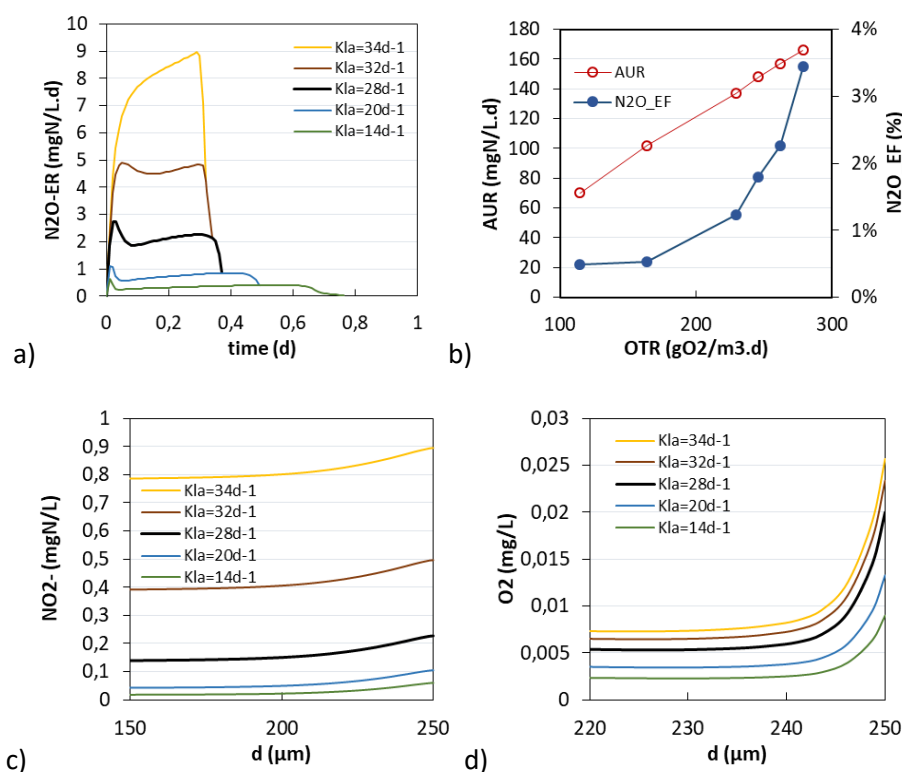


Figure 5.3: Effect of aeration on the N_2O emission rate (a), AUR and N_2O emission factor (b). NO_2^- in the biofilm (c) and DO in the biofilm (d).

In presence of NOB the effect of an increase of air flow rate is less important. With the concentration of NOB estimated in the reference case, the N_2O production decreased by 17% tempering the stimulating effect of oxygen transfer rate increase. Globally simulation shows that NOB presence can play a positive role in mitigating the N_2O production and emission. Even a few amount of NOB can play this role without too much negative impact on the performance. This suggests that suppression of NOB without an increase of anammox capabilities for consuming nitrite stimulates N_2O emission increase. Besides, since NOB grow faster and are more sensitive to the nitrite accumulation than anammox, anammox can benefit from the NOB repression. During this thesis we demonstrated that very low DO availability did not compromise autotrophic nitrogen removal, confirming the recent work of Abukaci et al. (2019). Micromolar DO allowed complete NOB suppression only with FA assistance (sidestream) but was sufficient to keep nitrification limited in any situation (Abukaci et al., 2019). During this thesis the presence of NOB was also detected by microbial analysis even if their activity was strongly repressed. Now we can say that such small amount of residual NOB activity was possibly positive for limiting the N_2O emissions.

3.4. Pathways analysis

As shown on Figure 5.4, N_2O is mainly produced at the surface of biofilm in the first layers (15 μm). This confirms the results of previous simulation studies (Wan et al, 2019) and experimental ones (Ali et al., 2016). N_2O is produced by both ND and NN pathway in reference condition, but in majority by ND pathway in a situation with high emission. This is true for situation of additional nitrite, as nitrite stimulates the ND pathway but also when air flow modification or NOB repression leads to high emission factor. The predominance of ND pathway for high emission period is in accordance with the isotopes analysis during this study. However the contributions of the two pathways seems more equilibrated when emissions are less stimulated. Such regulation may explain the contrasted results in literature concerning the most important pathways.

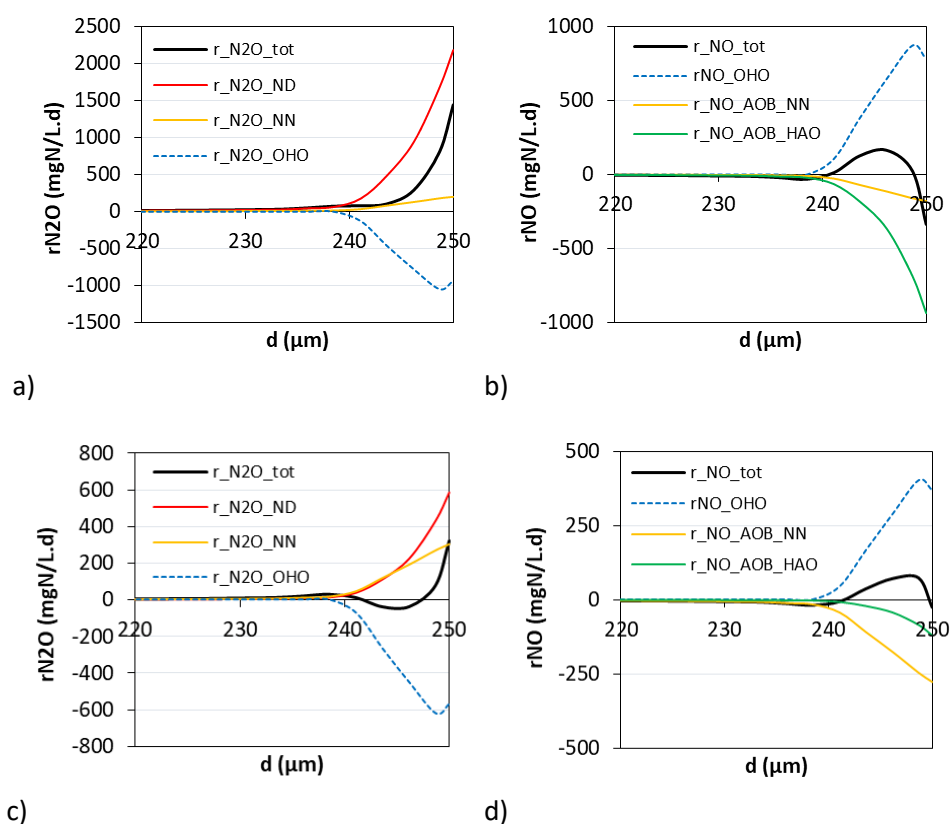


Figure 5.4: N_2O and NO production rate within the biofilm for two contrasted situation: high emission rate (a, b) for high AUR and OTR; reference case (c, d). Contribution of AOB (ND, NN pathways, HAO) and heterotroph (OHO).

In addition N_2O is significantly consumed by heterotroph denitrification at the surface (Figure 5.4). This conclusion is comparable to those of Wan et al. (2019). However as we operated under very low DO in this work, heterotroph is a sink of N_2O even without COD in the influent. This means that low DO allows heterotroph to reduce N_2O through endogenous denitrification using decay products at the surface of the biofilm. This was much less observed by Wan et al. (2019) without influent COD, operating at higher DO as heterotroph consumed preferentially oxygen. This means that low DO operation permits to take more benefit of the N_2O mitigation

by heterotroph. Obviously this is a simulation which is not validated experimentally and this mechanism may be overestimated by our model.

More surprisingly simulations also reveal that NO is an important intermediate molecule which is likely to be exchanged by heterotroph and AOB in the biofilm. The model predicts relatively low level of NO in the liquid (around 5-10 $\mu\text{gN/L}$) and low emission factors (0.1-0.15 % of ammonium removed), which are in accordance with our experimental observations. However the NO consumption and production rates in the biofilm are significant as all the nitrogen pass through the state of NO in heterotroph and autotroph pathways in the multiple step models.

As shown of Figure 5.4 (b, d) simulation indicates that heterotroph NO rate is positive whereas AOB rates are negative (rate HAO1-HAO2 and rate NN). Hence heterotroph seems to produce NO in excess, whereas AOB is a sink of NO. In reference scenario NO is mainly consumed by NN pathway (d), while NO is consumed in majority by HAO at high rate (b).

This means that heterotroph denitrification can enhance locally the N_2O emission of AOB through NN pathway by producing NO in excess. This interesting phenomenon definitively makes the mechanisms of N_2O emission from PNA even more complex. In addition, such NO loop is relatively speculative as the model do not take into account that NO is also an intermediate of ND pathway as well as Anammox reaction. So in reality the NO emitted by heterotrophs could also stimulate ND pathway. Hence this simplification probably make the N_2O produced by NN pathway slightly overestimated. As NO is also an intermediate compound for Anammox, it would be interesting to include it in the future evolution of the model.

Total NO and N_2O rates show inverse profiles in the layers closed to the surface. N_2O is produced at the surface of the biofilm by AOB but consumed in the deeper layers by heterotroph. In contrast NO is more produced in the deeper layers by heterotroph but consumed at the surface by AOB due to higher oxygen availability. Thanks to NO consumption on the surface less NO diffuse into the bulk.

This first simulation work shows that mechanisms involved in N_2O emission, including NO reactions, are highly complex in the situation of extremely low DO. Very small variation of local concentration of oxygen and nitrite in the biofilm surface, which are hard to access in practice, control the different reactions of heterotroph, AOB, NOB and Anammox. In addition, for the first time it is revealed that interactions between AOB and heterotroph in the NO and N_2O metabolism is more complex that it is usually considered. However, this metabolism is able to be simulated by assuming the different NO resources and sinks. Despite only small emission of NO are generally observed, it is here pointed out that NO can play a major role in the interaction between AOB and OHO and possibly in the N_2O emission regulation.

4. Conclusion

- The model combining N_2O emission with growth of AOB, NOB, OHO, Anammox was calibrated with experimental data from a PNA process working under oxygen

limitation for 300 days. Reduction of affinity constants (especially for oxygen) was the major adaptation compared to previous sets of values.

- The stimulating effect of nitrite on the N_2O emission was correctly predicted. This is the major source of high emission situation through the ND pathway.
- The model predicts variation of emission factor in a range which is closely comparable to the experimental observation of our study (0.5% to 6%).
- Under very low DO, heterotroph is a sink of N_2O (at the biofilm surface) even without COD in the influent, using decay products.
- Simulation indicates that significant NO is produced by heterotroph and consumed by AOB through HAO or NOR reaction, which means that heterotroph could also enhance locally the N_2O emission of AOB through NO stimulation.
- The level of repression of NOB was identified as a factor affecting very significantly N_2O emission even for relatively comparable observed condition (extremely low DO, small variation of nitrite)
- On a short term increase of air flow rate increase both AUR and N_2O -ER. But this is compensated on a long term by AOB densification on the biofilm surface and possibly mitigated by the presence of residual NOB.
- Future simulation works could be oriented to assess the effect of operational conditions: feeding mode (continuous, SBR, step feed), COD dosing, or air flow rate control in order to find the best conditions for mitigating N_2O emissions.

5. Appendix

5.1. Parameter, matrix and process description in the biofilm model

Table 5.S1: State variables

No.	Variable	Description	Unit
1	S_{N_2O}	Dissolved nitrous oxide (N_2O) concentration	$g\ N.m^{-3}$
2	S_{NH}	Dissolved ammonia (NH_3 and NH_4^+) concentration	$g\ N.m^{-3}$
3	S_{N_2}	Dissolved dinitrogen gas (N_2) concentration	$g\ N.m^{-3}$
4	S_{NH_2OH}	Dissolved hydroxylamine (NH_2OH) concentration	$g\ N.m^{-3}$
5	S_{NO}	Dissolved nitric oxide (NO) concentration	$g\ N.m^{-3}$
6	S_{NO_2}	Dissolved nitrite (NO_2^-) concentration	$g\ N.m^{-3}$
7	S_{NO_3}	Dissolved nitrate (NO_3^-) concentration	$g\ N.m^{-3}$
8	S_{O_2}	Dissolved oxygen (DO) concentration	$g\ O_2.m^{-3}$
9	S_S	Readily biodegradable substrate concentration	$g\ COD.m^{-3}$
10	X_{AOB}	Suspended ammonia oxidizing bacteria biomass concentration	$g\ COD.m^{-3}$
11	X_{NOB}	Suspended nitrite oxidizing bacteria biomass concentration	$g\ COD.m^{-3}$
12	X_{AMX}	Suspended anammox bacteria biomass concentration	$g\ COD.m^{-3}$
13	X_{BH}	Suspended heterotrophic biomass concentration	$g\ COD.m^{-3}$
14	X_I	Inert biomass concentration	$g\ COD.m^{-3}$

Table 5.S2: Model parameters

Name	Definition	Unit	Value	source
Stoichiometric parameters				
f_{XI}	Fraction of inert COD in biomass	g COD.g COD ⁻¹	0.08	<i>Henze et al. (2000)</i>
i_{NXB}	Nitrogen content of biomass	g N.g COD ⁻¹	0.086	<i>Henze et al. (2000)</i>
i_{NXI}	Nitrogen content of particulate inerts	g N.g COD ⁻¹	0.06	
$K_{H,NH}$	Total ammonium half-saturation coefficient for heterotrophs	g N.m ⁻³	10 ⁻¹²	<i>artificial</i>
AOB kinetic parameters				
Y_{AOB}	Yield of AOB	g COD.g N ⁻¹	0.15	<i>Pocquet et al. (2016)</i>
μ_{AOB}	Growth rate of AOB	d ⁻¹	0.78	<i>Pocquet et al. (2016)</i>
b_{AOB}	Decay rate of AOB	d ⁻¹	0.13	<i>Wiesmann (1994)</i>
$\eta_{AOB,ND}$	Reduction factor for maximum production rate by ND pathway	-	0.25	<i>Lang et al., (2017)</i>
$\eta_{AOB,NN}$	Reduction factor for maximum production rate by NN pathway	-	0.0015	<i>Lang et al. (2017)</i>
$K_{AOB,1,O}$	DO half-saturation coefficient for AOB in ammonium oxidation	g O ₂ .m ⁻³	0.045	<i>estimated</i>
$K_{AOB,2,O}$	DO half-saturation coefficient for AOB in NO ₂ ⁻ production	g O ₂ .m ⁻³	0.045	<i>estimated</i>
$K_{AOB,HAO,NO}$	NO half-saturation coefficient for AOB in NO ₂ ⁻ production	g N.m ⁻³	0.0003	<i>Pocquet et al. (2016)</i>
$K_{AOB,HNO2}$	HNO ₂ half-saturation coefficient for AOB	g N.m ⁻³	0.00073	<i>Pocquet et al. (2016)</i>
$K_{AOB,NH2OH}$	Hydroxylamine half-saturation coefficient for AOB	g N.m ⁻³	0.005	<i>estimated</i>
$K_{AOB,I,O}$	N ₂ O constant for production inhibition by DO	g O ₂ .m ⁻³	4.5	<i>Pocquet et al. (2016)</i>
$K_{AOB,ND,O}$	AOB constant for DO effect on ND	g N.m ⁻³	0.019	<i>Pocquet et al. (2016)</i>
$K_{AOB,NH}$	Total ammonium half-saturation coefficient for AOB	g N.m ⁻³	0.25	<i>Estimated</i>
$K_{AOB,NN,NO}$	NO half-saturation coefficient for AOB (NN pathway)	g N.m ⁻³	0.008	<i>Pocquet et al. (2016)</i>
NOB kinetic parameters				
Y_{NOB}	Yield of NOB	g COD.g N ⁻¹	0.041	
μ_{NOB}	Growth rate of NOB	d ⁻¹	1.45	
b_{NOB}	Decay rate of NOB	d ⁻¹	0.06	<i>Wiesmann (1994)</i>

$K_{NOB,NH}$	Total ammonium half-saturation coefficient for NOB	$g\ N.m^{-3}$	10^{-12}	<i>artificial</i>
K_{NOB,NO_2}	Total nitrite half-saturation coefficient for NOB	$g\ N.m^{-3}$	0.5	<i>Wiesmann (1994)</i>
$K_{NOB,O}$	DO half-saturation coefficient for NOB	$g\ O_2.m^{-3}$	0.12	<i>estimated</i>
Anammox kinetic parameters				
Y_{AN}	Yield of AN	$g\ COD.g\ N^{-1}$	0.186	<i>Strouss et al. (1998)</i> <i>Hubaux et al. (2014)</i>
μ_{AN}	Growth rate of AN	d^{-1}	0.04	<i>estimated</i>
b_{AN}	Decay rate of AN	d^{-1}	0.003	<i>Hubaux et al. (2014)</i>
$K_{AN,NH}$	Total ammonium half-saturation coefficient for AN	$g\ N.m^{-3}$	0.07	<i>Hubaux et al. (2014)</i>
K_{AN,NO_2}	Total nitrite half-saturation coefficient for AN	$g\ N.m^{-3}$	0.1	<i>Lotti et al. (2014)</i>
$K_{I,O_2,AN}$	DO Inhibition coefficient of for AN	$g\ O_2.m^{-3}$	0.005	<i>estimated</i>
Heterotrophs kinetic parameters				
Y_H	Yield of heterotrophs	$g\ COD.g\ N^{-1}$	0.666	<i>Henze et al. (2000)</i>
μ_H	Growth rate of heterotrophs	d^{-1}	6	<i>Henze et al. (2000)</i>
b_H	Decay rate of heterotrophs	d^{-1}	0.62	<i>Henze et al. (2000)</i>
$K_{H,I_3,NO}$	NO inhibition coefficient of heterotrophs, R3 – NO ₂ red	$g\ N.m^{-3}$	0.5	<i>Hiatt and Grady (2008)</i>
$K_{H,I_4,NO}$	NO inhibition coefficient of heterotrophs, R4 – NO red	$g\ N.m^{-3}$	0.3	<i>Hiatt and Grady (2008)</i>
$K_{H,I_5,NO}$	NO inhibition coefficient of heterotrophs, R5 – N ₂ O red	$g\ N.m^{-3}$	0.075	<i>Hiatt and Grady (2008)</i>
K_{H,N_2O}	N ₂ O half-saturation coefficient for heterotrophs	$g\ N.m^{-3}$	0.05	<i>Hiatt and Grady (2008)</i>
$K_{H,NO}$	NO half-saturation coefficient for heterotrophs	$g\ N.m^{-3}$	0.05	<i>Hiatt and Grady (2008)</i>
K_{H,NO_2}	Total nitrite half-saturation coefficient for heterotrophs	$g\ N.m^{-3}$	0.2	<i>Hiatt and Grady (2008)</i>
K_{H,NO_3}	Nitrate half-saturation coefficient for heterotrophs	$g\ N.m^{-3}$	0.2	<i>Hiatt and Grady (2008)</i>
$K_{H,O}$	DO half-saturation coefficient for heterotrophs	$g\ O_2.m^{-3}$	0.1	<i>Hiatt and Grady (2008)</i>
$K_{I,H,O}$	DO inhibition coefficient for heterotrophs	$g\ O_2.m^{-3}$	0.1	<i>Hiatt and Grady (2008)</i>

$K_{H,S}$	COD half-saturation coefficient for heterotrophs	g N.m^{-3}	20	<i>Hiatt and Grady (2008)</i>
$K_{H,S,S}$	COD half-saturation coefficient heterotrophs for N_2O reduction	g N.m^{-3}	40	<i>Hiatt and Grady (2008)</i>
η_Y	Reduction factor for yield under anoxic conditions	-	0.75	<i>Hiatt and Grady (2008)</i>
η_{g2}	Reduction factor for maximum growth rate under anoxic conditions with NO_3	-	0.28	<i>Hiatt and Grady (2008)</i>
η_{g3}	Reduction factor for maximum growth rate under anoxic conditions with NO_2	-	0.16	<i>Hiatt and Grady (2008)</i>
η_{g4}	Reduction factor for maximum growth rate under anoxic conditions with NO	-	0.35	<i>Hiatt and Grady (2008)</i>
η_{g5}	Reduction factor for maximum growth rate under anoxic conditions with N_2O	-	0.35	<i>Hiatt and Grady (2008)</i>
$K_{H,NH}$	Total ammonium half-saturation coefficient for heterotrophs	g N.m^{-3}	10^{-12}	<i>artificial</i>

Table 5.S3: Reactor physical model parameters

Name	Definition	Value	Unit
V_R	Total Volume of reactor	11	L
X	Concentration (MLSS)	1.5	g m^{-3}
ϵ	Biofilm porosity	0.6	-
ρ	Density of autotrophic biomass and particulate inert material	100 000	g COD. m^{-3}

Table 5.S4: Stoichiometric matrix

	Process	S_{N2O} [g N.m ⁻³]	S_{NH} [g N.m ⁻³]	S_{N2} [g N.m ⁻³]	S_{NH2OH} [g N.m ⁻³]	S_{NO} [g N.m ⁻³]	S_{NO2} [g N.m ⁻³]	S_{NO3} [g N.m ⁻³]	S_{O2} [g O ₂ .m ⁻³]	S_S [g COD.m ⁻³]	X_{AOB} [g COD.m ⁻³]	X_{NOB} [g COD.m ⁻³]	X_{AMX} [g COD.m ⁻³]	X_{BH} [g COD.m ⁻³]	X_I [g COD.m ⁻³]
Ammonia-oxidizing bacteria															
1	Ammonia oxidation		-1		1				$-\frac{12}{7}$						
2	NO production		$-i_{NXB}$		$-\frac{1}{Y_{AOB}}$	$\frac{1}{Y_{AOB}}$			$-\frac{(\frac{12}{7} - Y_{AOB})}{Y_{AOB}}$		1				
3	NO ₂ ⁻ production					-1	1		$-\frac{4}{7}$						
4	N ₂ O production (NN pathway)	4			-1	-4	1								
5	N ₂ O production (NN pathway)	2			-1		-1								
6	Decay		$i_{NXB} - f_{XI}i_{NXI}$							$1 - f_{XI}$	-1				f_{XI}
Nitrite oxidizing bacteria															
7	Nitrite oxidation		$-i_{NXB}$				$-\frac{1}{Y_{NOB}}$	$\frac{1}{Y_{NOB}}$	$-\frac{(\frac{8}{7} - Y_{NOB})}{Y_{NOB}}$			1			
8	Decay		$i_{NXB} - f_{XI}i_{NXI}$							$1 - f_{XI}$		-1			f_{XI}
Anammox bacteria															
9	Nitrite reduction and ammonium oxidation		$-i_{NXB} - \frac{1}{Y_{AN}}$	$\frac{2}{Y_{AN}}$			$-\frac{1}{Y_{AN}} - \frac{1}{1.14}$	$\frac{1}{1.14}$					1		
10	Decay		$i_{NXB} - f_{XI}i_{NXI}$							$1 - f_{XI}$			-1		f_{XI}
Heterotrophs															
11	Aerobic growth		$-i_{NXB}$						$-\frac{1 - Y_H}{Y_H}$	$-\frac{1}{Y_H}$				1	
12	Anoxic growth from NO ₃ ⁻ reduction to NO ₂ ⁻		$-i_{NXB}$				$\frac{1 - \eta_{Y,H}Y_H}{8\eta_{Y,H}Y_H}$	$-\frac{1 - \eta_{Y,H}Y_H}{8\eta_{Y,H}Y_H}$		$-\frac{1}{\eta_{Y,H}Y_H}$				1	

13	Anoxic growth from NO ₂ ⁻ reduction to NO		$-i_{NXB}$			$\frac{1 - \eta_{Y,H} Y_H}{\frac{4}{7} \eta_{Y,H} Y_H}$	$-\frac{1 - \eta_{Y,H} Y_H}{\frac{4}{7} \eta_{Y,H} Y_H}$			$-\frac{1}{\eta_{Y,H} Y_H}$			1	
14	Anoxic growth from NO reduction to N ₂ O	$\frac{1 - \eta_{Y,H} Y_H}{\frac{4}{7} \eta_{Y,H} Y_H}$	$-i_{NXB}$			$-\frac{1 - \eta_{Y,H} Y_H}{\frac{4}{7} \eta_{Y,H} Y_H}$				$-\frac{1}{\eta_{Y,H} Y_H}$			1	
15	Anoxic growth from N ₂ O reduction to N ₂	$-\frac{1 - \eta_{Y,H} Y_H}{\frac{4}{7} \eta_{Y,H} Y_H}$	$-i_{NXB}$	$\frac{1 - \eta_{Y,H} Y_H}{\frac{4}{7} \eta_{Y,H} Y_H}$						$-\frac{1}{\eta_{Y,H} Y_H}$			1	
16	Decay		$-i_{NXB} - f_{XI} i_{NXI}$							$1 - f_{XI}$			-1	f_{XI}
g COD/unit component		-2.29	0	-1.71	-1.14	-2.86	-3.43	-4.57	-1	1	1	1	1	1

Table 5.S5: Dynamic processes

	Process	Rate
Ammonia-oxidizing bacteria		
1	Ammonia oxidation	$\frac{\mu_{AOB}}{Y_{AOB}} \frac{S_{O_2}}{S_{O_2} + K_{AOB,1,O}} \frac{S_{NH}}{S_{NH} + K_{AOB,NH}} X_{AOB}$
2	NO production from NH ₂ OH to NO	$\frac{\mu_{AOB}}{Y_{AOB}} \frac{S_{O_2}}{S_{O_2} + K_{AOB,2,O}} \frac{S_{NH2OH}}{S_{NH2OH} + K_{AOB,NH2OH}} \frac{S_{NH}}{S_{NH} + 10^{-12}} X_{AOB}$
3	NO ₂ ⁻ production from NO to NO ₂ ⁻	$\frac{\mu_{AOB}}{Y_{AOB}} \frac{S_{O_2}}{S_{O_2} + K_{AOB,2,O}} \frac{S_{NO}}{S_{NO} + K_{AOB,HNO,NO}} X_{AOB}$
4	N ₂ O production (NN pathway)	$\frac{\mu_{AOB}}{Y_{AOB}} \eta_{AOB,NN} \frac{S_{NH2OH}}{S_{NH2OH} + K_{AOB,NH2OH}} \frac{S_{NO}}{S_{NO} + K_{AOB,NN,NO}} X_{AOB}$
5	N ₂ O production (ND pathway)	$\frac{\mu_{AOB}}{Y_{AOB}} \eta_{AOB,ND} \frac{S_{NH2OH}}{S_{NH2OH} + K_{AOB,NH2OH}} \frac{S_{HNO_2}}{S_{HNO_2} + K_{AOB,HNO_2}} \frac{S_{O_2}}{K_{AOB,ND,O} S_{O_2} + S_{O_2} (1 - 2\sqrt{K_{AOB,ND,O}/K_{AOB,1,O}}) + S_{O_2}^2/K_{AOB,1,O}} X_{AOB}$
6	Decay	$b_{AOB} X_{AOB}$
Nitrite oxidizing bacteria		
7	Growth	$\mu_{NOB} \frac{S_{NH}}{S_{NH} + 10^{-12}} \frac{S_{NO_2}}{S_{NO_2} + K_{NOB,NO_2}} \frac{S_{O_2}}{S_{O_2} + K_{NOB,O}} \frac{K_{I,NH,NOB}}{S_{NH} + K_{I,NH,NOB}} X_{NOB}$
8	Decay	$b_{NOB} X_{NOB}$
Anammox bacteria		
9	Growth	$\mu_{AMX} \frac{S_{NH}}{S_{NH} + K_{AN,NH}} \frac{S_{NO_2}}{S_{NO_2} + K_{AN,NO_2}} \frac{K_{I,O_2,AN}}{S_{O_2} + K_{I,O_2,AN}} X_{AMX}$

10	Decay	$b_{AN}X_{AMX}$
Heterotrophs		
11	Aerobic growth	$\mu_H \frac{S_{NH}}{S_{NH} + 10^{-12}} \frac{S_{O_2}}{S_{O_2} + K_{H,O}} \frac{S_s}{S_s + K_{H,S}} X_{BH}$
12	Anoxic growth from NO_3^- reduction to NO_2^-	$\eta_{g2} \mu_H \frac{S_{NH}}{S_{NH} + 10^{-12}} \frac{S_s}{S_s + K_{H,S}} \frac{K_{H,O}}{S_{O_2} + K_{H,O}} \frac{S_{NO_3}}{S_{NO_3} + K_{H,NO_3}} X_{BH}$
13	Anoxic growth from NO_3^- reduction to NO	$\eta_{g3} \mu_H \frac{S_{NH}}{S_{NH} + 10^{-12}} \frac{S_s}{S_s + K_{H,S}} \frac{K_{H,O}}{S_{O_2} + K_{H,O}} \frac{S_{NO_2}}{S_{NO_2} + K_{H,NO_2}} \frac{K_{H,I3,NO}}{S_{NO} + K_{H,I3,NO}} X_{BH}$
14	Anoxic growth from NO reduction to N_2O	$\eta_{g4} \mu_H \frac{S_{NH}}{S_{NH} + 10^{-12}} \frac{S_s}{S_s + K_{H,S}} \frac{K_{H,O}}{S_{O_2} + K_{H,O}} \frac{S_{NO}}{S_{NO} + K_{H,NO}} + \frac{S_{NO} * S_{NO}}{K_{H,I4,NO}} X_{BH}$
15	Anoxic growth from N_2O reduction to N_2	$\eta_{g5} \mu_H \frac{S_{NH}}{S_{NH} + 10^{-12}} \frac{S_s}{S_s + K_{H,S}} \frac{K_{H,O}}{S_{O_2} + K_{H,O}} \frac{S_{N_2O}}{S_{N_2O} + K_{H,N_2O}} \frac{K_{H,I5,NO}}{S_{NO} + K_{H,I5,NO}} X_{BH}$
16	Decay	$b_H X_{BH}$

5.2 Effect of Temperature and pH dependency

The temperature dependency is considered in the model in two aspects. One aspect is the maximum reaction rate for all the biomass (Equation 5.S1).

Equation 5.S1

$$K(T) = K(T_{ref})\exp(0.094(T - T_{ref}))$$

in which T and T_{ref} is the real and referred (20°C) temperature respectively, with $K(T)$ and $K(T_{ref})$ is the process rate under the corresponding temperature.

The other aspect is that it is generally known that ammonia (NH_3) and nitrous acid (HNO_2) are the real substrates for AOB. Therefore, NH instead of NH_3 is applied in the model for as for both AOB and anammox. Meanwhile, HNO_2 instead of NO_2^- is applied in the model for calculating the N_2O production from AOB through the ND pathway as shown in process 5, according to the following equations:

Equation 5.S2

$$S_{NH} = S_{NH_3} \left(1 + e^{6344/(273.15+T)} 10^{-pH} \right)$$

Equation 5.S3

$$S_{NO_2} = S_{HNO_2} \left(1 + e^{-(2300/(273.15+T))} 10^{pH} \right)$$

in which S_{NH} ($g\ N.m^{-3}$) is the nitrogen concentration of total ammonium; S_{NH_3} ($g\ N.m^{-3}$) is the nitrogen concentration of free ammonia; S_{NO_2} ($g\ N.m^{-3}$) represents the nitrogen concentration in the form of nitrite, and S_{HNO_2} ($g\ N.m^{-3}$) represents the nitrogen concentration of free nitrous acid.

In addition, the effect of pH dependency is also explored in the Equation 5.S2 and 5.S3.

5.3 The effect of DO on the ND pathway.

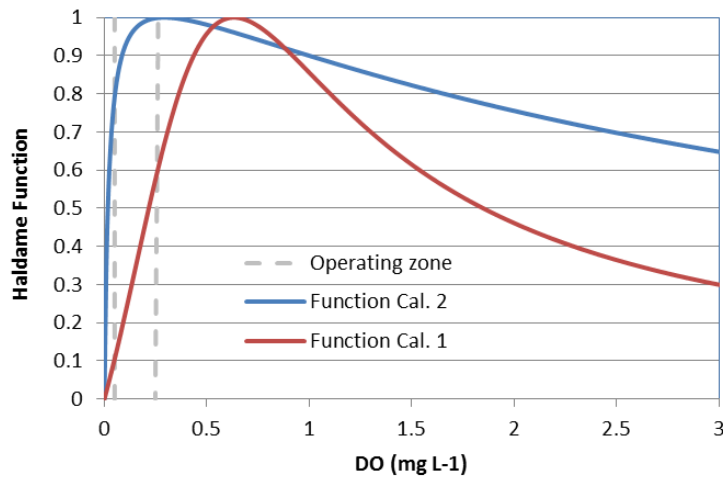


Figure 5.S1. The oxygen inhibition function for different dissolved oxygen concentrations based on 2 different calibrations of Haldane. The calibration 2 was used in this thesis (Lang et al., 2017).

5.3 Gas transfer calculations

The transport coefficients of N₂O, NO and N₂ at were calculated with K_{LaO_2} based on the diffusivity coefficients:

Equation 5.S4

$$K_{La_i} = K_{LaO_2} \sqrt{\frac{D_i}{D_{O_2}}}$$

The external mass transfer resistance (diffusion boundary layer) was neglected. Therefore, the concentration at the biofilm surface was equal to that in the reactor bulk liquid. The effective diffusion coefficients in the granules were calculated from their diffusion coefficients in water (multiplied by a reduction coefficient).

References

- Akaboci, T.R.V., Gich, F., Rusalleda, M., Balaguer, M.D., Colprim, J., 2018. Effects of extremely low bulk liquid DO on autotrophic nitrogen removal performance and NOB suppression in side- and mainstream one-stage PNA. *J. Chem. Technol. Biotechnol.* 0. <https://doi.org/10.1002/jctb.5649>
- Ali, M., Rathnayake, R.M.L.D., Zhang, L., Ishii, S., Kindaichi, T., Satoh, H., Toyoda, S., Yoshida, N., Okabe, S., 2016. Source identification of nitrous oxide emission pathways from a single-stage nitrification-anammox granular reactor. *Water Res.* 102, 147–157. <https://doi.org/10.1016/j.watres.2016.06.034>
- Hellinga, C., Van Loosdrecht, M.C.M., Heijnen, J.J., 1999. Model based design of a novel process for nitrogen removal from concentrated flows. *Math. Comput. Model. Dyn. Syst.* 5, 351–371.
- Henze, M., Gujer, W., Mino, T., van Loosdrecht, M.C.M., 2000. Activated sludge models ASM1, ASM2, ASM2d and ASM3. IWA Publ. 121. <https://doi.org/10.1007/s13398-014-0173-7.2>
- Hiatt, W.C., Grady, C.P.L., 2008. An Updated Process Model for Carbon Oxidation, Nitrification, and Denitrification. *Water Environ. Res.* 80, 2145–2156. <https://doi.org/10.2175/106143008X304776>
- Hulle, S.W.H.V., Callens, J., Mampaey, K.E., Loosdrecht, M.C.M. van, Volcke, E.I.P., 2012. N₂O and NO emissions during autotrophic nitrogen removal in a granular sludge reactor – a simulation study. *Environ. Technol.* 33, 2281–2290. <https://doi.org/10.1080/09593330.2012.665492>
- Lang, L., Pocquet, M., Ni, B.-J., Yuan, Z., Spérandio, M., 2017. Comparison of different two-pathway models for describing the combined effect of DO and nitrite on the nitrous oxide production by ammonia-oxidizing bacteria. *Water Sci. Technol. J. Int. Assoc. Water Pollut. Res.* 75, 491–500. <https://doi.org/10.2166/wst.2016.389>
- Mozumder, M.S.I., Picioreanu, C., Van Loosdrecht, M.C.M., Volcke, E.I.P., 2014. Effect of heterotrophic growth on autotrophic nitrogen removal in a granular sludge reactor. *Environ. Technol. U. K.* 35, 1027–1037. <https://doi.org/10.1080/09593330.2013.859711>
- Ni, B.J., Yuan, Z., Chandran, K., Vanrolleghem, P.A., Murthy, S., 2013. Evaluating four mathematical models for nitrous oxide production by autotrophic ammonia-oxidizing bacteria. *Biotechnol. Bioeng.* 110, 153–163. <https://doi.org/10.1002/bit.24620>
- Peng, L., Liu, Y., Ni, B.-J., 2016. Nitrous oxide production in completely autotrophic nitrogen removal biofilm process: A simulation study. *Chem. Eng. J.* 287, 217–224. <https://doi.org/10.1016/j.cej.2015.11.026>
- Pocquet, M., Wu, Z., Queinnec, I., Spérandio, M., 2016. A two pathway model for N₂O emissions by ammonium oxidizing bacteria supported by the NO/N₂O variation. *Water Res.* 88, 948–959. <https://doi.org/10.1016/j.watres.2015.11.029>
- Sabba, F., Picioreanu, C., Nerenberg, R., 2017. Mechanisms of nitrous oxide (N₂O) formation and reduction in denitrifying biofilms. *Biotechnol. Bioeng.* 114, 2753–2761. <https://doi.org/10.1002/bit.26399>
- Sabba, F., Picioreanu, C., Pérez, J., Nerenberg, R., 2015. Hydroxylamine Diffusion Can Enhance N₂O Emissions in Nitrifying Biofilms: A Modeling Study. *Environ. Sci. Technol.* 49, 1486–1494. <https://doi.org/10.1021/es5046919>
- Strous, M., Heijnen, J.J., Kuenen, J.G., Jetten, M.S.M., 1998. The sequencing batch reactor as a powerful tool for the study of slowly growing anaerobic ammonium-oxidizing microorganisms. *Appl. Microbiol. Biotechnol.* 50, 589–596. <https://doi.org/10.1007/s002530051340>

- Wan, X., Baeten, J.E., Volcke, E.I.P., 2019. Effect of operating conditions on N₂O emissions from one-stage partial nitritation-anammox reactors. *Biochem. Eng. J.* 143, 24–33. <https://doi.org/10.1016/j.bej.2018.12.004>
- Wiesmann, U., 1994. Biological nitrogen removal from wastewater, in: *Biotechnics/Wastewater*. pp. 113–154. <https://doi.org/10.1007/BFb0008736>

Chapter 6: Conclusions and perspectives

This PhD thesis aimed to clarify the N₂O emission mechanisms from the single-stage PNA process through the combination of experimentation and modelling work. Results give new insights and better understanding of the N₂O emission in autotrophic nitrogen removal system, supporting future strategies for mitigating greenhouse gas emissions, and reducing the carbon footprint of the nitrogen removal in wastewater systems.

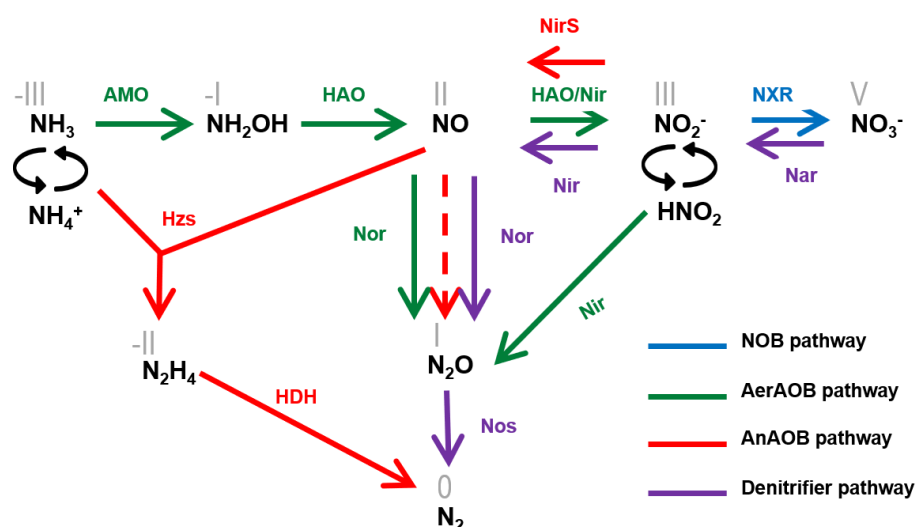


Figure 6.1: Biological nitrogen conversions possibly involved in the single-stage PNA process.

1. Conclusions

1.1 Properties of the one stage PNA process under OTR-controlled condition

In this work, one stage PNA process was successfully controlled by oxygen transfer rate at extremely low DO during 300 days at 26.5°C. Increasing the aeration strength allowed to improve specific nitrogen removal rate up to 0.130 g N g VSS⁻¹ d⁻¹ with a very limited amount of NOB activity (TN removal of 84%). This confirms that DO limitation is not detrimental for complete ammonium oxidation at a satisfying rate. Meanwhile the bulk DO concentration in the reaction phase changes from micromolar (0.02 to 0.2 mg O₂ L⁻¹) during the initial 100 days to almost zero for the rest of the study. Oxygen demand progressively decreased under DO limitation, and was very low (OTR/AUR = 1.3-1.5 gO₂ gN⁻¹), i.e. value slightly lower than theoretical stoichiometry. This was correlated to low NO emission but significant N₂O emissions. The maximal N₂O emission factor reached 6% of removed ammonium but was limited to 2% at the end of the study after adapting the air flow rate.

Regarding granule size distribution a very specific segregation process was observed among two categories of sizes. Granular sludge was naturally segregated into two categories of sizes (300-400 µm, 1100-1400 µm). Combination of the FISH and 16s rRNA results showed that AOB (*Nitrosomonas Europaea*) were found mainly on the surface of small granules, whereas anammox (*Candidatus Kuenenia*) were in majority in big granules, NOB and OHO being

homogeneously distributed. Such species distribution suggests that AOB develop a specific strategy for improving oxygen accessibility by colonizing the biofilm of smallest particles developing much higher specific surface. This leads to lower apparent affinity constant for oxygen and partly explains the relatively high specific activity despite very small DO level.

1.2 Deeper insights into the N₂O emission dynamics

Long and short term dynamics of N₂O emissions from PNA process operated under oxygen limitation were studied.

First, the N₂O emission factor progressively increased ($0.4 \pm 0.1\%$ - $5.8 \pm 0.3\%$) within 5 months, but finally stabilized ($2.1 \pm 0.2\%$) after increasing air flow rate over 100 days. This was correlated to increasing AUR and decreasing oxygen demand. The reason for such important increase was not only the intensification of ammonium oxidation generating more local oxygen limitation but also likely the repression of NOB which generated higher nitrite level (small but impactful). This phenomenon was confirmed by the last simulations.

The nitrite stimulating effect on N₂O emission was confirmed and seemed even more important than in a systems operated at high DO. It means that for controlling N₂O emission it is important to compensate the loss of NOB by high anammox activity for removing nitrite.

N₂O emission level measured at the end of the study finally indicate that N₂O emission level from PNA operated under very low oxygen level can be controlled in a range which is not that different from PNA system working under higher level of oxygen.

Increase of oxygen transfer rate led to instantaneous increase of both AUR and N₂O emission rate on a short term. However on a long term both N₂O emission rate and emission factor decreases towards a constant level reached after several weeks. This dynamic could be explained by the initial stimulating effect of both higher ammonium oxidation rate and higher nitrite, followed by microbial adaptation. AOB and anammox biomass growth reorganizes the AOB and Anammox among the granules and a small reactivation of NOB is also observed. Aeration optimization for N₂O mitigation should be definitively considered on a long term horizon in the future and not only with short term assays.

1.3 Deeper insights into the N₂O emission pathways

Analysis of nitrogen isotopes and site preference (SP) during the highest N₂O emission period tend to show that the major N₂O emission pathway was the nitrite reduction. This was confirmed by the modelling work, the model being able to predict the stimulating effect of nitrite on the N₂O emission through the ND pathway.

The anoxic experiment suggests that heterotrophs did not contribute that much to the N_2O emission, and the simulation even showed that heterotroph denitrification was a sink of N_2O . Under very low DO indeed, our model shows that heterotroph is a sink of N_2O (at the biofilm surface) even without COD in the influent, using decay products. Then the possible contribution of heterotrophic denitrification was not completely precluded by the much lower (3 times less) N_2O emission factor during the nitrite addition tests. If this pathway occurred, only a small contribution to the overall N_2O emission would be expected.

According to modelling work it comes that NO plays a role as a central molecule due to its ability to be exchanged by heterotroph and AOB on the surface layers of biofilm. The model indicates that significant NO is produced by heterotroph and consumed by AOB through HAO or NOR reaction, which means that heterotroph could also enhance locally the N_2O emission of AOB by providing excess of NO. Despite this is relatively speculative, it opens a new vision on the possible mechanisms involved in the PNA biofilm. As NO is also an intermediate of Anammox, it would be interesting to include the NO as an intermediate in the Anammox model in the future.

1.4 Combined effect of DO and nitrite on N_2O emission: modelling

progress

The combined effect of DO and nitrite on N_2O production is crucial for understanding and predicting the mechanisms involved in short-cut nitrogen removal and PNA system. In order to achieve this goal, first the 2-pathway model proposed by our group was compared to the metabolic electron transport model proposed by AWMC group.

Despite their different mathematical structures both the two pathway models were able to describe accurately the synergetic effect of DO and nitrite on the N_2O emissions. The results did not demonstrate strong difference in their application ranges (e.g. higher or lower NO_2^-) for experience with nitrifying culture. The calibration allows to provide a new set of parameters for future works.

The biofilm model combining N_2O emission with growth of 4 microbial groups was calibrated to experimental data from PNA process working under oxygen limitation. Reduction of a set of affinity constants (especially for oxygen) was the major adaptation compared to previous sets of values.

After calibrating the overall model to PNA under extremely low DO, the effect of operational parameters were much more directly influenced by the variation of nitrite than by the oxygen level or only indirectly. For instance lower DO in the biofilm reduces anammox inhibition which decreases the nitrite which limits N_2O emission.

As a consequence the level of repression of NOB was identified as an important factor which can affect very significantly N_2O emission even for relatively comparable condition (low DO,

small variation of nitrite). Consequently, presence of NOB, as a minority species, may be beneficial for N₂O mitigation in PNA system, without necessarily impacting significantly the overall performances.

The model predicts variation of emission factor in a range which very comparable to the experimental observation of our study (0.5% to 6%).

2. Future perspectives

2.1 N₂O mitigation measures

This work provides some recommendations for limiting N₂O emissions. For instance it was proven that anaerobically feeding reduces transient emissions of N₂O by reducing nitrite peak. Limiting the peaks of oxygen at the end of the reaction phase was also avoided by maintaining very low maximal DO setpoint.

A control strategy which could adapt the oxygen transfer rate to maintain OTR/AUR ratio closed to 1.7-1.75 seems and not less than 1.6 seems positive for N₂O mitigation. Higher ratio should be tested with a consideration on a long term of possible disturbance by variation of organic carbon demand.

The possible link between the segregation of AOB in small granules and the N₂O emission should be investigated. Maintaining high shear stress can be used for encouraging biomass repartition and could possibly influence such behavior, but this still needs to be further analyzed.

2.2 Modelling aspects

Pursuing the calibration work with new experience obtained with real wastewater and new conditions seems important as it is the first work with a confrontation of PNA model and experience on N₂O.

Future simulation works could be oriented to analyze the effect of feeding mode (continuous, SBR, step feed), COD dosing, temperature, or air flow rate control in order to find the best conditions for mitigating N₂O emissions.

Acknowledgements

Here we are, four years and a half after starting my PhD research on 21 October 2014, with this thesis to show for. This contribution could not have been possible without the help of a lot of people, whom I all thank dearly.

First of all, I had the privilege to have performed the research under the guidance of my supervisor, prof. Mathieu SPERANDIO. I am very grateful for your enthusiasm, patience and help until the last minute rush. Thank you for accurate and effective direction, no matter how busy your schedule was. I've appreciated the received trust and freedom, even I have made some stupid things. At the same time, I also thank all reviewers- Fabrice BÉLINE, Nicolas BERNET, Eveline VOLCKE, Ahlem FILALI, Mathieu SEBILO for their thorough review and contribution to this thesis.

The second thanks will be given to:

- All the technicians and colleagues for helping me out of the swamp in technology, work and life. - Evrard MENGELLE, Mansour BOUNOUBA, Simon DUBOS, Delphine DELAGNES, Chantha KIM, Etienne PAUL, Youlaine BESSIERE, Xavier LEFEBVRE, Claire DUMAS, Guillermina HERNANDEZ-RAQUET, Matthieu Peyre-Lavigne, Michel MAURET, Sebastien POMMIER....
- All PhD and post-docs students in my lab for your company and communication – Zhen Jun WU, Laura DIGAN, Mathilde BESSON, Yan Rafrafi, Amaury Buignet, Amr Aboulela, Mathieu POCQUET, Irene Gonzalez, Louison Dumond, Marie Giroudon, Thomas Etcheberry, Lea Laguillaumie, Gerald Matar, Emilie Alaux, Anil Shewani, Ana Barbara Bisinella-De Faira, Ana Morgado Ferreira, Pieter De Cocker, Erika Varga, Sidonie Durieux, Emeline Flajollet, Fiat Justine....
- All my Chinese friends for enriching my spare life – LIAO Qian, HUANG Yayu, TIAN Zeye, WANG Wenjuan, WANG Rui, YANG Xu, YANG Lin, ZHU Chongwei, ZHAO Zhihua, WANG Jinhui, Qiu Donghai, WANG Zhi, Zhao Jiao, NAN Zibin, ZHANG Wulong, GUO Xuan, PAN Qiang, Deng Hui, ZHANG Nan, WANG Yinping, Qiu Jieru, Guo Lijie, ZHANG Enxi, YU Yaning, Hu Luyang, WU Haiyang, YANG Zhuo.....

Last but not least my parents, for all the support and encouragement in what I do behind me.

Longqi LANG
EAD9-LISBP, INSA de Toulouse
Toulouse, July 2019